

Modeling air quality in a changing climate

Dissertation zur Erlangung des akademischen Grades
des Doktors der Naturwissenschaften
am Fachbereich Geowissenschaften
an der Freien Universität Berlin

Vorgelegt von

Andrea C. Mues

im April 2013

Freie Universität Berlin



1. Gutachter: Prof. Dr. Peter Builtjes

2. Gutachter: Prof. Dr. Ulrich Cubasch

Table of Contents

1	Introduction	1
1.1	Regional air quality	1
1.2	Particulate matter and Ozone.....	3
1.3	Emission and air quality	6
1.4	Meteorology and air quality	7
1.5	Research questions	10
2	Method	12
2.1	Modeling air quality	12
2.1.1	LOTOS-EUROS	12
2.1.2	REM/Calgrid	15
2.2	RACMO.....	16
2.3	Measurements	17
3	Presentation of the papers	19
3.1	Paper I: Impact of the extreme meteorological conditions during the summer 2003 in Europe on particulate matter concentrations	19
3.2	Paper II: The impact of differences in large-scale circulation output from climate models on the regional modeling of ozone and PM.....	20
3.3	Paper III: Differences in particulate matter concentrations between urban and rural regions under current and changing climate conditions	21
3.4	Paper IV: Sensitivity of air pollution simulations with LOTOS-EUROS to temporal distribution of emissions.....	22
4	Overall discussion and conclusions.....	24
5	Outlook	27
6	Summary and Zusammenfassung	29
6.1	Summary	29
6.2	Zusammenfassung	30
	References	33
7	Paper I: Impact of the extreme meteorological conditions during the summer 2003 in Europe on particulate matter concentrations ¹	
8	Paper II: The impact of differences in large-scale circulation output from climate models on the regional modeling of ozone and PM ¹	
9	Paper III: Differences in particulate matter concentrations between urban and rural regions under current and changing climate conditions ¹	

10 Paper IV: Sensitivity of air pollution simulations with LOTOS-EUROS to temporal distribution of emissions

11 Publication list

11.1 Scientific articles

11.2 Presentations

11.3 Posters

Appendix

Danksagung

¹ The papers have been reprinted with kind permission from the corresponding journals.

1 Introduction

The quality of ambient air is of large societal and environmental relevance. Adverse air quality, caused by high concentrations of air pollutants, has an undesirable effect on human health and ecosystems. The most severe health effects can be attributed to particulate matter (PM) and ozone (EEA, 2012). Particulate matter consists of many different primary and secondary components with different chemical and physical properties emitted by a large variety of sources. Ozone is a secondary pollutant formed by a chain of reactions following the emission of different precursors gases. The air quality situation in a region is essentially determined by emission strength and meteorology. Due to the strong relation between meteorological conditions and air quality, a changing climate is anticipated to impact the concentrations of pollutants in the atmosphere. Hence, it is important to understand and to assess the impact of climate change on air quality. To investigate this relation numerical models are important tools and several approaches are possible using climate models and chemistry transport models.

The main research questions addressed in this thesis are: Which conclusions can be drawn on the impact of a changing climate on air quality using different model approaches? What are the strengths and weaknesses of these approaches and the applied models in this context? The emphasis of this study is on particulate matter as its behavior as function of meteorology has not been well investigated yet, whereas for ozone, this relation is already better understood. Furthermore, the focus is on the regional scale and Europe.

In this first chapter, a general introduction to the air quality issue (1.1) with a focus on particulate matter and ozone (1.2) is given. Furthermore, the relation between air quality and emission (1.3) and air quality and meteorology (1.4) is described in more detail. In section 1.5 the research questions addressed here are formulated. In the second chapter the numerical models and the measurements used in the study are described. In chapter three a summary of the four papers is given. Chapter four and five present a discussion and conclusion of the main results as well as an outlook.

1.1 Regional air quality

The main chemical constituents of the atmosphere are nitrogen (~78%), oxygen (~21%), argon (~0.93%) and carbon dioxide (~0.033%) (Warneck, 2000) (relative fraction in dry air). Nitrogen, oxygen and argon alone account for 99.96% of the total contributions from all constituents. Whereas the mixing ratio of these gases is fairly constant in time and show no spatial variation up to an altitude of 100km, the ratio of water vapor is highly variable (Warneck, 2000). The vertical structure of the atmosphere is distributed into different layers, mainly determined by the vertical behavior of meteorological parameters. For regional air quality the main focus is on the troposphere. The height of the troposphere is of approximately 10-15km, but often only the lowest couple of kilometers are directly modified by the underlying surface. This part is called the planetary boundary layer (PBL) and is defined by Stull, (1988) “as that part of the troposphere which is directly influenced by the presence of the earth’s surface, and responds to surface forcing (including e.g. heat transfer and pollutant emissions) with a timescale of about an hour or less”. The planetary boundary layer thickness is quite variable in time and space, ranging from about one hundred meters to a few kilometers. In relation to atmospheric chemistry this layer is important due to the fact that most of

the natural and anthropogenic trace gases and particles are emitted from and transported within this layer. Despite their comparable low concentrations compared to the above mentioned chemical constituents of the atmosphere, some of them cause damage to ecosystems, living species and material and are therefore called air pollutants. A condition of “air pollution” or “adverse **air quality**” in a region may be defined as a situation in which chemical species that result from anthropogenic activities are present at concentration levels which produce a measurable effect on humans, animals, vegetation or materials (Seinfeld and Pandis, 1998).

The **impacts of air pollutants** on human health, the environment and climate are varied. The range of health effects which can be ascribed to air pollutants is already broad, but predominantly to the respiratory and cardiovascular systems (WHO, 2006). Concerning its potential to harm human health, particulate matter is one of the most important pollutants as it reaches sensitive regions of the respiratory system and can lead to health problems such as lung diseases, heart attacks and arrhythmias and can cause cancer (EEA, 2012). As a powerful and aggressive oxidizing agent ozone can decrease lung functions, aggravate asthma and other lung diseases. Particulate matter as well as ozone can lead to premature mortality. Up to 12 months of lower life expectancy can be attributed to man-made emissions of PM2.5 in large part of Europe (EEA, 2007). The most important effects of pollutants on ecosystems such as lakes, rivers and forests are eutrophication, acidification and damage to vegetation resulting from exposure to ozone. Mainly ammonia (NH_3) emitted from agricultural activities and nitrogen oxides (NO_x) emitted from combustion processes are the predominant acidifying and eutrophying air pollutants (EEA, 2012). Some air pollutants have a dual role in air quality and climate. Ozone for example is a short-lived greenhouse gas and contributes to global warming. Particulate matter, on the other hand, has a heating and cooling effect on the atmosphere dependent on the component and their characteristics and optical properties.

Since the beginning of the industrial revolution in the 19th century and the associated increase of anthropogenic emissions sources, a rising concentration and deposition of air pollutants has been observed. One of the first identified types of severe air pollution situations were smog episodes, first described in London. They were characterized by a mixture of fog and smoke of sulfur compounds and particles resulting from combustion of high-sulfur-containing coal. Such episodes do not often occur in Europe anymore mainly due to a shift to low-sulphur fuels e.g. natural gas as source of energy. An important aspect of a negative impact of pollutants on the ecosystem resulting from deposition processes is the phenomenon of acid rain, which caused severe damage on vegetation and forests, even in regions far away from the causing emission sources. Acid rain is related to an increased acid concentration in precipitation caused by anthropogenic emissions of sulfur dioxide from industries, for example. With increased knowledge of the potential damage air pollutants can do to the environment and human health, the terms “air pollution” and “air pollutants” came more and more in the focus of the public, politics and research.

Air quality in a region is largely determined by the interaction of the processes described in this section. The air pollution situation strongly depends on the **emission** strength and the origin of pollutants. The emission strength depends on the density and on the type of emission sources present in the region. In general, one can distinguish between natural and anthropogenic emission sources of primary pollutants and precursors ejected from point (e.g. power plants) or area (e.g. traffic, agriculture) sources. Next to primary emitted pollutants, secondary compounds can be formed in the atmosphere from precursor substances by **chemical reactions** and physical conversion processes. One example is the gas-to-particle conversion of gaseous precursors (ammonia, nitrogen oxides, sulphur dioxide) to secondary inorganic aerosols (ammonium, nitrate, sulphate). Another

type of reactions are photochemical reactions, important for the formation of ozone, for example. Once emitted or formed, the pollutants are mixed in the atmosphere that is determined by different atmospheric **transport** processes. The mean meridional (e.g. Hadley cells, Ferrel cell) and mean zonal (e.g. westerlies, polar jet stream) circulations lead to a large scale mixing of chemical constituents in the atmosphere. Bulk air exchange from the stratosphere into the troposphere lead to an intrusion of ozone downwards, affecting the concentration of tropospheric ozone. Advection which is mainly determined by the mean horizontal wind field is of special importance for regional air quality. It leads to a transport of pollutants into a region from emission sources with varies distances to the source region, as well as to transport of pollutants out of a region. Small scale turbulence dominates the vertical transport of pollutants. Turbulent flows are irregular and random and can be seen as the deviation from the mean wind flow. Sources of turbulence can be mechanical (friction processes) or thermal (convection) processes. Dry and wet **deposition** are removal processes of pollutants from the atmosphere. Whereas dry deposition is the removal of chemical compounds from the atmosphere onto the surface in the absences of precipitation, the wet deposition is related to processes by which species are scavenged by atmospheric hydrometeors (cloud and fog drops, rain, snow). The rate at which atmospheric compounds are absorbed by the surface by dry deposition depends on the chemical species, the atmospheric turbulence, the chemical properties of the depositing species and the nature of the surface itself. Wet deposition can be caused by the following different processes: Scavenging by precipitation (removal of species by raining clouds), cloud interception (impaction of cloud droplets on the terrain), fog deposition (removal of material by settling fog droplets) and snow deposition (removal of material during a snowstorm).

1.2 Particulate matter and Ozone

According to epidemiological studies (e.g. Eeftens et al., 2012 and references therein), the most severe health effects from air pollution can be attributed to particulate matter and, to a lesser extent, to ozone (EEA, 2012). Limit and target values for PM, ozone and many other pollutants are defined in European directives (EU, 2008) to avoid, prevent or reduce harmful effects of air pollutants on human health and the environment.

The term **particulate matter** is used for a mixture of particles (solid, liquid and mixed variety) suspended in the air with a wide range of size, chemical composition and origin which varies in space and time (EEA, 2012). The term “particulate matter”, predominantly related to air quality issues, is mainly used as an equivalent to the term “aerosol” which is in turn generally used in the context of climate issues. Atmospheric particulate matter is in general considered to be particles that range in size from a few nanometers (nm) to tens of micrometers (μm) (Seinfeld and Pandis, 1998). The size distribution of tropospheric particles shows two main different ranges. Particles less than $2.5\mu\text{m}$ are referred to as ‘fine’, summarized in the term PM2.5, and those greater than $2.5\mu\text{m}$ as ‘coarse’. PM10 includes all particles with a diameter of up to $10\mu\text{m}$. In general, the physical behavior, the sources and composition as well as the health effect differ between the fine and coarse mode particles. Fine particles can roughly be divided into two modes: the nuclei mode (about 0.005 to $0.1\mu\text{m}$ diameter) and the accumulation mode ($1\mu\text{m}$ to about $2.5\mu\text{m}$ diameter). Particles in the nuclei mode are formed from condensation of hot vapors during combustion processes and from nucleation of atmospheric compounds to form fresh particles. The source of particles in the accumulation mode is

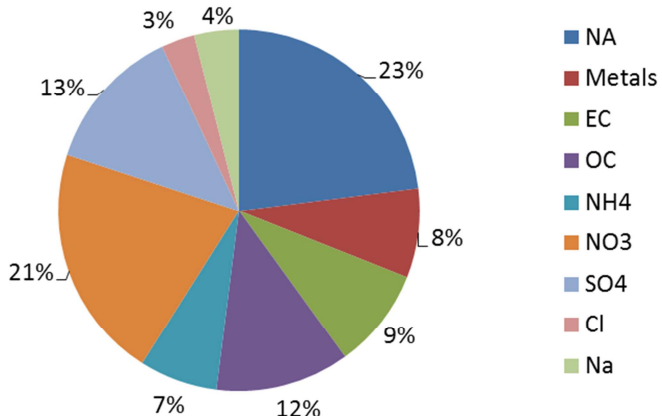


Figure 1
Measured relative distribution of the components in PM10 at the Dutch rural background station in Hellendoorn.
Data from Schaap et al. (2010).

the coagulation of particles in the nuclei mode, which is the main loss processes of the nuclei mode and from condensation of vapors onto existing particles, causing them to grow into size range. The term “accumulation mode” derives from the fact that particle removal mechanisms are least efficient in this regime, causing particles to accumulate there. The particles in the coarse mode are mainly formed by mechanical processes and usually consists of anthropogenic and natural dust particles. Coarse particles have such large sedimentation velocities that they settle out of the atmosphere in a reasonably short time.

Particulate matter consists of a variety of different chemical components, which are either primary because the particles enter the atmosphere directly from their emission sources or secondary because they are formed in the atmosphere from oxidation and transformation of primary precursor gases. In general one can distinguish between natural and anthropogenic emission sources of particulate matter. Natural emission sources are, for instance, erosion of soil dust, sea spray, natural biomass burning, volcanic action and reactions between natural gases, whereas categories for anthropogenic emissions are for example fuel combustion (e.g. in the energy and household sector), industrial processes, nonindustrial diffuse sources (e.g. construction activities), road transport (e.g. vehicle exhaust, brake wear), agriculture as well as reactions between gases emitted by anthropogenic sources.

Figure 1 illustrates an example of the chemical composition of measured particulate matter (PM10) at the rural background station of Hellendoorn in the Netherlands (Schaap et al., 2010). The following components are measured at this site: Sulfate (SO₄), nitrate (NO₃) and ammonium (NH₄), a variety of trace metals (plus silicium), elemental (EC) and organic carbon (OC) as well as sodium (Na) and chloride (Cl). The largest fraction of the chemical analysed components at this station is found for the secondary components nitrate (21%) and sulphate (13%). Elemental and organic carbon contribute in a sum of 21% to the measured total PM10 concentration. Whereas elemental carbon is a primary component, predominantly produced by combustion processes, particulate organic carbon can also be secondary forming the group of secondary organic aerosols (SOA). Secondary organic aerosols are formed by a large range of complex production mechanisms with a variety of precursor gases of anthropogenic and especially biogenic origin which are strongly sensitive to meteorological conditions. Examples for emission sources of primary organic carbon are meat cooking, road dust,

fireplaces, noncatalyst and diesel vehicles. There are still large uncertainties on the concentration and origin of organic carbon including the formation routes of secondary organic aerosols. Metals (8%) are emitted by a large range of abrasion processes and the metallurgical industry. Mineral dust summarizes a collection of components (e.g. Si, Al, Ca, K, Fe, and Ti) including all fugitive wind-blown and mechanically resuspended soil dusts which have composition comparable to that of the earth's crust. An estimation of the mineral dust contribution to the total PM10 level can be derived from the measured tracers Al and Si by means of the mass closure method (Schaap et al, 2010). Sodium and chloride (7%) are two common tracers which reflect the composition of pure sea salt aerosols. The sea salt contribution to particulate matter can be estimated using the measured sodium concentrations. Chloride is very reactive in the presence of sulphuric and nitric acid, resulting in loss of chloride in the aerosol therefore this component is not suitable to estimate the concentration of sea salt. The largest fraction (23%) of measured PM10 at Hellendoorn are not chemically analysed (NA – not analysed). This part includes non-analysed oxides present in particulate matter and the contribution of non-carbon atoms (e.g. H, O, N) in organic matter (Schaap et al., 2010) as well as elements contributing to mineral dust. Another substantial part of the 'not-analysed' fraction is thought to be due to the presences of water which gets lost as a result of the measurement techniques.

The sum of the **secondary inorganic aerosols** represent a considerable fraction of the total PM10 concentrations especially at rural stations, e.g. about 40% at Hellendoorn (Fig.1). Secondary inorganic aerosols are mainly of anthropogenic origin because their precursor gases are mostly emitted by energy production, road transport, industry and agriculture. The gaseous precursor of secondary inorganic aerosols are sulphur dioxide (SO_2), nitrogen oxides (NO and NO_2 , summarized in the term NO_x) and ammonia (NH_3). Sulphur dioxide is emitted by coal-burning power plants and diverse industrial processes (e.g. cement industry). Nitrogen monoxides and dioxides are mostly released during fossil fuel combustion, especially in vehicles, power plants and other industrial sources. The major anthropogenic emission source of ammonia are agricultural activities, only a small contribution comes from non-agricultural sources (e.g. oil refineries and fuel combustion). The main chemical components of the secondary inorganic aerosols are acids (sulphuric acid and nitric acid), ammonium sulphate ($(\text{NH}_4\text{HSO}_4)$, $(\text{NH}_4)_2\text{SO}_4$) and ammonium nitrate (NH_4NO_3) salts. In the following paragraph the formation pathways for secondary inorganic aerosols are briefly described following Weijers et al. (2010).

Sulphur dioxides converts into particulate sulphate on a gas-phase or aqueous-phase transformation path. In case of the gas-phase pathway, sulphur dioxide reacts first with hydroxyl radicals (OH) ($\text{OH} + \text{SO}_2 \rightarrow \text{HSO}_3$), the product oxidizes than to SO_3 ($\text{HSO}_3 + \text{O}_2 \rightarrow \text{HO}_2 + \text{SO}_3$), which finally reacts with small amounts of water vapor to sulphuric acid gas ($\text{SO}_3 + \text{H}_2\text{O} \rightarrow \text{H}_2\text{SO}_4$). Sulphuric acid gas condenses on existing particles and nucleates at high relative humidity, to form a H_2SO_4 droplet. A second path is that it becomes, in the presence of NH_3 gas, neutralized as (bi-)ammonium sulphate ($\text{H}_2\text{SO}_4 + \text{NH}_3 \rightarrow \text{NH}_4\text{HSO}_4$; $\text{NH}_4\text{HSO}_4 + \text{NH}_3 \rightarrow (\text{NH}_4)_2\text{SO}_4$). The aqueous pathway takes place when sulphur dioxide is dissolved in a fog or cloud droplet. Sulphur dioxide is quickly oxidized to H_2SO_4 with the available ozone and hydrogen peroxides (H_2O_2) in the droplet. If, also NH_3 is present the product (H_2SO_4) is neutralized to NH_4HSO_4 . The aqueous pathway depends on the cloudiness and is much faster than the gas-phase conversion of SO_2 to particulate sulphate. Generally, atmospheric nitrate originates from the oxidation of nitrogen dioxide (NO_2) to nitric acid (HNO_3), particles are then produced as the result of reactions with ammonia or sodium chloride. During daytime, the main production path of nitric acid is the reaction of nitrogen dioxide with hydroxyl radicals

$(OH^- + NO_2 \rightarrow HNO_3)$. Afterwards ammonia gas reacts reversibly with nitric acid to form the ammonium salt NH_4NO_3 ($NH_3 + HNO_3 \leftrightarrow NH_4NO_3$). The ammonium nitrate formation is limited by the available ammonia in a region as it can only be formed if the available sulphate is neutralized by ammonia. In marine and coastal atmosphere, HNO_3 is also converted into sodium nitrate ($NaNO_3$) through the reaction with sea salt particles.

Ozone (O_3) is formed in the atmosphere from a chain of chemical reactions involving primarily nitrogen monoxide (NO), nitrogen dioxide (NO_2) and volatile organic compounds (VOC). Emission sources of the precursor gases are fuel combustion by e.g. industrial facilities and road traffic for the nitrogen oxides, VOC are emitted by a large number of sources including paint, road transport, refineries and vegetation. Because the formation is also driven by the energy from the sun, ozone is labeled as a photochemical pollutant. The formation of ozone in the troposphere is complex and a result of the photolysis of nitrogen dioxide and the subsequent reaction of the reactive atomic oxygen (O) with molecular oxygen (O_2) to form ozone. In the destruction process, ozone reacts with NO, which oxides to NO_2 and is then again available for the photolysis process. This is known as the titration reaction. This chemical mechanism describes the equilibrium state in the atmosphere, and observed high ozone levels cannot be explained with this mechanism. Further formation paths for NO_2 from NO which are independent from ozone have to be involved. This process results from the chemical destruction processes of VOCs. By the degradation of VOC through the action of the hydroxyl radical formed by the action of sunlight, substances are produced that react with NO to produce NO_2 without consuming ozone. Thus, the net result of these reactions is that more ozone molecules are formed than VOC molecule are degraded. In contrast to other pollutants, ozone levels are generally highest at rural locations. This is due to the contribution of NO to the destruction of ozone, which is mainly emitted in urban and industrial area.

1.3 Emission and air quality

Along with meteorology, emission of pollutants is the most important controlling factor of air quality. Relevant characteristics of emission are the quantity of the emitted mass per pollutant, the emission sources, their spatial density and their height as well as the point in time of emission. The quantity of the emitted mass varies strongly per pollutant and country. Important natural sources are the resuspension of dust, sea spray, vegetation, and natural wild fires. Important anthropogenic sources are the energy, industry and road transport sector as well as agriculture. To give examples, the most contributing emission sources for PM precursor in Europe in 2004 were the energy (49%) and transport sectors (25%), followed by industry (15%), agriculture and waste (11%) and for ozone precursor emission the road transport sector (34%) was the dominate source, followed by energy (26%) and industry (26%) (EEA, 2007). The spatial density of anthropogenic emission sources is especially high in urban and industrial areas. The main contributor to air pollution in cities is road transport but also emission from the industry, power production and household sectors contribute substantially in many parts of Europe (EEA, 2007). In rural regions intensive agriculture is a large source of anthropogenic emissions. The emission strength varies in time with activity patterns, region, species, emission process and meteorology. Furthermore, it depends on the sources at which vertical height it is emitted, as area sources like road traffic or agriculture are close to the ground, whereas a stack height can be hundreds of meters high. The atmospheric conditions in time and height during release and transport impact the fate of the emitted air pollutants. The emission of

pollutants also depend directly (e.g. isoprene, windblown dust) or indirectly (e.g. heating, cooling) on meteorology. This holds for both the emitted mass and the point in time of emission.

Emissions of the main air pollutants declined in the period 2001-2010 in Europe, resulting for some of the pollutants in improved air quality across the region (EEA, 2012). An example are emissions of primary PM10 and PM2.5 which decreased between 2001 and 2010 by 14% and 15%, respectively, in the EU and also PM precursor emissions, except those of ammonia, decreased considerably during this time period (EEA, 2012). Most of the reductions in emissions of primary PM10 and PM precursors in the period 2000-2004 were in the energy supply and road transport sectors (EEA, 2007). Also ozone precursor gas emissions declined considerably between 2001 and 2010 by 26% for NOx, 27% for NMVOC and 33% for CO in the EU (EEA, 2012). Despite these emission reductions, many European countries still do not fulfill one or more emission ceilings defined in EU and United Nations (UN) conventions (EEA, 2012). Anthropogenic emission of air pollutants including precursors of key pollutants such as ozone and particulate matter are regulated in several EU directives, setting national emission limits for these pollutants. Likewise several directives and international conventions regulate emissions specifically for certain sources and sectors. This is done by either setting emission limits, by requiring the use of the best available technology, or by setting requirements on fuel compositions (EEA, 2012). One has to consider that due to the non-linear relationship between emission and pollutant concentrations, emission reduction do not always cause a corresponding drop of pollutant concentrations, especially for particulate matter and ozone. In large parts of Europe the emissions of air pollutants are projected to decline further until 2020 as a result of progressive implementation of current and planned emission control legislation and continuing structural changes in the energy system (EEA, 2007). Consequently, the largest projected reductions are for energy-related emissions (especially for SO₂, NOx, VOCs and primary PM2.5) but also with lower reductions for agriculture-related emissions (EEA, 2007). Emissions of primary PM10 and PM precursor are also expected to decline because the further application of improved vehicle technologies and emission from stationary fuel combustion are controlled through reduced usage or use of other fuels, e.g. natural gas (EEA, 2007).

1.4 Meteorology and air quality

The processes relevant for air quality discussed in chapter 1.1. strongly depend on meteorology. This includes the impact of individual meteorological parameters, synoptic situations, the state of the planetary boundary layer and large circulation patterns. In the following paragraph some examples are given for these dependencies. The emission of several natural and anthropogenic pollutants and precursor gases are directly or indirectly influenced by weather conditions. Examples are the dependency of windblown dust emissions on wind speed, the increase of isoprene emissions, which are important for the formation of secondary organic aerosols, with temperature or the indirect effect on anthropogenic emissions through the impact on activity patterns (e.g. heating, energy consumption). Horizontal wind (speed and direction) and the state of the planetary boundary layer highly impacts the horizontal and vertical transport of pollutants. The impact of meteorological parameters on chemistry is also very various. Photochemical reactions for example, relevant for ozone formation, depend on the incoming solar radiation and thus also on cloudiness. Regarding the formation of secondary particulate matter higher temperature can lead to increased sulfate concentrations due to faster SO₂ oxidation (Tai et al., 2012). Furthermore, the state of the

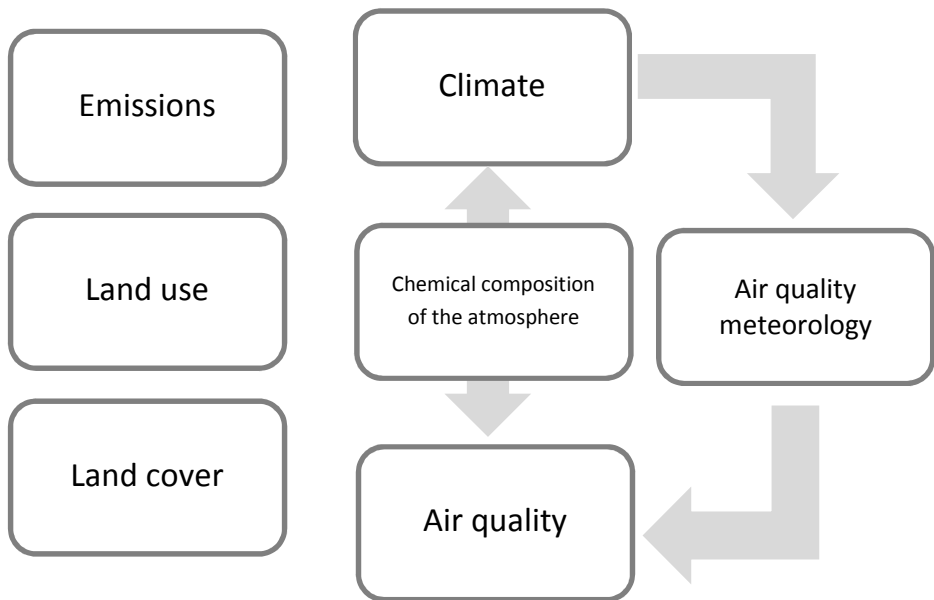


Figure 2
Schematically illustration of the processes taking part in the chemistry-climate system.

phase (particle or gas phase) of semi-volatile components such as nitrate and organics is among others a function of temperature (Seinfeld and Pandis, 1998). Dry deposition is mainly dependent on the level of atmospheric turbulence. Wet deposition is highly determined by precipitation and rather by the frequency of events than by their intensity. Several of these relations are well known and described in models, others are more uncertain. Since particulate matter consists of many components with different physical and chemical properties, the effect of the meteorological parameters on the individual components varies and is more uncertain than for ozone (Tai et al., 2012).

The present air quality situation in a region is mainly determined by the current synoptic situation in combination with the strength of emissions. Certain synoptic situations favor the accumulation of pollutants leading to enhanced concentrations of pollutants. These situations can be for example connected to stable high-pressure systems in summer (e.g. Vautard et al., 2007a) and winter (e.g. Stern et al., 2008), which are often characterized by stagnation, little precipitation and low wind speeds. In winter the low mixing height is another relevant impairing parameter. Other weather situations, such as frontal passages connected to precipitation events, are leading to the removal of air pollutants from the atmosphere. The variability of pollutant concentrations between years and within one year is mainly driven by weather. The variation of emissions between years is in general smaller, e.g. only by 5% between the years 2003 until 2007 (Kuenen et al., 2011). Thus changes in the meteorological conditions on short as well as long timescales have an impact on the concentrations of pollutants.

The interactions in the chemistry-climate system are very complex and are schematically illustrated in Figure 2. The right branch illustrates the impact of climate on surface air quality via its effect on the air quality meteorology, which describes the meteorological conditions affecting air quality. Climate and air quality are also related through the chemical composition of the atmosphere in the entire vertical column. The chemical composition of the atmosphere influences climate by regulating the radiation budget. The thermal structure of the atmosphere is highly influenced by the presence of greenhouse gases (e.g. CO₂, CH₄, N₂O, O₃) and aerosols. The main effect of the gases is

through absorbing of outgoing surface thermal radiation and reradiating at the local temperature and thus having a heating effect on the atmosphere (greenhouse effect). Aerosols on the other hand have a heating or cooling effect on the atmosphere dependent on their characteristics and the optical properties of the particles which affect the solar and thermal radiation. Black carbon for instance has a warming effect (positive forcing) while sulphate and nitrate may have a cooling effect (negative forcing) (direct effect) (Seinfeld and Pandis, 1998). Particles may also have an indirect effect on climate through their contribution to the formation and characteristics of clouds which influence climate by the albedo effect and the greenhouse effect. Furthermore, the albedo of surfaces such as snow and ice can be influenced by the deposition of particles such as black carbon. Because the main pollutants particulate matter and ozone are also recognized as important climate forcers they have a dual role in air quality and climate.

The climate varies with a natural variability on a long (millenniums) and on a comparatively short (decades) timescale. Changes in the concentration of greenhouse gases and aerosols as well as changes in land cover and solar radiation alter the energy balance of the climate system and are therefore drivers to climate change (IPCC, 2007). Radiative forcing (W/m^2) expresses the resulting positive or negative effect on the energy balance due to these factors. Global atmospheric concentration of greenhouse gases (e.g. CO_2 , CH_4 , and N_2O) increased as a result of anthropogenic activities and are anticipated to increase further in the future (IPCC, 2007). CO_2 is the most important greenhouse gas, its annual emissions have grown between 1970 and 2004 by about 80%, and represented 77% of total anthropogenic greenhouse gas emissions in 2004 (IPCC, 2007). This leads to an anthropogenic reinforcement of the greenhouse effect and a positive radiative forcing. Anthropogenic contribution to aerosols together produces a cooling effect, but the total radiative forcing is more uncertain than for the greenhouse gases (IPCC, 2007). Thus, the resulting climate change depends on a number of factors, including the size of the concentration increase and the radiative properties of each greenhouse gas, interactions with other radiatively important atmospheric constituents and climate feedbacks (Seinfeld and Pandis, 1998). Global and regional climate models are used to investigate possible trends in the future climate by means of greenhouse gas emission scenarios (SRES-scenarios) (IPCC, 2007) and to assess the impact on regional weather conditions.

Due to the interaction between climate and regional air quality as illustrated in Figure 2 climate change is anticipated to impact air quality. This impact is through a variety of effects which are not only connected to changes in mean values of meteorological variables (e.g. temperature, precipitation) but also to changes in their variances. Examples of possible effects of climate change in Europe which are also relevant for air quality are an increase in average temperature, changes in the frequency of heat waves, local changes in precipitation, impact on cloud cover and changes in circulation patterns (e.g. frequency of cold frontal passages) (Jacob and Winner, 2009; Vautard and Hauglustaine, 2007b; Forkel and Knoche, 2006). These effects can be direct or indirect, including the modification of anthropogenic and biogenic emissions, changes in chemical reaction rates or changes in mixing layer heights that affect the mixing of pollutants.

An important external forcing of the climate-chemistry system (and changes therein) come from emissions (and changes therein) of greenhouse gases, aerosols and air pollutants. Also changes in land cover and land use are expected in future both as a consequence of climate change and by anthropogenic activities. To focus on the impact of changes in the meteorological conditions on air quality, future changes in emissions of air pollutants as described in section 1.3 are not taken into account in this study, the same holds for changes in land use and land cover.

1.5 Research questions

In the previous section it was stated that it is important to assess the consequences of climate change for the different chemical species relevant for air quality. The impact of a changing climate on pollutant concentrations can be investigated using different modeling approaches. In this context the central question addressed in the present work is:

- Which conclusions can be drawn on the impact of a changing climate on air quality with a focus on particulate matter using different model approaches? What are the strength and weaknesses of these approaches and the applied models?

In more detail:

One approach is to analyze a synoptic situation in the past (e.g. summer 2003) which is expected to occur more frequently in the future in terms of its effects on air quality. The advantages of this approach are that such an effect can be directly analyzed using measurements and that an evaluation of chemistry transport models for these situations is possible. Hence, such an investigation also indicates the strengths and weaknesses of the chemistry transport model simulations as a function of meteorological conditions which is also important when chemistry transport models are used in coupled climate – air quality model systems. Thus, the following questions are addressed:

- Did the meteorological conditions during the summer 2003 have a clear impact on measured PM10 concentrations and its components?
- Are state-of-the-art regional chemistry transport models able to reproduce the measured PM10 concentrations during this episode?

A second approach is to use a one-way coupled model systems consisting of a regional chemistry transport model forced by a regional climate model. In this approach the output from an SRES (e.g. A1B) constraint transient scenario run with a global climate model (GCM) is dynamically downscaled with a regional climate model and used to force a constant emission run with a chemistry transport model. The application of two different GCMs which differ in terms of zonal mean flow for present-day conditions and in climate change response show the bandwidth of possible future climate scenarios. The discussed questions in this context are:

- What are common findings and differences – in meteorology and air quality - using two different GCMs as input for the RCM?
- What is the impact of biases in climate models on the outcomes of air quality modeling?

Urban areas are very important in view of air quality because they represent the main areas of anthropogenic emissions and threshold values at hot spot locations in urban and industrial areas are still exceeded on many locations. PM10 concentrations and composition were found to differ substantially between an urban area and its surrounding rural region, resulting in a positive urban increment of PM concentrations. The research questions in this context are:

- What is the size of the measured PM10 concentration difference between an urban and its surrounding rural region and does the resulting urban increment depend on the urban area?
- Is a regional state-of-the-art chemistry transport model able to reproduce the measured urban increment?

- Which conclusions can be drawn on the impact of a changing climate on the urban increment based on the two approaches discussed above using regional models?

Chemistry transport models have been developed to assess the fate of air pollutants. Large efforts have been devoted to improve the process descriptions and meteorological input data. Still, models underestimate the variability of air pollutant levels in time and as function of meteorology compared to observations. The emission data used in chemistry transport models might well be too static and the emission strength of the different sectors should be explicitly related to the meteorological variability. This is also relevant for climate studies. Here the stated questions are:

- Is the model performance sensitive for improved temporal emission information and the fact that specific emissions are a function of meteorology?
- Is it worthwhile to make the effort to improve the emission description to an explicit temporal emission model?

In order to address these research questions simulations with numerical models have been performed. These models are introduced and described in the following chapter (2.1.2.-2.1.4.). Furthermore, measurements of air pollutants from two different networks have been used which are described in section 2.2.

2 Method

To address the research questions stated in section 1.5. different model simulations have been performed and measurements have been used. In sections 2.2., 2.3., 2.4. and 2.5. the models and measurement networks used in the study are described.

2.1 Modeling air quality

Numerical modeling is an important tool to study complex processes in the atmosphere. It is also widely-used in many other fields (e.g. biology, economy) and can be classified between theory and experiment which are the basis for the development of numerical models. A common tool for air quality research are regional eulerian chemistry transport models aimed to simulate the concentration and deposition of atmospheric chemical components in the troposphere. These chemistry transport models deliver information on a continuous concentration field in contrast to measurements which are selective in space and time. They are required to understand interactions between different processes and events related to air quality as described in section 1.1. such as between emissions/meteorology and adverse concentrations of air pollutants. Fields of applications of chemistry transport models are the estimation of the current air quality situation in a region, air quality forecasting, assessing the effectiveness of emission reduction measures or to isolate certain processes to better understand their impacts. Furthermore they are used to study the effects of changes in the complex system of atmospheric chemistry such as changes in emission and meteorology. Thus, they are also common tools to investigate the impact of a changing climate on air quality.

It is important to consider that a model is a limited tool with missing processes and uncertainties. This should also be accounted for in the designing phase of a planned study as well as for the interpretation of the model results. Thus, a central and essential aspect is the evaluation of the model performance with measurements. This holds for the overall model performance as well as for individual processes.

2.1.1 LOTOS-EUROS

The LOTOS-EUROS (LOng Term Ozone Simulation - EUROpean Operational Smog) (Schaap et al., 2008) is a three-dimensional eulerian chemistry transport model, aimed to simulate air pollution in the lower troposphere on the regional scale. Regarding its complexity, it can be viewed as an operational model, containing in principle all relevant processes and being capable of calculating a large number of scenarios on an hour-by-hour basis over extended periods of at least a year on the European, national or regional domain. The default modelled species in LOTOS-EUROS are: ozone (O_3), nitrogen oxides (NO_x), sulphur dioxide (SO_2), ammonia (NH_3), chemically unspecified primary particulate matter in the fine (PPM2.5) and coarse (PPM10, excluding PPM2.5 and EC) mode, elemental carbon (BC), ammonium (NH_4^+), sulphate (SO_4^{2-}), nitrate (NO_3^-), and sea salt (Na in the fine and coarse mode) as well as species relevant as precursors and oxidants. Particulate matter is defined as the sum of the following individual components: $PM10 = PPM2.5 + PPM10 + EC + NH_4^+ + SO_4^{2-} + NO_3^- + 3.26 * (Na_{fine} + Na_{coarse})$.

The horizontal master domain of the model covers Europe and is bound at 35° and 70° North and 10° West and 40° East. The standard horizontal resolution is 0.5° x 0.25° (approximately 25x25km²) on a regular longitude-latitude grid. The choice of a smaller domain and a higher horizontal resolution (up to a factor of 8) is optional. For the lateral boundary conditions climatological background observations or the simulation output from the TM5-Model are used, while for nested simulations, output from a LOTOS-EUROS simulation with a larger domain serves as boundary information. The vertical grid is based on terrain following vertical coordinates and extends 3500m above sea level. The vertical layers vary in space and time as they are orientated on the mixing layer height to follow, in a simplified way, the vertical structure of the planetary boundary layer and especially the vertical mixing within it. The lowest model layer, which represents the surface layer, has a fixed vertical depth of 25m over ground. The top of the second layer follows the course of the mixing layer height in space and time and thus changes for every hour and grid cell. The corresponding mixing layer height is derived from the meteorological input data. The two reservoir layers are equally thick with a minimum of 50m and their height is determined by the difference between the top of the coordinate system and the mixing height. In the output, ground level concentration fields are given at measurement height diagnosed by the constant flux approach that relates the dry deposition velocity and the pollutant concentrations.

The main prognostic equation in the LOTOS-EUROS model is the continuity equation that describes the change in time of the components concentration as a result of the following processes: Emissions, transport (advection, diffusion and entrainment), chemistry, dry and wet deposition. The transport of pollutants consist of advection in three dimensions, horizontal and vertical diffusion and entrainment. Mean wind, given by meteorological input fields, is responsible for very rapid horizontal transport or advection. The, generally, much smaller vertical mean winds are calculated as the result of the divergence/convergence of the horizontal wind fields. The monotonic advection scheme developed by Walcek (2000) is used to solve the system in the model and the number of steps in the advection scheme is chosen such that the Courant restriction is fulfilled. The planetary boundary layer, next to the mean wind, is also characterized by subscale processes which are important for the mixing of pollutants, especially in the vertical. Vertical diffusion is described using the standard local K-approach. The K_z values are calculated based on stability parameters (e.g. Monin-Obukhov-Length) which delivers information about the thermal structure of the boundary layer. During daytime and for an appropriate solar radiation, the planetary boundary layer is characterized by a vertical growing turbulent mixing height which goes along with entrainment of air and strong vertical mixing in an instable layer leading to a strong dilution of pollutants. This intensified vertical mixing of emissions and pollutants and the entrainment during day is not only considered by the K-Theory in the model, but also by an ‘indirect’ parameterization of the convection driven turbulent mixing by use of time-depending layers. The accumulation of pollutants in a stable boundary layer, mainly occurring during night, is considered additionally by a decrease in height of the second layer associated to the mixing height. For the gas-phase chemistry the modified CBM-IV chemical mechanism (Schaap et al., 2005) based on the original CBM-IV (Whitten et al., 1980) is used in LOTOS-EUROS. In the default setting the aerosol chemistry is represented using ISORROPIA2 (Nenes et al., 1998; Fountoukis and Nenes, 2007). The dry deposition of gases is parameterized using the resistance approach (Erisman et al., 1994), based on the idea of electrical resistance. The dry deposition of particles is based on empirically derived values from IDEM. For the description of wet deposition only below cloud scavenging of gases and aerosols is explicitly treated in the LOTOS-EUROS but over the whole vertical domain and therefore also inside clouds.

SNAP (level 1)	SNAP name
01	Combustion in energy and transformation industries
02	Non-industrial combustion plants
03	Combustion in manufacturing industry
04	Production processes
05	Extraction and distribution of fossil fuels and geothermal energy
06	Solvent and other product use
07	Road transport
71	Road transport exhaust emissions, gasoline
72	Road transport exhaust emissions, diesel
73	Road transport exhaust emissions, other fuels
74	Road transport non-exhaust emissions, evaporation of gasoline
75	Road transport non-exhaust emissions, road, brake and tyre wear
08	Other mobile sources and machinery
09	Waste treatment and disposal
10	Agriculture

**Table 1.:
SNAP level 1 source categories.**

However, an explicitly treatment of in-cloud scavenging is neglected due to missing information of clouds in the meteorological input. It is planned to improve the description of aqueous-phase chemistry and wet deposition processes including variable droplet pH (Banzhaf et al., 2012) in the LOTOS-EUROS. In the improved wet deposition scheme it will be explicitly distinguished between in-cloud and below-cloud scavenging for gases and particles. In-cloud scavenging will be dependent on the cloud liquid water content and cloud water pH.

Input data: The anthropogenic emissions used in the studies are the TNO-MACC emission database (Kuenen et al., 2011) which is based on the TNO 2005 gridded emission inventory (Denier van der Gon et al., 2010). The TNO 2005 emission inventory is a European-wide, high-resolution ($0.125^\circ \times 0.0625^\circ$ lon-lat) inventory for NO_x, SO₂, NMVOC, CH₄, NH₃, CO, primary PM10 and primary PM2.5 for the year 2005. It is set up using official emissions reported by countries themselves. Elemental carbon emission are separated from the chemically unspecified primary PM2.5 emissions following Schaap et al. (2004) and primary organic carbon is included as a part of primary PM2.5. Natural emissions are calculated on-line using the actual meteorological data. Sea salt emissions are calculated following Monahan et al. (1986) from wind speed at ten meters and biogenic isoprene emissions are calculated following Guenther et al. (1993). Emissions have been split in point and area sources and are given in aggregated sources categories (SNAP levels) as a total annual sum. SNAP (Selected Nomenclature for Air Pollutants) level one is the highest aggregation level, distinguishing 10 different source sectors given in Table 1. The total of annual anthropogenic emissions are broken down to hourly emission estimates, using time factors for the temporal variation of emission strength over the months, day of the week and the hour of the day per SNAP category (Builtjes et al., 2003). The land use dataset describes the type of land that covers the surface in a grid cell. This is important for the determination of the deposition velocities and in particular of the uptake rate and the surface roughness. It is also required to determine the biogenic emission fluxes, such as isoprene and terpene emissions from forests. The land use data set used in the model is based on the CORINE/Smiatek (EEA, 2000), with a grid resolution of 0.0167° in longitude and latitude over Europe and 13 land use categories. The model has an off-line meteorology: The meteorological fields are input every 3-hours. Currently the default input fields are

provided by ECMWF meteorology, but data from the regional climate model RACMO can be used for long-term scenario runs as well. Meteorological fields are interpolated from the ECMWF grid (resolution $0.5625^\circ \times 0.5625^\circ$) to the grid as used in LOTOS-EUROS.

This description of the LOTOS-EUROS model is valid for the model version 1.6. which was used in paper I-III, whereas the updates to the model version 1.8. used in paper IV is described in the corresponding paper.

2.1.2 REM/Calgrid

The three dimensional chemistry transport model REM/Calgrid (RCG) (Stern et al., 2006; Beekmann et al., 2007) was developed at the Freie Universität Berlin. The RCG can be viewed as an operational model with a similar complexity as the LOTOS-EUROS and is used on the regional and the urban scale for short-term and long-term simulations of oxidant and aerosol formation. Examples for modeled gaseous species in the RCG are: ozone (O_3), nitrogen oxides (NOx), sulphur dioxide (SO_2) and ammonia (NH_3). The gas-phase chemistry carbon bond mechanism used in RCG is updated version of the CBM-IV (Gipson and Young, 1999) but differs from the one used in LOTOS-EUROS. The following different chemical components are considered to contribute to particulate matter in the RCG: $PM10 = PPM2.5 + PPMCO + EC + OC + Na^+ + Cl^- + SO_4^{2-} + NO_3^- + NH_4^+ + SOA$. PPM2.5 and PPMCO is primary particulate matter in the fine and coarse mode ($PPMCO = PM10 - PPM2.5$) emitted by anthropogenic and natural sources. In contrast to the LOTOS-EUROS, RCG considers road dust (Denier van der Gon et al., 2010) and windblown dust (Loosmore and Hunt, 2000; Claiborn et al., 1998). The resuspension of windblown dust is calculated as a function of friction velocity and the nature of soil. Organic carbon (OC) in RCG it is taken as an extra component, in contrast to LOTOS-EUROS, and is along with elemental carbon (EC) separated from the PPM2.5 emissions. Sea salt, composed by sodium (Na^+) and chloride (Cl^-), is simulated in the coarse mode and emitted by sea water. The equilibrium module for the formation of the secondary inorganic aerosols (SO_4^{2-} , NO_3^- , NH_4^+) is the ISORROPIA thermodynamic scheme (Nenes et al., 1998) optimized for urban and regional pollution conditions. The formation of secondary organic aerosols (SOA) is described by a modified version of the SORGAM module (Schell et al., 2001).

The horizontal master domain covers the area from 35° to 66.25° North and 10.5° West to 35.5° East, with a standard horizontal resolution of $0.5^\circ \times 0.25^\circ$ in latitude and longitude. The use of a higher horizontal resolution and the choice of a smaller domain is possible. The choice of time dependent layers, as described in section 2.1.1. for LOTOS-EUROS, and in time and height fixed layers is optional. Both vertical coordination systems are based on terrain-following layers. Lateral boundary conditions are taken from climatological background concentrations, for nested simulations, output from a lower resolution model run can be used as boundary information.

The change in time of the components concentrations is described by the continuity equation, considering the following processes: Emission, transport, chemistry, dry and wet deposition. For the horizontal advection, the scheme developed by Waleck (2000) is used. The non-advection horizontal pollutant fluxes are described in the RCG using the simplified K-theory closure based on the description in Yamartion et al. (1992). The description of the vertical diffusion is based on the Monin-Obukhov similarity theory and calculated using the vertical diffusion coefficient (K_z). The calculation of the dry deposition of gases in the RCG is based on a resistance approach (Erisman et al., 1994). Dry deposition of particles is treated with a theoretical approach based on the resistance analogy (Yamartino et al., 1992). In the used model version of RCG only wet deposition of gases and

particles due to below cloud scavenging is explicitly considered, based on a scavenging coefficient approach. Just as in the LOTOS-EUROS model, it is planned to improve the description of aqueous-phase chemistry and wet deposition processes in RCG considering also in-cloud scavenging.

The anthropogenic emissions used in this study are, as in the LOTOS-EUROS, based on the TNO-MACC emission dataset for 2005 (Kuenen et al., 2011) but the German emissions have been replaced by a high resolution distribution from the national PAREST project (Denier van der Gon et al., 2010), having the same emission total as the MACC database. Natural emissions are calculated online based on the actual, relevant meteorological parameters. An important difference between the two chemistry transport models LOTOS-EUROS and RCG is the off-line meteorology used in the models. Whereas for LOTOS-EUROS the fields are delivered by the ECMWF model, the input fields for the RCG are produced by the diagnostic meteorological analysis system Tramper (Reimer and Scherer, 1992). Tramper is based on an optimum interpolation procedure on isentropic surface developed at the Freie Universität Berlin. The scheme uses all available synoptic surface and upper air observations as well as topographical and land use information.

2.2 RACMO

A one-way coupled model system consisting of the regional climate model RACMO2 and the chemistry transport model LOTOS-EUROS is used in this study. The output from the SRES-A1B constraint transient runs with two global climate models (GCMs), i.e. ECHAM5 (Roeckner et al., 2003; Jungclaus et al., 2006) and MIROC-hires (K-1 Model Developers, 2004), have been dynamically downscaled with the regional climate model RACMO2 and used to force a constant emission run with the chemistry transport model LOTOS-EUROS covering the period 1970-2060. Additionally, the output of a RACMO2 simulation forced by ERA-Interim reanalysis are used as input for a LOTOS-EUROS simulation for a present-day climate period (1989-2009).

RACMO2 is the regional atmospheric climate model of the Dutch weather service KNMI (Lenderink et al., 2003; Van Meijgaard et al., 2008). The RACMO 2.2 version used for this study consists of the 31r1 cycle of the ECMWF physics package embedded in the semi-Lagrangian dynamical kernel of the numerical weather prediction model HIRLAM (Undén et al., 2002) and a few routines to link the dynamics and physics parts. RACMO2 employs a rotated longitude-latitude grid to ensure that the distance between neighboring grid points is more or less the same across the entire domain. For the coupled run, a RACMO2 domain was configured just encompassing the standard LOTOS-EUROS domain. It has a horizontal resolution of 0.44° with 114 points distributed from 25.04°W to 24.68°E longitude and 100 points from 11.78°S to 31.78°N latitude in the rotated grid. The South Pole is rotated to 47° S and 15°E. In the vertical, 40 pressure levels were used. At this resolution RACMO2 uses a model time step of 15 min and output for coupling with LOTOS-EUROS was generated every three hours. The analysis of atmospheric parameters is limited to the interior of the RACMO2 domain, here obtained by omitting an 8-point wide boundary zone. The model has participated in ensemble studies with other regional climate models (Jacob et al., 2007; Christensen and Christensen, 2007), which showed that the regional models did reproduce the large-scale circulation of the global driving model, albeit with biases, and that RACMO2 was not one of the extreme models.

2.3 Measurements

The continuous measuring of atmospheric chemical compounds, such as particulate matter, ozone, VOCs, heavy metals and organic pollutants, in air and in precipitation as well as their chemical, physical and optical properties is fundamental to assess their impact on ecosystems, health and climate. The measurements ensure the air quality monitoring on the short-term as well as the long-term basis. Short-term monitoring is used to identify exceedances of limit values which are defined in EU directives (EU, 2008), based on this, appropriate short-term actions can be taken and warnings can be circulated. Long-term monitoring helps to identify locations which have constant high concentrations and where actions on a long-term basis could be most effective. Furthermore, measurements are important to detect temporal and spatial concentration trends and to determine major emission sources. For air quality modeling, measurements are highly important for the validation of the models and are also used for data assimilation inside the models.

Several measurement station networks on the European, country and local/city scale were established in the last decades. Examples for European measurement networks and databases which are also used in the present study are the EMEP and the AirBase networks. The main objective of **EMEP** (European Monitoring and Evaluation Programme) is to provide governments with Europe-wide information on the concentration and deposition of air pollutants as well as of the quantity and significance of long-range transport of air pollutants across boundaries (Tørseth et al., 2012). The EMEP data are available in the public EMEP database (www.emep.int). Regarding PM the following compounds are part of the EMEP monitoring program: Secondary inorganic aerosols, organic and elemental carbon, sea salt, base cations, and mineral dust. But the number of sites reporting these components varies, and often, they are not measured continuously but only for a few selected sites during measurement campaigns. The EMEP monitoring network only includes sites which are classified as regional or global and which are therefore representative for a larger area. These sites are located in that way that significant local influences, for example local emission sources and sinks as well as topographic features, are minimized, and influences from local large industrial or transport related sources are avoided. The number of stations measuring PM10 and PM2.5 has steadily increased throughout the last decade.

AirBase is the public air quality database system of the European Environmental Agency (EEA). It contains air quality monitoring data and information submitted by participating countries throughout Europe (38 countries in 2012). The air quality database consists of a multi-annual time series of air quality measurement data and statistics for a number of pollutants. The most frequently reported pollutants in the AirBase database are: Sulphur dioxide (SO₂), nitrogen dioxide (NO₂), nitrogen oxides (NOx), ozone (O₃), carbon monoxide (CO), particulate matter (PM10, PM2.5), benzene (C₆H₆) and lead (Pb) (Snel, 2004). The number of reporting countries and stations varies per component. Monitoring stations in the AirBase database must be classified according to certain criteria including the type of station (traffic, industrial, background), the type of zone (urban, suburban, rural) and the characterization of zone (residential, commercial, industrial, agricultural, nature, unknown and combination of these). For stations located inside a city the zone is called urban. Residential areas just outside the main city represent the suburban zone. If a station is located outside a city far from city source, the type of zone is defined as rural. In these type of zones a distinction can be made regarding the location of the station defining the type of station. The type of station is called traffic (or street), if the station is located such that its pollution level is determined predominantly by emissions from nearby traffic. The level of pollution of industrial

stations is mainly determined by emissions from nearby single or multiply industrial sources. When the pollution level close to a station is not determined significantly by any single source or street, but by the integrated contribution from all sources upwind the station, the type of station is called background. All of these types of stations can be located in urban, suburban or rural zones. These characteristics affect the measured pollution concentration at a station.

Important for measurement networks is that the measurements need to be made in a comparable way at all sites and consistent in time to allow the assessment of temporal and spatial trends. But different methodologies are often used at stations in one network, hampering the comparability across the station in a network. Ideally, the spatial density of measurement sites should reflect the gradients in the air concentrations and deposition fluxes. However, the implementation of an adequate monitoring program has been difficult in some regions which are characterized by a lack of monitoring sites (e.g. Mediterranean area and Eastern Europe region (Tørseth et al., 2012)). A further problem is that several sites have unsatisfactory data coverage, so that data for a full year is rarely available, but rather for a few selected sites during research campaigns.

3 Presentation of the papers

In this chapter the objectives, a short method description and the main findings of the scientific papers are presented. The papers are put into a combined context and the motivation of the papers is discussed.

3.1 Paper I: Impact of the extreme meteorological conditions during the summer 2003 in Europe on particulate matter concentrations

Published: Mues, A., Manders, A., Schaap, M., Kerschbaumer, A., Stern, R., Builtjes, P., 2012. Impact of the extreme meteorological conditions during the summer 2003 in Europe on particulate matter concentrations. *Atmospheric Environment* 55, 377-391.

In the first paper an observation and model study was carried out to investigate the effect of climate change on the concentration of particulate matter in the lower troposphere. The method used in this first paper was to select a synoptic situation in the past which is expected to occur more often in the future and to analyze it in terms of its effect on air quality. An advantage of this approach is the availability of measurements and therefore also the possibility to evaluate state-of-the-art numerical chemistry transport models for such meteorological conditions. Furthermore, the overall ability of the models to simulate the dependency of air quality on meteorological conditions was investigated, as this is important to consider when investigating the impact of climate change on air quality with coupled climate – air quality model systems as it was done in paper II and III.

In this study the summer 2003 was chosen as an example for an extreme summer which is expected to occur more often in the future in Europe. It was characterized by heat waves with high temperature, stagnation and little precipitation over large parts of Europe. In order to investigate whether the meteorological conditions in the summer 2003 had a clear effect on the measured concentration of pollutants, the observations of the EMEP network in Europe of the summer 2003 were compared to the average of the summers of a five year period (2003-2007). The focus was on PM10 and its components (elemental carbon, sea salt, organic matter, secondary inorganic aerosols and secondary organic aerosols). A second important aim of this study was to analyze whether the state-of-the-art chemistry transport models REM/Calgrid and LOTOS-EUROS are able to reproduce the observed concentrations during this episode. Therefore simulation runs were performed with two models for the years 2003-2007. The application of two different chemistry transport models instead of one gives the opportunity to generalize common results or to specify differences.

At stations in Europe, 1-10 $\mu\text{g}/\text{m}^3$ higher PM10 concentrations were measured during the synoptic situation in the summer 2003 compared to the five years average. We could show that high PM10 concentrations are often connected to meteorological conditions characterized by low and high daily maximum temperature. Low horizontal transport, associated with low wind speed, and the absence of wet deposition due to little precipitation connected to conditions with high and low temperature favor the accumulation of pollutants in the lower troposphere leading to increased concentrations. Although these conditions were reflected in the two chemistry transport models, they did not reproduce the extent of the observed increase of concentrations in the low and high temperature range and underestimated also the increase of PM10 concentrations during the summer 2003 at most of the stations. Furthermore both models underestimated the measured total PM10

concentrations and showed substantial difference in their PM10 simulations. We concluded that the underestimation of the variability of PM with meteorology is due to missing but important components and connected emission sources (e.g. secondary organic aerosols, mineral dust, forest fires). To improve the simulation performance of the chemistry transport models as function of meteorology, a better representation of primary components such as dust, elemental carbon and components derived from forest fires as well as the formation of secondary organic aerosols have to be included. Another improvement would be to explicitly relate the emission strengths of the different sectors (e.g. traffic, agriculture) to meteorological variability. These aspects are taken up in paper IV where a study on the temporal profiles for emissions in the chemistry transport model LOTOS-EUROS was done.

3.2 Paper II: The impact of differences in large-scale circulation output from climate models on the regional modeling of ozone and PM

Published: Manders A.M.M., van Meijgaard E., Mues A.C., Kranenburg R., van Ulft L.H., Schaap M., 2012. The impact of differences in large-scale circulation output from climate models on the regional modeling of ozone and PM. *Atmospheric Chemistry and Physics Discussion*, 12, 9441-9458.

In the second paper, a model study was performed with the coupled model system RACMO2 (regional climate model) – LOTOS-EUROS (chemistry transport model) over Europe to investigate the impact of climate change on air quality. To use such a coupled model system is a common approach to study this effect. The regional climate model RACMO2 was used to downscale output from the SRES-A1B constraint transient runs with two GCMs, i.e. ECHAM5 and MIROC-hires. The resulting meteorological fields were then used to force a constant emission run with the chemistry transport model LOTOS-EUROS in a one-way coupled run covering the period 1970–2060 (RLE_ECHAM and RLE_MIROC). Global and regional climate models themselves are subject to considerable uncertainties and have significant biases dependent on the model and region. The focus of the present study is on the impact of these uncertainties and biases on the ozone and PM10 simulation output fields of the chemistry transport model. It also aims to provide more insight into the dependency of the air quality simulation results depending on which climate model is used.

To this end, results from the two climate simulations RLE_ECHAM and RLE_MIROC have been compared with a RACMO2–LOTOS-EUROS (RLE) simulation forced by the ERA-Interim reanalysis (RLE_ERA) for the period 1989–2009 (present-day period). Both RLE_ECHAM and RLE_MIROC showed considerable deviations from RLE_ERA for daily maximum temperature, precipitation and wind speed depending on the region and season. These differences have a substantial impact on the simulated ozone and PM10 concentrations. The differences in average present-day concentrations between the simulations were equal to (RLE_MIROC) or even larger than (RLE_ECHAM) the differences in concentrations between present-day and future climate (2041–2060). The climate simulations agreed on a future increase in average summer ozone daily maximum concentrations of 5–10 $\mu\text{g}/\text{m}^3$ in parts of Southern Europe and a smaller increase in Western and Central Europe. Overall, changes for total PM10 were small, both positive and negative changes were found, and for many locations the two climate runs did not agree on the sign of the change. This illustrates that results from individual climate runs can at best indicate tendencies and should therefore be interpreted with great care.

3.3 Paper III: Differences in particulate matter concentrations between urban and rural regions under current and changing climate conditions

Submitted to Atmospheric Environment in November 2012: A. Mues, A. Manders, M. Schaap, L.H. van Ulft, E. van Meijgaard, P. Builtjes. Differences in particulate matter concentrations between urban and rural regions under current and changing climate conditions.

In the third paper an observation and model study was carried out on the differences in air quality between urban areas and their surrounding rural regions under current and changing climate conditions. Pollution levels in urban areas and their surrounding rural regions differ due to different sources and density of emissions, different composition of pollutants as well as specific meteorological effects. These concentration differences for PM10, here defined as the urban increment, are investigated and compared in this study for three different north-west European urban agglomerations: The German Ruhr area, the Dutch Randstad and the German city of Berlin. Measurement data for PM10 for the years 2003-2008 at urban and rural background stations are selected from the AirBase database to quantify the PM10 concentration difference between these urban areas and their surrounding rural regions. The measured urban increment averaged over 2003-2008 is found to be $7.4\mu\text{g}/\text{m}^3$ for the Ruhr area, $3.1\mu\text{g}/\text{m}^3$ for the Randstad and $8.5\mu\text{g}/\text{m}^3$ for Berlin. To analyze whether the regional chemistry transport model LOTOS-EUROS is able to reproduce the measured urban increment simulation runs were performed for 2003-2008 on a $0.5^\circ \times 0.25^\circ$ lon-lat grid covering Europe and for the year 2008 on a finer grid of $0.125^\circ \times 0.0625^\circ$ covering the Netherlands and Germany, both with ECMWF meteorology as input. Although the model underestimates the absolute PM10 urban increment for the three areas, the relative concentration difference between urban and rural region for the Ruhr area and the Randstad is in general agreement with the measurements. The tested increase of the horizontal resolution gives no systematic improvement of the simulated urban increment. However, an even higher resolution than used here seems to be more appropriate to capture the urban increment (especially for Berlin). Nevertheless, model results could be used to interpret the measured increments.

The PM10 urban increment under changing climate conditions is studied using the approach introduced in the paper I (summer 2003) and by means of the RACMO2 – LOTOS-EUROS simulations introduced in paper II. Measured and simulated PM10 concentrations in summer 2003 were compared to the summer average of 2003-2008. The size and sign of the urban increment in the summer 2003 was found to depend on the urban area. In general the model reproduces the main features for this episode for the Randstad and Berlin. Simulated concentrations differ between the runs using ECHAM5 and MIROC-hires boundary conditions and both runs differ from the present-day simulations with ERA-interim forcing. The impact of climate change on the modeled PM10 concentrations and the urban increment was found to be small in both scenario runs. In contrast to the study in paper II the individual PM10 components were also looked at and the investigation showed only small differences between the result for the present-day and future climate period. However the concentration differences between the simulations forced by either ECHAM5 and MIROC-hires indicate that PM10 concentration levels are sensitive to circulation patterns rather than temperature change alone, and that PM10 concentration levels may thus change when circulation patterns change in the future. One has to keep in mind that expected changes in emissions and emission locations probably also heavily affect total PM10 concentrations and the urban increment.

3.4 Paper IV: Sensitivity of air pollution simulations with LOTOS-EUROS to temporal distribution of emissions

To be submitted to Atmospheric Chemistry and Physics: A. Mues, C. Hendriks, J. Kuenen, A. Manders, A. Segers, Y. Scholz, C. Hueglin, P. Builtjes, M. Schaap. Sensitivity of air pollution simulations with LOTOS-EUROS to temporal distribution of emissions.

In the fourth paper a model study with LOTOS-EUROS was carried out to investigate sensitivity of the model performance to the description of the temporal variability of emissions. Since the early nineties the handling of the temporal variability of anthropogenic emissions in chemistry transport models has not received much attention. For most of the emission sectors annual average emission totals per country are distributed across the domain and combined with average time profiles per sector to arrive at an emission at every point in time. In reality, the temporal distribution of emissions vary with activity patterns, region, species, emission process and meteorology. These are currently neglected but may be important as atmospheric conditions during release and transport impact the fate of the emitted air pollutants. The importance to consider this in more detail has been highlighted in the outcome of the first paper. The three sources dealt with in this study are combustion in energy and transformation industries (SNAP1), non-industrial combustion (SNAP2) and road transport (SNAP7). First the impact of neglecting the temporal emission profiles for these SNAP categories on simulated concentrations were explored. In a second step we constructed more detailed emission time profiles for the three categories and tested them in model simulations using each new profile separately and all three profiles simultaneously in one simulation. The results were compared for the pollutants NO₂, SO₂ and PM10 to measurements and to a simulation using the default LOTOS-EUROS emission time profiles.

In contrast to the default LOTOS-EUROS time profiles for SNAP1, the new profiles are country specific. The profiles are based on the timing of electricity production from fossil fuels which is made a function of the hourly availability of renewable electricity based on meteorological conditions. The new SNAP2 profiles are based on the concept of heating degree days which is a measure designed to reflect the demand for energy needed to heat a building. In contrast to the default profiles this method takes into account the actual daily mean temperature per grid cell and is therefore location specific. So far, the default time profiles for SNAP7 do not take the temporal release of emissions from road transport based on the driving behavior as a function of location, vehicle type and street type into account. To take this into account in more detail traffic count data for Light Duty Vehicles (LDV) and Heavy Duty Vehicles (HDV) at highway and urban street stations in Germany were used to construct new profiles. Pollutant dependent (here NOx) emission split factors were used to specify the fraction of emission per vehicle and street type for Germany.

In general the largest impact on the model performance was found when neglecting the default time profiles for the three categories. The daily average correlation coefficient for instance decreased by 0.04 (NO₂), 0.11 (SO₂) and 0.01 (PM10) at German urban background stations compared to the default simulation. A systematic increase of the correlation coefficient is found when using the new time profiles. The size of the increase depends on the source category, the component and station. Using national profiles for traffic showed important improvements of the explained variability over the weekdays as well as the diurnal cycle for NO₂. The largest impact of the SNAP1 and 2 profiles were found for SO₂. When using all new time profiles simultaneously in one simulation the daily average correlation coefficient increased by 0.05 (NO₂), 0.07 (SO₂) and 0.03

(PM10) at urban background stations in Germany. This exercise showed that the model is sensitive to changes in the temporal distribution of emissions and that more detailed emission time profiles lead to a systematically increase in the model performance. It also recommends to further work on enhanced and more detailed emission time profiles in the model.

4 Overall discussion and conclusions

Two different approaches have been used in this study to investigate the impact of a changing climate on particulate matter concentrations over Europe and on the PM10 urban increment of three different north-west European urban agglomerations. In the first approach measured and simulated PM10 concentrations of the extreme summer 2003 which was chosen as an example for a summer expected to occur more frequently in the future, were compared to an average summer over five years (2003-2007). To this end, model simulations for the time period of 2003-2007 have been performed on the European domain with the two different chemistry transport models LOTOS-EUROS and REM/Calgrid. For the second approach two long-term climate simulations have been performed with the one-way coupled model system RACMO2-LOTOS-EUROS, using meteorological boundary conditions from two different GCMs (ECHAM5 and MIROC3.2-hires) and the SERS-A1B. The two GCMs differ in terms of their representation of the general circulation patterns for present-day conditions. In addition, a 21-yr present-day simulation was performed using boundary conditions from reanalysis meteorology (ERA-interim) which serves as a reference for the present-day climate and air quality simulated by the two climate simulations. In the LOTOS-EUROS simulations no future emission scenario is considered. The results of the two long-term simulations were used to compute the difference in meteorology and air quality between a present-day (1989-2009) and a future climate period (2041-2060). Furthermore the sensitivity of the model performance of LOTOS-EUROS to the description of the temporal variability of emissions was investigated for the three SNAP categories 'combustion in energy and transformation industries' (SNAP1), 'non-industrial combustion' (SNAP2) and 'road transport' (SNAP7).

The advantages of the first approach are that the effect can be directly analyzed using measurements and that an evaluation of the chemistry transport model performance as function of meteorology with measurements is possible. In contrast to this approach, which only considers one specific synoptic situation, one-way coupled model systems consisting of a regional chemistry transport model forced by a regional climate model give the opportunity to take into account the variability of future climate.

PM10 concentrations in Europe may be affected by climate change, as indicated by the observed differences in PM10 concentrations between the extreme summer of 2003 and the summer average from 2003 to 2007. At rural stations in Europe 1-10 $\mu\text{g}/\text{m}^3$ higher PM10 concentration were measured in summer 2003. The stagnant weather conditions in this summer, characterized by high temperature, low wind speed and little precipitation, favored the increase of PM10 concentrations. It is well known that low horizontal transport and the virtual absence of wet deposition favor the accumulation of pollutants in the lower troposphere. Additionally, natural and anthropogenic emissions of PM10 components and precursors were concluded to increase during conditions represented by high temperatures (e.g. in summer 2003) as a consequence of the weather situation and thus contribute to higher PM concentrations. Examples are more efficient secondary organic aerosols formation due to enhanced photochemistry, increased potential of windblown dust emission due to dry soil, and the contribution of emission from wild fires. A possible increase of anthropogenic emissions could be attributed to enhanced road dust emission, higher energy demand due to air conditioning and cooling systems or barbecuing, for example. The respond of the secondary inorganic aerosols on meteorology depends on the component and location. Whereas sulphate was found to increase during conditions connected to high temperature, the respond of

nitrate and ammonium depends on the station which can be explained by the formation of the secondary inorganic aerosols and the availability of ammonia in a region.

The urban increment of the three selected regions, the Ruhr area, the Randstad and Berlin, differs per urban region which is mainly due to different rural background concentrations. Whereas the urban levels are similar, significantly smaller urban increments are observed for the Randstad ($3.1 \mu\text{g}/\text{m}^3$) than for the Ruhr area ($7.4 \mu\text{g}/\text{m}^3$) and Berlin ($8.5 \mu\text{g}/\text{m}^3$). A major part of the differences between the urban increments can be explained by the structure of land use and the related emission sources in the rural regions. The respond of the urban increment on the weather situation in the summer 2003 dependents on the region. For the Ruhr area and the Randstad the measured increase of the PM10 concentrations were found to be stronger at rural than at urban stations leading to a decreased or even negative urban increment, whereas this is the other way around for Berlin.

The simulated difference in meteorology between future and present-day climate in Europe in the second approach is mainly a considerable increase in temperature, whereas the circulation pattern, rain and wind show only a modest change. The climate simulations agreed on a future increase in averaged summer ozone daily maximum concentrations in Europe. The impact of climate change on the modeled PM10 concentrations and the urban increment was found to be small in both scenario runs ($\pm 4\%$), even at the component level. Both positive and negative changes were found, and for many locations the two climate runs did not agree on the sign of the changes. However, the concentration differences between the simulations forced by either ECHAM5 or MIROC-hires indicate that PM10 concentration levels are sensitive to circulation patterns rather than temperature change alone, and that PM10 concentration levels may thus change when circulation patterns change in future.

Another focus of this study was on the strengths and weaknesses of the model systems used in the two approaches in the context of the here discussed issue. This includes the performance of chemistry transport models as a function of meteorology, the meteorological input for the chemistry transport model delivered by the regional climate model and the handling of emissions in the chemistry transport models. The investigation of the impact of climate change on air quality with a numerical model system requires a good description of the processes related to meteorology in the chemistry transport model. Thus the ability of chemistry transport models to simulate particulate matter as a function of meteorology is investigated using the summer 2003 as a test case. One important outcome is that both chemistry transport models (LOTOS-EUROS and REM/Calgrid) failed to fully reproduce the increase of measured particulate matter concentrations during conditions with very low and high daily maximum temperature. The summer 2003 example showed that although the meteorological conditions were found to be reproduced in the meteorological input data (ECMWF, Tramper) of the two models, both models underestimated the extent of the observed increase at most of the stations. However, the observed variability of secondary inorganic aerosols, which accounts for a high fraction of simulated PM10 concentrations, with temperature was reproduced well by the models, indicating that the dependency of the chemistry on meteorology is represented in the models. But sources and formation of important components for such meteorological conditions as mentioned above (e.g. SOA, windblown dust) are still poorly understood and therefore not well represented in the emission database and models or not included at all. Together with the fact that in both models a dependency of anthropogenic emissions on meteorology is not considered, this leads to an underestimation of concentrations during weather conditions as observed in the summer 2003. The importance to improve the description of the

temporal distribution of emission in the chemistry transport model and to also consider its dependency on meteorology is indicated by the enhanced model performance found when more detailed emission time profiles are included in the LOTOS-EUROS model. As an example, an increase of the correlation coefficient is found for sulphur dioxide when emissions from household heating (SNAP2) were explicitly related to daily mean temperature. Thus, this is relevant to consider in climate studies also because climate change itself may affect the emission strength of natural and anthropogenic sources. An example is a change of fossil fuel combustion emission as a result of an intensified demand of air conditioning induced by higher temperature in summer on the one hand and a reduced demand of heating due to milder winters on the other hand.

It is important information how well urban areas are represented in regional models because long-term simulations with detailed urban scale models are still too time-consuming in terms of computation time. LOTOS-EUROS underestimated the absolute PM10 concentrations but was able to reproduce the relative urban increment for the Ruhr area and the Randstad and could be used to interpret the observe difference between the regions, despite the fact that the urban scale was not resolved. Nevertheless, a better representation of the meteorological characteristics of urban areas in regional chemistry transport models is required, especially for isolated cities like Berlin. The presented results indicate that regional scale-modeling is a useful tool in assessing air quality differences and resolves part of the urban increment. Such simulations can for example be used as boundary conditions for more detailed and more computationally intensive models assessing cities at higher resolution, using local bottom-up emission inventories and local-scale meteorology.

The results of studies using a climate – air quality model system depend amongst others on the quality of the meteorological input fields derived from the regional climate model as biases may impact the results of the chemistry transport model. The meteorological parameters from both climate simulations (RLE_ECHAM and RLE_MIROC) differ considerably from those of the reanalysis-driven simulation (RLE_ERA) for the present-day climate period, depending on the season and region. These differences have a substantial impact on the simulated ozone and PM10 concentrations and also affects the results for the urban increment. For the RLE_ECHAM run, differences in modeled PM10 concentrations between future and present-day climate are mainly smaller than the differences in present-day climate between RLE_ECHAM and RLE_ERA. In the RLE_MIROC simulation, the differences between future and present-day climate are of the same order of magnitude as the present-day differences between the simulations of RLE_MIROC and RLE_ERA.

Both model approaches presented in this study are useful tools to investigate the impact of a changing climate on particulate matter concentrations but due to considerable weaknesses in the model systems a qualitative rather than a quantitative interpretation of the simulation results is recommendable.

5 Outlook

For assessing the impact of climate change on air quality with climate – air quality model systems increased confidence in the model performance regarding this effect is required. This holds for both the climate and the chemistry transport model simulations. A good description of particulate matter as function of meteorology in chemistry transport models remains challenging. The relation between the emissions of particulate matter and also the formation of secondary particulate matter components with meteorology needs to be better understood. To improve the simulation performance of the two chemistry transport models REM/Calgrid and LOTOS-EUROS as function of meteorological conditions, a better representation of the emissions of primary components like dust, elemental carbon and from wild fire derived components as well as the formation of secondary organic aerosols have to be included. A further improvement would be to explicitly relate emission strengths of the different sectors to the meteorological variability. The inability of the particulate matter concentrations calculated by the chemistry transport models to correctly respond to meteorological changes may also partly explain the small and very uncertain responds of particulate matter to anticipated climate change in the model studies. Hence, these improvements are important to come to reliable results in climate scenario studies implying coupled climate – air quality model systems.

To relate the temporal release of emissions to meteorology is also relevant because climate change itself may affect the emission strength of both natural and anthropogenic sources. Increased aridity may enhance mineral dust emission through resuspension and wind erosion and also wild fires may become more frequent in the future. Moreover emission from fossil fuel combustion could change, as a result of for example an intensified demand of air conditioning induced by higher temperature in summer on the one hand and a reduced demand of heating due to milder winters on the other hand. Finally, a possible shift to biomass as a source of energy may enhance wood burning emission as well as secondary organic aerosols formation as a consequence of large scale land use changes. Hence climate change may indirectly affect particulate matter levels through feedback on emissions, which needs further research. Beyond that, anthropogenic emissions are anticipated to reduce in Europe due to stringent national and community legislation on emission controls. Anthropogenic emission of particulate matter and its precursor are expected to decline in Europe by approximately 40-45% between 2000 and 2020 (Cofala et al., 2006; EEA, 2007). These downward trends are expected to continue after 2020. This is neglected in the simulations in this study as anthropogenic emissions have been kept constant in the LOTOS-EUROS simulations. In order to assess the impact of the emission reduction on future PM levels in contrast to the impact of climate change, also emission scenarios should be taken into account in the chemistry transport model simulations. In this context long-term evaluation studies of chemistry transport model will help to assess the models ability to reproduce trends in pollutant concentrations both due to meteorology and emission variability. Furthermore, a change of land use and land cover may affect future air quality which has not been taken into account in this study either. Changes in land use and land cover would impact the deposition efficiency and the strength and composition of specific emissions and small scale thermal and dynamical processes affecting the dilution of pollution. This could be especially relevant when investigating specific regions. However, the size of this effect is still uncertain and might be comparably small. In the current study only one emission scenario (A1B) was used for the climate simulations, whereas using different emission scenarios would represent a broader bandwidth of possible future climate scenarios and thus also of the impact on air quality.

A general issue is the coupling of the global and the regional scale in the models. For climate studies dynamically downscaling of output from global climate models with regional climate models to better resolve regional patterns is necessary but maintaining consistency between GCM and RCM physics is still challenging. A proper representation of the global scale is also important for air quality simulations to describe the changes in background concentrations and inter-continental transport processes which are considered by using the output of a global model as boundary conditions for the regional chemistry transport model.

A multi-model approach can be used to get more confidence in results of climate - air quality studies by highlighting consistent results between model simulations with different models (GCM, RCM and CTM) but the same set-up (e.g. emissions, SRES). But this is only limitedly applicable as some uncertainties and errors are common to all models.

Beyond the scope of this study but an important issue for climate and air quality interactions are feedback processes between concentrations of chemical species and the ration budget of the atmosphere. To investigate this the use of online-coupled climate - air quality model systems is needed. A two-way coupling approach with relatively modest computational demands is currently being realized in the RACMO2 – LOTOS-EUROS system.

The model performance of the LOTOS-EUROS was found to be sensitive to improved temporal emission information. Thus to improve the model performance in view of the temporal variability of simulated pollutant concentration a better representation of the temporal release of anthropogenic emission in chemistry transport models by developing a dynamical emission module taking into account regional specific factors and meteorology is recommendable. This should also be extended to SNAP emission source categories which have not been tested in this study, an important example is agriculture which is very variable with location and meteorology.

Urban areas are not explicitly resolved in regional chemistry transport models which therefore do not take into account small scale features associated to the structure of a built-up area. Examples are the impact of roughness on the vertical mixing and deposition of pollutants as well as the impact of the urban cover on thermal and radiative properties of the surface which can lead to a large temperature gradient between the city and its surroundings resulting in an urban heat island. So far the urban characteristics are taken into account only by a high emission density and the roughness length, affecting dry deposition velocities. In order to enhance the representation of urban areas in regional chemistry transport models a more detailed description of the emission distribution and small scale meteorological features should be taken into account. For example by using a bottom-up instead of a top-down approach to assess the emissions in urban areas. Another possibility is to embed the output of a high resolution simulation for urban areas in a lower resolution run with a regional model, a third option is to use a more detailed parameterization of the urban structure (e.g. buildings) in the model.

Finally, both air quality and climate change receive a special interest in research and politics. So far the development and implementation of policies to prevent air pollution and to minimize the negative effect of climate changes have been established to a large extent independently, but there is an increasing awareness in policy and science of the many linkages between air pollution and climate changes. The air quality report of the European Environmental Agency (EEA, 2012) stated explicitly that this needs further attention: “Greater international cooperation, also focusing on links between climate and air pollution policies, is required more than ever to address air pollution.”.

6 Summary and Zusammenfassung

6.1 Summary

Air quality is strongly dependent on meteorology and thus is sensitive to climate change. In order to study the impact of a changing climate on particulate matter concentration over Europe and on the PM10 urban increment of three north-west European urban agglomerations (Ruhr area, Randstad and Berlin) two different model approaches have been used in this study. A second focus was on the strengths and weaknesses in this context of the model systems used in the approaches. The first approach was to analyze a synoptic situation in the past which is expected to occur more often in future, here the extreme situation in the summer 2003, in terms of its effect on the concentration of PM10 and its components. To this end measurements and model simulations with the chemistry transport models LOTOS-EUROS and REM/Calgrid of the summer 2003 were compared to the summer of a five years period (2003-2007). The second approach was to use the off-line coupled model system RACMO2 (regional climate model) – LOTOS-EUROS (air quality model) over Europe. Different sets of simulations were carried out using RACMO2 meteorology with ECHAM5 A1B and with MIROC-hires A1B boundary conditions for the time period 1970-2060, as well as with ERA-interim boundary conditions for the time period 1989-2009. In a third study the sensitivity of the model performance of the LOTOS-EUROS model to the description of the temporal variability of emissions with more detailed emission time profiles for the three source categories “combustion in energy and transformation industries” (SNAP1), “non-industrial combustion” (SNAP2) and “road transport” (SNAP7) were tested.

The synoptic situation in the summer 2003 resulted in higher observed PM10 concentrations compared to the five years average. Because the size of this increase differs per urban and rural station, the impact on the urban increment were found to differ in size and sign per urban region. Both chemistry transport models underestimated the variability of PM10 concentrations with meteorology. Low horizontal transport and the absence of wet deposition associated with conditions with high temperatures favor the accumulation of pollutants. Although these conditions are reflected in the meteorological input data, the chemistry transport models underestimated the extent of the observed increased PM10 concentration in summer 2003. Specific sources and formation of important components for such meteorological conditions (e.g. mineral dust, secondary organic aerosols, wild fire, energy consumption, road dust) are either not well represented or not included in the emission database and models. Furthermore, a dependency of anthropogenic emission on meteorology is not considered in the models but may enhance the model performance in this case. This is indicated by the sensitivity study because an increased correlation coefficient for sulphur dioxide was achieved when emissions from household heating (SNAP2) were explicitly related to the daily mean temperature. Improving the description of the temporal variation of the three considered SNAP codes in model leads to improved correlation coefficients also for nitrogen dioxide and PM.

The impact of climate change on the simulated PM10 concentrations and the urban increment was found to be small in both scenario runs performed with the RACMO2 – LOTOS-EUROS model system, even at the component level. Both positive and negative changes were found and for many locations the two climate runs did not agree on the sign of the changes. The meteorological parameters from both RACMO2 climate simulations differ considerably from those of the reanalysis-

driven simulation for the present-day climate period, depending on the season and region. These differences have a substantial impact on the simulated PM10 concentrations and also affects the urban increment.

Both model approaches presented in this study are useful tools to investigate the impact of a changing climate on particulate matter concentrations but due to considerable weaknesses in the model systems a qualitative rather than a quantitative interpretation of the simulation results is recommendable. An important point to enhance the model performance of the chemistry transport models as a function of meteorology is to include further emission sources and the formation of secondary organic aerosol and a better representation of the temporal distribution of anthropogenic emission by developing a dynamical emission model taking into account regional specific factors and meteorology is recommendable.

6.2 Zusammenfassung

Die Luftqualität einer Region wird zu einem hohen Maße von der Emissionsstärke von Schadstoffen und der Meteorologie bestimmt. Auf Grund dieses Zusammenhangs hat auch ein sich änderndes Klima Einfluss auf die Luftqualität. In dieser Arbeit wurden zwei verschiedene Ansätze verwendet, um den Einfluss des sich ändernden Klimas auf die Feinstaubkonzentration in Europa und auf den PM10 Konzentrationsunterschied zwischen drei nord-west europäischen urbanen Agglomerationen und deren ländlichen Umgebungen (Stadt-Land Konzentrationsdifferenz) zu untersuchen. In einer ersten Studie wurde der Effekt der meteorologischen Bedingungen während einer synoptischen Situation aus der Vergangenheit, deren Auftreten in der Zukunft häufiger erwartet wird, auf die Luftqualität untersucht. Dafür wurden gemessene und mit den zwei Chemie-Transportmodellen LOTOS-EUROS und REM/Calgrid simulierte PM10 Konzentrationen des extremen Sommers 2003 mit dem Sommermittel einer Fünfjahresperiode (2003-2008) verglichen. In einer zweiten Studie wurden Langzeitsimulationen mit dem off-line gekoppelten Modellsystem RACMO2 (regional Klimamodelle) – LOTOS-EUROS (Chemie-Transportmodell) durchgeführt. Dazu wurden zwei verschiedene Klimasimulationen mit den Globalmodellen ECHAM5 und MIROC-hires (mit SRES-A1B) (1970-2060) sowie ERA-Interim Daten (1989-2009) als Randbedingungen für das RACMO2 verwendet. Um die Sensitivität des LOTOS-EUROS gegenüber der zeitlichen Beschreibung von Emissionen zu untersuchen, wurden in einer dritten Studie neue und detailliertere Emissionszeitprofile für drei Emissionskategorien (combustion in energy and transformation industries (SNAP1), non-industrial combustion (SNAP2), road transport (SNAP7)) im Modell implementiert und getestet.

Für den Sommer 2003 wurden im Vergleich zu dem Fünfjahres-Sommermittel verbreitet erhöhte PM10 Konzentrationen an Stationen in Europa gemessen. Da die Stärke dieses Anstieges pro Gebiet in urbanen und ländlichen Hintergrundstationen unterschiedlich ist, variiert auch der Einfluss auf den Konzentrationsunterschied für die drei untersuchten urbanen Gebiete in Höhe und Vorzeichen. Die beiden Chemie-Transportmodelle unterschätzen für PM10 den Anteil an Variabilität, der durch meteorologische Einflüsse verursacht wird. Die Wettersituation im Sommer 2003, charakterisiert durch hohe Temperaturen, geringe Niederschläge und niedrige Windgeschwindigkeiten begünstigt die Akkumulation von Luftschatstoffen. Obwohl diese Bedingungen in den meteorologischen Eingangsfeldern der beiden Modelle repräsentiert sind, unterschätzen beide Modelle den gemessenen PM10 Anstieg im Sommer 2003. Einige für diese Wettersituation wichtige

Emissionsquellen und PM10 Komponenten (z.B. sekundäre organische Aerosole, Waldbrände, erhöhter Energieverbrauch) sind in den Emissionsdatenbasen und Modellen nicht ausreichend gut beschrieben oder nicht berücksichtigt. Des Weiteren ist eine Abhängigkeit der anthropogenen Emissionen von der Meteorologie nicht berücksichtigt. Dies könnte jedoch auch in dem hier betrachteten Kontext zu einer höheren Modellgüte führen. Darauf weisen auch die Ergebnisse einer Sensitivitätsstudie hin, in welcher z.B. höhere Korrelationskoeffizienten für Schwefeldioxid gefunden wurden, wenn die Emissionen von Hausbrand explizit als Funktion der Tagesmitteltemperatur berechnet werden. Eine verbesserte Beschreibung der Emissionszeitprofile der drei SNAP Kategorien 1, 2 und 7 führt ebenfalls zu höheren Korrelationskoeffizienten für Stickstoffdioxid und PM.

Die Auswirkungen von Klimaänderung auf die Konzentration von PM10 und dessen Komponenten und auf die Stadt-Land Konzentrationsdifferenz ist in beiden, mit dem RACMO2 – LOTOS-EUROS Modellsystem durchgeführten, Szenario-Läufen gering. Es wurden sowohl positive als auch negative Abweichungen gefunden und für viele Gebiete weisen die Abweichungen der beiden Klimaläufe unterschiedliche Vorzeichen auf. Abhängig von der Jahreszeit und der Region unterscheiden sich die meteorologischen Parameter der beiden RACMO2-Klimasimulationen von der RACMO2 – ERA-Interim Simulation. Dies hat einen erheblichen Einfluss auf die simulierten PM10 Konzentrationen und den Stadt-Land Konzentrationsunterschied.

Beide hier verwendeten Modellansätze sind eine gute Methode um den Einfluss von Klimaänderung auf Feinstaubkonzentrationen zu untersuchen. Allerdings weisen die verwendeten Modelle (Klimamodelle, Chemie-Transportmodelle) beträchtliche Schwächen in diesem Kontext auf. Daher ist eine qualitative anstatt einer quantitativen Interpretation der Modellergebnisse empfehlenswert. Möglichkeiten den Einfluss meteorologischer Variabilität auf die Schadstoffkonzentrationen im Chemie-Transportmodell zu verbessern sind weiter relevante Emissionsquellen und die Bildung von sekundären organischen Aerosolen im Modell zu berücksichtigen sowie eine verbesserte Beschreibung der zeitlichen Verteilung von anthropogenen Emissionen im Modell zu implementieren.

References

- Banzhaf S., Schaap M., Kerschbaumer A., Reimer E., Stern R., van der Swaluw E., Builtjes P., 2012. Implementation and evaluation of pH-dependent cloud chemistry and wet deposition in the chemical transport model REM-Calgrid. *Atmospheric Environment* 49, 378-390.
- Beekmann M., Kerschbaumer A., Reimer E., Stern R., Möller D., 2007. PM10 measurement campaign HOVERT in the Greater Berlin area: model evaluation with chemically specified particulate matter observations for a one year period. *Atmospheric Chemistry and Physics* 7, 55-68.
- Builtjes P.J.H., van Loon M., Schaap M., Teeuwisse S., Visschedijk A.J.H., Bloos J.P., 2003. Project on the modelling and verification of ozone reduction strategies: contribution of TNO-MEP. TNO-report, MEP-R2003/166, Apeldoorn, The Netherlands.
- Christensen J.H. and Christensen O.B., 2007. A summary of the PRUDENCE model projections of changes in European climate by the end of this century, *Climate Change*, 81, 7–30.
- Claiborn C., Lamb B., Miller A., Beseda B., Clode B., Vaughan J., Kang L., Newvine C., 1998. Regional measurements and modeling of windblown agricultural dust: The Columbia Plateau PM10 program. *J.G.R. VOL 103, D16*, 19753-19767.
- Cofala J., Klimont Z., Amann M., 2006. The potential for further control of emissions of fine particulate matter in Europe. IIASA Intermin Report IR-06-011.
- Denier van der Gon H.A.C., Visschedijk A., van den Brugh H., Dröge R., 2010. F&E Vorhaben: "Strategien zur Verminderung der Feinstaubbelastung" e PAREST: A high resolution European emission data base for the year 2005. TNO-Report, TNO-034-UT-2010-01895_RPT-ML, Utrecht.
- EEA, 2000. CORINE Land Cover 2000: dataservice.eea.eu.int.
- EEA, 2007. Europe's Environment. The Fourth Assessment. EEA, Copenhagen.
- EEA, 2012. Air quality in Europe — 2012 report. European Environmental Agency report No 4/2012, doi:10.2800/55823.
- Eeftens M. et al., 2012. Development of Land Use Regression Models for PM2.5, PM2.5 Absorbance, PM10 and PMcoarse in 20 European Study Areas; Results of the ESCAPE Project. *Environmental Science & Technology*, 46 (20), pp 11195-11205.
- Erisman J.W., van Pul A., Wyers P., 1994. Parametrization of surface-resistance for the quantification of atmospheric deposition of acidifying pollutants and ozone, *Atmos. Environ.*, 28, 2595–2607.
- EU, 2008. Directive 2008/50/EC of the European Parliament and of the Council on ambient air quality and cleaner air for Europe.
- Forkel R. and Knoche R, 2006. Regional climate change and its impact on photooxidant concentrations in southern Germany: Simulations with a coupled regional climate-chemistry model. *Journal of Geophysical Research*, 111, D12302.
- Fountoukis C. and Nenes A., 2007. ISORROPIA II: A Computationally Efficient Aerosol Thermodynamic Equilibrium Model for K^+ , Ca^{2+} , Mg^{2+} , NH_4^+ , Na^+ , SO_4^{2-} , NO_3^- , Cl^- , H_2O Aerosols. *Atmospheric Chemistry and Physics* 7, 4639-4659.

Gipson G. and Young J., 1999. Gas-phase chemistry. Chapter 8 in SCIENCE ALGORITHMS OF THE EPA MODELS-3 COMMUNITY MULTISCALE AIR QUALITY (CMAQ) MODELING SYSTEM Edited by: D. W. BYUN and J. K. S. CHING. Atmospheric Modeling Division National Exposure Research Laboratory U.S. Environmental Protection Agency Research Triangle Park, NC 27711, EPA/600/R-99/030.

Guenther A.B., Zimmerman P.R., Harley P.C., Monson R.K., Fall R., 1993. Isoprene and monoterpene emission rate variability: model evaluations and sensitivity analyses. *J. Geophys. Res.*, 98, 12609-12617, 1993.

IPCC, 2007. Climate change 2007: Synthesis Report.

Jacob D., Barring L., Christensen O.B., Christensen J.H., de Castro M., Deque M., Giorgi F., Hagemann S., Hirschi M., Jones R., Kjellstrom E., Lenderink G., Rockel B., Sanches E., Schar C., Seneviratne S.I., Somot S., van Ulden A., Van den Hurk B., 2007. An inter-comparison of regional climate models for Europe: model performance in present-day climate, *Climatic Change*, 81, 31–52.

Jacob D.J. and Winner D.A., 2009. Effect of climate change on air quality. *Atmospheric Environment* 43, 51-63.

Jungclaus J.H., Botzet M., Haak H., Keenlyside N., Luo J.J., Latif M., Marotzke J., Mikolajewicz U., Roeckner E., 2006: Ocean circulation and tropical variability in the AOGCM ECHAM5/MPI-OM, *J. Climate*, 19, 3952–3972.

K-1 Model Developers: K-1 Coupled Model (MIROC) Description, K-1 Technical Report 1, 2004. edited by: Hasumi, H. and Emori, S., Center for Climate System Research, University of Tokyo, Tokyo, Japan, 34 pp., available at: <http://www.ccsr.u-tokyo.ac.jp/kyosei/hasumi/MIROC/tech-repo.pdf>.

Kuenen J., Denier van der Gon H., Visschedijk A., van der Brugh H., van Gijlswijk R., 2011. MACC European emission inventory for the years 2003-2007. TNO report, TNO-060-UT-2011-00588, Utrecht.

Lenderink G., Van den Hurk B., Van Meijgaard E., Van Ulden A. P., Cuijpers J., 2003. Simulation of present-day climate in RACMO2: first results and model developments, KNMI technical report TR 252.

Loosmore and Hunt, 2000. Dust resuspension without saltation (2000). *J. Geophys. Res.* Vol 105, D16, 20,663 ff, August 27, 2000.

Monahan E.C., Speil D., Speil K., 1986. *Oceanic Whitecaps*. Reidel.

Nenes A., Pandis S.N., Pilinis C., 1998. ISORROPIA: a new thermodynamic equilibrium model for multiphase multicomponent inorganic aerosols. *Aquatic Geochemistry* 4, 123-152.

Reimer E. and Scherer B., 1992. An operational meteorological diagnostic system for regional air pollution analysis and long-term modeling. *Air Poll. Modelling and its Applications IX* (1992). Plenum Press.

Roeckner E., Bäuml G., Bonaventura L., Brokopf R., Esch M., Giorgetta M., Hagemann S., Kirchner I., Kornblueh L., Manzini E., Rhodin A., Schlese U., Schulzweida U., Tompkins A., 2003. The Atmospheric General Circulation Model ECHAM5, Part I: Model Description, MPI Report 349, Max Planck Institute for Meteorology, Hamburg, Germany, 127 pp.

Schaap M., Weijers E.P., Mooibroek D., Nguyen L., Hoogerbrugge R., 2010. Composition and origin of Particulate Matter in the Netherlands. Results from the Dutch Research Programme on Particulate Matter. Publication of the Netherlands Research Program on Particulate Matter Report 5000099007/2010.

Schaap M., Timmermans R.M.A., Sauter F.J., Roemer M., Velders G.J.M., Boersen G.A.C., Beck J.P., Builtes P.J.H., 2008. The LOTOS-EUROS model: description, validation and latest developments. International Journal of Environment and Pollution 32 (2), 270-289.

Schaap M., Roemer M., Sauter F., Boersen G., Timmermans R., Builtes P.J.H., 2005. LOTOS-EUROS Documentation, TNO Report B&O 2005/297, TNO, Apeldoorn, The Netherlands.

Schaap M., Denier Van Der Gon H.A.C., Dentener F.J., Visschedijk A.J.H., van Loon M., ten Brink H.M., Putaud J.-P., Guillaume B., Liousse C., Builtes P.J.H., 2004. Anthropogenic black carbon and fine aerosol distribution over Europe. Journal of Geophysical Research 109, D18201.

Schell B., Ackermann I. J., Hass H., Binkowski F. S., Ebel A., 2001. Modeling the formation of secondary organic aerosol within a comprehensive air quality model system, J. Geophys. Res., 106, 28275-28293.

Seinfeld J.H. and Pandis S.N., 1998. Atmospheric Chemistry and Physics: From Air Pollution to Climate Change. Wiley-Interscience, John Wiley & Sons, Inc.

Snel A., 2004. Improving of classifications European monitoring stations for AirBase. A quality control. ETC/ACC Technical Paper 2004/7. European Topic Centre on Air and Climate Change.

Stern R., Yamartino R., Graff A., 2006. Analyzing the response of a chemical transport model to emissions reductions utilizing various grid resolutions. Twenty-eighth ITM on Air Pollution Modelling and its Application, May 15 - 19 2006, Leipzig, Germany.

Stern R., Builtes P.J.H., Schaap M., Timmermans R., Vautard R., Hodzic A., Memmesheimer M., Feldmann H., Renner E., Wolke R., Kerschabumer A., 2008. A model inter-comparison study focusing on episodes with elevated PM10 concentrations. Atmospheric Environment 42. 4567-4588.

Stull R., 1988. An Introduction to Boundary Layer Meteorology. Atmospheric Science Library, Kluwer Academic Publisher.

Tai A.P.K., Mickley L.J., Jacob D.J., Leibensperger E.M., Zhang L., Fisher J.A., Pye H.O.T., 2012. Meteorological modes of variability for fine particulate matter (PM2.5) air quality in the United States: implications for PM2.5 sensitivity to climate change. Atmos. Chem. Phys., 12, 3131–3145.

Tørseth K., Aas W., Breivik K., Fjæraa A.M., Fiebig M., Hjelbrekke A.G., Lund Myhre C., Solberg S., Yttri K.E., 2012. Introduction to the European Monitoring and Evaluation Programme (EMEP) and observed atmospheric composition change during 1972-2009. Atmospheric Chemistry and Physics, 12, 5447-5481.

Unéden P. et al., 2002: HIRLAM-5 Scientific Documentation, available from SMHI, S-601 76 Norrköping, Sweden, 144 pp..

van Meijgaard E., Van Ulft L. H., Van de Berg W.J., Bosveld F.C., Van den Hurk B.J.J.M., Lenderink G., Siebesma A.P., 2008. The KNMI regional atmospheric climate model RACMO version 2.1, KNMI Technical report, TR-302.

Vautard R., Beekmann M., Desplat J., Hodzic A., Morel S., 2007a. Air quality in Europe during the summer of 2003 as a prototype of air quality in a warmer climate. C. R. Geoscience 339, 747-763.

Vautard R. and Hauglustaine D., 2007b. Impact of global climate change on regional air quality : Introduction to the thematic issue. C.R. Geoscience 339, 703-708.

Walcek C.J., 2000. Minor flux adjustment near mixing ration extremes for simplified yet highly accurate monotonic calculation of tracer advection. J. Geophy. Re., 105, D7 2000, 9335-9348.

Warneck P., 2000. Chemistry of the natural atmosphere. International Geophysics series, Volume 71, Academic press.

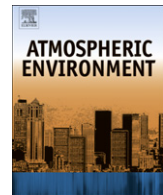
Weijers E.P., Sahan E., Ten Brink H.M., Schaap M., Matthijsen J., Otjes R.P., Van Arkel F., 2010. Contribution of secondary inorganic aerosols to PM10 and PM2.5 in the Netherlands; measurements and modelling results. Publication of the Netherlands Research Program on Particulate Matter, Report 500099006, ISSN: 1875-2322 (print) ISSN: 1875-2314 (on line).

Whitten G., Hogo H., Killus J., 1980. The Carbon Bond Mechanism for photochemical smog. Env. Sci. Technn. 14, 14690-700.

WHO, 2006. WHO Air quality guidelines for particulate matter, ozone, nitrogen dioxide and sulfur dioxide, global update 2005. WHO Air quality guidelines.

Yamartino R.J., Scire J., Carmichael G.R., Chang Y.S., 1992. The CALGRID mesoscale photo-chemical grid model-I. Model formulation. Atmos. Environ., 26A, 1493-1512.

7 Paper I: Impact of the extreme meteorological conditions during the summer 2003 in Europe on particulate matter concentrations



Impact of the extreme meteorological conditions during the summer 2003 in Europe on particulate matter concentrations

A. Mues ^{a,*}, A. Manders ^b, M. Schaap ^b, A. Kerschbaumer ^a, R. Stern ^a, P. Builjet ^{a,b}

^a Freie Universität Berlin, Institut für Meteorologie, Carl-Heinrich-Becker-Weg 6–10, 12165 Berlin, Germany

^b TNO, P.O. Box 80015, 3508 TA Utrecht, The Netherlands

ARTICLE INFO

Article history:

Received 9 November 2011

Received in revised form

24 February 2012

Accepted 2 March 2012

Keywords:

Chemistry transport models

PM10

Composition

Model evaluation

Meteorological variability

ABSTRACT

Due to the strong relation between meteorology and air quality, a changing climate is anticipated to significantly impact air pollution. To investigate this effect a synoptic situation in the past which is expected to occur more often in future is analyzed in terms of air quality. In this study the effect of the meteorological conditions in the extreme summer 2003 on the concentration of PM10 and its components is investigated over Europe. To this end measurements of the EMEP network in Europe of the summer 2003 were compared to the average of the summers of a five years period (2003–2007). Furthermore simulation runs were performed with the German chemistry transport model REM-Calgrid and the Dutch model LOTOS-EUROS, to analyze whether state-of-the-art chemistry transport models are able to reproduce the observed concentrations during this episode.

The synoptic situation in summer 2003 resulted in 1–10 $\mu\text{g m}^{-3}$ higher observed PM10 concentrations compared to the five years average. This increase was not reproduced to the same extent by the two models at most of the stations and the two models show evident differences in their PM10 simulations. The correlation between PM10 concentrations and meteorological parameters indicates that observed concentrations increase during weather conditions with high daily maximum temperature. The same holds for elemental carbon which is chosen as an example for a primary component. Low horizontal transport and the absence of wet deposition as a result of low wind speed and little precipitation associated with conditions with high temperatures favour the accumulation of pollutants in the lower troposphere. Although these conditions are reflected in the meteorological input data of the chemistry transport models used in this study, the models were not able to reproduce this relationship; they underestimate the observed high concentrations. This indicates that the underestimation of the variability of PM with meteorology is due to missing but important components and associated emissions or uncertainties therein, e.g. mineral dust, secondary organic aerosols and wild fires. To improve the simulation performance of the chemistry transport models as function of meteorological conditions these emission sources and the formation of secondary organic aerosols have to be included or improved and the dependency of anthropogenic emissions on meteorological conditions should be explicitly taken into account. These are essential issues for the simulation of such extreme conditions.

© 2012 Elsevier Ltd. All rights reserved.

1. Introduction

Impaired air quality has a large societal impact through its adverse effects on public health and the ecosystem. The air quality situation in an area is largely determined by the emission strength in combination with meteorology. The fate of air pollutants is highly dependent on meteorological parameters as they control natural emissions, transport, chemistry and deposition. Changing

meteorological conditions on short as well as on long timescales therefore affect the concentration of pollutants in the atmosphere. Changing climate is anticipated to significantly impact weather conditions in Europe. For example, extreme situations like heat waves characterized by high temperature, low precipitation and low wind speed conditions are expected to occur more frequently in the future (Fink et al., 2004). Hence, it is important to assess the consequences of climate change for the different chemical species relevant for air quality. Results, based on simulations with a coupled model system consisting of a chemistry transport model forced by a regional climate model, show that ozone increases under projected climate changes in summer European climate

* Corresponding author. Tel.: +49 30 83871130; fax: +49 30 83871128.

E-mail address: andrea.mues@met.fu-berlin.de (A. Mues).

(Meleux et al., 2007; Langner et al., 2005). This is mostly because of the large increase in temperature and decrease in cloudiness projected for summer European climate, which leads to higher photochemical production of ozone from biogenic species. In case of ozone, the available studies provide a consistent picture although the extent of the projected change is variable. For particulate matter however, the limited number of studies do not agree on the direction of the anticipated change (Jacob and Winner, 2009). Since particulate matter consists of many components with different physical and chemical properties, the effect of the meteorological parameters on the individual components varies and is more uncertain than for ozone (Tai et al., 2010).

To use such a coupled model system is a common approach to investigate the effect of climate change on air quality. An important prerequisite to come to reliable results with such model systems is a reasonable simulation of the variability of pollutant concentrations related to meteorological conditions. Evaluation of the model response to changing meteorological parameters is an important part of model evaluation (Dennis et al., 2010). A synoptic situation in the past which is expected to occur more often in the future is analyzed here in terms of air quality. An advantage of this approach is the availability of measurements and thus the possibility to evaluate chemistry transport models for these situations. Hence, such an investigation also indicates the strengths and weaknesses of the chemistry transport models if used in such climate change simulations. The summer 2003 is often taken as an example for an extreme summer which is expected to occur more often at the end of the 21st century in Europe (Vautard et al., 2007). It was characterized by persisting heat waves with high temperatures, stagnation and little precipitation over large parts of Europe. In order to investigate whether the meteorological conditions in the summer 2003 had a clear effect on the concentration of PM10 and its components, the observations of the EMEP network in Europe of the summer 2003 were compared to the average of the summers of a five years period (2003–2007). To analyze whether state-of-the-art chemistry transport models are able to reproduce the observed concentrations during this episode simulation runs were performed with the German model REM-Calgrid (Stern et al., 2006; Beekmann et al., 2007) and the Dutch model LOTOS-EUROS (Schaap et al., 2008) in this study.

2. Summer 2003 as an example for a summer by the end of the 21st century

The summer 2003 in Central Europe was exceptionally warm and dry and most regions were affected by a series of strong heat waves leading to high monthly mean temperatures with largest positive anomalies in June and August in a region reaching from south-west Germany across Switzerland to the eastern and southern parts of France (Fink et al., 2004). This summer was dominated by stagnant high-pressure systems which favour the development of heat and drought.

June 2003 was characterized by high temperatures throughout the entire month, with large positive temperature anomalies of up to 7 K over France, Switzerland and south Germany (BW, 2003). In Central Europe this month was +4.2 K warmer than the average at the stations Potsdam, De Bilt, Basel, and Vienna (BW, 2003). The heat period in June was exceptionally long with up to 18 heat days (days with a maximum of 30 °C or more) at several stations in the southern part of Germany. This is also shown by the number of summer days (days with at least 25 °C). In Freiburg and Konstanz summer days were observed throughout the entire month, that means 30 days instead of in average 9 or 10 days (BW, 2003). July 2003 in Central Europe was less extreme compared to the unusual warm and dry summer months June and August. The measured

temperature anomalies were between +2.8 K in the north and +1.3 K in the south-east of Europe (BW, 2003). In contrast to June, with warm anomalies lasting throughout the entire month, one extreme heat wave occurred from about 1st to 10th of August 2003 (Fink et al., 2004). The most affected regions were especially the western and southern part of Germany as well as western and southern Europe. At the German station Karlsruhe temperatures up to 40.2 °C were measured. For Central Europe the positive temperature anomaly was 4.2 K compared to the 1761–1990 average. In the middle of the month the synoptic situation became less stable and the rest of the August was characterized by more moderate weather conditions. June and August were accompanied by strong negative precipitation anomalies, whereas July was only slightly drier than normal in large parts of the West and Central Europe (Fink et al., 2004). As a result of the constant high temperatures and drought, large forest fires were observed in different parts of Europe. While small-scale forest fires occurred all over Central Europe and the western Mediterranean, the forest fires on the Iberian peninsula were especially devastating (Fink et al., 2004; Hodzic et al., 2007). These weather conditions make the summer of 2003 a good test case in view of the expected climate change by the end of the 21st century (Vautard et al., 2007).

3. Model descriptions and observation network

The application of two different chemistry transport models instead of one gives the opportunity to generalize common results or to specify differences. A comparison of the model setups may give information about the differences in model performances. Moreover, the use of two models provides insight in the uncertainty associated with chemistry transport modelling. The two three-dimensional regional chemistry transport models REM-Calgrid (RCG) and LOTOS-EUROS participated in this study. Both models are aimed to simulate air pollution in the lower troposphere and have a similar complexity. They can be viewed as operational models and have been used for several studies related to long-term air quality policy issues. Furthermore they have participated frequently in international model comparisons aimed at ozone (van Loon et al., 2007; Hass et al., 1997) and particulate matter (Cuvelier et al., 2007; Hass et al., 2003; Stern et al., 2008). The RCG model has been applied for a number of projects to develop pollution reduction plans as for example the Parest (PArtikel-REDuktions-Strategien)-Project aimed to identify strategies to reduce the particulate matter burden in Germany (Buitjes et al., 2010). Furthermore the model can also be used for short-term ozone forecasts (Tilmes et al., 2002). The LOTOS-EUROS model has been used for the assessment of particulate air pollution in a number of studies directed to PM10 (Denby et al., 2008; van Zelm et al., 2008; Manders et al., 2009), secondary inorganic aerosols (Schaap et al., 2004a; Erisman and Schaap, 2004; Barbu et al., 2009), primary carbonaceous components (Schaap et al., 2004b; Schaap and Dernier van der Gon, 2007) and trace metals (Denier van der Gon et al., 2007). The model participates in the MACC (Monitoring atmospheric composition & climate) atmospheric core service providing operational air quality forecasts for Europe. For a detailed model description we refer to the above mentioned publications.

Our focus is to analyze the ability of the models, in their operational setup, to reproduce the variability of PM10 concentrations with meteorology with a focus on an extraordinary summer like that of 2003. Therefore, the model setups, including the emission inventory and meteorological driver, are not standardized. For the interpretation of the results the model setups are discussed below and summarized in Table 1. The vertical grid in both models is based on terrain following vertical coordinates. The vertical layers

Table 1

Model specifications of REM-CALGRID and LOTOS-EUROS.

Model	REM-CALGRID	LOTOS-EUROS
Horizontal grid	0.50° longitude × 0.25° latitude	0.50° longitude × 0.25° latitude
Vertical grid	5 fixed layers: 25, 100, 500, 1500, 3000 m	4 time depending layers
Model domain	35° and 66.25° North, 10.5° West and 30.5° East	35° and 70° North, 10° West and 40° East
Time resolution	Hourly output	Hourly output
Emissions	Parest Project (www.parest.de) emission data of the year 2005	MACC emission database of the year 2005
Meteorological input	Tramper, Diagnostic Optimal Interpolation scheme	12 h forecast data from the operational ECMWF stream with analyses at noon and midnight at a horizontal resolution of about 25 × 25 km
Boundary conditions	Climatological background observations	Climatological background observations
Aerosol size distribution	2 modes: A fine mode (PM2.5) and a coarse mode (PM10–PM2.5)	2 modes: A fine mode (PM2.5) and a coarse mode (PM10–PM2.5)
PM10 components	Primary PM2.5 (PPM25), Primary PM10 without PM2.5 (PPMCO), Elemental carbon (EC), Organic carbon (OC), Windblown dust, Sea salt (Gong et al., 1997; Monahan et al., 1986), Secondary inorganic aerosols (SIA) (SO ₄ , NH ₄ , NO ₃), Secondary organic aerosols (SOA)	Primary PM2.5 (PPM25), Primary PM10 without PM2.5 (PPMCO), Elemental carbon (EC) (Schaap et al., 2004b), Sea salt (Monahan et al., 1986), Secondary inorganic aerosols (SIA) (SO ₄ , NH ₄ , NO ₃)
Gas phase chemistry	Modified CBM-IV	Modified CBM-IV
Inorganic aerosols	Thermodynamic equilibrium with ISORROPIA	Thermodynamic equilibrium with ISORROPIA
Organic aerosols	Modified SORGAM module	Not included
Dry deposition module	Of gases: Resistance approach (Erisman and van Pul, 1994) Of particles: Resistance approach	Of gases: Resistance approach (Erisman and van Pul, 1994) Of particles: Empirically derived values from IDEM
Wet deposition	Scavenging coefficients	Scavenging coefficients

in the RCG model are fixed in space and time, whereas they vary in space in time in LOTOS-EUROS as they are orientated on the mixing layer height, aimed to follow the vertical structure of the boundary layer and the vertical mixing within it. Hence, mixing within the boundary layer is dealt differently. Furthermore, both models use a different set of input meteorology. For the RCG model the meteorological input is derived from the diagnostic Optimal Interpolation scheme Tramper (Reimer and Scherer, 1992) which is based on surface and upper air observations. Tramper includes a model for the planetary boundary layer and simulates fields on the European scale. The meteorological input fields for the LOTOS-EUROS model are the 12 h forecasts after the noon and midnight analyses of the ECMWF model with a resolution of about 25 × 25 km. The anthropogenic emissions used in both models are based on the TNO-MACC emission dataset for 2005 (Kuenen et al., 2011). Within RCG the German emissions have been replaced by a high resolution distribution from the national PAREST project (Denier van der Gon et al., 2010), having the same emission total as the MACC database. Elemental carbon emissions in both models are separated from the PM2.5 emissions following Schaap et al. (2004b). Primary organic carbon is separated from the PM2.5 emissions in the RCG model, whereas the LOTOS-EUROS model includes it as a part of the chemically unspecified primary PM2.5 (PPM25) component and not as an extra component. Furthermore, RCG includes road dust emissions (Denier van der Gon et al., 2010) in the PPM25 as well as in the coarse fraction of primary PM10 (PPMCO). Windblown dust (Loosmore and Hunt, 2000; Claiborn et al., 1998) and the formation of secondary organic aerosols (SOA) (Schell et al., 2001) are only taken into account in the RCG model. Resuspension of crustal material by wind or traffic and SOA are not yet incorporated in the operational model version of LOTOS-EUROS. Both models do not include forest fire emissions. The chemistry description of the models is similar in complexity and approach, but both models use different versions of the carbon bond mechanism CBM-4 (Gipson and Young, 1999). The equilibrium module for the secondary inorganic aerosols (SIA) is the same. Wet deposition is treated with slightly different scavenging ratios. Dry deposition of particles is treated differently in the models with a theoretical approach based

on the resistance analogy (Yamartino et al., 1992) in the RCG whereas LOTOS-EUROS uses an empirical approach.

For this investigation observations and model simulations for the years 2003 until 2007 were used. This period of five years was chosen because it represents a reliable average for a summer period for which also an adequate set of observations is available. The summer 2003 is included because the five years are supposed to represent an average of summers in which also extreme summers may be included. Periods declared as summer averages in this study are the average over the month June, July and August. To extract the effect of the meteorology the emission data of 2005 are used for every year. This is justified by the conclusion that the emission differences between the years 2003 until 2007 are in general about 5% (Kuenen et al., 2011). As the total uncertainty of emission estimates is much larger, the emissions of the central year 2005 are considered representative for the whole period.

Most of the air quality observations for this study are provided by the European network EMEP (Hjellbrekke and Fjæraa, 2009; www.emep.int), and two of the chosen stations are operated by the Federal States of Germany. All stations are background stations and are situated in rural areas. No mountain stations (above 700 m) are chosen and the data coverage is over 40% for the analyzed periods. More information about the stations is summarized in a table in the Appendix.

For the figures in Section 5, for each station the five years of modelled (Tramper, ECMWF) daily maximum temperature, daily average wind speed, daily sum of precipitation and daily maximum mixing height as well as the observed and modelled daily concentration of different pollutants for the whole year were used. The data are sorted along the daily maximum temperature and then averaged over 50 days, one data point represents approximately 2–3% of the whole dataset. Data points were disregarded if no measurements were available for that day. Because the shown stations do not coincide with meteorological observation locations, the model output of Tramper and ECMWF is used here. Furthermore, it gives the opportunity to illustrate differences between the different meteorological drivers of the two chemistry transport models.

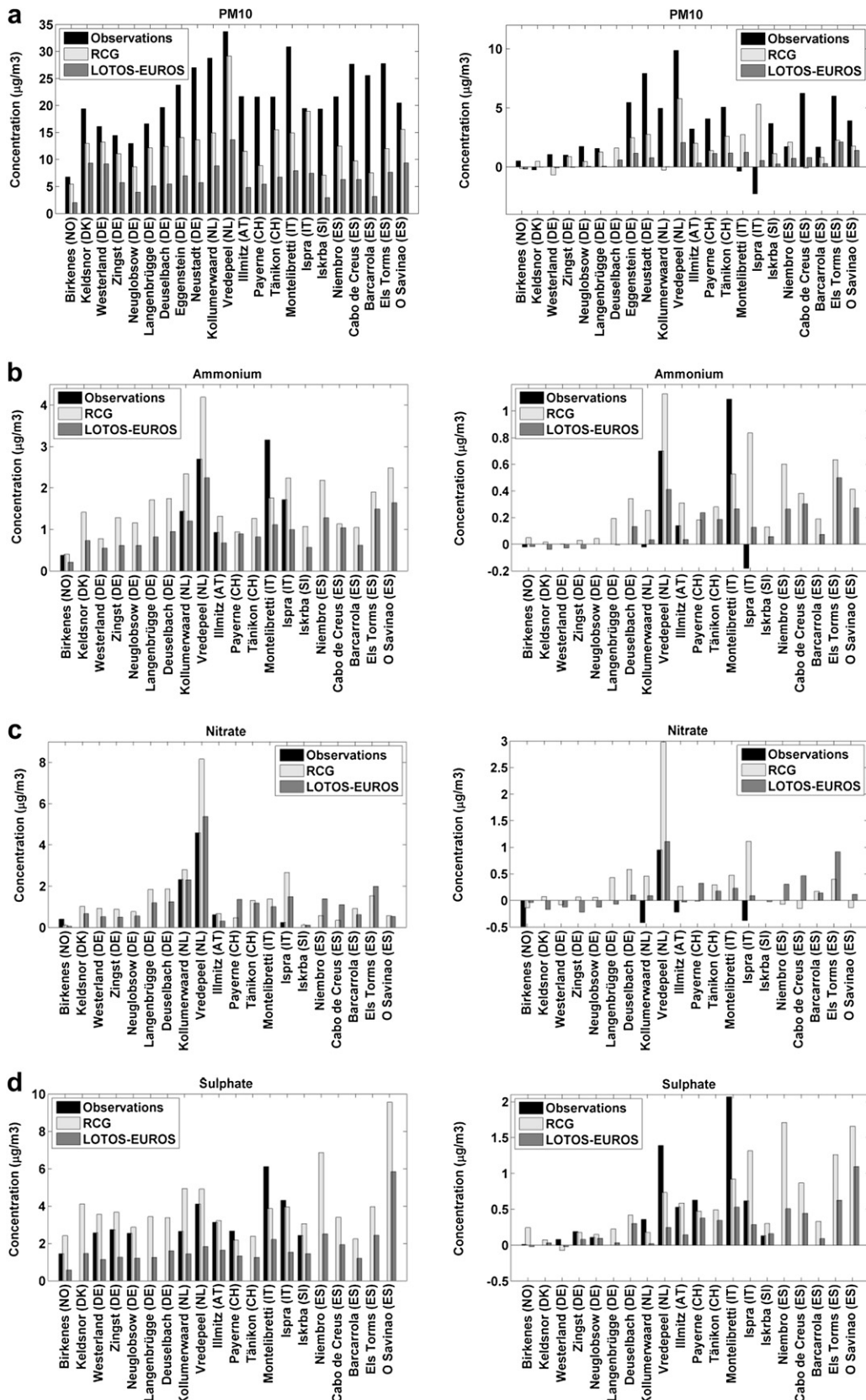


Fig. 1. Observed and modelled 2003 summer average concentrations ($\mu\text{g}/\text{m}^3$) (left) and absolute differences between the 2003 and 2003–2007 summer averages (right) for PM10 (a), Ammonium (b), Nitrate (c), Sulphate (d), and primary PM10 (without sea salt) (e) on different stations in Europe.

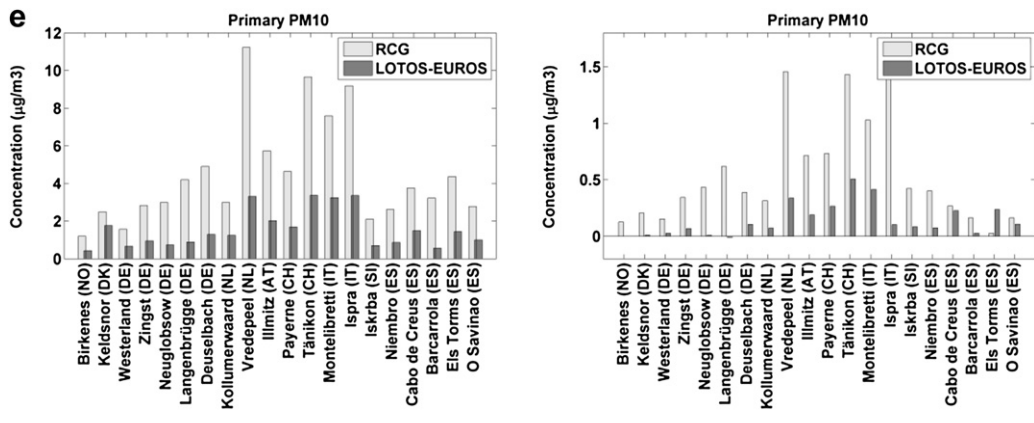


Fig. 1. (continued).

4. Observed and modelled concentrations of PM10 and its components in the summer 2003

4.1. PM10

The spatial distribution of the measured PM10 concentrations averaged over the summer 2003 (Fig. 1a) shows a north to south gradient, with lowest concentrations at the Norwegian station and the northern part of Germany ($13\text{--}17 \mu\text{g m}^{-3}$) and higher concentrations in southern Germany, Austria, and Switzerland ($20\text{--}27 \mu\text{g m}^{-3}$). In Spain the concentrations are in a similar range with $20\text{--}28 \mu\text{g m}^{-3}$. The highest PM10 concentrations are measured in the densely populated and industrial regions represented by two Dutch stations (29 and $34 \mu\text{g m}^{-3}$) and an Italian station ($30 \mu\text{g m}^{-3}$). Compared to the average of the summers 2003–2007, measured PM10 concentrations are higher in the summer 2003 at most of the stations (Fig. 1a). The highest differences are observed in the south part of the domain at stations in south Germany and Switzerland ($4\text{--}8 \mu\text{g m}^{-3}$), in some parts of Spain ($6 \mu\text{g m}^{-3}$) as well as in the densely populated regions in the Netherlands ($5\text{--}10 \mu\text{g m}^{-3}$). At most of the stations the summer averages of the single years 2004, 2005, 2006 and 2007 are smaller than the summer average of the period 2003–2007 (not shown). Hence the averaged concentration in summer 2003 is indeed exceptionally high compared to the other years.

The simulation results of the RCG and LOTOS-EUROS models for PM10 show regions with elevated pollution levels in urban and industrial regions as in the Netherlands, the German Ruhr area and northern Italy in summer 2003 (Fig. 2a), as well. The observed north to south gradient on the other hand is not reproduced. Both models underestimate the observed PM10 concentrations especially in regions with high concentrations. Compared to the RCG-field the PM10 concentrations simulated with the LOTOS-EUROS model are lower. The modelled spatial PM10 distributions are very similar, but not evident in Fig. 2a as a consequence of the common scale. The difference between the 2003 and 2003–2007 summer periods of the PM10-fields simulated by the RCG model shows mostly positive values ($0\text{--}6 \mu\text{g m}^{-3}$), but the differences are smaller than for the measurements (Figs. 1a and 2b). The model results reproduce the measured gradient of differences between northern and southern Germany and between Germany and the Netherlands. The differences shown by LOTOS-EUROS are up to $+2 \mu\text{g m}^{-3}$ with highest differences in the urban and industrial regions and are considerably smaller than for the measurements and the RCG results (Figs. 1a and 2b). The Italian station Ispra is situated in a valley with strong local effects and the station Montelibretti is close to Rome with high local emissions. Therefore the

meteorological conditions in 2003 might have a minor effect at these stations, which may explain the negative observed differences, whereas for these stations the local effects on pollution levels are not resolved by the models. By comparing the results of the relative differences of the two summer periods for the models, the difference in the absolute value of simulated concentrations between the two models is disregarded. This gives the possibility to compare the quality of the parameterized processes in the models in view of their ability to react on the conditions in summer 2003. The spatial distribution and level of the relative differences are very similar for the two models except for the northern part of the domain (Fig. 2c). In areas most affected by the heat periods in summer 2003 the relative difference between the simulated PM10 concentrations are between -10 and $+30\%$ for both models. The differences between the models regarding the relative differences are smaller than for the absolute differences between the two time periods indicating that the processes causing the differences of PM10 concentration between the two time periods have a similar effect in both models.

The absolute and relative differences between the two summer periods for the PM10 concentrations simulated with RCG (Fig. 2b and c) are comparatively high above the sea. This might be due to uncertainties of the wind speed in the Tramper model as they are derived from observations which are rarely available in this region. This affects the emission of sea salt, which represents a high part of the PM10 concentration here.

4.2. PM10 components

In order to analyze the contribution of the different components to the PM10 concentration and their importance during the summer 2003 conditions, the measured and modelled PM10 components are investigated in this section.

Time series of measured and modelled PM10 and its components for the summer 2003 are shown at the Dutch station Vredespeel and the Austrian station Illmitz (Fig. 3), but only measurements for PM10 and sulphate, nitrate and ammonium particles were available. The difference between the sum of the SIA and the PM10 concentrations can be attributed to the primary components (as anthropogenic, mineral dust, sea salt) and the SOA. These components represent the major part of the measured PM10 concentrations especially at the Austrian station. This station shows high measured PM10 concentrations during June, decreasing concentrations for July and highest concentrations during the strong heat wave in the beginning of August which reflects the described weather conditions. At the Dutch station, the sum of the SIA is for a small time period higher than the PM10 concentration.

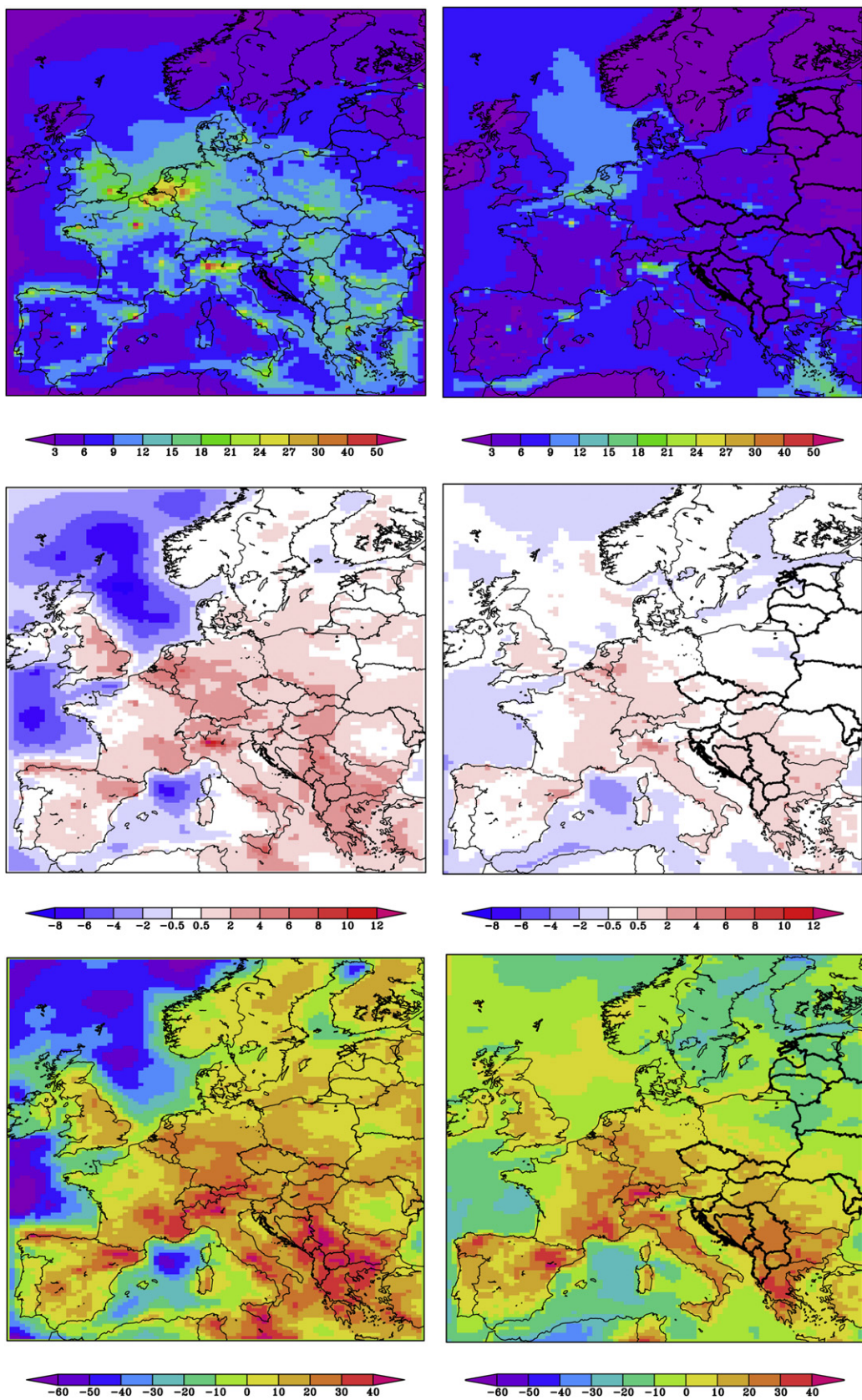


Fig. 2. Distributions of the modelled 2003 summer average for PM10 ($\mu\text{g m}^{-3}$) (a); modelled absolute difference between the 2003 and 2003–2007 summer averages for PM10 ($\mu\text{g m}^{-3}$) (b); relative difference between the 2003 and 2003–2007 summer averages for modelled PM10 (%) (c). Results for both RCG (left) and LOTOS-EUROS (right) are given.

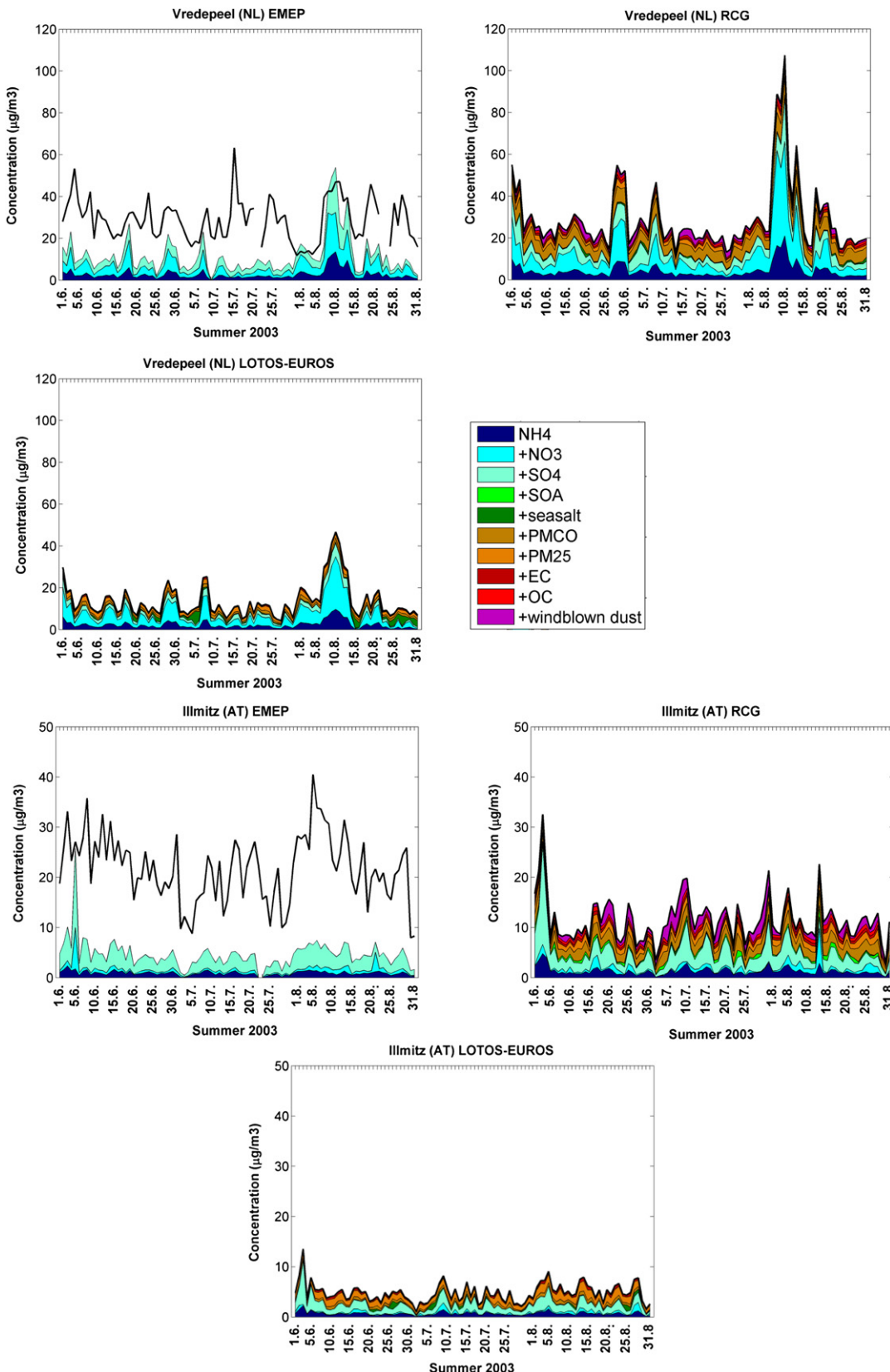


Fig. 3. Summer 2003 time series of PM10 and added concentrations of PM10 components at the stations Vredepeel and Illmitz for the EMEP observations, the RCG and the LOTOS-EUROS simulation results.

This might be due to uncertainties in the measurements. Compared to the other stations in Europe the measurements of the SIA are especially high at the two Dutch stations (Fig. 1b–d) and represent a high portion of the PM10 concentration as is shown for Vredepeel (Fig. 3). The differences between the two summer periods for the SIA are highly depending on the station and component (Fig. 1b–d). For stations with increased observed ammonium concentrations in summer 2003 differences are between 0.1 and 1.1 $\mu\text{g m}^{-3}$ (Fig. 1b) whereas concentrations differences at the other stations are close to zero. The observed nitrate concentrations are higher for the five years summer average (0.3–0.5 $\mu\text{g m}^{-3}$) except for the Dutch station Vredepeel (Fig. 1c). Sulphate measurements are higher for the summer 2003 (Fig. 1d) at every shown station with differences up to 2 $\mu\text{g m}^{-3}$. The differences represent around 5% of the sulphate concentration measured for the five years average and are especially high for the Dutch station Vredepeel (50%) where the concentrations of the SIA are always relatively high. The same holds for the station Montelibretti where sulphate concentrations are highest.

In contrast to the measurements, the SIA represent the major part of the modelled PM10 concentrations at the two stations Vredepeel and Illmitz (Fig. 3) and both models underestimate the measured PM10 concentrations. Apparently both models miss a substantial part of the primary components and also the RCG simulation results for SOA are low. The contribution of SIA to the PM10 differences between the two summer periods and also the performance of the models for SIA depends on the component and location of the station (Tables 2–4). Besides the bias and the time correlation, the standard deviation of error is given in the tables which is defined as the normalized differences between the standard deviation of observations and model results. It evaluates the non-systematic part of the error and should be zero for an ideal simulation. For most stations and components the biases and the standard deviation of error are lower and correlations are higher for LOTOS-EUROS compared to RCG. The RCG model tends to overestimates the observed concentrations of every component in both time periods whereas LOTOS-EUROS rather underestimates the concentrations. Both models simulate increased ammonium concentrations for the summer 2003 on most of the stations and the differences are higher for the RCG model (Fig. 1b). The modelled nitrate concentrations are mostly higher in summer 2003, apart from the northern part of the domain of the LOTOS-EUROS simulations (Fig. 1c). The sign of the differences for nitrate differ between the models and the observations for most of the stations. For both models the concentrations of sulphate are higher in 2003

(Fig. 1d). The LOTOS-EUROS model underestimates the observed sulphate differences, whereas the RCG model over- as well as underestimates the differences depending on the station.

Although a comparison with measurements for primary PM10 components is not possible, the comparison between the simulation results of the two models helps to understand differences between the model performances. It gives information about the ability of the models to react to the meteorological conditions in terms of transport processes and to which extent the primary components contribute to the simulated PM10 differences between the two time periods. The highest concentrations of primary PM10 are modelled in urban and industrial regions during both time periods (Fig. 1e), but concentrations are much higher for RCG (1–11 $\mu\text{g m}^{-3}$) than for LOTOS-EUROS (0.5–3.5 $\mu\text{g m}^{-3}$). Differences between the two time periods modelled with the RCG are depending on the area. Whereas differences are only up to 0.5 $\mu\text{g m}^{-3}$ in Spain and northern Europe, differences in most of the other parts, especially in urban regions, are up to 1.7 $\mu\text{g m}^{-3}$. Differences for LOTOS-EUROS are smaller with maximum differences of 0.5 $\mu\text{g m}^{-3}$ in urban regions.

For both summer periods lower PM10 concentrations are simulated with LOTOS-EUROS than with RCG (Figs. 1 and 3). This is partly due to the additional emission sources and components (road dust, windblown dust and SOA) in the RCG model but also the different treatment of dry deposition is important to consider here. In the PMCO emission used for RCG road dust is included which explains a major part of the differences between the PMCO simulation results of the two models. At the Austrian station the simulated concentrations of primary PM2.5 are slightly higher for LOTOS-EUROS as this model includes OC in PPM25 (Fig. 3). In view of the extra components included in the RCG model wind-blown dust, especially at the Austrian station, plays an important role for the differences of PM10 concentration between the two models.

5. Meteorological parameters and air quality

5.1. Meteorological parameters at different stations

To analyse the effect of meteorological conditions on air quality with a focus on situations with high temperature as in summer 2003, the relation between meteorological parameters and pollutant concentrations is investigated in this section.

Meteorological parameters as temperature, wind speed, precipitation and mixing height are especially important in terms

Table 2
Statistical comparison between measured and modelled ammonium concentrations for the 2003 and 2003–2007 summer averages for the RCG and LOTOS-EUROS model in $\mu\text{g m}^{-3}$ at different stations in Europe. Observed and modelled mean, as well as bias, time correlation and standard deviation of error (stde) are given.

Ammonium	Summer 2003–2007					Summer 2003					Differences summers 2003–ave (2003–2007)		
	Station	Observed mean	Modelled mean	Correlation	Bias	Stde	Observed mean	Modelled mean	Correlation	Bias	Stde	Observed differences	Modelled differences
			RCG					RCG					RCG
Illmitz (AUT)	0.79	1.01	0.41	0.22	0.68	0.93	1.33	0.54	0.40	0.66	0.14		0.32
Montelibretti (ITA)	2.07	1.42	0.28	-0.65	1.26	3.16	1.76	0.34	-1.40	1.17	1.09		0.34
Ispra (ITA)	1.90	1.74	0.19	-0.16	1.86	1.72	2.23	0.30	0.51	1.71	-0.18		0.49
Kollumerwaard (NL)	1.46	2.04	0.56	0.58	1.14	1.44	2.31	0.59	0.87	1.31	-0.02		0.27
Vredepeel (NL)	2.00	3.34	0.72	1.34	1.74	2.70	4.19	0.89	1.49	1.68	0.70		0.85
Birkenes (NOR)	0.40	0.38	0.53	-0.02	0.41	0.38	0.46	0.62	0.08	0.2	-0.02		0.08
			LOTOS-EUROS					LOTOS-EUROS					LOTOS-EUROS
Illmitz (AUT)	0.79	0.64	0.56	-0.15	0.40	0.93	0.68	0.71	-0.25	0.29	0.14		0.04
Montelibretti (ITA)	2.07	0.87	0.49	-1.20	1.07	3.16	1.12	0.51	-2.04	0.98	1.09		0.25
Ispra (ITA)	1.90	0.92	0.24	-0.98	1.35	1.72	1.00	0.56	-0.72	0.90	-0.18		0.08
Kollumerwaard (NL)	1.46	1.19	0.70	-0.27	0.68	1.44	1.18	0.76	-0.26	0.62	-0.02		-0.01
Vredepeel (NL)	2.00	1.95	0.73	-0.05	1.17	2.70	2.26	0.88	-0.44	1.09	0.70		0.31
Birkenes (NOR)	0.40	0.25	0.63	-0.15	0.34	0.38	0.24	0.69	-0.14	0.34	-0.02		-0.01

Table 3

Statistical comparison between the measured and modelled nitrate concentrations for the 2003 and 2003–2007 summer averages for the RCG and LOTOS-EUROS model in $\mu\text{g m}^{-3}$ on different stations in Europe. Observed and modelled mean, as well as bias, time correlation and standard deviation of error (stde) are given.

Nitrate	Summer 2003–2007					Summer 2003					Differences summers 2003–ave (2003–2007)		
Station	Observed mean	Modelled mean	Correlation	Bias	Stde	Observed mean	Modelled mean	Correlation	Bias	Stde	Observed differences	Modelled differences	
RCG													
Illmitz (AUT)	0.84	0.47	-0.06	-0.37	1.40	0.62	0.67	0.03	0.05	1.25	-0.22	0.20	
Ispra (ITA)	0.62	1.91	0.02	1.29	3.34	0.24	2.55	0.18	2.31	3.39	-0.38	0.64	
Kollumerwaard (NL)	2.74	2.45	0.43	-0.29	2.22	2.32	2.80	0.41	0.48	2.38	-0.42	0.35	
Vredepeel (NL)	3.64	5.82	0.67	2.18	4.61	4.59	8.16	0.82	3.57	5.53	0.95	2.34	
Birkenes (NOR)	0.89	0.24	0.05	-0.65	1.40	0.40	0.10	0.02	-0.30	0.33	-0.49	-0.14	
LOTOS-EUROS													
Illmitz (AUT)	0.84	0.36	0.03	-0.48	1.27	0.62	0.30	-0.04	-0.32	0.99	-0.22	-0.06	
Ispra (ITA)	0.62	1.61	0.14	0.99	2.15	0.24	1.63	0.50	1.39	1.73	-0.38	0.02	
Kollumerwaard (NL)	2.74	2.39	0.64	-0.35	1.74	2.32	2.25	0.66	-0.07	1.82	-0.42	-0.14	
Vredepeel (NL)	3.64	4.56	0.70	0.92	2.86	4.59	5.38	0.82	0.79	2.73	0.95	0.82	
Birkenes (NOR)	0.89	0.09	0.05	-0.80	1.36	0.40	0.05	0.42	-0.35	0.25	-0.49	-0.04	

of air quality. The wind speed is an indicator for the horizontal transport or ventilation of pollutants, precipitation gives information about the loss processes through wet deposition. The mixing height describes the vertical condition of the troposphere and is an indicator for the vertical mixing of pollutants. The effect of temperature is different for the individual chemical components as it affects for example chemical reaction rates, deposition velocities and gas aerosol partitioning. The total effect of the meteorological parameters on the PM10 concentration is a result of many processes and is different for the compounds of PM10. However, the mentioned meteorological parameters are not independent. To investigate the relationship of these parameters, the daily average wind speed, the daily sum of precipitation, as well as the daily maximum mixing height at different stations are correlated with the daily maximum temperature for the whole years of the time period 2003–2007 (Fig. 4). Wind direction is not investigated, since the effect of wind direction will be different for each station due to the geographical distribution of emission sources. Although the two different meteorological drivers are not evaluated here,

differences between the two meteorology input sets may help to understand differences in model performances.

Low daily maximum temperature is related to low wind speed, low daily maximum mixing height and little precipitation (Fig. 4). The low daily maximum mixing height in winter is often connected to a stable boundary layer with weak vertical transport and low wind speed which results in little horizontal transport. Very high daily maximum temperatures are also correlated with low wind speed, little precipitation but high daily maximum mixing height. Since both situations are connected to stagnant condition and are related to little precipitation as shown in the figures, these conditions favour high concentrations of pollutants because of their impact on mixing, transport and deposition. The very high temperatures are often connected to long persistent high-pressure systems as observed in summer 2003. Moderate daily maximum temperatures go along with high wind speed and a high amount of precipitation; this situation is often connected to the passing of Atlantic low pressure systems. These situations have a cleaning effect on air quality as there is strong transport, and high wet

Table 4

Statistical comparison between the measured and modelled sulphate concentrations for the 2003 and 2003–2007 summer averages for the RCG and LOTOS-EUROS model in $\mu\text{g m}^{-3}$ on different stations in Europe. Observed and modelled mean, as well as bias, time correlation and standard deviation of error (stde) are given.

Sulphate	Summer 2003–2007					Summer 2003					Differences summers 2003–ave (2003–2007)		
Station	Observed mean	Modelled mean	Correlation	Bias	Stde	Observed mean	Modelled mean	Correlation	Bias	Stde	Observed differences	Modelled differences	
RCG													
Illmitz (AUT)	2.60	2.93	0.32	0.33	2.46	3.13	3.25	0.28	0.12	2.68	0.53	0.32	
Westerland (DEU)	2.55	3.63	0.59	1.08	1.96	2.74	3.47	0.61	0.73	1.75	0.19	-0.16	
Neuglobosw (DEU)	2.43	2.72	0.44	0.29	1.57	2.54	2.87	0.59	0.33	1.52	0.11	0.15	
Zingst (DEU)	2.48	3.47	0.40	0.99	1.89	2.56	3.64	0.43	1.08	1.74	0.08	0.17	
Montelibretti (ITA)	4.31	3.34	0.21	-0.97	2.95	6.43	3.86	0.31	-2.57	3.04	2.12	0.52	
Ispra (ITA)	3.68	2.97	0.30	-0.71	2.87	4.30	4.14	0.24	-0.16	2.87	0.62	1.17	
Kollumerwaard (NL)	2.28	5.01	0.48	2.73	2.83	2.64	4.94	0.41	2.30	2.49	0.36	-0.07	
Vredepeel (NL)	2.72	4.38	0.52	1.66	2.59	4.11	4.91	0.70	0.80	2.54	1.39	0.53	
Birkenes (NOR)	1.44	2.15	0.49	0.71	1.75	1.45	2.40	0.64	0.95	1.86	0.01	0.25	
Iskrba (SI)	2.30	2.73	0.07	0.43	2.22	2.43	3.07	0.06	0.64	2.04	0.13	0.34	
LOTOS-EUROS													
Illmitz (AUT)	2.60	1.50	0.59	-1.10	1.29	3.13	1.64	0.66	-1.49	1.36	0.53	0.14	
Westerland (DEU)	2.55	1.16	0.70	-1.39	1.03	2.74	1.11	0.65	-1.63	0.99	0.19	-0.05	
Neuglobosw (DEU)	2.43	1.11	0.68	-1.32	0.93	2.54	1.21	0.70	-1.33	1.23	0.11	0.10	
Zingst (DEU)	2.48	1.19	0.63	-1.29	0.92	2.56	1.28	0.62	-1.28	0.92	0.08	0.09	
Montelibretti (ITA)	4.31	1.73	0.55	-2.58	2.46	6.43	2.21	0.43	-4.22	2.80	2.12	0.48	
Ispra (ITA)	3.68	1.27	0.47	-2.41	2.20	4.42	1.53	0.51	-2.89	2.06	0.74	0.26	
Kollumerwaard (NL)	2.28	1.46	0.69	-0.82	1.00	2.64	1.43	0.65	-1.21	0.98	0.36	-0.03	
Vredepeel (NL)	2.72	1.65	0.66	-1.07	1.94	4.11	1.83	0.82	-2.28	2.42	1.39	0.18	
Birkenes (NOR)	1.44	0.60	0.62	-0.84	0.91	1.45	0.57	0.75	-0.88	0.69	0.01	-0.03	
Iskrba (SI)	2.30	1.24	0.60	-1.06	1.17	2.43	1.45	0.62	-0.98	0.95	0.13	0.21	

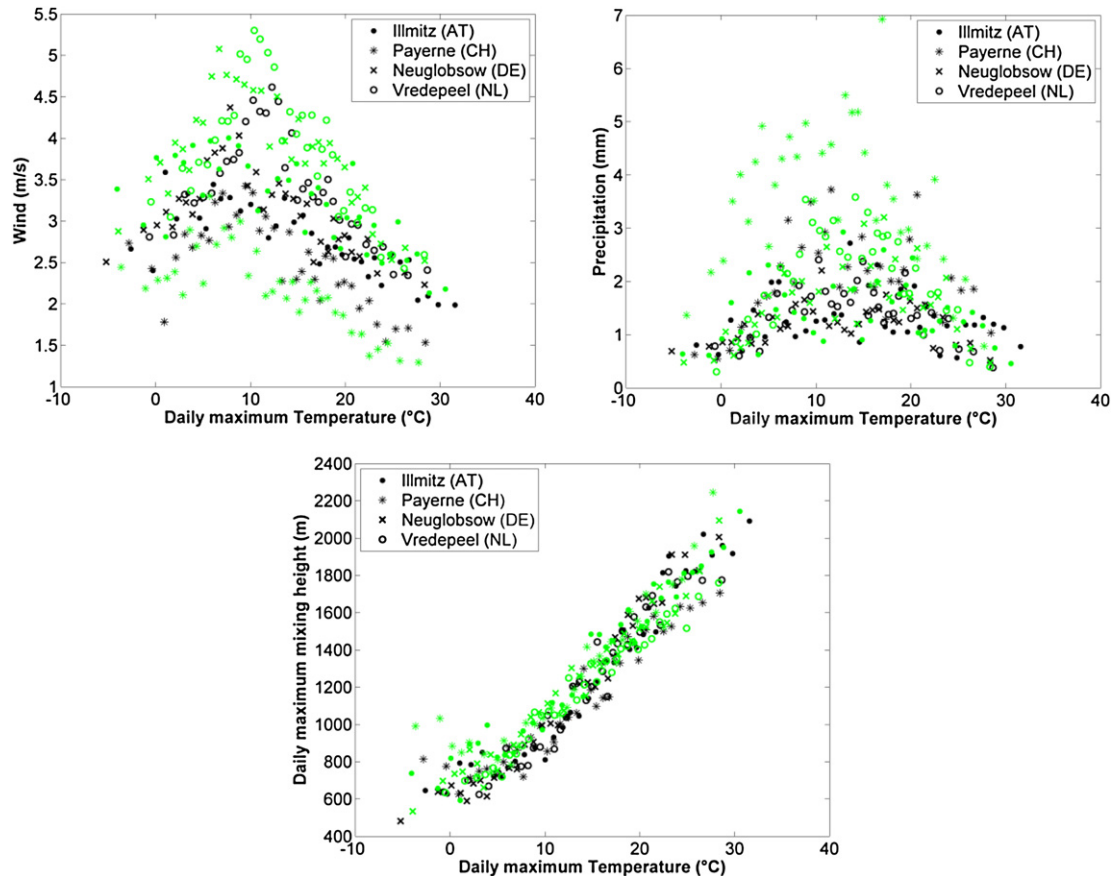


Fig. 4. Scatter plots of sorted and binned modelled meteorological data (wind, sum of precipitation and daily maximum mixing height) for 2003–2007, Tramper (black) and ECMWF (green), at different stations in Europe. (For interpretation of the references to colour in this figure legend, the reader is referred to the web version of this article.)

deposition through precipitation. Both meteorological drivers show these general features.

5.2. Relation between temperature and PM10 concentrations

The daily maximum temperature is clearly related to the other meteorological parameters and provides important implicit information about meteorological conditions at the stations. Hence,

this enables to investigate the model's ability to respond to meteorological variability by focussing on the relationship between daily maximum temperature and pollutant concentration.

High observed PM10 concentrations are connected with low maximum temperature for all stations (**Fig. 5**), and therefore, concluding from **Fig. 4**, also with low wind speed, little precipitation and low mixing height. With increasing daily maximum temperature the measured PM10 concentration decreases until about

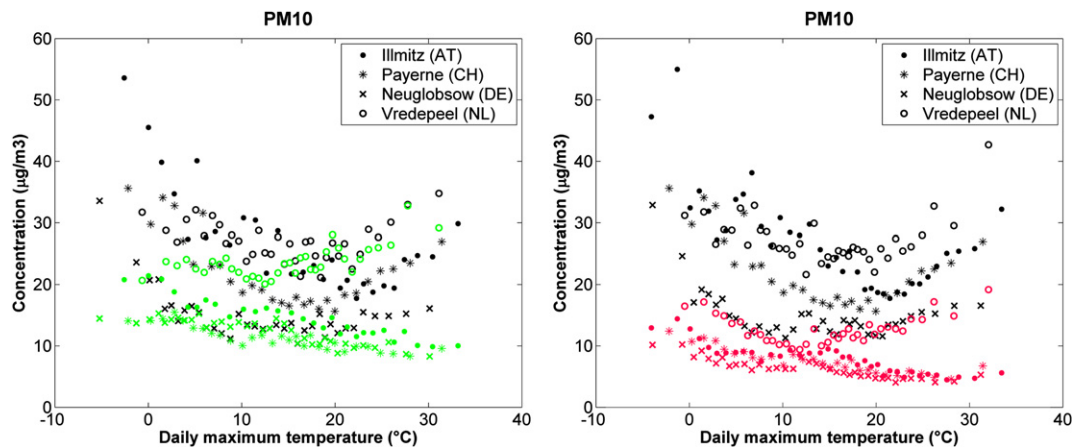


Fig. 5. PM10 concentrations versus daily maximum temperature, sorted and averaged for 2003–2007, observations (black) and RCG results (green) with Tramper meteorology (left) and observations and Lotos-Euros results (red) with ECMWF meteorology (right) at different stations in Europe. (For interpretation of the references to colour in this figure legend, the reader is referred to the web version of this article.)

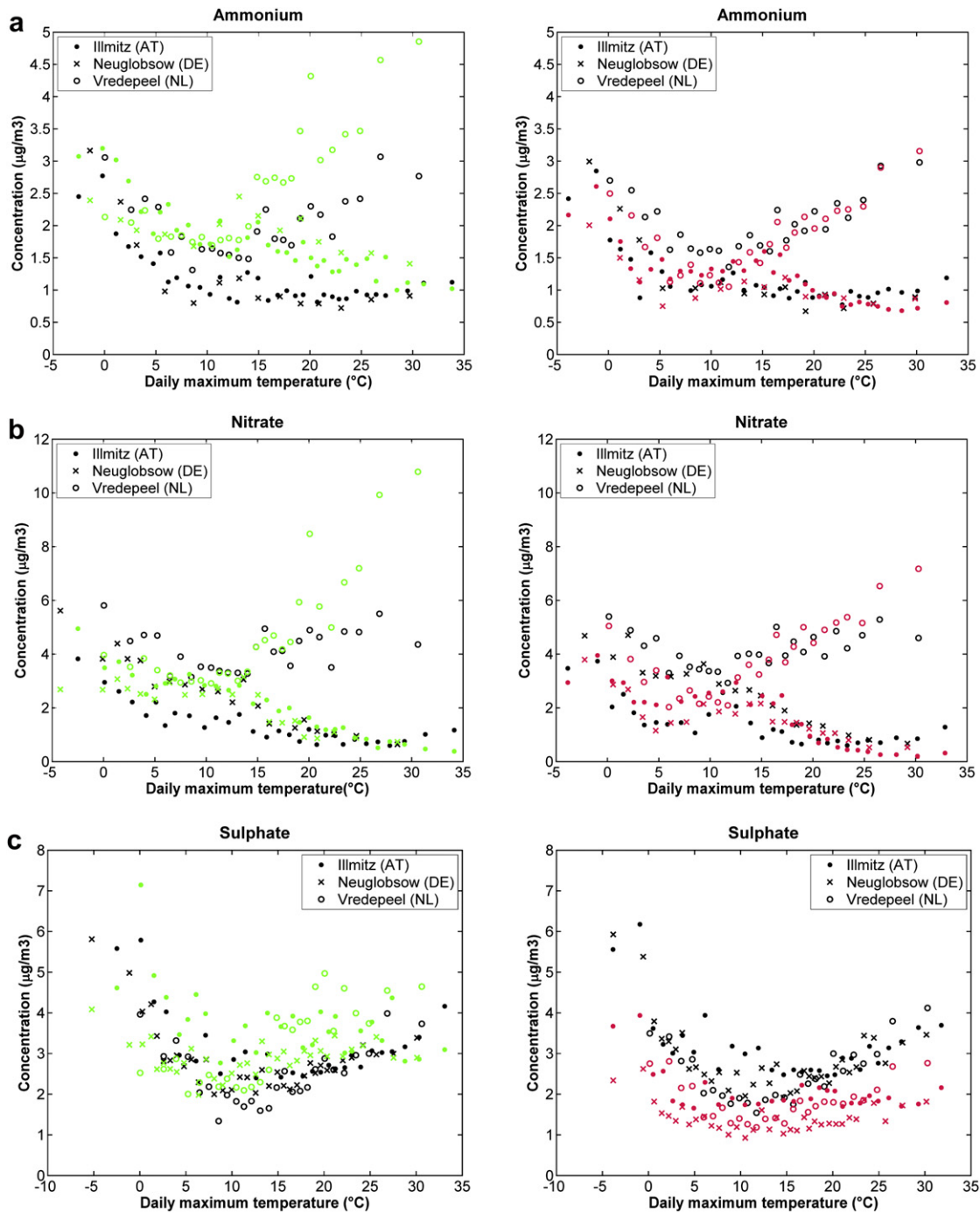


Fig. 6. Concentrations of the secondary inorganic components (Ammonium (a), Nitrate (b), Sulphate (c)) versus daily maximum temperature, sorted and averaged for 2003–2007, observations (black) and RCG results (green) with Tramper meteorology (left) and observations and LOTOS-EUROS results (red) with ECMWF meteorology (right) on different stations in Europe. (For interpretation of the references to colour in this figure legend, the reader is referred to the web version of this article.)

10–20 °C. In that range a broad minimum concentration is measured at most of the stations. The measured PM10 concentrations increase again with higher daily maximum temperature, but not for all stations. This dependency is very similar for the temperature output of both meteorological models.

Beside the fact that the models underestimate the measured PM10 concentrations, the described relation between measured PM10 concentrations and temperature is not fully reproduced by the two models (Fig. 5). RCG shows a rather flat PM10 concentration as function of daily maximum temperature. The increased concentrations connected to low temperature are, to a lower

extent, reproduced only for the Austrian station. Only at the Dutch station RCG follows the observed correlation between PM10 and high daily maximum temperature. For the other stations RCG tends to simulate the lowest concentrations for the highest temperatures. In contrast to RCG, Lotos-Euros reproduces an increase of PM10 concentrations for low temperatures. But similar to RCG, Lotos-Euros reproduces the observed connection between PM10 concentration and daily maximum temperature only for the Dutch station in the full temperature range. Note that the results for both models show less variability than the observations at most of the stations.

PM10 consists of different components and to explain the behaviour of PM10 the relation between temperature and the individual component needs to be addressed. For that reason in the next sections the correlation between the daily maximum temperature and SIA and elemental carbon (EC) is studied.

5.3. Relation between temperature and SIA concentrations

As for PM10, the concentrations of the observed SIA are high for conditions with low daily maximum temperature and decrease with increasing daily maximum temperature until about 10–15 °C (Fig. 6a–c). For higher temperatures the relation depends on component and station. For sulphate the concentrations increase for high temperatures for all shown stations. Therefore, the generally observed increase of PM10 with high daily maximum temperature is partly determined by sulphate. The formation of sulphate depends on the availability of sulphur dioxide in the atmosphere, and on meteorological conditions affecting the chemical reactions and the dynamical processes responsible for the transport and mixing of sulphate. The increase of sulphate concentration with high daily maximum temperature might be partly due to accumulation of sulphate and sulphur dioxide during stagnant conditions and partly due to chemical processes as a higher sulphur dioxide oxidation rate with increasing temperature (Tai et al., 2010). Both models reproduce the observed relationship between daily maximum temperature and sulphate concentrations, although the LOTOS-EUROS model underestimates whereas the RCG model overestimates the concentrations.

In contrast to sulphate, the ammonium and nitrate concentrations decrease, or only increase slightly, with increasing daily maximum temperature at the Austrian and German station. At the Dutch station the concentrations increase with increasing temperature for both components. The different behaviour in the high temperature range can be explained by the chemical formation of the SIA. Ammonium nitrate can only be formed if the available sulphate is neutralized by ammonia to form ammonium sulphate. In regions with low ammonia emissions (ammonia/sulphate ratio lower than 2) the ammonia concentration is insufficient to neutralize the available sulphate and the aerosol phase will be acidic. Then no ammonia is available to form ammonium nitrate. In ammonia rich regions (ratio ammonia/sulphate higher than 2) the excess ammonia that was not needed to neutralize sulphate will be available to combine with nitric acid to produce

ammonium nitrate, a semi volatile component. The equilibrium constant for the formation of ammonium nitrate strongly increases with increasing temperature. Therefore, more ammonia is needed to stabilize a certain concentration of ammonium nitrate at high temperatures than at low temperatures (Seinfeld and Pandis, 1998). Hence, the behaviour of ammonium nitrate with temperature is strongly dependent on the availability of ammonia. Measured ammonia concentrations at the investigated stations differ substantially. For the Dutch station the summer average ammonia concentration during 2003–2007 is 18.12 µg m⁻³, mainly due to high emissions from agriculture in the area, whereas the concentration at the Austrian and German station are 2.2 and 0.85 µg m⁻³, respectively. This can explain the observed differences in behaviour of the ammonium and nitrate concentrations between the shown stations at high daily maximum temperature.

The described processes are also included in the aerosol modules in the models (Nenes et al., 1998) and the described differences in the behaviour for the components and stations are reproduced by both models. The reproduction of the nitrate behaviour and its high mass contribution in the Netherlands explain why both models reproduce rising PM10 concentrations in the high temperature range for this region.

5.4. Relation between temperature and elemental carbon concentrations

As an example for primary components the relation between daily maximum temperature and observed and modelled EC concentrations is discussed in this section. Reliable measurements of EC for such a long time period (5 years) are rarely available, therefore only measurements at one station are used here. The observed EC concentrations are derived from black smoke measurements at the Dutch station Vredepeel and converted to EC concentrations following Schaap and Dernier van der Gon (2007). Stagnant winter time conditions are connected with highest observed and modelled concentrations (Fig. 7). This is followed by a decrease of concentrations with increasing temperature. For very high daily maximum temperature (above 25 °C) the observed concentrations increase again. The models do not reproduce this feature and modelled EC levels are rather flat in the high temperature range. Observed EC concentrations are overestimated by both models over the whole temperature range especially by the RCG model on this station even though EC concentrations in model evaluation studies are shown to be rather underestimated (e.g.

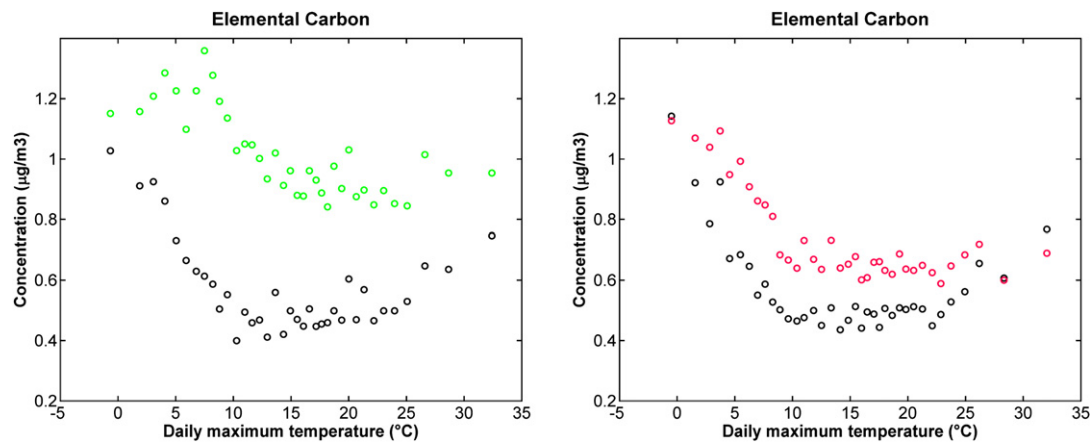


Fig. 7. Concentrations of elemental carbon versus daily maximum temperature, sorted and averaged for 2003–2007, observations (black) and RCG results (green) with Tramper meteorology (left) and observations and LOTOS-EUROS results (red) with ECMWF meteorology (right) for the Dutch station Vredepeel. (For interpretation of the references to colour in this figure legend, the reader is referred to the web version of this article.)

Table 5

Overview of the main findings for the two models.

- Both CTMs did not reproduce the extent of the observed increase in PM10 concentrations in the high temperature range such as in summer 2003
- In contrast to the RCG, LOTOS-EUROS shows the observed increased PM10 concentrations in the low temperature range
- The larger bias for PM10 in LOTOS-EUROS may be largely due to the different deposition velocities
- The observed variability of NO₃, SO₄ and NH₄ with temperature was reproduced by both models
- The observed variability of EC was not reproduced by the two models
- RCG included dust and SOA, but did not better represent the variability of PM10

Beekmann et al., 2007). Because the emissions are the same in both model versions the differences between the models are mainly a result of the different input meteorology and the description of deposition (see below).

6. Discussion and conclusions

The meteorological conditions in summer 2003 had a significant effect on the observed concentrations of PM10 and are therefore a good test case for the models in view of their ability to simulate extreme summer conditions. Depending on the area the observed PM10 concentrations in summer 2003 were found to be 1–10 µg m⁻³ higher than for the summer average of the years 2003–2007. It is well known that low horizontal transport and the virtual absence of wet deposition as a result of low wind speed and little precipitation favour the accumulation of pollutants in the lower troposphere. Although these conditions are reflected in the meteorological input data of the chemistry transport models used in this study, both models did not reproduce the extent of the observed increase in PM10 concentrations during the summer 2003 at most of the stations. This leads to the conclusion that important processes for the simulation of the high PM10 concentrations are not included or not described correctly in these models.

To understand the behaviour of PM, one needs to understand its components. The highest fraction of modelled PM10 is represented by the SIA. Comparison to observations reveals that LOTOS-EUROS tends to underestimate the SIA concentrations whereas RCG overestimates. The general increase of observed sulphate concentrations with temperature during summer is reproduced by both models. Moreover, the models are also capable to correctly simulate the dual response of ammonium and nitrate. Ammonium nitrate concentrations rise with temperature in summer in areas with a high emission density of ammonia, e.g. the Netherlands, whereas at most locations their concentrations decrease. The exceptional behaviour in the ammonia rich areas explains why Vredenpeel is the only station at which the modelled relationship between PM10 and temperature is in good agreement with the observations. As the SIA response is reproduced and sulphate is only a small contribution, the reason for not reproducing the increasing PM10 concentrations with temperature needs to be sought elsewhere.

Organic carbon (OC) represents a significant fraction (10–50%) of PM10 (e.g. Yttri et al., 2009). Primary OC is mostly released from incomplete combustion of fossil fuels or wood while the secondary components (SOA) are formed through oxidation products of volatile organic compounds (VOC) in the atmosphere. In Tai et al. (2010) OC in the USA is found to be positively correlated with temperature, mostly during the summer months. This was suggested to reflect the impact of wild fires and the enhanced emission of biogenic VOC (e.g. isoprene) due to their temperature and light

dependency combined with more efficient SOA formation due to enhanced photochemistry (Simpson et al., 1999; Jacob and Winner, 2009). The uncertainties in the description of the biogenic SOA formation and in the emissions of the precursors are large. The low contribution by the scheme in RCG and the absence of biogenic SOA formation in LOTOS-EUROS may contribute significantly to the underestimation of OC by the chemistry transport models (e.g. Beekmann et al., 2007).

In a model study (CHIMERE model) Hodzic et al. (2007) found wild fires to result in a significant increase in PM2.5 mean concentrations (from 20 to 200%) over several regions in Europe during the heat wave in the first half of August 2003. The largest increase is found close (200 km) to the fire sources (e.g. Portugal) (up to 40 µg m⁻³), while a more moderate increase (3–5 µg m⁻³) is observed over the southern Mediterranean basin and Benelux countries. The missing emission source of wild fires in the models might therefore significantly contribute to local underestimations of PM10 concentrations in August 2003 but as wild fires only occur occasionally this fails to explain fully the high EC concentrations in the high temperature range for the five year period. Further possible emission sources relevant for EC during such conditions could be barbecuing and a higher energy demand due to air conditioning and cooling systems. The life time of elemental carbon is dependent on its mixing state. We anticipate the ageing of EC to be fast under conditions with active photochemistry associated with high temperature and high pollution levels (Tsyro et al., 2007; Riemer et al., 2004). Therefore, the fact that it is not modelled explicitly has no impact on the disagreement between modelled and observed EC concentrations in the high temperature range.

Another candidate to explain an increase of PM10 in the high concentration range is mineral dust. The emission of windblown dust is depending mainly on aridity and wind speed (Schaap et al., 2010). As wind speed conditions are rather low it is not anticipated that windblown dust contributes significantly. However, other emission sources for mineral dust include agricultural land management, resuspension of road dust, construction activities and other mechanical activities. The dry soil as a result of little precipitation may lead therefore to an increase of dust emissions and can therefore contribute to the high PM10 concentrations during conditions with high temperature. Road dust emissions are only included in the RCG but do not depend on meteorological or soil conditions. Although it is an important contribution to PM10, the sources of mineral dust are still poorly understood and therefore not well represented in emission data bases and models (Vautard et al., 2005).

Concluding from the findings above natural and anthropogenic emissions increase during conditions represented by high temperatures (e.g. summer 2003) as consequence of the weather situation and contribute to higher PM concentrations. In both models a dependency of anthropogenic emissions on the meteorological variability is not taken into account which leads to an underestimation of concentrations.

Differences between the simulation results of the two models are mostly due to the additional components in RCG, the different meteorological input data as well as the deposition efficiency. Although the description of the laminar layer and surface resistance for gases is the same in both models, the laminar layer resistance for particulate matter is very different. In RCG this value is defined with a theoretical approach based on the resistance analogy (Yamartino et al., 1992) whereas LOTOS-EUROS uses empirically derived values from IDEM (Integral Deposition Model). The large differences in resulting dry deposition velocities (Flechard et al., 2011) cause large differences, up to a factor 2 for the coarse PM, in the resulting aerosol concentrations

(Manders et al., 2010). Additional differences derive from the meteorological input data as ECMWF shows slightly higher values for wind speed and more precipitation than Tramper at most stations leading to higher dilution and more effective wet deposition in LOTOS-EUROS. Besides these evident implications, previous experience learns that the stability parameters deduced from the meteorological input may also differ significantly among models (Stern et al., 2008). Model simulations performed with LOTOS-EUROS using Tramper and ECMWF meteorological input, show that concentrations for PM10 components when driven with Tramper meteorology are higher than with ECMWF input. Finally, the RCG model includes more components. Especially road dust contributes to a large part to the higher simulated PM10 concentrations in this model. SOA, on the other hand, does not as it contributes only to a small extent to the modelled PM10 concentration in RCG. An overview about the main findings for the models is given in Table 5.

So far, we have discussed PM10 and its components, but did not explicitly mention PM2.5. The reason is that there is very little data available on PM2.5 in the period under investigation. In reality, PM2.5 contributes typically 70% to PM10 mass (Putaud et al., 2010). The coarse fraction is enriched with dust and sea salt, whereas the majority of the carbonaceous and secondary inorganic components are in the PM2.5 size range. Hence, the results presented for the latter can be directly linked to PM2.5. Moreover, most of the shortcomings identified here encompass the components in both PM2.5 and PM10. We conclude that our findings for PM10 can be projected on PM2.5.

To improve the simulation performance of the chemistry transport models as function of meteorological conditions, a better representation of primary components like dust, elemental carbon and from wild fire derived components as well as the formation of SOA have to be included. A further improvement would be to explicitly relate the emissions strengths of the different sectors to the meteorological variability. The inability of the chemistry transport models to correctly respond to meteorological changes may also partly explain the low but very uncertain response of particulate matter to anticipated climate change in model studies (Jacob and Winner, 2009). Hence, these improvements are important to come to more reliable results in climate scenario studies implying both one and two way coupled climate – air quality model systems.

Acknowledgement

We would like to thank the EMEP for providing their data from the EBAS-dataset, as well as the measurement networks of the Federal States of Germany. Furthermore, this work was financially supported by the Milieu-Project at the Freie Universität Berlin.

Appendix. Observation network

Station	Country	Lat	Lon	Reference
Illmitz (AT0002R)	AUT	47.77	16.77	EMEP
Payerne (CH0002R)	CH	46.82	6.95	EMEP
Tänikon (CH0003R)	CH	47.48	8.9	EMEP
Srvatouch (CZ0001R)	CZE	49.73	16.03	EMEP
Kosetice (CZ0003R)	CZE	49.58	15.08	EMEP
Keldsnor (DK0005R)	DEN	54.73	10.73	EMEP
Westerland (DE0001R)	DEU	54.92	8.31	EMEP
Langenbrügge (DE0002R)	DEU	52.8	10.75	EMEP
Deuselbach (DE0004R)	DEU	49.75	7.05	EMEP
Neuglobsw (DE0007R)	DEU	53.14	13.03	EMEP
Zingst (DE0009R)	DEU	54.43	12.73	EMEP
Melpitz (DE0044R)	DEU	52.53	12.93	EMEP
Eggenstein (DEBW004)	DEU	49.08	8.4	German network

(continued)

Station	Country	Lat	Lon	Reference
Neustadt a.d. Donau (DEBY049)	DEU	48.85	11.77	German network
Niembro (ES0008R)	ESP	43.43	-4.85	EMEP
Cabo de Creus (ES0010R)	ESP	42.32	-3.32	EMEP
Barcarrola (ES0011R)	ESP	38.47	-6.92	EMEP
Els Torms (ES0014R)	ESP	41.4	-0.72	EMEP
O Saviñao (ES0016R)	ESP	43.22	-7.68	EMEP
Montelibretti (IT0001R)	ITA	42.1	12.63	EMEP
Ispra (IT0004R)	ITA	45.8	8.63	EMEP
Kollumerwaard (NL0009R)	NL	53.33	6.28	EMEP
Vredepeel (NL0010R)	NL	51.53	5.85	EMEP
Birkenes (NO0001R)	NOR	58.38	8.25	EMEP
Diabla Gora (PL0005R)	POL	54.15	22.07	EMEP
Iskrba (SI0008R)	SI	45.57	14.87	EMEP

References

- Barbu, A.L., Segers, A.J., Schaap, M., Heemink, A.W., Buitjes, P.J.H., 2009. A multi-component data assimilation experiment directed to sulphur dioxide and sulphate over Europe. *Atmospheric Environment* 43, 1622–1631.
- Beekmann, M., Kerschbaumer, A., Reimer, E., Stern, R., Möller, D., 2007. PM10 measurement campaign HOVERT in the Greater Berlin area: model evaluation with chemically specified particulate matter observations for a one year period. *Atmospheric Chemistry and Physics* 7, 55–68.
- Buitjes, P.J.H., Jörß, W., Stern, R., Theloke, J., 2010. F&E Vorhaben: "Strategien zur Verminderung der Feinstaubbelastung" – PAREST: Zusammenfassender Abschlussbericht FKZ 206 43 200-01, Report.
- BW, "Berliner Wetterkarte", 2003. Berliner Wetterkarte e.V. www.berliner-wetterkarte.de.
- Claiborn, C., Lamb, B., Miller, A., Beseda, J., Clode, B., Vaughan, J., Kang, L., Newvine, C., 1998. Regional measurements and modeling of windblown agricultural dust: the Columbia Plateau PM10 Program. *Journal of Geophysical Research* 103 (D16), 19,753–19,767. doi:10.1029/98JD00046.
- Cuvelier, C., Thunis, P., Vautard, R., Amann, M., Bessagnet, B., Bedogni, M., Berkowicz, R., Brandt, J., Brochetton, F., Buitjes, P., Carnavale, C., Coppalle, A., Denby, B., Douros, J., Graf, A., Hellmuth, O., Hodzic, A., Honoré, C., Jonson, J., Kerschbaumer, A., de Leeuw, F., Minguzzi, E., Moussiopoulos, N., Pertot, C., Peuch, V.H., Pirovano, G., Rouil, L., Schaap, M., Stern, R., Tarrason, L., Vignati, E., Volta, M., White, L., Wind, P., Zuber, A., 2007. CityDelta: a model intercomparison study to explore the impact of emission reductions in European cities in 2010. *Atmospheric Environment* 41, 189–207.
- Denby, B., Schaap, M., Segers, A., Buitjes, P., Horalek, J., 2008. Comparison of two data assimilation methods for assessing PM10 exceedances on the European scale. *Atmospheric Environment* 42, 7122–7134.
- Denier van der Gon, H.A.C., Hulskotte, J.H.J., Visschedijk, A.J.H., Schaap, M., 2007. A revised estimate of cooper emissions from road transport in UNECE Europe and its impact on predicted copper concentrations. *Atmospheric Environment* 41, 8697–8710.
- Denier van der Gon, H.A.C., Visschedijk, A., van den Brugh, H., Dröge, R., 2010. F&E Vorhaben: "Strategien zur Verminderung der Feinstaubbelastung" – PAREST: A high resolution European emission data base for the year 2005. TNO-Report, TNO-034-UT-2010-01895_RPT-ML, Utrecht.
- Dennis, R., Fox, T., Fuentes, M., Gilliland, A., Hanna, S., Hogrefe, C., Irwin, J., Trivikrama Rao, S., Scheffe, R., Schere, K., Steyn, D., Venkatram, A., 2010. A framework for evaluating regional-scale numerical photochemical modeling systems. *Environmental Fluid Mechanics* 10, 471–489.
- Erisman, J.W., Schaap, M., 2004. The need for ammonia abatement with respect to secondary PM reductions in Europe. *Environmental Pollution* 129, 159–163.
- Erisman, J.W., van Pul, A., 1994. Parametrization of surface resistance for the quantification of atmospheric deposition of acidifying pollutants and ozone. *Atmospheric Environment* 39, 2595–2607.
- Fink, A.H., Brücher, T., Krüger, A., Leckebusch, G.C., Pinto, J.G., Ulbrich, U., 2004. The 2003 European summer heatwaves and drought – synoptic diagnosis and impacts. *Royal Meteorological Society, Weather* 59, 209–216.
- Flechard, C.R., Nemitz, E., Smith, R.I., Fowler, D., Vermeulen, A.T., Bleeker, A., Erisman, J.W., Simpson, D., Zhang, L., Tang, Y.S., Sutton, M.A., 2011. Dry deposition of reactive nitrogen to European ecosystems: a comparison of inferential models across the NitroEurope network. *Atmospheric Chemistry and Physics* 11, 2703–2728.
- Gipson, G., Young, J., 1999. Gas phase chemistry (Chapter 8). In: Byun, D.W., Ching, J.K.S. (Eds.), *Science Algorithms of the Epa Models-3 Community Multiscale Air Quality (Cmaq) Modeling System*. Atmospheric Modeling Division National Exposure Research Laboratory U.S. Environmental Protection Agency Research Triangle Park, NC 27711, EPA/600/R-99/030.
- Gong, S.L., Barrie, L.A., Blanchet, J.-P., 1997. Modelling sea-salt aerosols in the atmosphere. 1. Model development. *Journal of Geophysical Research* 102, 3805–3818.
- Hass, H., Buitjes, P.J.H., Simpson, D., Stern, R., 1997. Comparison of model results obtained with several European regional air quality models. *Atmospheric Environment* 31, 3259–3279.

- Hass, H., van Loon, M., Kessler, C., Stern, R., Matthijssen, J., Sauter, F., Zlatev, Z., Langner, J., Foltescu, V., Schaap, M., 2003. Aerosol Modelling: Results and Intercomparison from 15 European Regional-scale Modelling Systems. EURO-TRAC-2 Special report. Eurotrac-ISS, Garmisch Partenkirchen, Germany.
- Hjellbrekke, A.-G., Fjæraa, A.M., 2009. Data Report 2007, Acidifying and Eutrophying Compounds and Particulate Matter. EMEP/CCC-Report 1/2009.
- Hodzic, A., Madronich, S., Bohn, B., Massie, S., Menut, L., Wiedinmyer, C., 2007. Wildfire particulate matter in Europe during summer 2003: meso-scale modeling of smoke emissions, transport and radiative effects. *Atmospheric Chemistry and Physics* 7, 4043–4064.
- Jacob, D.J., Winner, D.J., 2009. Effect of climate change on air quality. *Atmospheric Environment* 43, 51–63.
- Kuenen, J., Denier van der Gon, H., Visschedijk, A., van der Brugh, H., van Gijlswijk, R., 2011. MACC European Emission Inventory for the Years 2003–2007. TNO report, TNO-060-UT-2011-00588, Utrecht.
- Langner, J., Bergström, R., Foltescu, V., 2005. Impact of climate change on surface ozone and deposition of sulphur and nitrogen in Europe. *Atmospheric Environment* 39, 1129–1141.
- Loosmore, G.A., Hunt, J.R., 2000. Dust resuspension without saltation. *Journal of Geophysical Research* 105 (D16), 20,663–20,671. doi:10.1029/2000JD900271.
- Manders, A.M.M., Schaap, M., Hoogerbrugge, R., 2009. Testing the capability of the chemistry transport model LOTOS-EUROS to forecast PM10 levels in the Netherlands. *Atmospheric Environment* 43, 4050–4059.
- Manders, A.M.M., Schaap, M., Querol, X., Albert, M.F.M.A., Vercauteren, J., Kuhlbusch, T.A.J., Hoogerbrugge, R., 2010. Sea salt concentrations across the European continent. *Atmospheric Environment* 44, 2434–2442.
- Meleux, F., Solmon, F., Giorgi, F., 2007. Increase in summer European ozone amounts due to climate change. *Atmospheric Environment* 41, 7577–7587.
- Monahan, E.C., Speil, D., Speil, K., 1986. Oceanic Whitecaps. Reidel.
- Nenes, A., Pandis, S.N., Pilinis, C., 1998. ISORROPIA: a new thermodynamic equilibrium model for multiphase multicomponent inorganic aerosols. *Aquatic Geochemistry* 4, 123–152.
- Putaud, J.-P., Van Dingenen, R., Alastuey, A., Bauer, H., Birmili, W., Cyrys, J., Flentje, H., Fuzzi, S., Gehrig, R., Hansson, H.C., Harrison, R.M., Herrmann, H., Hitzenberger, R., Hüglin, C., Jones, A.M., Kasper-Giebl, A., Kiss, G., Kousa, A., Kuhlbusch, T.A.J., Löschau, G., Maenhaut, W., Molnar, A., Moreno, T., Pekkanen, J., Perrino, C., Pitz, M., Puxbaum, H., Querol, X., Rodriguez, S., Salma, I., Schwarz, J., Smolik, J., Schneider, J., Spindler, G., ten Brink, H., Tursic, J., Viana, M., Wiedensohler, A., Raes, F., 2010. A European aerosol phenomenology e 3: physical and chemical characteristics of particulate matter from 60 rural, urban, and kerbside sites across Europe. *Atmospheric Environment* 44, 1308–1320.
- Reimer, E., Scherer, B., 1992. An operational meteorological diagnostic system for regional air pollution analysis and long-term modeling. In: Dop, H.v., Kallos, G. (Eds.), Air Pollution Modelling and Its Applications. NATO Challenges of Modern Society, vol. IX. Kluwer Academic/Plenum Publisher, New York.
- Riemer, N., Vogel, H., Vogel, B., 2004. Soot aging time scales in polluted regions during day and night. *Atmospheric Chemistry and Physics* 4, 1885–1893.
- Schaap, M., Denier van der Gon, H.A.C., 2007. On the variability of Black Smoke and carbonaceous aerosols in the Netherlands. *Atmospheric Environment* 41, 5908–5920.
- Schaap, M., van Loon, M., ten Brink, H.M., Dentener, F.D., Builtjes, P.J.H., 2004a. Secondary inorganic aerosol simulations for Europe with special attention to nitrate. *Atmospheric Chemistry and Physics* 4, 857–874.
- Schaap, M., Denier Van Der Gon, H.A.C., Dentener, F.J., Visschedijk, A.J.H., van Loon, M., ten Brink, H.M., Putaud, J.-P., Guillaume, B., Liouesse, C., Builtjes, P.J.H., 2004b. Anthropogenic black carbon and fine aerosol distribution over Europe. *Journal of Geophysical Research* 109, D18201. doi:10.1029/2003JD004330.
- Schaap, M., Timmermans, R.M.A., Sauter, F.J., Roemer, M., Velders, G.J.M., Boersen, G.A.C., Beck, J.P., Builtjes, P.J.H., 2008. The LOTOS-EUROS model: description, validation and latest developments. *International Journal of Environment and Pollution* 32 (2), 270–289.
- Schaap, M., Timmermans, R.M.A., Denier van der Gon, H.A.C., 2010. Assessment of Anthropogenic Versus Natural Aerosols in Europe. TNO Report, TNO-034-UT-2010-00318_RPT-ML, Utrecht.
- Schell, B., Ackermann, I.J., Hass, H., Binkowski, F.S., Ebel, A., 2001. Modeling the formation of secondary organic aerosol within a comprehensive air quality model system. *Journal of Geophysical Research* 106, 28275–28293. doi:10.1029/2001JD000384.
- Seinfeld, J.H., Pandis, S.N., 1998. Atmospheric Chemistry and Physics: From Air Pollution to Climate Change. Wiley-Interscience, John Wiley & Sons, Inc.
- Simpson, D., Winiwarter, W., Börjesson, G., Cinderby, S., Ferreiro, A., Guenther, A., Hewitt, C.N., Janssen, R., Khalil, M.A.K., Owen, S., Pierce, T.E., Puxbaum, H., Shearer, M., Skiba, U., Steinbrecher, R., Tarrasón, L., Öquist, M.G., 1999. Inventorying emissions from nature in Europe. *Journal of Geophysical Research* 104, 8113–8152.
- Stern, R., Yamartino, R., Graff, A., 2006. Analyzing the Response of a Chemical Transport Model to Emissions Reductions Utilizing Various Grid Resolutions. Twenty-eighth ITM on Air Pollution Modelling and its Application, May 15–19 2006, Leipzig, Germany.
- Stern, R., Builtjes, P.J.H., Schaap, M., Timmermans, R., Vautard, R., Hodzic, A., Memmesheimer, M., Feldmann, H., Renner, E., Wolke, R., Kerschbaumer, A., 2008. A model inter-comparison study focussing on episodes with elevated PM10 concentrations. *Atmospheric Environment* 42, 4567–4588.
- Tai, A.P.T., Mickley, L.J., Jacob, D.J., 2010. Correlations between fine particulate matter (PM2.5) and meteorological variables in the United States: implications for the sensitivity of PM2.5 to climate change. *Atmospheric Environment* 44, 3976–3984.
- Tilmes, S., Brandt, J., Flatøy, F., Bergström, R., Flemming, J., Langner, J., Christensen, J.H., Frohn, L.M., Hov, O., Jacobson, I., Reimer, E., Stern, R., Zimmermann, J., 2002. Comparison of five eulerian air pollution forecasting systems for the summer of 1999 using the German ozone monitoring data. *Journal of Atmospheric Chemistry* 42, 91–121.
- Tsyro, S., Simpson, D., Tarrasón, L., Klimont, Z., Kupiainen, K., Pio, C., Yttri, K.E., 2007. Modeling of elemental carbon over Europe. *Journal of Geophysical Research* 112, D23S19. doi:10.1029/2006JD008164.
- van Loon, M., Vautard, R., Schaap, M., Bergström, R., Bessagnet, B., Brandt, J., Builtjes, P.J.H., Christensen, J.H., Cuvelier, K., Graf, A., Jonson, J.E., Krol, M., Langner, J., Roberts, P., Rouil, L., Stern, R., Tarrasón, L., Thunis, P., Vignati, E., White, L., Wind, P., 2007. Evaluation of long-term ozone simulations from seven regional air quality models and their ensemble average. *Atmospheric Environment* 41, 2083–2097.
- van Zelm, R., Huijbregts, M.A.J., den Hollander, H.A., van Jaarsveld, H.A., Sauter, F.J., Struijs, J., van Wijnen, H.J., van de Meent, D., 2008. European characterization factors for human health damage of PM10 and ozone in life cycle impact assessment. *Atmospheric Environment* 42 (3), 441–453.
- Vautard, R., Bessagnet, B., Chin, M., Menut, L., 2005. On the contribution of natural Aeolian sources to particulate matter concentrations in Europe: testing hypotheses with a modelling approach. *Atmospheric Environment* 39, 3291–3303.
- Vautard, R., Beekmann, M., Desplat, J., Hodzic, A., Morel, S., 2007. Air quality in Europe during the summer of 2003 as a prototype of air quality in a warmer climate. *Comptes Rendus Geoscience* 339, 747–763.
- Yamartino, R.J., Scire, J.S., Carmichael, G.R., Chang, Y.S., 1992. The CALGRID meso-scale photochemical grid model-I. Model formulation. *Atmospheric Environment* 26A, 1493–1512.
- Yttri, K.E., Aas, W., Tøtseth, K., Stebel, K., Tsyro, S., Simpson, D., Merckova, K., Wankmüller, R., Klimont, Z., Bergström, R., Denier van der Gon, H., Holzer-Popp, T., Schroedter-Homscheidt, M., 2009. Transboundary Particulate Matter in Europe. Chapter 2 in Emeep Status Report 4/2009.

8 Paper II: The impact of differences in large-scale circulation output from climate models on the regional modeling of ozone and PM



The impact of differences in large-scale circulation output from climate models on the regional modeling of ozone and PM

A. M. M. Manders¹, E. van Meijgaard², A. C. Mues³, R. Kranenburg¹, L. H. van Ulft², and M. Schaap¹

¹TNO, P.O. Box 80015, 3584 TA Utrecht, The Netherlands

²KNMI, De Bilt, The Netherlands

³FUB, Berlin, Germany

Correspondence to: A. M. M. Manders (astrid.manders@tno.nl)

Received: 2 March 2012 – Published in Atmos. Chem. Phys. Discuss.: 11 May 2012

Revised: 26 September 2012 – Accepted: 30 September 2012 – Published: 19 October 2012

Abstract. Climate change may have an impact on air quality (ozone, particulate matter) due to the strong dependency of air quality on meteorology. The effect is often studied using a global climate model (GCM) to produce meteorological fields that are subsequently used by chemical transport models. However, climate models themselves are subject to large uncertainties and fail to reproduce the present-day climate adequately. The present study illustrates the impact of these uncertainties on air quality. To this end, output from the SRES-A1B constraint transient runs with two GCMs, i.e. ECHAM5 and MIROC-hires, has been dynamically down-scaled with the regional climate model RACMO2 and used to force a constant emission run with the chemistry transport model LOTOS-EUROS in a one-way coupled run covering the period 1970–2060.

Results from the two climate simulations have been compared with a RACMO2-LOTOS-EUROS (RLE) simulation forced by the ERA-Interim reanalysis for the period 1989–2009. Both RLE_ECHAM and RLE_MIROC showed considerable deviations from RLE_ERA for daily maximum temperature, precipitation and wind speed. Moreover, sign and magnitude of these deviations depended on the region. The differences in average present-day concentrations between the simulations were equal to (RLE_MIROC) or even larger than (RLE_ECHAM) the differences in concentrations between present-day and future climate (2041–2060). The climate simulations agreed on a future increase in average summer ozone daily maximum concentrations of 5–10 $\mu\text{g m}^{-3}$ in parts of Southern Europe and a smaller increase in Western and Central Europe. Annual average PM_{10} concentrations increased 0.5–1.0 $\mu\text{g m}^{-3}$ in North-West Europe and

the Po Valley, but these numbers are rather uncertain: overall, changes for PM_{10} were small, both positive and negative changes were found, and for many locations the two climate runs did not agree on the sign of the change. This illustrates that results from individual climate runs can at best indicate tendencies and should therefore be interpreted with great care.

1 Introduction

Ozone and particulate matter (PM) have an adverse impact on the health of human beings and other organisms. They also play a role in the climate system by their interaction with radiation and/or clouds (Raes et al., 2010; Zhang et al., 2010). The day-to-day and even sub-daily variability of concentrations strongly depends on atmospheric conditions, since these govern transport, dilution and deposition, as well as chemical conversions (cloud processes, photochemistry). There is a strong correlation between ozone concentrations and temperature. The correlation of particulate matter with meteorological parameters is more complex and depends on the component (e.g. Tai et al., 2010; Jimenez-Guerrero et al., 2011; Manders et al., 2011; Mues et al., 2012). Due to changes in meteorology associated with a changing climate, ambient concentrations are expected to change even if anthropogenic emissions are kept constant. The quantification of expected changes in concentrations is highly relevant for policy making, as there are strict regulations for concentrations (e.g. EU, 2008; US EPA NAAQS, 2012). Additional emission reductions may be needed to comply with

regulations under expected warmer conditions and changes in other meteorological fields that influence air pollution (e.g. longer stagnant episodes).

A common approach to study the impact of climate change on air quality is to directly use output of climate models in an air quality model (one-way coupling), with many examples for different meteorological models coupled to different air quality models, both at the global and the regional scale (e.g. Dentener et al., 2006; Forkel and Knoche, 2007; Giorgi and Meleux, 2007; Andersson, 2009). The overview by Jacob and Winner (2009) shows that the impact of climate change on air quality depends on the time horizon, region and component, and simulations with various models have resulted in both increases and decreases in concentrations. Results generally show an increase in ozone concentration, related to an increase in temperature. The response of PM to changes in meteorology is weaker and less conclusive, with the different model simulations not even resulting in the same sign of the change.

Climate models themselves are subject to considerable uncertainties due to assumptions and parameterizations and simplifications of processes. All climate models, both global and regional, have significant biases, which are different for each model and region (Christensen et al., 2007). They may represent for example too strong or too weak zonal flow. This is why a multi-model approach is crucial, and this approach is taken by IPCC. Despite the regional differences, there is a general consensus that there is global warming, with very likely an increase in frequency of hot extremes, heat waves and heavy precipitation and a poleward shift of extratropical storm tracks with consequent changes in wind, precipitation and temperature patterns (IPCC, 2007).

So far, the impact of biases in climate models on the outcomes of air quality modeling has not received much attention, and authors have based their estimates of the impact of climate change on air quality on simulation with a single model (e.g. Giorgi and Meleux, 2007; Andersson, 2009; Carvalho et al., 2010). A commonly applied assumption is that a climate model exhibits the same bias structure in both the present-day and the future climate simulation, so that concentration differences can be identified and interpreted straightforwardly. Most one-way coupled simulations only used one realization of the future climate, or two scenarios using the same climate model. But using two scenarios with the same climate model results in a change in amplitude of the change rather than shifts in patterns (Mitchell et al., 1999). Alternatively, Liao et al. (2007) produced a high and a low extreme of a meteorological baseline scenario, based on uncertainty estimates for the individual variables for future climate in terms of their probabilistic distributions. When results from an individual climate model are used, e.g. for flood predictions, bias-corrected precipitation fields are made prior to the application. However, it is very difficult to make *consistent* bias corrections for all meteorological fields at once, which would be required for use in air quality models.

To bypass the use of climate models, an extremely warm summer episode in the present-day climate can be investigated as being representative for an average future summer (Vautard et al., 2007a; Mues et al., 2012). This has the advantage that one can verify the ability of models to represent such conditions with observations (Mues et al., 2012), but in this way it is difficult to look into the variability of the future climate and obtain statistics about extremes. Another way is to directly manipulate the output of a meteorological model to represent expected warmer future conditions (e.g. Im et al., 2011, 2012) and use that as input for the air quality model. The drawback of the latter method is that temperature, precipitation and wind are often modified independently and not in a dynamically consistent way. Therefore, these sensitivity studies can at most be used to identify the most relevant meteorological parameters for air quality, and indicate the possible change due to the change in this meteorological parameter. Since changes due to changes in e.g. temperature, wind and precipitation separately do not simply add up it is only possible to arrive at qualitative results.

Owing to regional biases in global climate models and nonlinear responses of air quality to simulated climate change, results may strongly depend on which climate model is used. The present study aims to provide more insight in this dependency. This is done by using a one-way coupled system consisting of the regional chemistry transport model LOTOS-EUROS and the regional climate model RACMO2. A simulation driven by meteorology from ERA-Interim reanalysis at the boundaries is regarded as reference, best representing the present-day climate. In Manders et al. (2011), the coupled system was compared with LOTOS-EUROS using ECMWF analysis meteorology and observations of concentrations, justifying this approach. Within the EU-Ensembles project RACMO2 participated in an evaluation study in which model output of 16 regional climate models (RCMs) driven by ERA-40 reanalyses was compared with high-resolution daily temperature and precipitation observations in Europe (Kjellström et al., 2010). More recently, RACMO2 simulations forced with ERA-Interim fields have been evaluated with the same set of observations (van Meijgaard et al., 2012). Both studies show that RACMO2 is capable of realistically downscaling re-analyzed meteorology at the 50-km scale, however one should remain aware that local meteorological parameters like wind speed and precipitation derived from (re)analyses should not be used as a substitute for observations. LOTOS-EUROS has been compared with observations for ozone (Curier et al., 2012) and PM (Manders et al., 2009; Mues et al., 2012). In the latter two studies also the dependency of concentration on meteorology has been studied explicitly, showing good general trends but also shortcomings due to species that are not taken into account and flaws in the emissions. Model intercomparison studies (e.g. Vautard et al., 2007b; van Loon 2007; Solazzo et al., 2012) indicate that LOTOS-EUROS is performing very comparable to other models. Since the general performances of

RACMO2 and LOTOS-EUROS separately are assessed comprehensively in the literature mentioned above, output from the coupled system forced with reanalyses will be not compared with observations, but is regarded as the reference in the present article.

Two transient climate runs for the period 1970–2060 have been carried out with the coupled system RACMO2-LOTOS-EUROS. They were driven by boundary conditions from two different GCMs, i.e. ECHAM5 (Roeckner et al., 2003; Jungclaus et al., 2006), henceforth referred to as ECHAM5, and MIROC3.2-hires (K-1 Model Developers, 2004), hereafter referred to as MIROC. Results were complemented by a present-day climate simulation for the period 1989–2009 forced by reanalysis data from ERA-Interim (Dee et al., 2011). Van Ulden and Van Oldenborgh (2006) found that while ECHAM5 and MIROC were both among the five best performing climate models in representing present-day climate conditions in Central Europe, their behavior differs both in terms of zonal mean flow for present-day conditions and in climate change response, which has a strong impact on temperature and precipitation and changes therein.

This study is limited to examining the impact of meteorology only, without feedback mechanisms. Therefore, constant anthropogenic emissions were used in LOTOS-EUROS. However, the impact of meteorology on biogenic and sea salt emissions is included. The presented results are confined to the analysis of long-term average ozone and PM₁₀ concentrations over the European modeling domain, and the present and future relationships between concentrations and temperature. Model output from RACMO2 and LOTOS-EUROS is compared for two 20-yr periods, centered around 2000 and 2050, representing time slices of present-day and future climate conditions.

2 Description of models and method

2.1 RACMO2

RACMO2 is the regional atmospheric climate model of KNMI (Lenderink et al., 2003; Van Meijgaard et al., 2008). The RACMO 2.2 version used for this study consists of the 31r1 cycle of the ECMWF physics package embedded in the semi-Lagrangian dynamical kernel of the numerical weather prediction model HIRLAM (Undén et al., 2002) and a few routines to link the dynamics and physics parts. It has participated in ensemble studies with other regional climate models (Jacob et al., 2007; Christensen and Christensen, 2007), which showed that the regional models did reproduce the large-scale circulation of the global driving model, albeit with biases, and that RACMO2 was not one of the extreme models.

RACMO2 employs a rotated longitude-latitude grid to ensure that the distance between neighboring grid points is more or less the same across the entire domain. For the

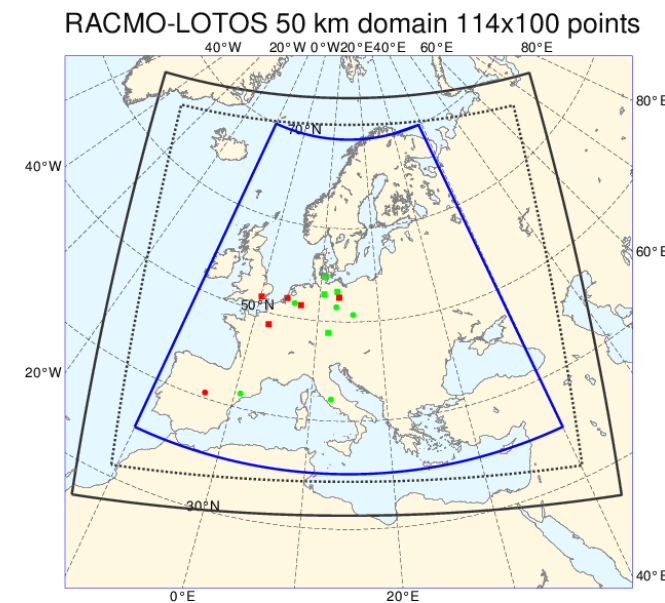
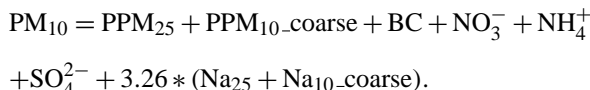


Fig. 1. RACMO domain in black, inner domain dashed, encompassing the LOTOS-EUROS domain (in blue). Points indicate locations that are used in the analyses: red markers indicate cities, green EMEP background locations.

coupled run a RACMO2 domain was configured just encompassing the standard LOTOS-EUROS domain (see Fig. 1). It has a horizontal resolution of 0.44° with 114 points distributed from 25.04° W to 24.68° E longitude and 100 points from 11.78° S to 31.78° N latitude in the rotated grid. The South Pole is rotated to 47° S and 15° E. In the vertical, 40 pressure levels were used. At this resolution RACMO2 uses a model time step of 15 min and output for coupling with LOTOS-EUROS was generated every three hours. The analysis of atmospheric parameters is limited to the interior of the RACMO2 domain, here obtained by omitting an 8-point wide boundary zone.

2.2 LOTOS-EUROS

LOTOS-EUROS is a Eulerian chemistry transport model on the European domain (Schaap et al., 2008). It has participated in model intercomparison studies (Vautard et al., 2007b; Van Loon et al., 2007; Solazzo et al., 2012) and is well evaluated for PM₁₀ in the Netherlands (Manders et al., 2009). It is used for the daily air quality forecast in the Netherlands and part of the MACC ensemble (<http://www.gmes-atmosphere.eu/services/raq/>). Modeled species are ozone, nitrogen oxides, sulfur dioxide, ammonia, primary PM_{2.5} and black carbon, primary PM₁₀ (excluding PM_{2.5} and black carbon), sulfate, nitrate, ammonium and sea salt and species relevant as precursors or reservoir (peroxy-acetyl nitrate, volatile organic carbon). Total PM is defined as:



For (photo)chemical gas reactions a modified CBM IV scheme is used, for secondary inorganic aerosol formation EQSAM (Metzger, 2000) is used.

The regional model is driven by climatological boundary conditions for gases and aerosols. In the present set-up, these boundary conditions were kept constant for consistency, although background concentrations are expected to change. In the present study, anthropogenic emissions for 2005 (MACC 2005 emissions, Kuenen et al., 2011) were used for the whole period to isolate the effect of climate change. Natural emissions of sea salt and isoprene emissions by trees are calculated on-line, as they depend on wind speed (sea salt, Monahan et al., 1986) and temperature (isoprene, Guenther et al., 1993). Dust emissions, forest fire emissions and secondary organic aerosols were not included since they are either too uncertain (secondary organic aerosols), mainly fall outside the domain (dust) or cannot be modeled in a realistic way in a climate run (fire emissions).

The horizontal model domain covered the region 10° W–40° E, 35° N–70° N on a $0.5 \times 0.25^\circ$ regular longitude-latitude grid. In the vertical, five dynamical layers up to 5 km were used, including a static surface layer, and a mixing layer and reservoir layers which vary in time. The horizontal projection of RACMO fields on the LOTOS-EUROS grid was carried out by bi-linear interpolation. The vertical projection of RACMO profiles on the much coarser LOTOS-EUROS vertical grid was achieved by mass-weighted averaging of those RACMO model layers that were contained – fully or partially – in each of the LOTOS-EUROS model layers. Friction velocity and Monin-Obukhov length could be taken from RACMO2 but were recalculated internally in LOTOS-EUROS for consistency with the grid size and land use in LOTOS-EUROS.

For the climate simulations, 3-hourly instantaneous concentrations were stored to reduce the amount of output. Since this may result in missing the daily maximum ozone concentration, this concentration was stored additionally.

2.3 Model runs and analysis method

RACMO2 and LOTOS-EUROS were configured to run side-by-side. Three model runs were performed, with RACMO2 downscaling the following meteorologies:

1. ERA-Interim boundaries, 1 January 1989–31 December 2009,
2. ECHAM5r3 A1B scenario boundaries, transient, 1 January 1970–31 December 2060,
3. MIROC-hires A1B scenario boundaries, transient, 1 January 1970–31 December 2060.

In the text, these runs will be referred to as RLE_ERA, RLE_ECHAM and RLE_MIROC, respectively. Results for the period 1 January 1989 to 31 December 2009 (present-day climate) will be compared to identify biases, and the results for the period 1 January 2041 to 31 December 2060 (future climate) will be compared to the present-day results to study the impact of climate change. Due to the natural variability of the meteorology, it is important to compare long periods. A 20-yr period is chosen to be able to compare with ERA-Interim, although in climate science 30-yr periods are used more commonly.

Exposure to pollutants takes place at ground level. Therefore, this paper considers only ground-level concentrations of ozone and PM_{10} , and their associated meteorology. Climate model output is generally assessed using average temperatures and wind fields. However, these are not the most relevant parameters in studying the impact of climate on ground-level air quality. The following meteorological parameters are considered of particular relevance in relation to air quality:

- Daily maximum surface temperature. High temperatures coincide with high ozone concentrations and both high and low temperatures are often related to stagnant conditions. In particular the number of summer days ($T_{\max} > 25^\circ\text{C}$) is used. For some regions low daily maximum temperatures ($T_{\max} < 5^\circ\text{C}$) are related to stagnant conditions in winter.
- Daily average surface wind speed. Low wind speed is related to stagnant conditions, in particular the number of calm days (daily average wind speed $< 2 \text{ m s}^{-1}$).
- Rain. Rain is related to wash-out of species, in particular the number of wet days. Since wet deposition is a very efficient removal process, the mere occurrence of precipitation is more important than its intensity and duration. To account for unphysical small amounts of drizzle that often occur in climate models, a threshold of 0.5 mm for daily accumulated rain was set.

These meteorological variables are not independent. For example very high and very low daily maximum temperatures are related to low wind speeds and little precipitation on most locations. In addition, working with threshold values can exaggerate differences when there are many days with values around this threshold. Mixing height is an important variable for PM, and is determined by both temperature (convection) and wind (turbulence). In our analysis, it is represented indirectly by the temperature and wind speed.

To analyze long periods, long-term average values and their standard deviations were calculated for surface temperature, surface wind speed, rain and surface PM concentrations. For surface ozone concentrations, the average daily maximum in summer (June, July, August) was calculated. Spatial patterns were investigated, as well as temporal variability at 15 locations (Fig. 1, Table 1). These locations are a

selection of major European cities and background locations (EMEP stations). The concentrations at the background locations will be representative for a relatively large area, however, for the cities they will only be an indication of the local behavior due to the higher concentrations in these areas with high emissions. Results will be illustrated for the locations Vredepeel and Madrid, which have the most contrasting signature in terms of meteorology and air quality. Vredepeel is situated in a rural area in the south-east of the Netherlands, but may be affected by the densely populated Randstad and nearby Ruhr area, and by local farming (in particular ammonia emissions). Its climate is moderate and affected by the sea. In contrast, Madrid is major city, situated in the central highlands in a much warmer and dryer climate. The model system is not able to resolve cities in detail, but since the emissions are high in these areas the concentrations in the model results are clearly elevated. For this reason cities are included in the analysis. For ozone and PM₁₀ the presence of local emission sources can lead to stronger gradients, and Vredepeel has relatively high concentrations for a rural location. Differences in behavior between these two and other analyzed locations will be described qualitatively. For Madrid, Vredepeel and five additional locations, results are presented in more detail. In the Supplement tables with statistics can be found for these locations. In addition to the time averaged values, average relationships between temperature and rain, temperature and wind, temperature and ozone, and temperature and PM₁₀ concentrations have been studied for the time series at these stations to study whether these relationships differ between the forcing GCMs and whether they are affected by climate change. For this purpose, all daily values per station were sorted by daily maximum temperature and subsequently averaged in 50 temperature bins. Since the temperature series differ between model runs and stations, the temperature bins differ as well, but do contain the same amount of data. In addition, histograms (probability density functions) were studied. Examples hereof are shown in the Supplement (Fig. S2).

3 Results: meteorology

The meteorological parameters from RLE.ERA, RLE.ECHAM and RLE.MIROC were compared with each other. For the climate simulations, good day-to-day correlations between temperature, wind and precipitation from RLE.ERA on the one hand and RLE.ECHAM or RLE.MIROC on the other hand cannot be expected. However, for the present-day climate, at least the frequency of occurrence of events and their amplitude should be similar. The mean sea level pressure is an indication of the general circulation and will be discussed first. Then the number of warm days, wet days and calm days will be compared to establish projected shifts in the more extreme conditions. In addition, the average annual cycle for temperature, rain

Table 1. Location of stations for detailed analysis (see also Fig. 1).

Country	station	lon	lat
Denmark	Keldsnor	10.73	54.72
France	Paris	2.35	48.85
Germany	Berlin	13.34	52.54
	Essen	6.96	51.40
	Melpitz	12.92	51.52
	Neuglobsow	13.03	53.14
	Neustadt (Donau)	11.77	48.81
	Waldhof	10.75	52.80
Italy	Montelibretti	12.63	42.10
Netherlands	Vredepeel	5.85	51.53
	Rotterdam	4.48	51.93
Poland	Sniezka	15.73	50.73
Spain	Els Torms	0.71	41.40
	Madrid	-3.70	40.41
United Kingdom	London	0.16	51.50

and wind speed was studied for a number of stations. In the Supplement, the statistics for a selection of locations is summarized.

3.1 General circulation

A first indication of the ability to represent the circulation properly can be derived from the average patterns of mean sea level pressure (mslp). As shown in Fig. 2a, the centers of low pressure during winter in both RLE.ECHAM and RLE.MIROC have shifted to the south compared to RLE.ERA, resulting in a more southerly average position of the Atlantic storm track. In RLE.ECHAM, this shift extends to the whole of Western Europe giving rise to a stronger zonal circulation in this region compared to RLE.ERA. In RLE.MIROC, on the other hand, the center of low pressure is positioned much more to the west over the Central Atlantic which weakens its influence over the European landmass, increasing the likelihood of stagnant conditions over the continent. Figure 2b shows that all simulations feature a prominent Azores anticyclone during summer, as expected. In RLE.ECHAM, the pressure over Northern Europe is on average lower than in RLE.ERA giving rise to a more predominant (north) westerly flow over Western Europe than in RLE.ERA and very stable conditions over the Mediterranean. RLE.MIROC, on the other hand, simulates a higher mslp over Scandinavia and the North-East Atlantic than RLE.ERA which weakens the north-south pressure gradient and reduces the oceanic influence of the weather over the continent. This results in more stable summertime conditions in Northern Europe and relatively more unsettled conditions in Southern Europe as compared to RLE.ERA. Thus, in general, the circulation structures of RLE.ECHAM and RLE.MIROC have mutually different characteristics, and they also differ from those of RLE.ERA. Furthermore, the

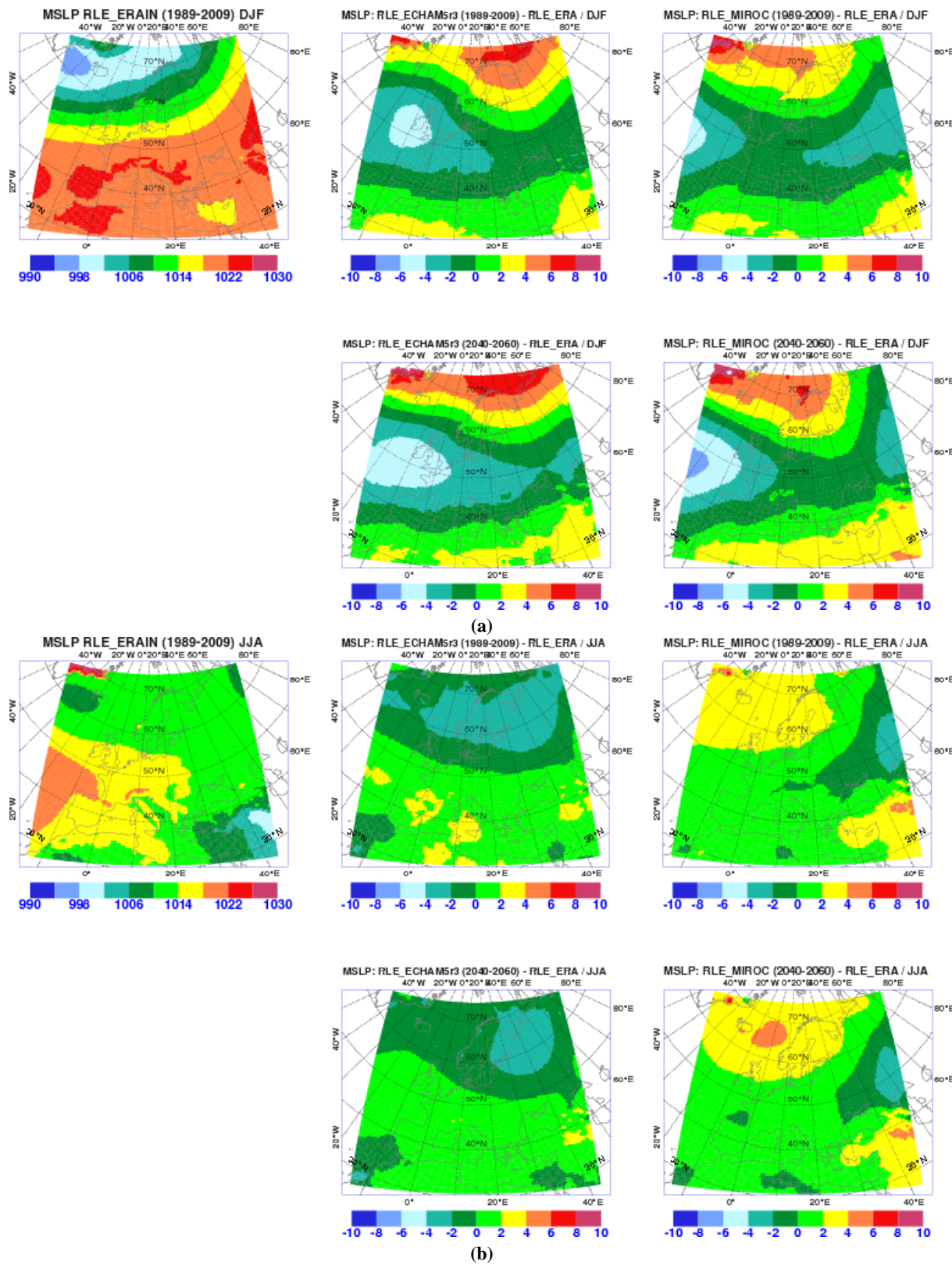


Fig. 2. (a) Top-left panel: average winter (December–January–February) mean sea level pressure (hPa) from RLE_ERA. Central (right-hand) panel: differences in mslp between RLE_ECHAM5 (RLE_MIROC) and RLE_ERA for the present-day climate (1989–2009, top row) and the future climate (2040–2060, bottom row). (b) Like (a) but for summer (June–July–August).

differences between future climate and present-day climate within each of the transient runs are much smaller than the differences between the models. The impact of these general findings on near-surface temperature and wind speed and on precipitation will now be discussed for the present-day and future climate.

3.2 Temperature

For most areas, the average daily maximum temperatures in summer for the present-day climate from RLE_ECHAM are up to 3°C lower (e.g. Vredepeel) than those from RLE ERA, and also the number of days with $T_{\max} > 25^{\circ}\text{C}$ is much lower (Figs. 3, S1, S2 and Table S1a). Differences in annual average daily maximum temperatures between RLE_ECHAM and RLE ERA are smaller than the interannual variability observed in RLE ERA. The differences are larger for the summer period, with the exception of the Spanish locations. In general the differences are significant at the 0.05 level, except for the analyzed locations Els Torms (annual mean) and Madrid (summer mean). In between periods 2000 and 2050, the increase in annual average daily maximum temperature is larger than the interannual variability of this parameter, but for the summer period the increase is of the same order of magnitude as the interannual variability. Both differences are significant at all stations. For North-West Europe, RLE_ECHAM future climate summer temperatures are close to the present-day RLE ERA summer temperatures. Furthermore, the seasonal cycle is weaker: the difference between summer and winter temperatures is smaller than for RLE ERA (Fig. 4). For Spain, the RLE_ECHAM present-day climate temperatures resemble those of RLE ERA more closely and the RLE_ECHAM future climate simulation gives the highest temperatures.

The difference in annual mean and summer mean daily maximum temperature between RLE_MIROC and RLE ERA is smaller than the interannual variability, with the exception of the Spanish stations (Fig. S1). Differences are found significant for all analyzed locations, except for Snieszka, Montelibretti, Paris and Neustadt. The difference between future and present-day annual and summer average daily maximum temperature is larger than the interannual variability for all stations and is significant. Temperatures from RLE_MIROC correspond better to the RLE ERA's present-day summer and summer-winter difference than RLE_ECHAM. However, RLE_MIROC tends to be somewhat warmer than RLE ERA (2 °C) in early summer for North-West Europe. Also in the future climate RLE_MIROC gives a 2 °C higher average summer daily maximum temperature than RLE_ECHAM. However, for Southern Europe RLE_MIROC tends to be the coldest model. In Spain, for example, RLE_MIROC clearly simulates the lowest temperatures in present-day summer, whereas in the future climate the temperatures from RLE_MIROC and RLE_ECHAM become comparable in summer, autumn and early winter. In

future late winter/early spring, RLE_MIROC is warmer than RLE_ECHAM. This is also reflected in Fig. 3, which shows that RLE ERA yields more warm days than RLE_ECHAM in a broad region around 50° N, the Sahara and the Mediterranean, whereas RLE_MIROC is comparable to the run using RLE_ECHAM in North-West Europe, is much warmer than RLE_ECHAM in Russia and parts over the Mediterranean Sea, while it is much colder than RLE_ECHAM in the Mediterranean countries. For the future climate, both simulations show an increase in summer days with a clear north-south gradient, but the changes are much larger for RLE_MIROC than for RLE_ECHAM. Figure S2 clearly illustrates the contrasting behavior of the two simulations for Vredepeel and Madrid, showing differences in both the shape of the distribution and the position of the maximum.

3.3 Precipitation

RLE_ECHAM and RLE_MIROC both produce more precipitation than RLE ERA, with RLE_ECHAM being the wettest almost everywhere (Table S1b). RLE_ECHAM simulates a larger number of wet days in Western Europe than RLE ERA, but it has less wet days near Norway and the Eastern Mediterranean and around the Black Sea (Fig. 5, Table S1b). For RLE_MIROC however, the number of wet days in Northern Europe, north of 50° N, is smaller than for RLE ERA, while it is larger south of this latitude. The difference between future and present-day climate is comparable for the two transient runs, with in the future less precipitation in the Mediterranean area and somewhat more in Central and Northern Europe, with a slightly stronger signal for RLE_MIROC in the Mediterranean. The annual cycle of monthly mean precipitation (Fig. 4) shows the same general pattern for several model runs and time windows. For most locations in North-West Europe (e.g. Vredepeel), the amount of precipitation is relatively constant throughout the year. RLE_ECHAM clearly is the wettest model, with little difference between present-day simulations for the first half of the year and larger differences in the second half. RLE_MIROC is close to RLE ERA for the present-day climate, except for late summer when it is wetter. For the future climate, RLE_MIROC becomes wetter, except for the late summer period. So in a future climate both transient runs generate a wetter spring/early summer and little change in autumn. In South-West Europe, there are regional differences. For Madrid and Montelibretti, there is a clear annual cycle, with dry summer months and a wet winter. RLE_ECHAM 2041–2060 is the most extreme case, with ca. 100 mm more rain in January than in June. RLE_MIROC 1989–2009 shows less variation during the year. In contrast, for Els Torms precipitation is relatively constant throughout the year with a small summer minimum in the RLE ERA and RLE_ECHAM runs, and a summer maximum in RLE_MIROC.

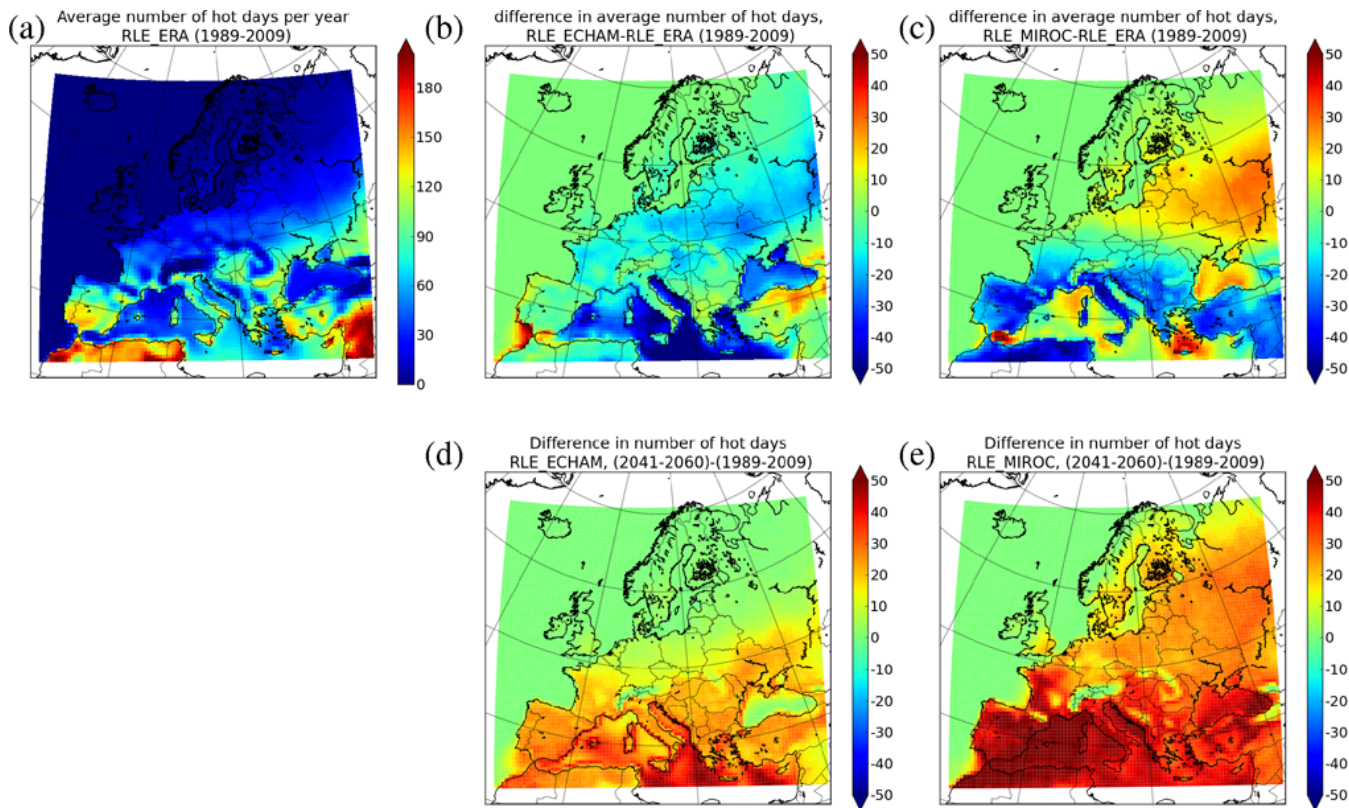


Fig. 3. Average number of summer days ($T_{\text{max}} > 25^{\circ}\text{C}$). (a) Present-day RLE.ERA, (b) difference present-day RLE.ECHAM and RLE.ERA, (c) difference present-day RLE.MIROC and RLE.ERA, (d) difference future climate and present-day climate RLE.ECHAM, and (e) difference future climate and present-day climate RLE.MIROC.

3.4 Wind speed

According to the model, 10-m wind speed in mountainous regions is in general lower than in flat areas at lower elevations. This is clearly illustrated by the spatial distribution of the annual mean number of calm days for RLE.ERA in Fig. 6. This behavior is caused by the high value of surface roughness length for momentum associated with mountainous terrain. While the contrast in number of calm days between flat and mountainous areas might not be confirmed by observations we want to emphasize that this study deals with differences or changes in parameters, and not with their absolute values. All 10-m wind speed output has been obtained with the same surface roughness map which considerably helps in the interpretation of the relative differences.

For the present-day climate, the number of calm days for RLE.ECHAM is comparable to that for RLE.ERA in Northern Europe, however, in Central and Southern Europe, and at the eastern boundary of the domain RLE.ECHAM predicts less calm days than RLE.ERA (Fig. 6). RLE.MIROC tends to simulate more calm days than RLE.ERA, except in North-West Africa and at the eastern boundary of the domain. The difference between future and present-day climate is small in both transient simulations: less than 10 days

on average in the RLE.ECHAM run, and slightly more for RLE.MIROC, which predicts there will be more calm days in larger areas in the future climate, although there are local exceptions. The annual cycles of wind speeds are similar for all runs and periods (Fig. 4). For North-West Europe (e.g. Vredepeel), RLE.ERA is in between RLE.ECHAM (more wind) and RLE.MIROC (less wind). The largest differences occur in summer which is the period with lowest wind speed (Fig. 4). Furthermore, in Vredepeel, also the differences between the present-day and future climate time series are small. For Southwestern Europe (e.g. Madrid, Els Torms), wind speeds tend to be lower, and are nearly constant throughout the year for RLE.ERA except for a weak late winter/spring maximum. The transient simulations show a stronger annual cycle, with more wind in (late) winter/early spring than RLE.ERA but in summer their wind speeds are close to those of RLE.ERA. RLE.ECHAM deviates most from RLE.ERA. Again, the difference between present-day and future average wind speed is very small in both transient simulations. For other locations in South Europe (Montelibretti) the behavior is similar, with a slightly stronger annual cycle.

For all investigated meteorological parameters, the observed differences are not just shifts in amplitude, but also

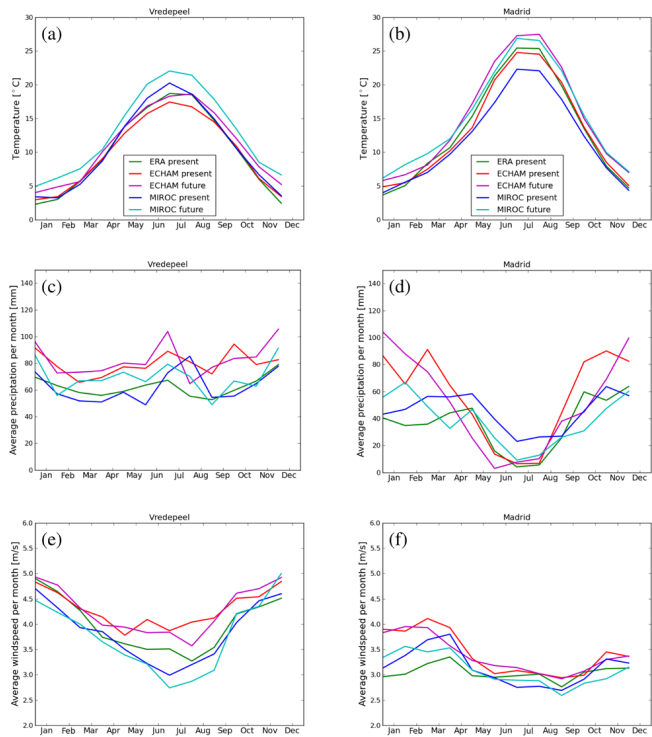


Fig. 4. Average annual cycles of monthly mean values for daily maximum temperature (**a, b**), monthly mean precipitation (**c, d**) and monthly mean wind speed (**e, f**) at Vredepeel (left) and Madrid (right) derived from various downscaling experiments with RACMO2.

shifts in the spatial patterns. The results are consistent with the conclusions derived from a comparison of global model simulations for present-day climate conditions by Van Ulden and Van Oldenborgh (2006). ECHAM5 predicted less easterly flow than observed for present-day climate, whereas MIROC tended to be more stagnant, which has a direct impact on temperature and rain. The output from two global models was rather consistent concerning the simulated change in annual mean temperature across Europe, but the models differed considerably in seasonality.

4 Results: concentrations of ozone and PM₁₀

4.1 Present-day climate

For ozone, the summer average daily maximum (June–July–August) was studied (Fig. 7a, Fig. S1). RLE_ERA shows a general north-south gradient. Ozone concentrations are highest above the Mediterranean Sea (up to $150 \mu\text{g m}^{-3}$), followed by lower concentrations ($110 \mu\text{g m}^{-3}$) in industrial areas in southern Europe (Po Valley, around Porto, Rhone delta) and in Central Europe. Figure 7b shows that PM₁₀ concentrations are highest in densely populated and industrialized areas (The Netherlands, Ruhr area, Po Valley, Poland

and major cities) and above the sea, due to the high local contribution of sea salt. Lowest concentrations are found above Scandinavia, Eastern Europe, Balkan, Ireland, Scotland, parts of Spain and Northern Africa. The low concentrations are partly unrealistic, since no dust and secondary organic aerosol (SOA) was taken into account. SOA may contribute significantly to PM in large parts of Europe (e.g. Gelencsér et al., 2007; Bergström et al., 2012), depending on anthropogenic and biogenic emissions and on the oxidative capacity of the atmosphere. Saharan dust mainly affects the Mediterranean area.

For the present-day climate, summer ozone concentrations in the RLE_ECHAM run are up to $12 \mu\text{g m}^{-3}$ lower than in the RLE_ERA run in a large part of the domain (Fig. 8a, Fig. S1), in particular in North-West Europe, the Baltic Sea region and the Mediterranean area. Only in a few small areas at the southern boundary of the domain, RLE_ECHAM yields higher concentrations than RLE_ERA. For RLE_MIROC it is the other way around, with concentrations of up to $12 \mu\text{g m}^{-3}$ higher in North-West Europe and some areas around the Mediterranean Sea. The differences in ozone concentration between the present-day transient runs and RLE_ERA are not clearly correlated with the spatial pattern of the ozone concentration from RLE_ERA, indicating a shift in patterns rather than just differences in amplitude. This is consistent with the notion that changes in meteorological conditions can (in part) be associated to changes in patterns. The difference in ozone concentration between the transient runs and RLE_ERA can only partly be related to the patterns of number of summer days, since the sensitivity of ozone to temperature depends on the location and the temperature, as will be illustrated further on. Relative differences (not shown) have a spatial pattern that follows the pattern of absolute differences. Over sea, differences with RLE_ERA concentrations are up to 20 % for both RLE_ECHAM and RLE_MIROC, in particular at the ship tracks. Over land, the relative differences are less than 10 %. For RLE_ECHAM, the difference with RLE_ERA is larger than the interannual variability, except for the Spanish locations, and was significant at all analyzed locations. For RLE_MIROC the differences with RLE_ERA tend to be smaller than the interannual variability (Fig. S1), although they were significant at most locations (not significant at Madrid and Montelibretti). The probability distribution function (pdf, Fig. S2) for Vredepeel falls off more steeply for RLE_ECHAM than for RLE_ERA and RLE_MIROC. In addition, concentrations between 100 and $150 \mu\text{g m}^{-3}$ occur more often for RLE_MIROC, though for higher concentrations the curves of all three simulations are close together for Vredepeel. This behavior is observed for all stations in North and Central Europe. For Madrid all curves decrease very rapidly for concentrations of more than $80 \mu\text{g m}^{-3}$. For Montelibretti and Els Torms the decrease is not as steep but the curves are also closely together for concentrations above $110 \mu\text{g m}^{-3}$, albeit with at Els Torms a

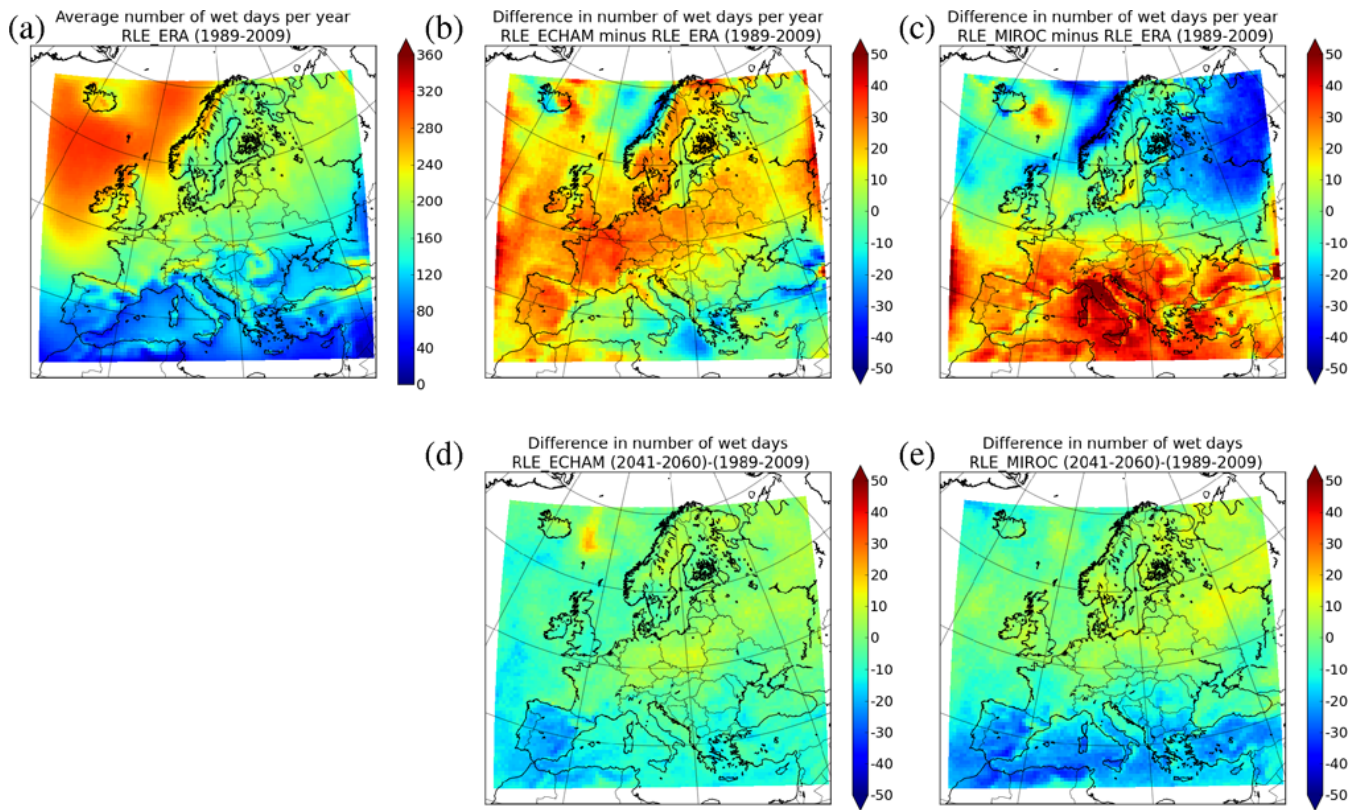


Fig. 5. Like Fig. 3, but showing the average number of wet days.

local maximum just below $100 \mu\text{g m}^{-3}$ for RLE_ERA and RLE_ECHAM and just above it for RLE_MIROC.

Over land, simulated total PM₁₀ concentrations in the present-day part of both transient runs are lower than in the RLE_ERA run. RLE_ECHAM differs much more from RLE_ERA than RLE_MIROC, with the exception of specific locations in Russia (Fig. 9). The spatial pattern of differences in PM₁₀ concentrations between RLE_ECHAM and RLE_ERA can be related to the spatial pattern of the (reduced) number of calm days (Fig. 6), reflecting the relationship between high PM concentrations and low wind speed (Manders et al., 2009, 2011), although also precipitation will play a role. For RLE_MIROC, the differences are smaller and the increase in number of wet days may contribute more to the lower PM₁₀ concentrations seen in this simulation than the changes in number of calm days. Over sea, the difference in total PM₁₀ is particularly large, and can easily be related to wind-generated sea salt. The generation of sea salt aerosol depends strongly on the 10m wind speed (Monahan et al., 1986). Above the Northern seas, RLE_MIROC tends to have lower wind speeds (not shown) than RLE_ERA and RLE_ECHAM, leading to reduced sea salt emissions. In the Mediterranean area, the wind speed tends to be lower in RLE_ERA than in RLE_ECHAM and RLE_MIROC (less calm days, Fig. 6, wind speeds for Els Torms, Table S1c), leading to more sea salt genera-

tion in the latter simulations. In RLE_ECHAM this effect is reinforced by a decrease in number of wet days, leading to less wet deposition, whereas in RLE_MIROC the increase in precipitation partly counterbalances the increase in sea salt aerosol production so that the concentration differences with RLE_ERA are smaller for RLE_MIROC than for RLE_ECHAM. Relative differences between the transient runs and RLE_ERA (not shown) of up to 25 % are found. The relative differences follow the spatial patterns of the absolute differences, except for Scandinavia where very low PM concentrations and large relative differences are found. The differences between RLE_ERA and RLE_ECHAM are equal to or larger than the interannual variability, while for RLE_MIROC the differences are smaller than the interannual variability (Fig. S1). For RLE_ECHAM, the differences were significant at nearly all analyzed stations (except for Neuglobsow and Keldsnor), while for RLE_MIROC they were not, except for Madrid, Els Torms and Montelibretti (and Waldhof, Neustadt and Keldsnor). The probability distribution plot of Vredepeel (Fig. S2) is clearly shifted towards the lower concentrations for RLE_ECHAM when compared with RLE_ERA and RLE_MIROC. For most other rural stations the differences between the models are very small and the pdf was narrow, reflecting the low concentrations except for Keldsnor which showed two maxima. For Madrid, RLE_ECHAM has a pdf with a maximum at $12 \mu\text{g m}^{-3}$, i.e.

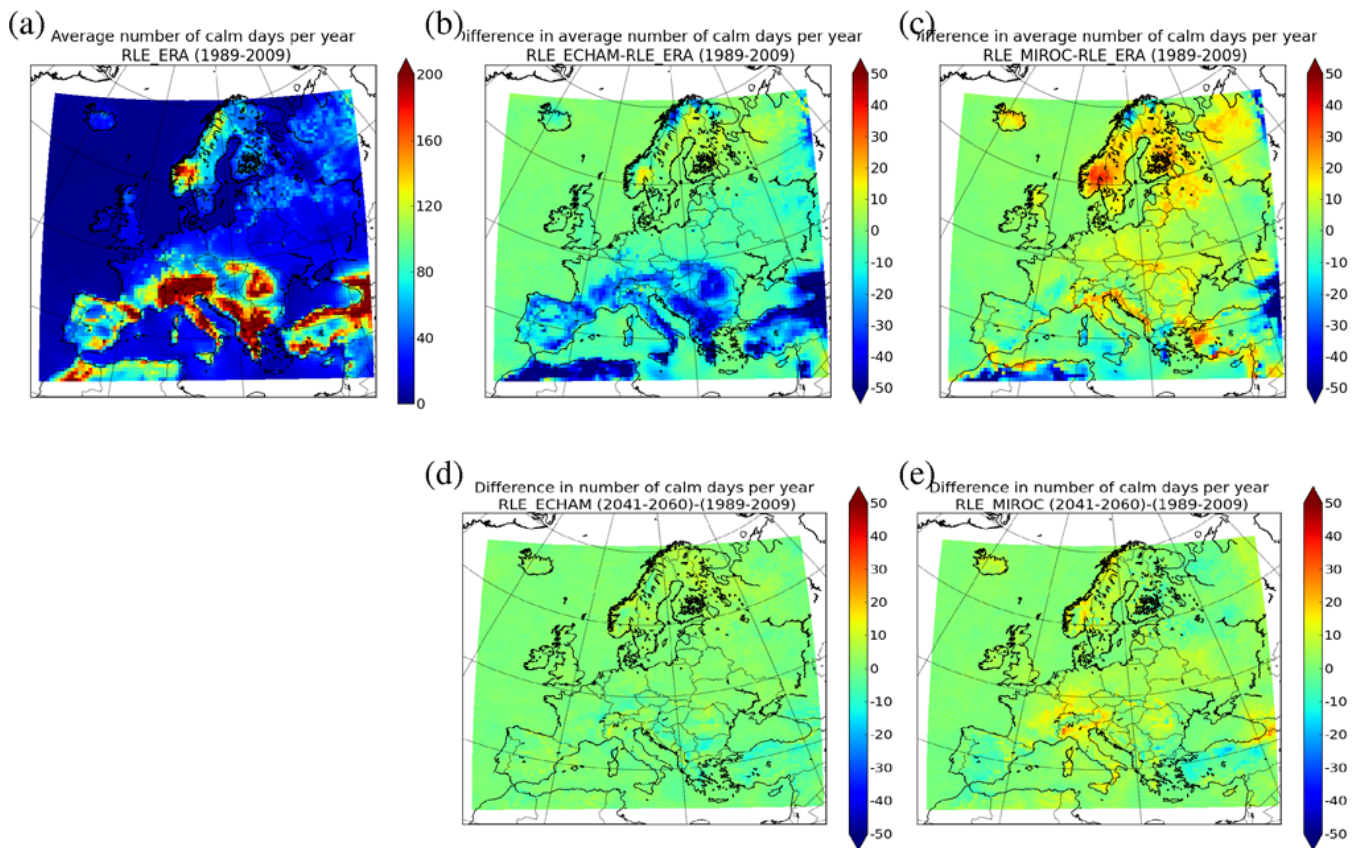


Fig. 6. Like Fig. 3, but showing the average number of calm days.

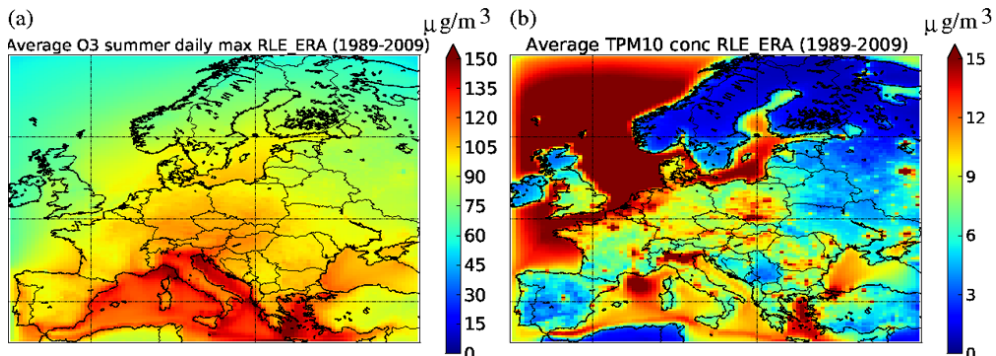


Fig. 7. Average O₃ daily maximum concentrations (June–July–August) (a) and annual average total PM₁₀ concentration (b) obtained with RLE_ERA (1989–2009).

at lower concentrations than RLE_ERA and RLE_MIROC, and without the second maximum at $22 \mu\text{g m}^{-3}$ displayed by RLE_ERA and RLE_MIROC. For Els Torms, the pdfs of RLE_ECHAM and RLE_ERA are shifted towards slightly lower concentrations compared to the pdf of RLE_ERA. For Montelibretti the location of the maximum is the same for the three simulations, but the distribution is much narrower for RLE_ECHAM and wider for RLE_MIROC.

4.2 Concentration changes due to climate change

Both RLE_ECHAM and RLE_MIROC show an increase in average O₃ summer maximum concentrations in the future, with values of up to $12 \mu\text{g m}^{-3}$ higher than in the present-day climate (Fig. 8). These differences are found over much larger areas in the RLE_MIROC than in the RLE_ECHAM simulation. This is consistent with Fig. 3, which illustrates that the increase in average maximum

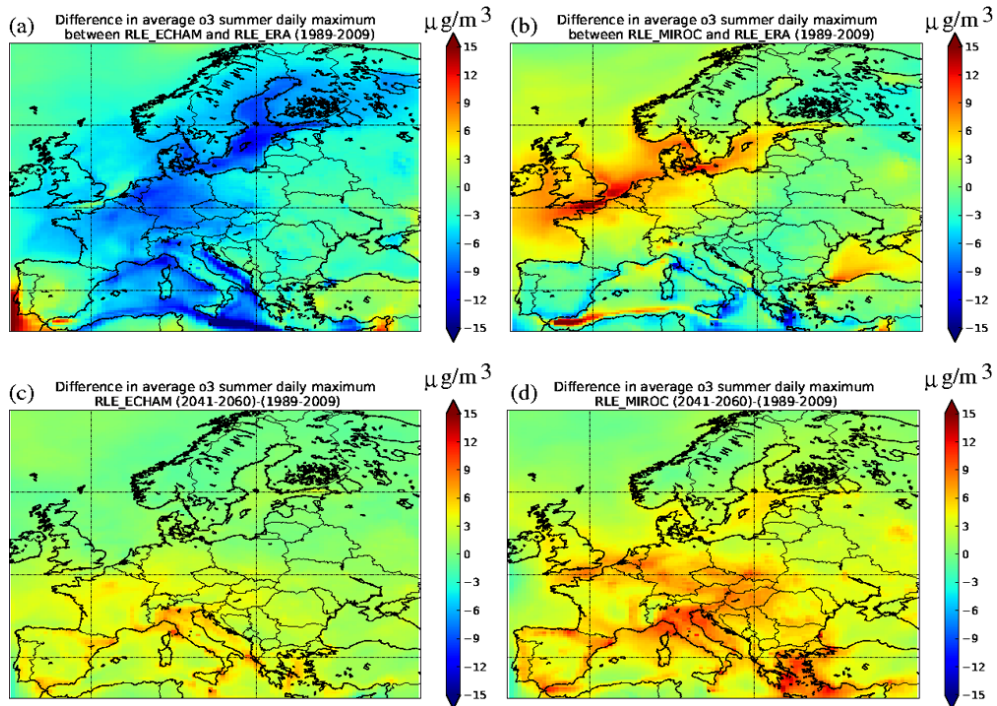


Fig. 8. Differences between 20-yr O₃ average daily maximum concentrations (June-July-August) in $\mu\text{g m}^{-3}$. Upper panels: (a) differences between present-day climate RLE_ECHAM and RLE ERA and (b) between present-day climate RLE_MIROC and RLE ERA. Lower panels: difference between future climate and present-day climate for (c) RLE_ECHAM and (d) RLE_MIROC.

temperature is larger and more widespread in RLE_MIROC than in RLE_ECHAM, leading to larger responses in ozone concentration. Moreover, the change in ozone concentration with temperature depends on the region since it is dependent on the availability of NO_x and VOC, so that the same temperature changes may lead to different changes in concentration for different regions. This point is further illustrated in the next section. Relative differences with the present-day climate simulation are up to 5 % for RLE_ECHAM and up to 10 % for RLE_MIROC. Again, the patterns of the relative differences closely follow those of the absolute differences. For RLE_ECHAM, the difference in ozone concentration between future and present-day climate is smaller than the interannual variability in Northern Europe and approximately equal to the interannual variability in Southern Europe. Differences are found significant for most locations in Fig. 1, except for Rotterdam and London and the EMEP locations Neuglobsow and Keldsnor. For RLE_MIROC the difference in ozone concentration induced by climate change is larger than the interannual variability (Fig. S1) and significant for all locations. For both Vredepeel and Madrid, the shift in temperature probability distribution is reflected in the frequency distribution of ozone (Fig. S2), with largest differences between future and present-day climate for RLE_MIROC. In all cases there is a clear extension of the tail of the pdf towards higher concentrations.

Differences in PM₁₀ concentrations between future and present-day climate are rather small. For RLE_ECHAM, concentrations are up to $2 \mu\text{g m}^{-3}$ lower above the Atlantic, east of Norway, which could be a combined effect of more precipitation in that region in the future climate (more wet deposition) and lower wind speeds (less sea salt generation). Differences over the continent are very small (less than $0.5 \mu\text{g m}^{-3}$), except for a small area around Moscow, where concentrations have decreased by more than $2 \mu\text{g m}^{-3}$. For the RLE_MIROC run, differences above the continent are somewhat larger but still small: concentrations increase up to $0.7 \mu\text{g m}^{-3}$ in the Netherlands and the North-East of Spain, and up to $2 \mu\text{g m}^{-3}$ in the Po Valley, while, again, the concentration decreases distinctly around Moscow. Relative differences are less than 10 % for RLE_ECHAM and up to 10 % for RLE_MIROC, with patterns related to the patterns of absolute differences. Only for Scandinavia the small absolute differences still yield large relative differences. For both RLE_ECHAM and RLE_MIROC the changes in PM₁₀ concentrations associated with climate change are found smaller than the present-day interannual variability derived for the analyzed locations (Fig. S1). These changes in PM concentration (future-present) are not significant at most analyzed locations, except for Sniezka, Keldsnor, Neuglobsow and Neustadt (RLE_ECHAM) and Vredepeel (RLE_MIROC). For RLE_MIROC, the PM₁₀ pdfs at Melpitz, Neuglobsow and Berlin change in shape from a single maximum for the

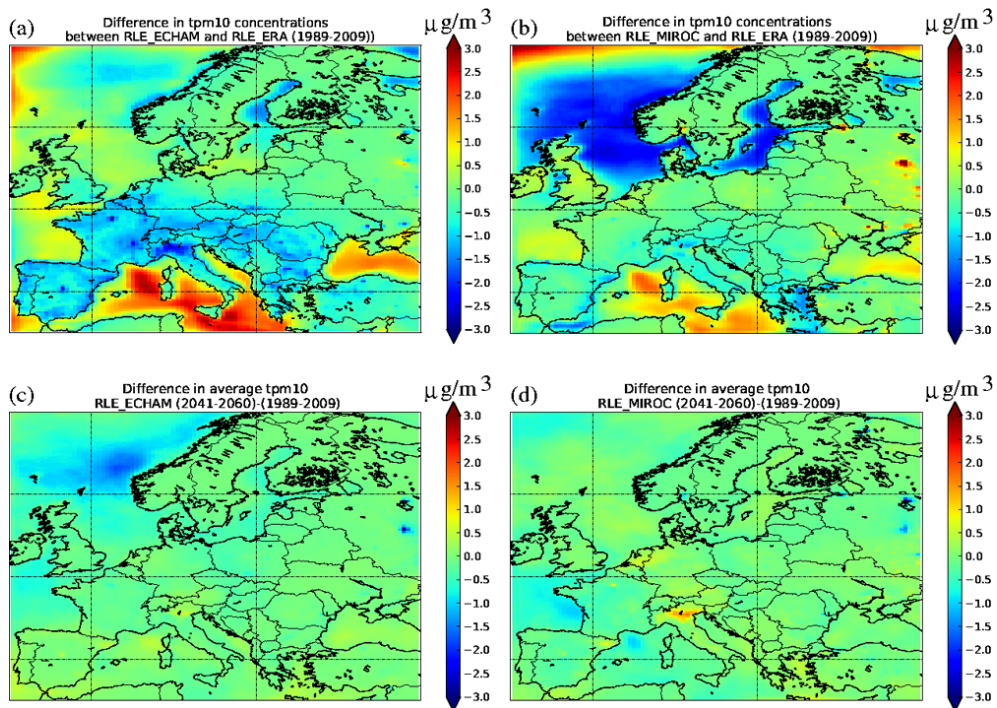


Fig. 9. Like Fig. 8, but showing differences between 20-yr total PM_{10} concentrations.

present-day to two maxima for the future climate (one at lower and one at higher concentrations), while the pdf at Madrid shows the opposite change (from two maxima to a single maximum). For other stations and for RLE_ECHAM, the shape of the pdf and the location of the maximum did not change clearly.

4.3 Changes in average correlations between temperature and ozone or PM_{10} concentrations

The average relationships between ozone or PM_{10} concentrations on the one hand and temperature on the other hand have been investigated for several sites. The results are again illustrated for Vredepeel and Madrid (Fig. 10). For each site the general tendencies are similar for the different model simulations, but there are notable differences between the various sites.

For ozone the relationship with temperature is very distinct and has little scatter. There is a gradual increase with temperature, but the slope is not constant with temperature and differs between locations. For Vredepeel, for example, the slope seems to become somewhat steeper for temperatures above 20°C , whereas for Madrid the figure shows a leveling-off for temperatures above 20°C . The value of the slope also differs slightly between model runs. Madrid shows the largest contrast with Vredepeel. The highest ozone concentrations in Madrid are nearly $40 \mu\text{g m}^{-3}$ lower than in Vredepeel, in spite of the higher temperatures. The summer average concentrations are highest at Montelibretti, but the maximum

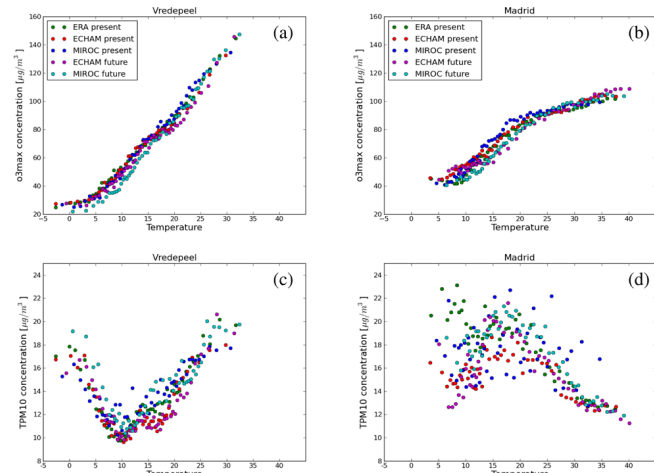


Fig. 10. Average relationship between either (a, b) ozone daily maximum or (c, d) total PM_{10} from LOTOS-EUROS and daily maximum temperature ($^\circ\text{C}$) for the meteorologies downscaled with RACMO.

ozone concentrations at that site are not higher than those observed at Vredepeel. This does not contradict the general north-south gradient in mean O_3 concentrations with high concentrations in the south, since the high temperatures favoring high ozone concentrations occur more frequently in the south. The leveling-off observed at Madrid is not seen to this extent at the other locations, like Montelibretti or

Paris. The difference in slope between the locations can probably be attributed in part to the local NO_x/VOC ratio. In the Netherlands, NO_x concentrations are generally high and ozone production is assumed to be VOC-limited. Here, increased VOC emissions from trees at higher temperatures accelerate the increase in ozone concentrations, leading to a steeper increase of ozone concentration with temperature. In contrast, on the Iberian Peninsula, the ozone formation is generally assumed to be NO_x-limited, so that the biogenic VOC production at higher temperatures would not lead to additional ozone formation, and here, a deep boundary layer associated to fair weather may result in more dilution. Moreover, for Madrid the local NO_x emissions contribute to the local destruction of ozone (titration).

Total PM₁₀ concentrations at Vredepeel show a minimum value around a daily maximum temperature of 10 °C. For Madrid the curve is the other way round: PM₁₀ concentrations are highest around 17 °C, with linear decreases for both higher and lower temperatures, except for the coldest days which have relatively high concentrations. In contrast, for Els Torms (not shown) PM₁₀ shows little variation with temperature while concentrations are considerably lower. There may be several causes for these differences. First of all, the differences can be caused by the relationships of wind speed and precipitation with temperature at the sites. At Vredepeel, higher wind speeds (mixing) and more precipitation (wet deposition) occur at temperatures around 12 °C, explaining the PM minimum at this temperature. In contrast, for Madrid high wind speeds and precipitation are associated with nearly the lowest temperatures (not shown). The decrease in PM₁₀ concentration for higher temperatures is counter-intuitive, since at these temperatures wind speeds and precipitation are generally lower than on average. However, at high temperatures the mixing layer is expected to be deeper, leading to more dilution. The effect may in part be due to the relatively coarse grid resolution, which may result in considerable dilution of the Madrid emissions since it is surrounded by areas with low emissions and concentrations. In this case, the results may strongly depend on the wind direction, which we did not take into account in our analysis since it is a local relationship. An indication for this is the large scatter in PM₁₀ for Madrid. Another cause may be the contribution of the different components of PM₁₀ (not shown). In Vredepeel, ammonium and nitrate concentrations are higher than at other locations used in the analysis, due to nearby ammonia emissions from intensive farming. There, temperature-dependent reactions involving secondary inorganic aerosol and the volatility of ammonium nitrate may have an impact. In contrast, in Madrid the inert black carbon contributes most to PM₁₀ and concentrations are determined more directly by dilution, transport and deposition. For other locations the behavior is somewhat in-between the illustrated results, with in general higher PM values for lower temperatures, a minimum for temperatures around 15 °C, however, the increase in PM concentration with temperature at high temperatures

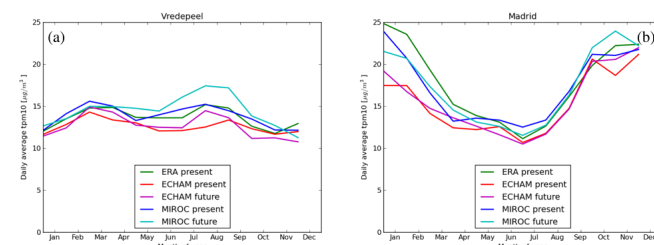


Fig. 11. Simulated daily mean PM₁₀ concentrations for Vredepeel (a) and Madrid (b) averaged over 20 yr.

was not reproduced everywhere. For Els Torms, for example, PM₁₀ concentrations vary little with temperature. However, the underlying modeled species at this site do show clear trends with temperature: the ammonium concentration increases with increasing temperature, while the concentration of black carbon decreases with increasing temperature (not shown). Such relationships can not be generalized and depend on the local relative contributions of the PM components. In addition, the large scatter indicates that the relationship between PM and meteorology is complex and that using only temperature as a proxy for meteorological conditions does not suffice to explain all observed variation.

Maximum ozone concentrations are reached in summer since ozone is formed by photochemical reactions. For PM₁₀, the annual cycle depends on the exact composition which varies per location. To investigate the annual cycle and in which periods the impact of climate change is largest, we analyzed the 20-yr records of simulated monthly means of daily mean PM₁₀ concentrations, which are shown for Vredepeel and Madrid (Fig. 11). PM₁₀ concentrations tend to be lowest in summer. Some locations show distinct periods of higher concentrations in spring/autumn (Melpitz, Els Torms), while others show a more gradual increase in the winter half year. For Madrid, high PM₁₀ concentrations are a winter phenomenon. The highest concentrations are seen in the RLE.ERA run, which has the lowest wind speeds and the least amount of precipitation in the winter months. Vredepeel however, has rather high PM₁₀ concentrations in early spring and late summer. This can be related partly to the relatively high ammonia emission in this area in these periods, and partly to wind speed, in particular for the RLE.MIROC future climate, which has the lowest wind speeds in late summer. Both RLE.MIROC and RLE.ECHAM show that PM₁₀ concentrations may increase due to climate change for late summer in Vredepeel. For Madrid, RLE.MIROC and RLE.ECHAM predict concentration changes of up to 2 µg m⁻³ due to climate change, but with opposite signs: future PM₁₀ concentrations will decrease according to RLE.MIROC and increase according to RLE.ECHAM. Most other rural locations that were analyzed show maximum concentrations in early spring and autumn, with a negligible impact of climate change. Figure 11 shows

that differences in annual mean concentrations between the runs and periods can be lower than the differences in monthly mean concentrations, and that the main impact of climate change may be observed in a specific season, depending on the region.

5 Discussion and conclusions

Two long-term climate simulations have been performed with the one-way coupled system RACMO2-LOTOS-EUROS, using meteorological boundary conditions from two different GCMs to study the impact of climate change on air quality. In addition, a 21-yr present-day simulation was performed using boundary conditions from reanalysis meteorology, which served as a reference for the present-day period air quality modeled by the two climate simulations. The two climate simulations using ECHAM and MIROC forcings differ significantly from the reference using ERA-Interim but also from each other, primarily owing to the differences in circulation patterns (meteorology).

The results of the two long-term simulations were used to compute the difference in air quality between the present-day (1989–2009) and the future climate (2041–2060). The difference in meteorology between future and present-day climate is mainly a considerable increase in temperature, whereas the circulation pattern, rain and wind show only a modest change. The increase in temperature yields an increase in mean daily summer maximum ozone concentrations of up to $12 \mu\text{g m}^{-3}$. Above the Northern Atlantic mean PM_{10} concentrations are up to $1\text{--}2 \mu\text{g m}^{-3}$ lower in future than in the present day climate. Over the continent changes are around $0.5 \mu\text{g m}^{-3}$, with positive changes over the Netherlands, North-West Germany, North-East Spain and the Po valley. Results from the two simulations are in agreement regarding general response (general increase in ozone concentration, weak response of PM_{10}), however, there are considerable differences in absolute values and between regions. For some regions the two models did not even agree on the sign of the change in PM_{10} . However, at most locations changes in PM_{10} are not significant.

The results obtained in this paper cannot be compared with results from literature in a straightforward way, due to the differences in metrics used (e.g. average 8-h maximum, averages over April–September, AOT40), the difference in time windows (most used are 1961–1990, 2071–2100), and differences in climate scenario (A2, A1B). Nevertheless, the results of this study appear to be generally in line with European studies (e.g. Giorgi and Meleux 2007, up to 10 ppbv difference in mean daily summer ozone concentrations, Andersson et al., 2009, up to 7 ppbv difference in mean daily maximum O_3 with future climate representing 2021–2050, Carvalho et al., 2010 are at the high end with up to $50 \mu\text{g m}^{-3}$ difference in monthly mean O_3 concentrations) and US studies (see the overview by Jacob and

Winner, 2009). For PM, usually annual or seasonal means are reported, sometimes given per component, with both increases and decreases of up to 10 %, or less than $1 \mu\text{g m}^{-3}$ (Jacob and Winner, 2009). Thus our results comply with results from literature. However, they also indicate a considerable sensitivity to the choice of the global climate model that serves as a driver for the air quality simulations.

The changes in concentrations of ozone and PM_{10} can be related to changes in temperature, i.e. daily maximum temperature, and to a lesser extent to changes in precipitation and wind speed. Average relationships between concentrations and temperature differ slightly between the different simulations and time windows. This implies that average relationships for the present-day climate cannot be directly extrapolated to the future. Furthermore, changes are not uniform over the year. High ozone concentrations are clearly a summer phenomenon but for PM_{10} the seasonal behavior is less uniform. In the Netherlands, for example, an increase in summertime PM_{10} seems a robust feature, but for other seasons the changes appear smaller. For Madrid, on the other hand, the model simulations indicate that high PM_{10} concentrations are mainly a winter phenomenon. This implies that although one could in principle carry out a bias correction for the portion of the climate simulation that represents the present-day climate, this bias correction would only be valid locally and would only be applicable to the future climate to a limited extent.

The meteorological parameters from both climate simulations (RLE_ECHAM and RLE_MIROC) differ considerably from those of the reanalysis-driven simulation RLE_ERA for the period 1989–2009, depending on the season and region, even though both ECHAM5 and MIROC are among the better-performing global climate models (Van Oldenborgh, 2006). These differences have a substantial impact on the modeled ozone and PM_{10} concentrations. For the RLE_ECHAM run, differences in modeled concentrations between future and present-day climate are smaller than the differences in present-day climate between RLE_ECHAM and RLE_ERA. In the RLE_MIROC simulation, the differences between future and present-day climate are of the same order of magnitude as the present-day differences between the simulations of RLE_MIROC and RLE_ERA. Yet, differences between either RLE_ECHAM or RLE_MIROC and RLE_ERA have divergent characteristics, illustrating the uncertainties in the global climate models. Results from a single transient simulation should therefore be interpreted in a qualitative rather than a quantitative way, merely as an illustration of one out of many possible climate change realizations. The two simulations analyzed in this paper show differences, but also consistent changes related to climate change. Nevertheless, ideally an ensemble approach should be taken, with ensemble members from different GCMs and different regional climate models.

In this paper only the impact of differences in meteorology has been considered. However, chemistry transport models

also have biases, and an ideal ensemble should include several CTMs as well. LOTOS-EUROS underestimates the daily ozone maximum (Curier et al., 2012). In particular the highest ozone peaks ($180 \mu\text{g m}^{-3}$) are underestimated by 10–20 $\mu\text{g m}^{-3}$. It also underestimates total PM₁₀, especially in summer (Manders et al., 2009). In Mues et al. (2012) the relation between temperature and PM₁₀ concentrations was investigated for LOTOS-EUROS and compared with observed concentrations. The observed increase in PM concentrations with temperature was not represented to the same extent by the model. For winter periods, during which PM is mainly determined by ventilation effects, the behavior is fairly good, but for summertime conditions the model is not performing adequately. LOTOS-EUROS lacks a good description of SOA, which may contribute significantly (typically up to a few $\mu\text{g m}^{-3}$) in summer through the temperature dependency of biogenic emissions and the dependency on photochemistry (oxidation) and volatility (Donahue et al., 2009 and references therein). Windblown dust will be more important under warmer and dryer conditions, in particular in Southern Europe, but is currently not taken into account. Furthermore, the contribution of forest fire emissions is not modeled. Forest fires can contribute significantly to ozone and PM concentrations during fire episodes and can cause serious and acute local air quality problems. Through long-range transport of emissions, forest fires have an impact on atmospheric conditions at distances of hundreds of kilometers away from the fire, not only on the concentrations but also on the radiation budget and atmospheric stability (e.g. Hodzic et al., 2007; Saarikoski et al., 2007). The emissions of forest fires are expected to increase for a warmer climate in the Mediterranean area (e.g. Moriondo et al., 2006). Therefore we must state that the changes in concentration in response to changes in meteorology as considered in this study are probably an underestimation of the impact of climate change on air quality.

In the present study, anthropogenic emissions have been kept constant at the 2005 level to focus on the impact of meteorology. The interannual variability in concentration is largely due to meteorological variability rather than interannual variability in emissions (Andersson et al., 2007), but the effect of changes in emissions between 2000 and 2050 on the long-term average concentrations may be as large as or even larger than the effect of climate change (Tagaris et al., 2007). Not only the amount of emissions, but also their timing may change due to changes in energy sources and in human activity patterns. The increase of observed elemental carbon concentrations with higher temperatures was not reproduced by LOTOS-EUROS (Mues et al., 2012), which may indicate an effect of meteorology on anthropogenic emissions. Emission scenarios should be taken into account when assessing air quality for a future period, in particular for the strong emission reductions expected for Europe for the coming decades.

Other sources of uncertainty in the interactions between climate change and air quality are the boundary conditions, enhanced stratosphere-troposphere exchange and

higher background levels. Andersson et al. (2009) conducted an impact study, and Hogrefe et al. (2011) studied the uncertainties associated with chemical boundary conditions from a global model, showing that the interannual variability was underestimated when time-invariant boundary conditions were used. Also land use changes may be relevant as they affect deposition efficiencies and biogenic emissions, although their effect may be small. And last but not least, two-way interactions between concentrations of species and the radiation budget of the atmosphere should be taken into account (Zhang et al., 2010). Unfortunately, most present-day coupled models are not capable of performing long-term climate studies due to the large computational effort that would be required. A two-way coupling approach with relatively modest computational demands is currently being realized in the RACMO2-LOTOS-EUROS system.

Supplementary material related to this article is available online at: <http://www.atmos-chem-phys.net/12/9441/2012/acp-12-9441-2012-supplement.pdf>.

Acknowledgements. This project was supported by the Dutch Knowledge for Climate Programme. We thank two anonymous reviewers for their constructive comment.

Edited by: P. Jöckel

References

- Andersson, C.: Air pollution dependency on climate variability and source region, PhD Thesis, Stockholm University, 2009.
- Andersson, C., Langner, J., Bergstrom, R.: Interannual variations and trends in air pollution over Europe due to climate variability during 1958–2001 simulated with a regional CTM coupled to the ERA-40 reanalysis, Tellus 59B, 77–98, 2007.
- Bergström, R., Denier van der Gon, H. A. C., Prévôt, A. S. H., Yttri, K. E., and Simpson, D.: Modelling of organic aerosols over Europe (2002–2007) using a volatility basis set (VBS) framework: application of different assumptions regarding the formation of secondary organic aerosol, Atmos. Chem. Phys., 12, 8499–8527, doi:10.5194/acp-12-8499-2012, 2012.
- Carvalho, A., Monteiro, A., Solman, S., Miranda, A. I., and Borrego, C.: Climate-driven changes in air quality over Europe by the end of the 21st century, with special reference to Portugal, Environ. Sci. Policy, 13, 445–458, 2010.
- Christensen, J. H. and Christensen, O. B.: A summary of the PRUDENCE model projections of changes in European climate by the end of this century, Climate Change, 81, 7–30, 2007.
- Curier, R. L., Timmermans, R., Eskes, H., Calabretta-Jongen, S., Segers, A., and Schaap, M.: Improving ozone forecasts over Europe by synergistic use of the LOTOS-EUROS chemical transport model and in-situ measurements, Atmos. Environ., 60, 217–226, 2012.
- Dee, D. P., Uppala, S. M., Simmons, A. J., Berrisford, P., Poli, P., Kobayashi, S., Andrae, U., Balmaseda, M. A., Balsamo, G., Bauer, P., Bechtold, P., Beljaars, A. C. M., van de Berg, L., Bidlot, J., Bormann, N., Delsol, C., Dragani, R., Fuentes, M., Geer,

- A. J., Haimberger, L., Healy, S. B., Hersbach, H., Hólm, E. V., Isaksen, L., Källberg, P., Köhler, M., Matricardi, M., McNally, A. P., Monge-Sanz, B. M., Morcrette, J.-J., Park, B.-K., Peubey, C., de Rosnay, P., Tavolato, C., Thépaut, J.-N., and Vitart, F.: The ERA-Interim reanalysis: configuration and performance of the data assimilation system, *Q. J. Roy. Meteorol. Soc.*, 137, 553–597, doi:10.1002/qj.828, 2011.
- Dentener, F., Stevenson, D., Ellingsen, K., van Noije, T., Schultz, M., Amann, M., Atherton, C., Bell, N., Bergmann, D., Bey, I., Bouwman, L., Butler, T., Cofala, J., Collins, B., Drevet, J., Doherty, R., Eickhout, B., Eskes, H., Fiore, A., Gauss, M., Hauglustaine, D., Horowitz, L., Isaksen, I. S. A., Josse, B., Lawrence, M., Krol, M., Lamarque, J. F., Montanaro, V., Müller, J.F., Peuch, V. H., Pitari, G., Pyle, J., Rast, S., Rodriguez, J., Sanderson, M., Savage, N. H., Shindell, D., Strahan, S., Szopa, S., Sudo, K., Van Dingenen, R., Wild, O., and Zeng, G.: The global atmospheric environment for the next generation, *Environ. Sci. Technol.*, 40, 3586–3594, doi:10.1021/es0523845, 2006.
- Donahue, N. M., Robinson, A. L., and Pandis, S. N.: Atmospheric organic particulate matter: From smoke to secondary aerosol, *Atmos. Environ.*, 43, 94–106, 2009.
- EPA: National Ambient Air Quality Standards, available at: <http://www.epa.gov/ttn/naaqs/> (last access: 9 October 2012), 2012.
- EU Directive 2008/50/EC of the European Parliament and of the Council of 21 May 2008 on ambient air quality and cleaner air for Europe, 2008.
- Forkel, R. and Knoche, R.: Nested regional climate-chemistry simulations for central Europe, *ComptesRendus – Geoscience* 339, 734–746, 2007.
- Gelencsér, A., May, B., Simpson, D., Sánchez-Ochoa, A., Kasper-Giebl, A., Puxbaum, H., Caseiro, A., Pio, C., Legrand, M.: Source apportionment of PM_{2.5} organic aerosol over Europe: Primary/secondary, natural/anthropogenic, and fossil/biogenic origin, *J. Geophys. Res.*, 112, D23S04, doi:10.1029/2006JD008094, 2007.
- Giorgi, F. and Meleux, F.: Modelling the regional effects of climate change on air quality, *C. R. Geoscience*, 339, 721–733, 2007.
- Guenther, A. B., Zimmerman, P. R., Harley, P. C., Monson, R. K., and Fall, R.: Isoprene and monoterpene emission rate variability: model evaluations and sensitivity analyses, *J. Geophys. Res.*, 98, 12609–12617, 1993.
- Hodzic, A., Madronich, S., Bohn, B., Massie, S., Menut, L., and Wiedinmyer, C.: Wildfire particulate matter in Europe during summer 2003: meso-scale modeling of smoke emissions, transport and radiative effects, *Atmos. Chem. Phys.*, 7, 4043–4064, doi:10.5194/acp-7-4043-2007, 2007.
- Hogrefe, C., Hao, W., Zalewsky, E. E., Ku, J.-Y., Lynn, B., Rosenzweig, C., Schultz, M. G., Rast, S., Newchurch, M. J., Wang, L., Kinney, P. L., and Sistla, G.: An analysis of long-term regional-scale ozone simulations over the Northeastern United States: variability and trends, *Atmos. Chem. Phys.*, 11, 567–582, doi:10.5194/acp-11-567-2011, 2011.
- Im, U., Markakis, K., Poupkou, A., Melas, D., Unal, A., Gerasopoulos, E., Daskalakis, N., Kindap, T., and Kanakidou, M.: The impact of temperature changes on summer time ozone and its precursors in the Eastern Mediterranean, *Atmos. Chem. Phys.*, 11, 3847–3864, doi:10.5194/acp-11-3847-2011, 2011.
- Im, U., Markakis, K., Koçak, M., Gerasopoulos, E., Daskalakis, N., Mihalopoulos, N., Poupkou, A., Kindap, T., Unal, A., and Kanakidou, M.: Summertime aerosol chemical composition in the Eastern Mediterranean and its sensitivity to temperature, *Atmos. Environ.*, 50, 164–173, doi:10.1016/j.atmosenv.2011.12.044, 2012.
- IPCC: Contribution of Working Groups I, II and III to the Fourth Assessment Report of the Intergovernmental Panel on Climate Change Core Writing Team, edited by: Pachauri, R. K. and Reisinger, A., IPCC, Geneva, Switzerland, pp. 104, 2007.
- Jacob, D. J. and Winner, D. A.: Effect of climate change on air quality, *Atmos. Environ.*, 43, 51–63, 2009.
- Jacob, D., Barrig, L., Christensen, O. B., Christensen, J. H., de Castro, M., Deque, M., Giorgi, F., Hagemann, S., Hirschi, M., Jones, R., Kjellstrom, E., Lenderink, G., Rockel, B., Sánchez, E., Schar, C., Seneviratne, S. I., Somot, S., van Ulden, A., and Van den Hurk, B.: An inter-comparison of regional climate models for Europe: model performance in present-day climate, *Climatic Change*, 81, 31–52, 2007.
- Jimenez-Guerrero, P., Jose Gomez-Navarro, J., Jerez, S., Lorente-Plazas, R., Garcia-Valero, J. A., and Montavez, J. P.: Isolating the effects of climate change in the variation of secondary inorganic aerosols (SIA) in Europe for the 21st century (1991–2100), *Atmos. Environ.*, 45, 1059–1063, 2011.
- Jungclaus, J. H., Botzet, M., Haak, H., Keenlyside, N., Luo, J. J., Latif, M., Marotzke, J., Mikolajewicz, U., and Roeckner, E.: Ocean circulation and tropical variability in the AOGCM ECHAM5/MPI-OM, *J. Climate*, 19, 3952–3972, 2006.
- K-1 Model Developers: K-1 Coupled Model (MIROC) Description, K-1 Technical Report 1, edited by: Hasumi, H. and Emori, S., Center for Climate System Research, University of Tokyo, Tokyo, Japan, 34 pp., available at: <http://www.ccsr.u-tokyo.ac.jp/kyosei/hasumi/MIROC/tech-repo.pdf>, 2004.
- Kjellström, E., Boberg, F., Castro, M., Christensen, H. J., Nikulin, G., and Sánchez, E.: Daily and monthly temperature and precipitation statistics as performance indicators for regional climate models, *Clim. Res.*, 44, 135–150, 2010.
- Kuenen, J., Denier van der Gon, H., Visschedijk, A., Van der Brugh, H., and Van Gijswijk, R.: MACC European emission inventory for the years 2003–2007, TNO report, UT-2011-00588, 2011.
- Lenderink, G., Van den Hurk, B., Van Meijgaard, E., Van Ulden, A. P., and Cuijpers, J.: Simulation of present-day climate in RACMO2: first results and model developments, KNMI technical report TR 252, 2003.
- Liao, K.-J., Tagaris, E., Manomaiphiboon, K., Wang, C., Woo, J.-H., Amar, P., He, S., and Russell, A. G.: Quantification of the impact of climate uncertainty on regional air quality, *Atmos. Chem. Phys.*, 9, 865–878, doi:10.5194/acp-9-865-2009, 2009.
- Manders, A. M. M., Schaap, M., and Hoogerbrugge, R.: Testing the capability of the chemistry transport model LOTOS-EUROS to forecast PM₁₀ levels in the Netherlands, *Atmos. Environ.*, 43, 4050–4059, 2009.
- Manders, A. M. M., van Ulft, B., van Meijgaard, E., and Schaap, M.: Coupling of the air quality model LOTOS-EUROS to the climate model RACMO, Dutch National Research Programme Knowledge for Climate Technical Report KFC/038E/2011, ISBN 978-94-90070-00-7, 2011.
- Metzger, S.: Gas/Aerosol Partitioning: A simplified method for global modeling. PhD Thesis, Utrecht University, 2000.
- Mitchell, J. F. N., Johns, T. C., Eagles, M., Ingram, W. J., and Davis, R. A.: Towards the construction of climate change scenarios, Cli-

- matic Change, 41, 547–581, 1999.
- Monahan, E. C., Spiel, D. E., and Davidson, K. L.: A model of marine aerosol generation via whitecaps and wave disruption, in: Oceanic Whitecaps and their role in air/sea exchange, edited by: Monahan, E. C. and Mac Niocaill, G., D. Reidel, Norwell, Mass., USA, 167–174, 1986.
- Mues, A., Manders, A., Schaap, M., Kerschbaumer, A., Stern, R., and Builtjes, P.: Impact of the extreme meteorological conditions during the summer 2003 in Europe on particle matter concentrations – an observation and model study. *Atmos. Environ.*, 55, 377–391, 2012.
- Moriondo, M., Good, P., Durão, R., Bindu, M., Giannakopoulos, C., and Corte-Real, J.: Potential impact of climate change on fire risk in the Mediterranean area, *Clim. Res.*, 31, 85–95, doi:10.3354/cr031085, 2006.
- Raes, F., Liao, H., Chen, W.-T., and Seinfeld, J. H.: Atmospheric chemistry-climate feedbacks, *J. Geophys. Res.*, 115, D12121, doi:10.1029/2009JD013300, 2010.
- Roeckner, E., Bäuml, G., Bonaventura, L., Brokopf, R., Esch, M., Giorgetta, M., Hagemann, S., Kirchner, I., Kornblueh, L., Manzini, E., Rhodin, A., Schlese, U., Schulzweida, U., and Tompkins, A.: The Atmospheric General Circulation Model ECHAM5, Part I: Model Description, MPI Report 349, Max Planck Institute for Meteorology, Hamburg, Germany, 127 pp., 2003.
- Saarikoski, S., Sillanpaa, M., Sofiev, M., Timonen, H., Saarnio, K., Teinila, K., Kukkonen, J., and Hillamo, R.: Chemical composition of aerosols during a major biomass burning episode over northern Europe in spring 2006: Experimental and modeling assessments, *Atmos. Environ.*, 41, 3577–3589, 2007.
- Schaap, M., Timmermans, R. M. A., Sauter, F. J., Roemer, M., Velders, G. J. M., Boersen, G. A. C., Beck, J. P., and Builtjes, P. J. H.: The LOTOS-EUROS model: description, validation and latest developments, *Int. J. Environ. Pollut.*, 32, 270–290, 2008.
- Solazzo, E., Bianconi, R., Vautard, R., Appel, K. W., Moran, M. D., Hogrefe, C., Bessagnet, B., Brandt, J., Christensen, J. H., Chemel, C., Coll, I., Denier van der Gon, H., Ferreira, J., Forkel, R., Francis, X. V., Grell, G., Grossi, P., Hansen, A. B., Jerièvæ, A., Kraljeviæ, Miranda, A. I., Nopmongcol, U., Pirovano, G., Prank, M., Riccio, A., Sartelet, K. N., Schaap, M., Silver, J. D., Sokhi, R. S., Vira, J., Werhahn, J., Wolke, R., Yarwood, G., Zhang, J., Rao, S. T., and Galmarini, S.: Model evaluation and ensemble modelling of surface-level ozone in Europe and North America in the context of AQMEII, *Atmos. Environ.*, 53, 60–74, doi:10.1016/j.atmosenv.2012.01.003, 2012.
- Tagaris, E., Manomaiphiphoon, K., Liao, K.-J., Leung, L. R., Woo, J. H., He, S., Amar, P., and Russell, A. G.: The impact of global climate change and emissions on regional ozone and fine particulate matter concentrations over the US, *J. Geophys. Res.-Atmos.*, 112, D14312, doi:10.1029/2006JD008262, 2007.
- Tai, A. P. K., Mickely, L. R., and Jacob, D. J.: Correlations between fine particulate matter ($PM_{2.5}$) and meteorological variables in the United States: implications for the sensitivity of $PM_{2.5}$ to climate change, *Atmos. Environ.*, 44, 3976–3984, doi:10.1016/j.atmosenv.2010.06.060, 2010.
- Undén, P. et al.: HIRLAM-5 Scientific Documentation, available from SMHI, S-601 76 Norrköping, Sweden, 144 pp., 2002.
- Van Loon, M., Vautard, R., Schaap, M., Bergstrom, R., Bessagnet, B., Brandt, J., Builtjes, P. H. J., Christensen, H. J., Cuvelier, C., Graff, A., Jonson, J. E., Krol, M., Langner, J., Roberts, P., Rouil, L., Stern, R., Tarrason, L., Thunis, P., Vignati, E., White, L., and Wind, P.: Evaluation of long-term ozone simulations from seven regional air quality models and their ensemble, *Atmos. Environ.*, 41, 2083–2097, 2007.
- van Meijgaard, E., Van Ulft, L. H., Van de Berg, W. J., Bosveld, F. C., Van den Hurk, B. J. J. M., Lenderink, G., and Siebesma, A. P.: The KNMI regional atmospheric climate model RACMO version 2.1, KNMI Technical report, TR-302, 2008.
- van Meijgaard, E., Van Ulft, L. H., Lenderink, G., de Roode, S. R., Wipfler, L., Boers, R., and Timmermans, R. M. A.: Refinement and application of a regional atmospheric model for climate scenario calculations of Western Europe, Climate changes Spatial Planning publication: KvR 054/12, ISBN/EAN 978-90-8815-046-3, pp. 44, 2012.
- van Ulden, A. P. and van Oldenborgh, G. J.: Large-scale atmospheric circulation biases and changes in global climate model simulations and their importance for climate change in Central Europe, *Atmos. Chem. Phys.*, 6, 863–881, doi:10.5194/acp-6-863-2006, 2006.
- Vautard, R., Beekmann, M., Desplat, J., Hodzic, A., and Morel, S.: Air quality in Europe during the summer of 2003 as a prototype of air quality in a warmer climate, *C. R. Geoscience*, 339, 747–763, 2007a.
- Vautard, R., Builtjes, P. H. J., Thunis, P., Cuvelier, P., Bedogni, M., Bessagnet, B., Honore, C., Moussiopoulos, N., Pirovano, G., Schaap, M., Stern, R., Tarrason, L., and Wind, P.: Evaluation and intercomparison of Ozone and PM_{10} simulation by several chemistry transport models over four European Cities within the City Delta project, *Atmos. Environ.*, 41, 173–188, 2007b.
- Zhang, Y., Wen, X.-Y., and Jang, C. J.: Simulating chemistry-aerosol-cloud-radiation-climate feedbacks over the continental US using the online-coupled Weather Research Forecasting Model with chemistry (WRF/Chem), *Atmos. Environ.*, 44, 3568–3582, 2010.

Supplementary material to ‘The impact of differences in large-scale circulation output from climate models on the regional modeling of ozone and PM’

Statistical evaluation

Table S1a. Annual average behavior of temperatures for the period 1989-2009. Standard deviations represent the day-to-day variability. Numbers in italics indicate that the difference with RLE_ERA is not significant at the P=0.05 level.

Station	RLE_ERA				RLE_ECHAM				RLE_MIROC			
	# T>25	# T<5	T _{max}	std	# T>25	# T<5	T _{max}	Std	# T>25	# T<5	T _{max}	std
Vredepeel	28	54	13.6	7.9	16	46	13.1	7.0	30	44	14.1	7.7
Sniezka	30	105	11.9	9.4	17	96	11.6	8.5	29	101	12.2	9.1
Melpitz	37	81	13.1	9.1	20	73	12.6	8.2	39	74	13.6	8.9
Paris	37	41	14.6	7.9	25	35	14.1	7.1	29	33	14.6	7.3
Els Torms	126	1	21.4	8.5	124	1	21.2	8.2	99	1	20.1	7.00
Madrid	109	6	19.2	9.3	105	7	18.6	9.4	76	4	17.4	7.9
Montelibretti	63	0	18.3	5.9	19	0	17.2	5.0	55	0	18.2	5.5

Table S1b. Annual average behavior of rain 1989-2009. Wet days are days with more than 0.5 mm rain.

Station	RLE_ERA		RLE_ECHAM		RLE_MIROC	
	wet days	yearly rain (mm)	wet days	yearly rain (mm)	wet days	yearly rain (mm)
Vredepeel	196	748	227	956	199	752
Sniezka	184	653	212	803	198	708
Melpitz	168	533	194	668	175	584
Paris	179	690	212	872	201	759
Els Torms	71	336	80	383	93	453
Madrid	93	431	124	675	116	544
Montelibretti	98	482	109	595	137	803

Table S1c. Annual averages wind speed 1989-2009

Station	RLE_ERA		RLE_ECHAM		RLE_MIROC	
	#v<2m/s	average v	#v<2m/s	average v	#v<2m/s	average v
Vredepeel	40	4.0	32	4.3	44	3.9
Sniezka	55	3.2	48	3.4	66	3.1
Melpitz	34	4.0	28	4.2	41	3.8
Paris	26	3.9	23	4.2	31	3.8
Els Torms	123	2.8	101	3.1	125	2.9
Madrid	64	3.0	52	3.4	67	3.1
Montelibretti	34	3.9	30	4.4	40	4.0

Table S2a. Average behavior of temperature, 2041-2060. Differences with respect to the present-day simulation are significant for all stations

Station	RLE_ECHAM				RLE_MIROC			
	# T>25 C	# T<5 C	T _{max}	std	# T>25 C	# T<5 C	T _{max}	Std
Vredepeel	25	33	14.3	7.1	55	21	16.3	7.7
Sniezka	26	76	12.8	8.4	53	65	14.4	9.0
Melpitz	27	53	13.8	8.0	65	42	15.7	8.7
Paris	38	21	15.2	7.3	65	12	17.0	7.5
Els Torms	148	0	22.9	8.6	145	0	23.2	7.5
Madrid	129	2	20.7	10.0	123	0	21.0	8.8
Montelibretti	59	0	18.5	5.3	102	0	20.8	5.8

Table S2b. Average rain 2041-2060. Wet days are days with more than 0.5 mm rain

Station	RLE_ECHAM		RLE_MIROC	
	wet days	yearly rain (mm)	wet days	yearly rain (mm)
Vredepeel	228	993	199	832
Sniezka	219	869	202	770
Melpitz	200	745	177	635
Paris	210	888	193	788
Els Torms	74	336	87	394
Madrid	104	617	97	464
Montelibretti	103	610	129	759

Table S2c. Average wind speed 2041-2060.

Station	RLE_ECHAM		RLE_MIROC	
	#v<2m/s	average v	#v<2m/s	average v
Vredepeel	31	4.3	50	3.8
Sniezka	47	3.4	68	3.0
Melpitz	31	4.2	47	3.7
Paris	23	4.2	34	3.7
Els Torms	99	3.2	123	2.9
Madrid	54	3.4	61	3.1
Montelibretti	26	4.4	41	4.0

Table S3. Summer (JJA) average daily maximum O₃ concentrations and annual average PM10 concentrations, present-day and future period for each of the model runs. Standard deviations represent the day to day variability.

RLE_ERA (1989-2009)				
	O _{3max}		PM10	
Station	average	stdev	average	stdev
Vredepeel	100	28	13.6	6.3
Sniezka	108	18	8.7	4.3
Melpitz	107	20	8.7	4.3
Paris	99	26	36.3	20.9
Els Torms	118	19	8.9	4.8
Madrid	98	15	17.8	7.4
Montelibretti	123	17	10.8	4.3

RLE_ECHAM	(1989-2009)				(2041-2060)				Relative change %		
	O _{3max}		PM10		O _{3max}		PM10		O ₃	PM10	
	station	average	stdev	average	stdev	average	stdev	average	stdev		
Vredepeel		91	24	12.6	5.9	93	27	12.6	6.0	+2.9	+0.5
Sniezka		102	17	8.2	4.1	106	20	7.8	3.9	+3.2	-4.2
Melpitz		100	19	8.2	4.1	103	21	8.0	4.0	+2.7	-2.7
Paris		91	24	32.3	20.1	96	27	31.7	19.6	+6.1	-2.0
Els Torms		113	19	7.6	4.4	119	21	7.8	4.5	+5.0	+2.6
Madrid		98	15	15.3	7.4	102	16	15.7	7.5	+4.0	+2.3
Montelibretti		120	17	10.1	4.0	124	19	10.0	4.1	+3.4	-0.4

RLE_MIROC	(1989-2009)				(2041-2060)				Relative change %	
	O ₃ max		PM10		O ₃ max		PM10			
station	average	stdev	average	stdev	average	stdev	average	stdev	O ₃	PM10
Vredepeel	107	26	13.8	6.4	115	29	14.5	7.2	+7.7	+4.6
Sniezka	110	16	8.6	4.2	116	18	8.4	4.3	+5.6	-2.0
Melpitz	111	19	8.5	4.3	117	20	8.5	4.6	+5.2	+0.2
Paris	105	27	35.6	20.4	113	30	36.4	19.7	+6.9	+2.0
Els Torms	115	18	8.0	4.5	122	19	8.2	4.6	+6.7	+0.1
Madrid	96	15	17.3	7.5	101	16	17.3	7.4	+4.8	+0.2
Montelibretti	123	17	10.1	4.2	130	12	10.3	4.3	+5.8	+1.6

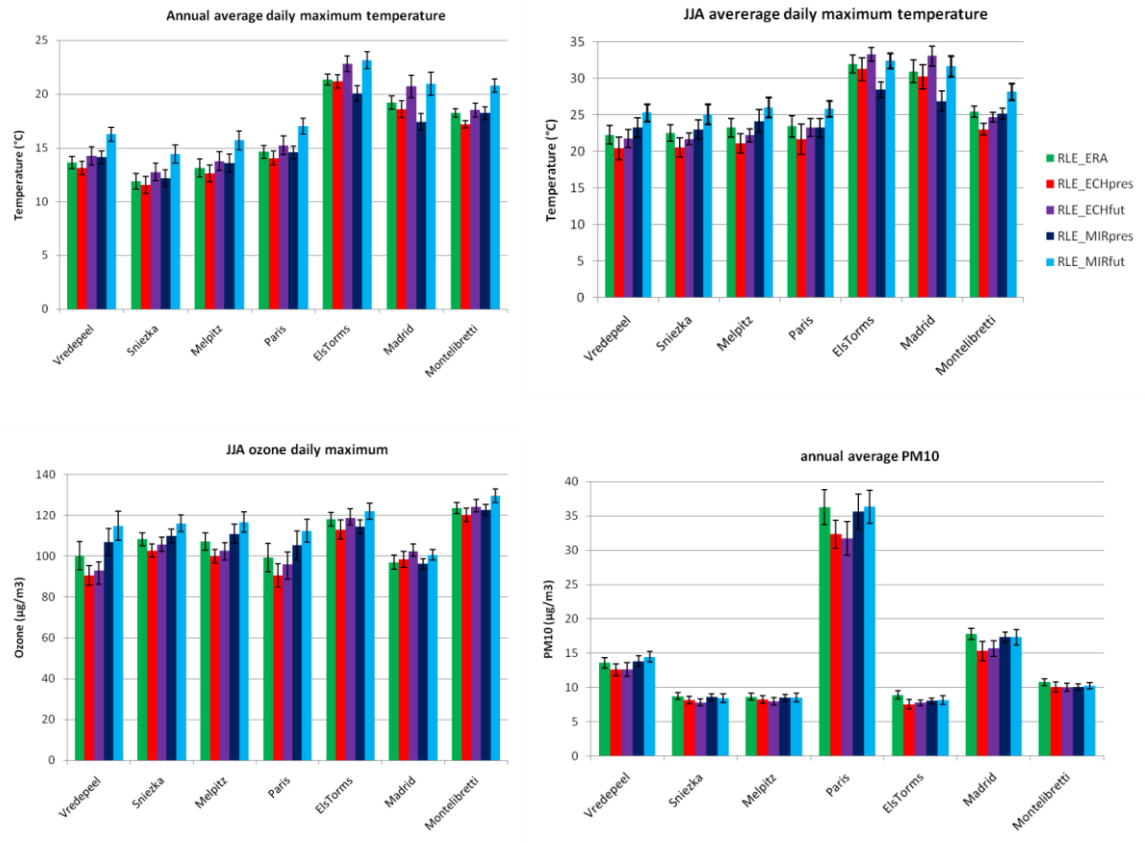


Figure S1. Average values for daily maximum temperature (annual and summer averages) and PM10 (annual) and ozone concentrations (summer averages), with standard deviations to indicate the interannual variability.

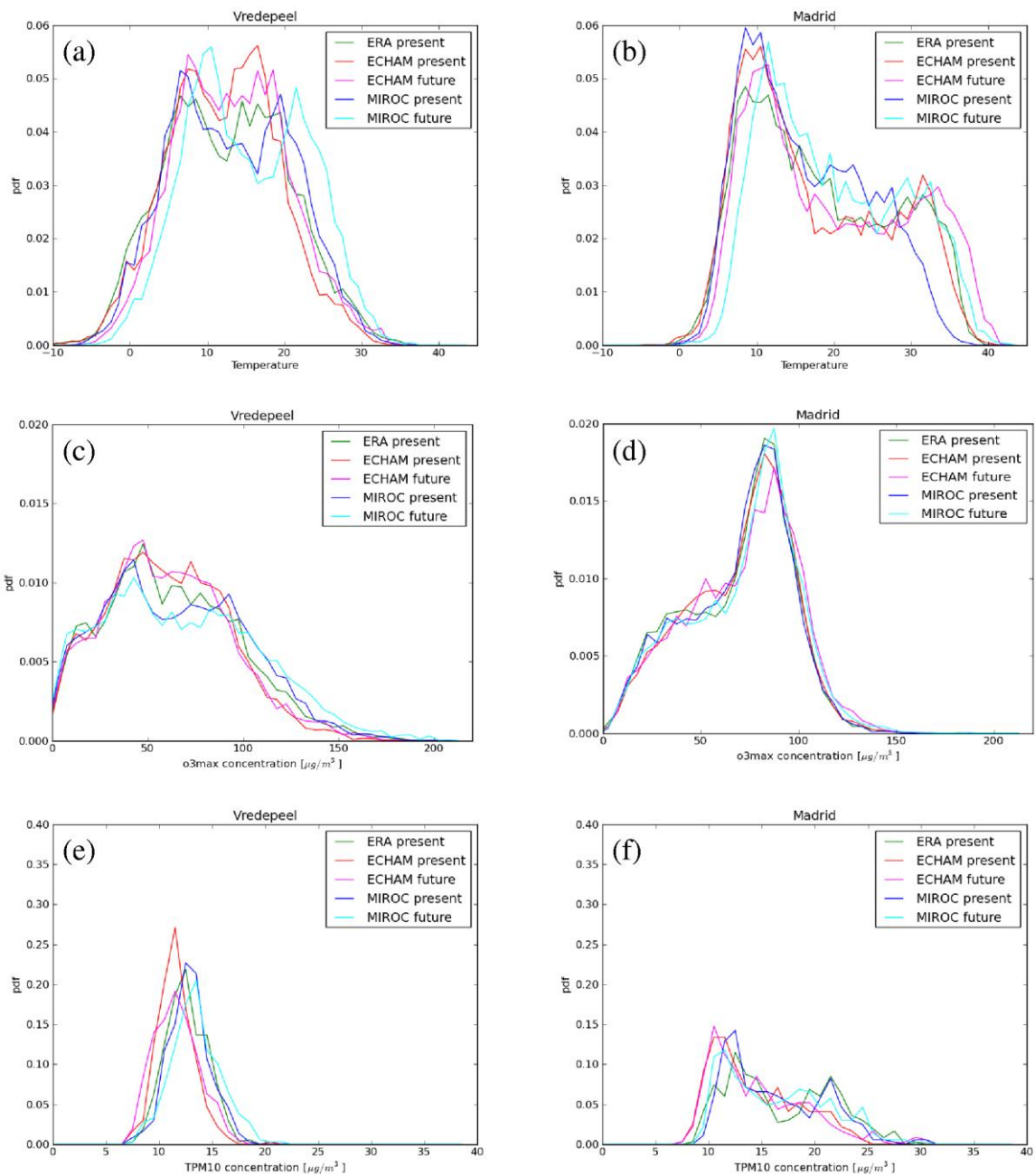


Figure S2. Histogram plots (probability distribution) of daily maximum temperature (a,b), daily maximum ozone concentration, not restricted to summer (c,d) and daily average total PM10 concentration(e,f) for Vredepeel (left) and Madrid (right).

9 Paper III: Differences in particulate matter concentrations between urban and rural regions under current and changing climate conditions

Differences in particulate matter concentrations between urban and rural regions under current and changing climate conditions

A. Mues^{1*}, A. Manders², M. Schaap², L.H. van Ulft³, E. van Meijgaard³, P. Builtjes^{1,2}

1) Freie Universität Berlin, Berlin, Germany, andrea.mues@met.fu-berlin.de

2) TNO, Utrecht, The Netherlands

3) KNMI, De Bilt, The Netherlands

*Corresponding author: Andrea Mues, Carl-Heinrich-Becker-Weg 6-10, 12165 Berlin, Germany, e-mail: andrea.mues@met.fu-berlin.de, Tel: 0049 30 83871130, Fax: 0049 30 83871128

Submitted to Atmospheric Environment in November 2012.

Abstract

Pollution levels in urban areas and their surrounding rural regions differ due to different sources and density of emissions, different composition of pollutants as well as specific meteorological effects. These concentration differences for PM10 are investigated and compared in this study for three different north-west European urban agglomerations: The German Ruhr area, the Dutch Randstad and the German city of Berlin. Measurement data for PM10 for the years 2003-2008 at urban and rural background stations are selected from the AirBase database to specify the PM10 concentration difference between these urban areas and their surrounding rural regions, here defined as the urban increment. The measured urban increment averaged over 2003-2008 is found to be 7.4 $\mu\text{g}/\text{m}^3$ for the Ruhr area, 3.1 $\mu\text{g}/\text{m}^3$ for the Randstad and 8.5 $\mu\text{g}/\text{m}^3$ for Berlin. To analyze whether the regional chemistry transport model LOTOS-EUROS is able to reproduce the measured urban increment simulation runs were performed for 2003-2008 on a 0.5°x0.25° lon-lat grid covering Europe and for the year 2008 on a finer grid of 0.125°x0.0625° covering the Netherlands and Germany, both with ECMWF meteorology as input. Although the model underestimates the absolute PM10 urban increment for the three areas, the relative concentration difference between urban and rural region for the Ruhr area and the Randstad is in general agreement with the measurements. The tested increase of the horizontal resolution gives no systematic improvement of the simulated urban increment. However, an even higher resolution than used here seems to be more appropriate to capture the urban increment (especially for Berlin). Nevertheless, model results could be used to interpret the observed increments.

The variability of the PM10 urban increment with weather is tested by means of the extreme summer 2003, such a synoptic situation is expected to occur more often in future. Measured and simulated PM10 concentrations in summer 2003 were compared to the summer average of 2003-2008. The response of the urban increment was found to depend on the urban area. In general the model reproduces the main features for the Randstad and Berlin.

In order to investigate the impact of a changing climate on the PM10 urban increment, simulations were performed with the off-line coupled model system RACMO2 (regional climate model) – LOTOS-EUROS (air quality model) over Europe. Different sets of simulations were carried out using RACMO2 meteorology with ECHAM5 A1B and with MIROC A1B boundary conditions for the time period 1970-2060, as well as with ERA-interim boundary conditions for the time period 1989-2009. Anthropogenic emissions were kept constant in the LOTOS-EUROS simulations. Simulated concentrations differ between the runs using ECHAM and MIROC boundary conditions and both runs differ from the present-day simulations with ERA-interim forcing. The impact of climate change on the modeled PM10 concentrations and the urban increment was found to be small in both scenario runs. However the concentration differences between the simulations forced by either ECHAM or MIROC indicate that PM10 concentration levels are sensitive to circulation patterns rather than temperature change alone, and that PM10 concentration levels may thus change when circulation patterns change in the future. One has to keep in mind that expected changes in emissions and emission locations probably also heavily affect total PM10 concentrations and the urban increment.

1 Introduction

Particulate matter (PM) receives a special interest in research and politics as the most severe health effects of air pollution are attributed to PM (EEA, 2012). Therefore, threshold values for PM10 and PM2.5 are defined in current EU directives (EU, 2008), but even below this threshold considerable health impacts (up to 12 months lower life expectancy (EEA, 2007)) are found. In this context urban areas are very important because they represent the main areas of anthropogenic emissions and threshold values at hot spot locations in urban and industrial areas are still exceeded on many locations (EEA, 2012). In order to develop mitigation strategies one needs to determine the origin of PM and its components as well as its response on emission reductions in urban areas. For air quality assessments it is important to consider both emissions and meteorology. Meteorological conditions in Europe are anticipated to change in future due to climate change. Hence it is important to also assess the impact of a changing climate on the concentration of pollutants. This is of special interest for urban areas because a high and even increasing proportion of the population lives in urbanized regions and is therefore exposed to the consequences of climate change and to air pollution.

The urban air quality depends on the pollution regime inside as well as outside an urban area. There is a large interest to specify the contribution of the regional background concentration, determined by regional emission sources and long-term transport, and of the concentration resulting from the local urban emissions to the urban pollution level. PM concentrations and composition were found to differ substantially between an urban area and its surrounding rural region (e.g. Lenschow et al., 2001; Putaud et al., 2010), resulting in a positive urban increment of PM concentrations. However, the size of the urban increment might differ per area because of differences in its size and structure (isolated city versus urban agglomeration), climate, population density, as well as in main emission sources and the contribution from long-range transport. A central question in the present paper is: what is the PM10 concentration difference between an urban and its surrounding rural region and how much does the resulting urban increment depend on the urban area.

It is a common approach to use regional chemistry transport models (CTM) to evaluate air quality policies and the impact of emission reduction strategies on the national and European scale (e.g. Builtjes et al., 2010). Hence it is important that regional CTMs are able to reproduce the concentration level and the different response of emission reductions in urban and rural regions. A central question in this context is therefore if a state-of-the-art regional CTM like LOTOS-EUROS (Schaap et al., 2008) is able to reproduce the measured urban increment.

In many model evaluation studies aiming PM a considerable underestimation of PM10 concentrations in CTM simulations of up to 50% (e.g. Cuvelier et al., 2007; Stern et al., 2008) are shown. This is mainly due to missing but important components and emissions sources or uncertainties therein (e.g. windblown dust, secondary organic aerosols, wild fires). As a consequence it is expected that the absolute urban increment is also underestimated in the models. However, assuming that the relative ratio between emissions in the urban and rural regions is captured, we can expect a reproduction of the measured relative urban increment. In general, the horizontal resolution of a regional CTM ($7 \times 7 \text{ km}^2$ to $25 \times 25 \text{ km}^2$), which is needed to cover an appropriate area and time period is not sufficient to reproduce the concentration variability within an urban agglomeration (Stern et al., 2010). Furthermore small scale features associated to the structure of a built-up area (e.g. urban heat-island, modified wind field) are not explicitly taken into account in these models. Hence, with such a model system the focus should be

on large-scale feature (synoptic situations). In view of recent studies on the impact of climate change on air quality, it is relevant information how well such a model performs, because long-term simulations with urban scale models are still too time-consuming in terms of computation time.

One method to investigate the impact of climate change on air pollution is to analyze a specific synoptic situation in the past (e.g. extreme summer 2003) which is expected to occur more often in future in terms of its effect on air quality (Vautard et al. 2007a; Mues et al., 2012). The advantages of this approach are that such an effect can be directly analyzed using observations, and that an evaluation of the CTM performance as function of meteorology is possible. In contrast to this approach, which only considers one specific synoptic situation, one-way coupled model systems consisting of a regional CTM forced by a regional climate model (RCM) give the opportunity to take into account the variability of the future climate. The available studies using such a model system (e.g. Meleux et al., 2007; Langner et al., 2005; Manders et al., 2012) show a consistent picture of increasing summer ozone concentrations but the extent of the changes differ. For PM the response to changes in climate is weaker and the limited number of studies do not even agree on the sign of the change (Jacob and Winner, 2009). Furthermore PM consists of several components which may respond differently to meteorology and therefore it is reasonable to look into changes of the individual PM components (Tai et al., 2012). The question discussed here is which conclusions can be drawn on the impact of a changing climate on the urban increment based on the two approaches using regional models.

In the present study we aim to quantify the size of the average measured PM10 urban increment for the time period 2003-2008. The urban increment is here defined as the difference between the urban and regional background concentrations represented by PM10 concentrations at urban and rural background stations located in the urban and its surrounding rural region, respectively. We selected three different areas in north-west Europe: the German Ruhr area, the Dutch Randstad and the city of Berlin (Germany). In a second step we tested whether the state-of-the-art regional CTM LOTOS-EUROS (Schaap et al, 2008) is able to reproduce the observed urban increment as a function of the urban area. To this end model simulations were produced for the years 2003-2008 on a $25 \times 25 \text{ km}^2$ grid resolution covering Europe. To test the sensitivity of the simulation results to the spatial resolution of the model a simulation with a higher resolution of $7 \times 7 \text{ km}^2$ for the year 2008 was performed. These measurement and simulation data were also used to compare the urban increment for the extreme summer 2003 to the summer 2003-2008 average. To investigate the impact of climate change on the urban increment a model study was done with a climate - air quality model system consisting of the regional atmospheric climate model of KNMI (Royal Netherlands Meteorological Institute), RACMO (2.2 version) (Lenderink et al., 2003; Van Meijgaard et al., 2008) which is one-way coupled to the LOTOS-EUROS model. To assess the impact of using two different global climate models (GCMs), which differ in terms of zonal mean flow for present-day conditions and in climate change response (Manders et al., 2012), on modeled PM10 concentrations the two GCMs ECHAM5 (Roeckner et al., 2003; Jungclaus et al., 2006) and MIROC3.2-hires (K-1 Model Developers, 2004) were used as boundary conditions for RACMO. In both simulations SRES-A1B for the time period 1970-2060 are used. Simulation results of a present-day climate period (1989-2009) are then compared to the results of a future climate period (2041-2060).

2 Methods and data

2.1 Study regions

The main focus in this study will be on the Ruhr area, which is located in the west of Germany on the Dutch border. With an area of approximately 4435km² and 1167 inhabitants per km² this area is one of the largest densely populated agglomerations in Europe. The Ruhr area is characterized by an agglomeration of middle-size cities, which partly merge and the intersections between them are often diffuse and mainly characterized by suburbs. But the area also contains not built-up area as parks and even small agricultural areas. The Ruhr area has a dense road network and industries like automobile industry and coal mining. The surrounding region of the Ruhr area is characterized by intensive agriculture especially in the north and west, and by forests in the east. In the south the Rhineland, with middle-size cities which are further apart, borders to the Ruhr area. The second urban area under investigation is the densely populated Dutch Randstad located in the west of the Netherlands, relatively close to the coast. This area accounts for only 20% (about 5600km²) of the whole area of the Netherlands but 40% (about 6.6 million inhabitants) of the Dutch population lives in this part of the country. Similar to the Ruhr area it is characterized by an agglomeration of cities, the largest being Amsterdam, Rotterdam, Den Haag and Utrecht. The road network between the cities is very dense, furthermore Rotterdam has a big harbor with related industry, and a furnace is located at the seaside, about 20km west of Amsterdam. The region surrounding the Randstad is still relatively densely populated and characterized by intensive agriculture and grassland. The third urban region is the city of Berlin. Different to the agglomerations Ruhr area and the Randstad, Berlin is a single big city which has an area of 892km² with about 3942 inhabitants per km². In the south-west of Berlin lies the city of Potsdam which is part of the federal state of Brandenburg. Brandenburg surrounds Berlin completely and is mainly characterized by rural areas with agriculture and forests.

2.2 Definition of the urban increment and selection of measurements

An averaged PM10 concentration difference between the three individual urban areas and their surrounding rural regions is quantified for the period 2003-2008 and will be referred to as the 'urban increment' in this study. The aim of the study is to determine a temporal and spatial average urban increment. Therefore a period of six years was chosen as it represents a reliable average which takes into account different meteorological and air pollution situations and averages out the interannual variability. The urban increment is defined as the concentration difference between the urban and rural background concentrations. It is quantified by subtracting averages over PM10 concentrations from stations inside the urban area from averages over PM10 concentrations from stations in its surrounding rural region. The urban increment is given as an absolute as well as a relative value $((C_u - C_r)/C_r) * 100$, C_u : average concentration at urban stations, C_r : average concentration at rural stations). In order to quantify the measured urban increment, PM10 measurement data from the AirBase (AIRBASE, 2012) database are used. According to the definition of the urban increment only urban and rural background stations were selected and kerbside stations are excluded from the analysis. The stations were selected for their location, displayed in Figure 1, and the availability of the data in the six years. Table 1 gives an overview

of the stations, their classification and the availability of measurement data. Whenever possible, rural stations in every geographical direction of the urban agglomerations were selected to account for up- and downwind effects. In general we followed the station classifications given in the AirBase database. But because we count suburbs of cities within the Ruhr area and the Randstad as part of the agglomerations we decided to classify also the suburban stations Gelsenkirchen and Den Haag as urban background stations in this study. Stations which are located in the center of an urban agglomeration but not in a city (Zegveld) or are located in a suburb of Berlin (Friedrichshagen) were classified as suburban stations in this study, although the Airbase classification is rural. This change in classification can also be justified for this study because these stations are quantitative similar to the urban and suburban stations, respectively (see Fig.2). The distances between the selected stations vary per region. Within the Ruhr area the urban stations are about 10km apart, while the rural stations are located 40 (Borken) to 110km (Vredepeel) from the center of the urban area. The stations in the Randstad have a distance of up to about 67km to each other and the rural stations have a distance from about 50km (Utrecht-Wekerom) until 110km (Utrecht-Hellendoorn) to the Randstad. Stations in Berlin have a distance of about 8-21km to each other and the rural stations are located 30-60km from the center of the city.

2.3 Model simulations and statistical methods

In this study the three dimensional Eulerian chemistry transport model LOTOS-EUROS is used. LOTOS-EUROS is an operational model used to calculate air pollution concentrations and deposition focusing on the lower troposphere. Model simulations are performed on the regional scale over the European domain. The model has been used and developed in a large number of European research projects and in several policy support studies in the Netherlands, Germany and Europe. It has participated frequently in model intercomparison studies aimed at particulate matter (Cuvelier et al., 2007; Stern et al., 2008) and ozone (Solazzo et al., 2012). The model is part of the MACC (Monitoring atmospheric composition & climate) ensemble and is used for daily air quality forecasts in the Netherlands (Manders et al., 2009). The modeled species in LOTOS-EUROS include gaseous species as well as the following PM components: Primary anthropogenic PM2.5 (PPM2.5), black carbon (BC), primary anthropogenic PM10 (PPM10) (excluding PM2.5 and BC), ammonium (NH_4^+), sulfate (SO_4^{2-}), nitrate (NO_3^-), and sea salt (Na in fine and coarse mode, which is translated to total sea salt by using a factor 3.26 to account for other sea water components like chloride and sulfate (Millero, 2004)). Thus total PM in LOTOS-EUROS is defined as the sum of the following individual components: $\text{PM10} = \text{PPM2.5} + \text{PPM10} + \text{BC} + \text{NO}_3^- + \text{NH}_4^+ + \text{SO}_4^{2-} + 3.26 * (\text{Na_fine} + \text{Na_coarse})$. The anthropogenic emissions used for the LOTOS-EUROS simulation in this study are taken from the TNO-MACC emission database for the year 2005 (Kuenen et al., 2011; Denier van der Gon et al., 2010). This inventory is a European-wide, high-resolution ($0.125^\circ \times 0.0625^\circ$ lon-lat) inventory. It is set up using official emissions reported by countries themselves. However, natural sea spray emission are calculated on-line using the actual meteorological data.

In order to quantify the simulated urban increment and to compare it to the measured value, simulations with the LOTOS-EUROS for the years 2003-2008 on the European domain with a resolution of ca. $25 \times 25 \text{ km}^2$ ($0.5^\circ \times 0.25^\circ$) were performed (LE_eu). To analyze the model performance as a function of the horizontal grid resolution, a model simulation for the year 2008 on a smaller domain covering Germany and the Netherlands has been performed with a resolution of ca. $7 \times 7 \text{ km}^2$ ($0.125^\circ \times 0.0625^\circ$). The

year 2008 is chosen because an adequate set of PM10 measurement data is available, and the meteorological conditions in 2008 were not remarkably extreme (BW,2008). The higher grid resolution has mainly an impact on the dilution of the emitted mass of pollutants and therefore on the concentration in one grid cell. The description of the deposition in the 25x25km² simulation is already based on the highest resolution of the land use class and the same meteorological fields are used in both simulations.

The LE_eu simulations are also used to analyze the impact of the summer 2003 meteorological conditions on the PM10 concentrations. For these two simulations (LE_eu and LE_zoom) the meteorological input fields for the LOTOS-EUROS model are delivered by the ECMWF model. Lateral boundary conditions are taken from climatology for the LE_eu simulation, while for the LE_zoom simulation output from the LE_eu simulation serves as boundary condition.

For the climate - air quality model system the regional atmospheric climate model of KNMI, RACMO (2.2 version) is one-way coupled to the LOTOS-EUROS model. Ensemble studies, in which RACMO2 participated (Jacob et al., 2007; Kjellström et al., 2010), showed that the regional models did reproduce the large-scale circulation of the global driving model, albeit with biases. These studies also showed that RACMO2 was not one of the extreme models. Different sets of simulations were produced, for which the output of the GCMs ECHAM5 and MIROC3.2-hires with SRES-A1B for the time period 1970-2060 as well as ERA-interim data (Dee et al., 2011) for the time period 1989-2009 were dynamically downscaled with RACMO2 at 50km resolution. Simulations with LOTOS-EUROS at 25x25km² resolution were then subsequently forced with the meteorological fields produced by the simulations with RACMO2 (RLE_ERA, RLE_ECHAM and RLE_MIROC). For the LOTOS-EUROS simulations the anthropogenic emissions were kept constant for the year 2005 to concentrate on the effect of changing meteorological conditions. The impact of meteorology on biogenic and sea salt emissions is included. A more detailed technical description of the RACMO – LOTOS-EUROS one-way coupled system is given in Manders et al., (2012).

The specification of all model simulations including the aims and the acronyms of the runs are summarized in Table 2. In Tables 3-5 the measured and modeled PM10 averages of the years 2003-2008 and 2008 as well as the summers of 2003-2008 and 2003 are displayed. For these averages model data are disregarded for days on which no measurements were available. Furthermore, the average of a station is disregarded in the Tables 3-5 if the availability of data is below 40% for the particular given time period (see Tab.1). Because the focus is on the Ruhr area the statistic for every station in this area is given in Table 3a. For the Randstad and Berlin only the averages over the rural, suburban and urban stations are given in Table 4 and 5. Also the long-term averages of the RACMO - LOTOS-EUROS simulations for a present-day climate period (1989 -2009) and a future climate period (2041 – 2060) are given in Tables 3-5. The modeled urban increment were quantified according to the description in section 2.2.

3 The measured PM10 urban increment

3.1 Ruhr area

In the Ruhr area measured 2003-2008 average PM10 concentrations are between 27.6 (Dortmund) and $29.5\mu\text{g}/\text{m}^3$ (Essen) at urban stations and between 14.8 (Westerwald) and $26.8\mu\text{g}/\text{m}^3$ (Vredepeel) at stations in the surrounding rural region (Fig.2a, Tab.3a). Measured concentrations are rather uniform within the urban area as the urban stations tend to be closely grouped in the Ruhr area and thus similar emission sources apply to all stations. In contrast the spatial variability in measured PM10 concentrations among rural stations is found to be higher with decreasing concentrations between stations located in the west (Vredepeel, Borken) and the east (Bad Arolsen, Westerwald) of the rural region (Fig.2a). Distances between the rural stations are larger and therefore the individual stations may be affected by different emission sources, e.g. agriculture (Vredepeel, Borken); forests (Westerwald). But also the up- and downwind effect from the different surrounding areas (e.g. Ruhr area, the Netherlands) have to be considered. The differences in concentration between stations in the urban and the rural region vary widely between 0.8 and $14.7\mu\text{g}/\text{m}^3$ depending on the station pair (Tab.3a). When averaging over all urban and all rural stations, as defined in section 2.2., the measured urban increment for the 2003-2008 average is $7.4\mu\text{g}/\text{m}^3$ and 35%, respectively (Tab.3b). The variation of the urban increment during the year, represented by the annual cycle based on monthly means in Figure 3, is between 6 and $11\mu\text{g}/\text{m}^3$, with highest values in the winter months. The urban increment varies less than the concentrations during the year.

3.2 Randstad

In the Dutch Randstad the measured 2003-2008 average PM10 concentrations vary between 26.0 (Den Haag) and $33.1\mu\text{g}/\text{m}^3$ (Rotterdam) in the urban area and between 24.6 (Hellendoorn) and $28.2\mu\text{g}/\text{m}^3$ (Wekerom) in the surrounding rural region (Fig.2b). The concentrations measured at urban stations depend strongly on the city they are located in. In contrast the PM10 concentrations at rural stations are rather similar although distances between rural stations around the Randstad are relatively large. But different emission sources are likely to have a higher contribution at the individual rural stations e.g. sea salt (De Zilk, Westmaas) and agriculture (Vredepeel). The suburban station Zegveld is located in a rural region between the cities Amsterdam, Utrecht and Den Haag and thus in the center of the Randstad and is affected by one of the three cities depending on the wind direction. But with $25\mu\text{g}/\text{m}^3$ Zegveld is one of the stations with the lowest concentrations, suggesting that no direct large emission source is close to this station. The concentration differences for the period 2003-2008 between the individual urban and rural stations vary between -2.2 and $8.5\mu\text{g}/\text{m}^3$. The negative difference hints at a high rural background concentration around the Randstad. The measured urban increment averaged over 2003-2008 for the Randstad is $3.1\mu\text{g}/\text{m}^3$ and 12% (Tab.4).

3.3 Berlin

In Berlin the measured 2003-2008 average PM10 concentrations are between 25.6 (Amrumer Str.) and $27.9\mu\text{g}/\text{m}^3$ (Nansenstr.) at urban stations and ranges from 14.5 (Neuglobsow) to $21.2\mu\text{g}/\text{m}^3$ (Spreewald) in the surrounding rural region (Fig.2c). PM10 concentration at urban as well as at rural stations were found to be rather uniform, except for Neuglobsow. Thus no strong impact of up- and downwind effects from the city was found at the rural stations. Also measured concentrations at the two suburban stations of around $23\mu\text{g}/\text{m}^3$ are rather uniform. Both stations are located eastward of the city and are therefore affected by the same up- and downwind effects of the city and long-range transports (especially from east of the city). The average for the suburban stations is found to be in between the urban and rural stations with a difference of about $-3\mu\text{g}/\text{m}^3$ to the urban and $+5\mu\text{g}/\text{m}^3$ to the rural stations (Tab.5). Thus the stations show a negative concentration gradient from the urban to the suburban and rural region. The measured concentration difference for the 2003-2008 average between the individual urban and rural station pairs ranges from 4.4 to $13.4\mu\text{g}/\text{m}^3$. The measured PM10 urban increment for Berlin is $8.5\mu\text{g}/\text{m}^3$ and 46%.

3.4 Comparison of the measured PM10 urban increment in the three regions

Although the urban agglomerations discussed in this paper differ in many aspects, they have in common that measured 2003-2008 average PM10 urban background concentrations are quite similar with differences of less than $3\mu\text{g}/\text{m}^3$. The air quality in a region is mainly determined by meteorological conditions and emission strength. Whereas the meteorology in the Randstad is characterized by a maritime influence (southwesterly wind from the sea, more precipitation) favoring the dilution and removal of pollutants, Berlin has a more continental climate favoring stagnation (wind from the continent, less precipitation) which leads to a higher accumulation of pollutants. Nevertheless, PM10 concentrations are higher in the Randstad ($29.6\mu\text{g}/\text{m}^3$) than in Berlin ($26.7\mu\text{g}/\text{m}^3$), which may be explained by the higher emission density in and around the Randstad area (Kuenen et al., 2011). Note that in contrast to Berlin, the Randstad and the Ruhr area are agglomerations of many smaller cities. Concerning air pollution these cities affect each other, intensified by the presence of a dense road network and industries.

Whereas the urban levels are similar, significantly smaller urban increments are observed for the Randstad ($3.1\mu\text{g}/\text{m}^3$) than for the Ruhr area ($7.4\mu\text{g}/\text{m}^3$) and Berlin ($8.5\mu\text{g}/\text{m}^3$). Note that due to the proximity of the urban area of the Randstad to the sea, part of the urban increment is induced by differences in sea salt concentrations. But a major part of the differences between the urban increments can be mostly explained by the structure of land use and the related emission sources in the rural regions. Within the rural regions in Germany many more large forest areas are present, while levels of population density and agricultural intensity are less than in the Netherlands. Hendriks et al. (2012) established that agriculture was the largest contributor to regional-scale PM in the Netherlands, followed by traffic. Ammonium nitrate is the most important contributor to PM in the Netherlands (Weijers et al., 2011) and can be used to illustrate the difference in agricultural impact. The high ammonia emissions in the Netherlands cause the semi-volatile ammonium nitrate concentrations to be high during stagnant conditions in winter and summer (ten Brink et al., 1997). In regions with lower

ammonia emissions ammonium nitrate levels show a summer minimum leading to a lower annual average concentration (Schaap et al., 2002). This is confirmed by the fraction of ammonium nitrate in PM10 at rural background stations in the Netherlands of around 30% (Weijers et al., 2011), whereas the fraction is about 15-20% around Berlin (John and Kuhlbusch, 2004).

4 The simulated urban increment

4.1 Impact of the horizontal grid resolution on model results

The two simulations LE_eu and LE_zoom produce in general similar spatial distributions of PM10 concentrations averaged over the year 2008, showing a west-east PM10 concentration gradient (Fig.1). Highest concentrations are simulated above the sea due to high sea salt concentrations but both model simulations produce also high PM10 concentrations in the Ruhr area and parts of the Netherlands including the Randstad. Simulated concentrations in Berlin are lower but in comparison to its surrounding region concentrations in the city are also relatively high. Owing to the lower horizontal resolution of LE_eu for some cases stations (Gelsenkirchen and Dormtund, Mühlheim and Essen; Westmaas and Rotterdam; De Zilk and Amsterdam; Buch and Amrumer Str.) are located in the same grid cell. The LE_zoom simulation gives more detailed information about the spatial distribution of PM10 concentrations within an area. But the observed spatial variability in concentration between stations is also for LE_zoom only captured for the Ruhr area (Tab.3a). For the other two regions the resolution of 7x7km² is not sufficient to resolve the spatial variability that is seen in the measurements.

At most stations in the three urban and rural regions LE_eu produces higher concentrations than LE_zoom. Differences range between -0.5 and +2.9µg/m³ for the 2008 average in the Ruhr area (Tab.3a), between +0.4 and +2µg/m³ in the Randstad and between -0.7 and +0.7µg/m³ in Berlin. In particular in the Ruhr area very high concentrations, simulated with the LE_zoom version, are confined to only a few grid cells which are in collocation with the main emission sources. But for LE_eu high emissions are diluted in the larger grid cells and therefore high concentrations tend to cover larger areas (Fig.1). Concentrations are therefore higher for LE_eu if a station is not located in a LE_zoom grid cell including a strong emission source. This can affect both the concentration of primary components as well as of precursor gases which are then available for the formation of SIA. The models ability to reproduce the measured temporal variability, here given by the correlation coefficient, is similar for LE_zoom and LE_eu (Ruhr area: Tab.3a). Lowest correlations are found for stations in Berlin (not shown). The observed variability of PM10 concentrations in the year 2008, here presented as the standard deviation, increases from rural to urban stations (Ruhr area: Tab.3a). This increase is reproduced by both model simulations but the value of the standard deviation is underestimated. Also the fact that the standard deviations at most stations is slightly higher for the LE_eu compared to the LE_zoom simulation, hints that stations in the urban Ruhr area are not located in a grid cell including strong emission sources in LE_zoom.

In the Ruhr area the simulated urban increment for the year 2008 has a value of 2.5µg/m³ (32%) for LE_zoom and 3.0µg/m³ (35%) for LE_eu, instead of 8.1µg/m³ (44%) for the measurements (Tab.3b). The urban increment for the Randstad is 2.1µg/m³ (20%) for the LE_zoom run and 2.0µg/m³ (18%) for LE_eu, in contrast to an observed urban increment of 4.7 µg/m³ (20%) (Tab.4). In Berlin the PM10 urban increment is 1.8µg/m³ (34%) for the LE_zoom run and 1.4µg/m³ (24%) for LE_eu whereas the measured concentration difference is 6.9µg/m³ (41%) (Tab.5). The simulated absolute and relative urban increments are very similar for LE_eu and LE_zoom for the Ruhr area and the Randstad, only for Berlin the relative urban increment for LE_zoom is closer to the measured value.

These findings lead to the conclusion that using a resolution of $7 \times 7 \text{ km}^2$ instead of $25 \times 25 \text{ km}^2$ do not represent a general improvement of the simulations regarding the PM10 concentrations at rural and urban stations and the urban increment.

4.2 The simulated (LE_eu) PM10 urban increment in comparison to measurements

4.2.1 Ruhr area

The simulated 2003-2008 average PM10 concentrations are between 12.8 (Gelsenkirchen) and $13.8 \mu\text{g}/\text{m}^3$ (Essen) in the urban Ruhr area and between 7.7 (Bad Arolsen) and $12.5 \mu\text{g}/\text{m}^3$ (Vredepeel) in the surrounding rural region (Fig.2a, Tab.3a). In general the model captures the observed variation of concentrations between the different stations inside the urban and rural region as well as between urban and rural stations (Fig.2a). Differences in concentrations between urban and rural stations vary between 0.3 and $6.1 \mu\text{g}/\text{m}^3$, which is a lower variation than observed. Thus, the model does not reproduce the measured absolute urban increment ($7.4 \mu\text{g}/\text{m}^3$), in fact it is much lower in the LE_eu simulation ($3.3 \mu\text{g}/\text{m}^3$) (Tab.3b). However, the simulated relative urban increment of 33% is close to the measured value of 35%. The model simulations allow to analyze the differences in the composition of PM10 in urban and rural regions. The main components of the modeled PM10 concentrations in the rural region are the secondary inorganic components (Fig.2a). Mainly the primary PM2.5 component and to a lesser extent also primary PM10 and BC account for the higher concentrations in the urban area.

4.2.2 Randstad

Simulated 2003-2008 average PM10 concentrations vary between 13.2 (Dordrecht) and $14.7 \mu\text{g}/\text{m}^3$ (Den Haag) in the urban area and between 11.0 (Wekerom) and $14.2 \mu\text{g}/\text{m}^3$ (Westmaas) in the rural region (Fig. 2b). The model fails to reproduce the differences in measured PM10 concentrations between the stations, which is mainly due to the fact that some urban and rural stations are in the same grid cell (see section 4.1.). The concentration differences for the period 2003-2008 between the individual urban and rural stations vary between -0.5 and $3.7 \mu\text{g}/\text{m}^3$. The simulated absolute urban increment of $1.5 \mu\text{g}/\text{m}^3$ is lower than observed. Nevertheless, the simulated relative urban increment of 12.4% is very close to the observed value of 11.5%. The composition of modeled PM10 is not very different between the stations in and around the Randstad (Fig.2b). The modeled sum of the SIA is slightly higher at the rural stations, whereas the amount of primary PM2.5 and PM10 as well as BC is higher at the urban stations. The results for sea salt show that for the Netherlands the distance to the coast is a relevant parameter for PM concentrations, affecting the urban increment based on the large-scale averages as defined in this study.

4.2.3 Berlin

In Berlin the simulated 2002-2008 average concentrations are between 7.9 (Amrumer Str.) and $8.2 \mu\text{g}/\text{m}^3$ (Nansenstr.) at urban stations and are around $6.3 \mu\text{g}/\text{m}^3$ at all rural stations. The variability between the stations is only poorly reproduced by the LE_eu simulation, although the observed increase

towards the urban stations is reproduced qualitatively in Figure 2c. The simulated absolute urban increment for Berlin is only $1.7\mu\text{g}/\text{m}^3$, while the measured value is $8.5\mu\text{g}/\text{m}^3$ (Tab.5). Also the simulated relative urban increment is with only 27% lower than observed (46%). The model simulates an increase of primary PM2.5 and to a lesser extent primary PM10 and BC towards the urban area (Fig.2c).

4.3 Evaluation of the simulated PM10 urban increment

In section 3 the measured urban background concentration in the Ruhr area and the Randstad were found to be similar. But due to lower concentration in the rural surrounding the Ruhr area has a higher urban increment. Both findings are reproduced by the LE_eu simulations. But as stated before LOTOS-EUROS underestimates observed PM10 concentrations and thus also the absolute urban increment. The agreement between the modeled and observed relative PM10 urban increment for the Ruhr area and the Randstad hints at a similar underestimation of secondary and primary PM10 components in the model. The simulated three urban increments are mainly determined by higher concentrations of the primary components at urban stations (BC, PPM2.5, PPM10). Elemental carbon concentrations in observation studies (e.g. Putaud et al., 2010; John and Kuhlbusch, 2004) were also found to increase slightly from rural towards urban background stations but especially towards street stations (e.g. 6%, 17% EC contribution to PM10 at rural and kerbside stations in Central Europe (Putaud et al., 2010)). The model tends to overestimate sea salt by a factor of about 1.5 (Schaap et al., 2009). However, the inland gradient from the coast is represented well, which is especially relevant for the urban increment in the Randstad. From Schaap et al., (2011) it is already known that the model tends to underestimate regional background SIA concentrations by about 30%. But the observed decrease of sulphate and nitrate contribution to PM10 when moving from rural to kerbside sites in Europe (19% (SO₄), 13% (NO₃) at rural stations; 9%, 8% at kerbside stations in Central Europe are given in Putaud et al. (2010)) is also shown by the model.

Several components are not included in the model but might contribute the urban increment. Mineral dust is accounting for only 5-10% of the PM10 mass in north-west Europe (Putaud et al., 2010; Weijers et al., 2011) and the contribution from individual emission sources is very uncertain. The most important emission sources of mineral dust in the domain of interest are agricultural land management, road dust, constructions, and wind erosion of bare soils. However, experimental data show a small positive concentration difference of mineral dust between urban and rural areas (Putaud et al., 2004; Weijers et al., 2011; Vercauteren et al., 2011) indicating significant urban sources. Organic matter contributes up to 30-50% (Querol et al., 2008; Putaud et al., 2010) to the PM10 mass and the primary part which is included in primary PM is largely underestimated by LOTOS-EUROS (Hendriks et al., 2012). But the contribution of organic matter to PM10 was found to be notably similar at all types of stations including rural and kerbside stations in Europe (Putaud et al., 2010) and would therefore probably not affect the urban increment. Although the process descriptions are highly uncertain the model should be extended by a SOA description. This is important for the improvement of the simulated total PM10 concentrations but probably without impact on the urban increment. Note also that new sources as cooking and wood burning are recognized to be important in populated areas (e.g. Crippa et al., 2012). Measurement campaigns pointed out that the unspecified part of PM10 as well as metals contribute to a considerable part to the concentration differences between urban and rural stations (John and

Kuhlbusch, 2004; Weijers et al., 2011). The difference in the concentration of metals indicates that emissions from diffuse sources are important.

In section 4.1. it has been concluded that an increase of the horizontal resolution from $25 \times 25 \text{ km}^2$ to $7 \times 7 \text{ km}^2$ gives no systematic improvement of the simulated urban increment. Earlier studies have shown that higher resolutions (e.g. $2 \times 2 \text{ km}^2$) are needed to capture the urban increment for PM10 and NOx (Stern et al., 2010). This could be of special relevance for Berlin because in contrast to the other two areas the measured relative urban increment is not reproduced for Berlin. This is mainly caused by the fact that the underestimation of PM10 concentrations is higher at urban than at rural stations for Berlin. This might be due to too much dilution of the localized urban emissions as a consequence of the low grid resolution.

5 The impact of changing climate conditions on the urban increment

5.1 The impact of the extreme summer 2003 on the urban increment

In this section the measured urban increment as a function of meteorology is investigated using the example of the extreme summer 2003 and the model performance for this situation is discussed. The extreme summer 2003 was characterized by several stagnant heat waves with high temperatures, low wind speed and few precipitation events (Fink et al., 2004). During these meteorological conditions measured PM10 concentrations at background stations in Europe were found to be high compared to a five years summer average (2003-2007) (differences of 1-10 $\mu\text{g}/\text{m}^3$) (Mues et al., 2012).

In the present study increased measured PM10 concentrations in the summer 2003 compared to the summer 2003-2008 average were found at both urban and rural stations in the three areas (Tab.3-5). For example in the Ruhr area measured concentration increases range from 2.7 $\mu\text{g}/\text{m}^3$ (Dortmund) to 10.4 $\mu\text{g}/\text{m}^3$ (Vredepeel) (Tab.3a). However, the size of this concentration increase is different at urban and rural stations in the individual area and thus also the impact on the urban increment differs per area. For the Ruhr area the 2003-2008 average annual cycle (Fig.3) shows only a small impact of the summer conditions on the urban increment. But in summer 2003 the urban increment decreases to a concentration of 4.9 $\mu\text{g}/\text{m}^3$ and 19% compared to the 2003-2008 summer average (6.9 $\mu\text{g}/\text{m}^3$, 37%) (Tab.3b). This is mainly caused by a higher increase of PM10 concentrations in summer 2003 at rural stations, especially at Vredepeel and Westerwald. In the Randstad region the measured increase of PM10 concentrations in summer 2003 is even larger at the rural stations. This results in a negative urban increment in summer 2003 (-2.1 $\mu\text{g}/\text{m}^3$, -7%) (Tab.4). In contrast, in Berlin the measured concentration increase for the summer 2003 average is higher in the urban area (up to 2.4 $\mu\text{g}/\text{m}^3$) than in the rural region (0.6 and 1.7 $\mu\text{g}/\text{m}^3$). This results in a higher urban increment for the summer 2003 average (7.5 $\mu\text{g}/\text{m}^3$, 46%) compared to the summer 2003-2008 average (6.3 $\mu\text{g}/\text{m}^3$, 42%) (Tab.5). Note that the differences are only small and due to missing data not all stations could be included in the summer average.

In order to illustrate the temporal variability of PM10 concentrations at urban and rural stations as well as of the urban increment in the three areas, the summer 2003 time series is shown in Figure 4. In general the temporal variability of the urban and rural averages is similar in the individual areas. The urban increment of the Ruhr area in summer 2003 varies mainly between 0 and 10 $\mu\text{g}/\text{m}^3$ (Fig.4a). But during a severe heat wave in the beginning of August the magnitude of the urban increment changes to values between -10 and +20 $\mu\text{g}/\text{m}^3$. The temporal variation of the urban increment in the Randstad varies mainly between -10 and +10 $\mu\text{g}/\text{m}^3$ and declines up to -40 $\mu\text{g}/\text{m}^3$ in August 2003 (Fig.4b), indicating a strong increase of concentrations at rural stations. The observed urban increment in Berlin varies between 0 and 10 $\mu\text{g}/\text{m}^3$ during the summer 2003 with a maximum in August of up to 20 $\mu\text{g}/\text{m}^3$ (Fig.4c). Thus the temporal variability at urban and rural stations is similar, but especially the heat wave in August has a considerable impact on the urban increment.

LOTOS-EUROS reproduces the increase of PM10 concentrations in summer 2003 compared to the summer 2003-2008 average in the three areas but the differences are smaller than observed (Tab3-5). In contrast to the measurements, the simulated urban increment for the Ruhr area is slightly higher for the summer 2003 (4.2 $\mu\text{g}/\text{m}^3$, 41%) compared to the summer 2003-2008 average (3 $\mu\text{g}/\text{m}^3$, 35%) (Tab.3b).

This is due to a stronger increase in simulated PM10 concentrations at urban stations. For the Randstad the simulated summer 2003 urban increment is indeed negative as it was observed, but much smaller in magnitude (-0.08 $\mu\text{g}/\text{m}^3$) (Tab.4). For Berlin the measured increase of the urban increment in the summer 2003 compared to the summer 2003-2008 average is reproduced by the model albeit with smaller magnitude. The simulated relative urban increment (44%) in summer 2003 on the other hand is close to the measurements (46%) (Tab.5).

5.2 Results from the off-line coupled model system RACMO – LOTOS-EUROS

5.2.1 Present-day climate period (1989 - 2009)

In this study we used two different GCMs to downscale with RACMO2. RACMO2_ECHAM and RACMO2_MIROC show considerable differences in their representation of the overall circulation and meteorological parameters in north-west Europe (Manders et al., 2012). RACMO2_ECHAM shows more unstable conditions with lower temperature, more precipitation and higher wind speed compared to RACMO_MIROC, resulting in lower modeled total PM10 concentrations. Both simulations differ also compared to the reanalysis forced RACMO2_ERA simulation, which is taken as a reference to assess the performance of the transient simulations for the present-day period. The results of the three simulations are here illustrated by annual mean values over the 1989-2009 period of the station Vredepeel, the value for the individual parameter is given in brackets behind the simulation name. The station Vredepeel is chosen because it is included in both analysis for the Ruhr area and the Randstad and it is a continental station. In the domain of interest the number of hot days (days with $T_{\max}>25^\circ$) is much lower for RACMO2_ECHAM (16), whereas the values is somewhat higher for RACMO2_MIROC (30) compared to RACMO2_ERA (28). While the number of wet days (days with more than 0.5mm rain) for RACMO2_MIROC (199) are similar to RACMO2_ERA (196), RACMO2_ECHAM (227) produces more precipitation and shows more wet days. The number of calm days (daily average wind speed $<2\text{ms}^{-1}$) for RACMO2_ECHAM (32) is somewhat lower compared to RACMO2_ERA (40), whereas RACMO2_MIROC (44) tends to simulate more calm days. For a more detailed discussion we refer to Manders et al., (2012).

As a consequence of these differences the use of the three different sets of meteorological input data (RACMO2_ERA, RACMO2_ECHAM and RACMO2_MIROC) for LOTOS-EUROS yields differences in the resulting modeled PM10 concentrations in the three areas, which is here discussed by means of the Ruhr area. Whereas RLE_ECHAM underestimates the RLE_ERA results at every station (up to 1.5 $\mu\text{g}/\text{m}^3$), RLE_MIROC overestimates at most of the stations (up to 0.3 $\mu\text{g}/\text{m}^3$) (Tab.3a). These differences are illustrated in the frequency distributions of PM10 concentrations in Figure 5a. Compared to RLE_ERA, the distribution for RLE_ECHAM is shifted to lower concentrations for both the rural and urban stations. The position of the maximum is at lower concentrations and at a higher frequency of occurrence. At the same time, the occurrence of high concentrations (above 10 $\mu\text{g}/\text{m}^3$) in RLE_ECHAM is less frequent than in RLE_ERA. The distribution for RLE_MIROC, on the other hand, is slightly shifted to higher concentrations compared to RLE_ERA, especially at urban stations.

These differences in simulated PM10 concentrations also impact the urban increment. The highest urban increment is modeled with RLE_MIROC (4.24 $\mu\text{g}/\text{m}^3$), followed by RLE_ERA (4.03 $\mu\text{g}/\text{m}^3$) and RLE_ECHAM (3.55 $\mu\text{g}/\text{m}^3$) (Tab.3b). The simulated urban increment is reflected in the frequency

distribution but it differs substantially from the observed distribution for the 2003-2008 measurements (Fig.5a). In the simulations the urban and rural regions show a maximum peak at similar concentrations ($8\text{-}10\mu\text{g}/\text{m}^3$) but with different frequency of occurrence (about 6% and 8-9%) and the distribution for the urban stations is flatter and broader. The distribution of the measurements has its maximum for the urban average at higher concentrations but with lower frequency of occurrence compared to the rural average and shows a broader distribution.

Also for the Randstad and Berlin the present-day average for PM10 concentrations differ between the three model simulations, again with lowest concentrations for RLE_ECHAM, followed by RLE ERA and RLE_MIROC. This affects the urban increment in the following way. For the Randstad the values are $1.45\mu\text{g}/\text{m}^3$ (RLE ERA), $1.49\mu\text{g}/\text{m}^3$ (RLE_ECHAM) and $1.36\mu\text{g}/\text{m}^3$ (RLE_MIROC), and for Berlin $1.86\mu\text{g}/\text{m}^3$ (RLE ERA), $1.72\mu\text{g}/\text{m}^3$ (RLE_ECHAM) and $1.98\mu\text{g}/\text{m}^3$ (RLE_MIROC) (Tab.4+5).

5.2.2 Future climate conditions (2041-2060)

Temperature differences between the future and present-day climate are obvious in both simulations, in particular for RACMO2_MIROC, whereas the climate change signal in wind speed and precipitation is on average only small in north-west Europe. At Vredepeel the number of hot days increases for both RACMO2_ECHAM (25) and RACMO2_MIROC (55) compared to the present-day climate. The number of wet days remains more or less the same for both simulations. The same holds for the number of calm days for RACMO2_ECHAM (31) but for RACMO2_MIROC (50) this parameter increases slightly for the future climate period. The characteristics of simulated PM10 concentrations and the urban increment in the Ruhr area, as derived for the present-day period, is found maintained in the future climate simulations with both RLE_ECHAM and RLE_MIROC. The corresponding frequency distributions of PM10 concentrations (Fig.5b) clearly show that the climate change signal of the individual transient simulations is much smaller than the difference between the two transient simulations for the present-day period. This modest effect of climate change is also seen in the responses of the absolute PM10 values at the individual stations which are only up to $0.64\mu\text{g}/\text{m}^3$ in the Ruhr area (Tab.3a). Whereas the PM10 concentration averaged over all rural and urban stations in the Ruhr area (Tab.3b) and the Randstad (Tab.4) show mostly a small increase in both transient simulations, these averages in the area of Berlin are found to be reduced slightly in both transient simulations (Tab.5). Likewise, the responses in the urban increment are also small, e.g. in the Ruhr area they decrease with $0.07\mu\text{g}/\text{m}^3$ for RLE_ECHAM and increase with $0.03\mu\text{g}/\text{m}^3$ for RLE_MIROC.

Since PM10 consists of several components which may respond differently to changing climate conditions we have also looked into the changes of the individual PM10 components (Fig.6). The relative differences between the results of the future and the present-day period for PM10 and the individual components are only between $\pm 6\%$ for RLE_ECHAM and $\pm 8\%$ for RLE_MIROC in the three regions. In the RLE_ECHAM simulation sea salt concentrations are increasing while concentrations of the other PM10 components are generally decreasing at most of the stations in the Ruhr area and the Randstad. In the RLE_MIROC simulation the opposite response is seen. Also in the RLE_MIROC simulations, at the majority of stations in both areas it is the response in the concentrations of secondary inorganic components which is found most pronounced after sea salt. Largest differences are found for nitrate and ammonium at rural stations around the Randstad and at the stations Vredepeel and Borken in the Ruhr

area. In Berlin, a somewhat different response is seen for the individual components (Fig.6). Concentrations of all components, besides sea salt, are found to decrease for RLE_ECHAM with highest reductions found for secondary inorganic components of up to 6%. In contrast, in RLE_MIROC the concentrations of sulphate, primary PM2.5 and primary PM10 as well as BC increase whereas all other components decrease under the modeled future climate conditions. In general, for the RLE_ECHAM simulation differences for the PM components concentrations are only small, but for Berlin a small increase of the number of wet days could be relevant for the decrease of pollutant concentrations. The increase of the number of calm days found for the RACMO2_MIROC simulation could lead to lower dilution of pollutants and thus to increasing concentrations. An increase of temperature could be especially relevant for the concentration of SIA as it will be discussed in section 5.3.

5.3 The PM10 urban increment under changing climate conditions

The variability of the urban increment with weather and its dependency on the urban area is investigated by means of one specific summer episode and by two transient climate runs. For summer 2003, the response of the urban increment on this weather situation depends on the urban region. For the Ruhr area and the Randstad the measured increase of the PM10 concentrations were found to be stronger at rural than at urban stations. That the model is able to reproduce the inverse urban increment for the Randstad, hints a high contribution of SIA at rural stations (e.g. Vredepeel). The SIA concentrations were found to increase with high temperature which is reproduced by the model (Mues et al., 2012). The stronger increase of PM10 concentrations at urban stations in Berlin might be due to a stronger accumulation of pollutants in the urban area and a less high contribution of SIA at rural stations. In this study the impact of climate change on the modeled PM10 concentrations and the urban increment was found to be small in both scenario runs, even at the component level. This small response has been found in several other studies (see Jacob and Winner, 2009). However the concentration differences between the simulations forced by either ECHAM or MIROC indicate that PM10 concentration levels are sensitive to circulation patterns rather than temperature change alone, and that PM10 concentration levels may thus change when circulation patterns change in the future.

In the simulations discussed in this paper anthropogenic emissions have been kept constant (year 2005) to focus on the impact of a changing climate. However, anthropogenic emissions of PM and its precursors in Europe are expected to decline by approximately 40-45 percent between 2000 and 2020 due to stringent national and community legislation on emission controls (Cofala et al., 2006). These downward trends are expected to continue after 2020 (Cofala et al., 2007). The low impact of climate change on PM10 concentrations, contrasted to the expected emission reduction, indicates that the evolution of future PM levels will be dominated by emission changes. This has also been illustrated for the US by Tagaris et al., (2007). Note, however, that current studies neglect that climate change itself may affect the emission strength of both natural sources and anthropogenic sources. Increased aridity may enhance mineral dust emission through resuspension and wind erosion. Also wild fires may become more frequent in the future (e.g. Moriondo et al., 2006). Moreover fossil fuel combustion emissions could change, for example, as a result of an intensified demand of air conditioning induced by higher temperatures in summer on the one hand (Jacob and Winner, 2009) and a reduced demand of heating due to milder winters on the other hand. Finally a shift to biomass as a source of energy may enhance

wood burning emissions (Ashworth et al., 2011) and may enhance SOA formation as a consequence of large scale land use changes (Lathière et al., 2006). Hence climate change may indirectly affect PM levels through feedback on emissions, which needs further research. The impact of these reductions on total PM₁₀ and on the urban increment needs detailed emission and spatial planning scenarios and therefore goes far beyond the scope of the present study.

6 Summary and Conclusion

We have determined average PM10 urban increments for three densely populated regions in North-West Europe, based on Airbase measurements and model simulations with the regional-scale CTM LOTOS-EUROS. Although the measured urban background concentrations were quite comparable ($27\text{-}30\mu\text{g}/\text{m}^3$) for the three areas, the surrounding rural concentrations differed considerably between the regions, resulting in a different urban increment.

LOTOS-EUROS underestimated the absolute concentrations but was able to reproduce the relative urban increment for the Ruhr area and the Randstad area, and could be used to interpret the observed differences between the regions, despite the fact that the urban scale was not resolved. The resolution of $0.5^\circ\text{x}0.25^\circ$ was high enough to produce the general features, although measurements at individual stations were not always well represented. Going to a higher resolution ($0.125^\circ\text{x}0.0625^\circ$) resulted in more spatial detail but did not improve the model performance for the measurement locations significantly. A better representation of the characteristics of urban areas in regional CTMs seem to be required, especially for isolated cities like Berlin. So far characteristics of urban areas in regional CTMs are taken into account by a high emission density and the roughness length, affecting dry deposition velocities. However, a model study using the example of Paris, described in Sarrat et al. (2006), showed that the consideration of small-scale dynamical processes generated by an urban area are crucial for a good model representation of primary pollutants such as nitrogen oxides. Urban cover affects not only turbulence, leading for example to the dilution of primary pollutants inside a higher boundary layer during night, but also chemistry and deposition velocities, whereby the net result of these effects is depending on the component (Sarrat et al., 2006). Concerning emissions a bottom-up instead of a top-down approach could increase the representation of the emission distribution in urban areas, and could increase the consistency of simulated concentrations and concentration gradients with observations as it was for example found in a MEGAPOLI study for Paris.

The urban increment may be affected by climate change, as indicated by the observed differences in urban increments between the extremely warm summer of 2003 and the summer average 2003-2008. This change was partly reproduced by the model. In addition, two long-term transient climate simulations were used. These indicated that at the studied scale, the impact of climate change on PM for a single climate realization was small, but that changes in circulation could have an impact. Both simulations retained their circulation characteristics in the transient run, mainly showing a temperature increase, but mutually differed in their circulation characteristics. One has to keep in mind that expected changes in emissions and emission locations probably also heavily affect total PM10 concentrations and the urban increment.

The present approach indicates that regional scale-modelling is a useful tool in assessing air quality differences and resolves part of the urban increment. Such simulations can be used as boundary conditions for more detailed and more computationally intensive models addressing cities at far higher resolution, using local bottom-up emission inventories and local-scale meteorology.

Acknowledgments

We would like to thank the EEA for providing the measurement data from the AirBase database and the Dutch Knowledge for Climate Programme for providing the simulations of the coupled model system RACMO2 LOTOS-EUROS. Furthermore, this work was financially supported by TNO and the Milieu-Project of the Freie Universität Berlin. We thank the reviewers for their constructive comments.

References

- AIRBASE, 2012. European Topic Centre on Air and Climate Change.
<http://acm.eionet.europa.eu/databases/airbase>.
- Ashworth K., Folberth G., Hewitt C.N., Wild O., 2011. Impacts of near-future cultivation of biofuel feedstocks on atmospheric composition and local air quality. *Atmospheric Chemistry and Physics* 11, 24857-939.
- Builtjes P.J.H., Jörß W., Stern R., Theloke J., 2010. F&E Vorhaben: "Strategien zur Verminderung der Feinstaubbelastung" e PAREST: Zusammenfassender Abschlussbericht FKZ 206 43 200-01, Report.
- BW, "Berliner Wetterkarte", 2008. Berliner Wetterkarte e.V. www.berlinerwetterkarte.de.
- Cofala J., Klimont Z., Amann M., 2006. The potential for further control of emissions of fine particulate matter in Europe. IIASA Intermin Report IR-06-011.
- Cofala J., Amann M., Klimont Z., Kupiainen K., Höglund-Isaksson, 2007. Scenarios of global anthropogenic emission of air pollutants and methane until 2030. *Atmospheric Environment* 41, 8486 – 8499.
- Crippa M., DeCarlo P.F., Slowik J.G., Mohr C., Heringa M.F., Chirico R., Poulain L., Freutel F., Sciare J., Cozic J., Di Marco C.F., Elsasser M., José N., Marchand N., Abidi E., Wiedensohler A., Drewnick F., Schneider J., Borrmann S., Nemitz E., Zimmermann R., Jaffrezo J.-L., Prévôt A.S.H., and Baltensperger U., 2012. Wintertime aerosol chemical composition and source apportionment of the organic fraction in the metropolitan area of Paris. *Atmopheric Chemistry and Physics Discussions*, 12, 22535 – 22586. Discussion Paper
- Cuvelier C., Thunis P., Vautard R., Amann M., Bessagnet B., Bedogni M., Berkowicz R., Brandt J., Brocheton F., Builtjes P., Carnavale C., Coppalle A., Denby B., Douros J., Graf A., Hellmuth O., Hodzic A., Honoré C., Jonson J., Kerschbaumer A., de Leeuw F., Minguzzi E., Moussiopoulos N., Pertot C., Peuch V.H., Pirovano G., Rouil L., Schaap M., Stern R., Tarrason L., Vignati E., Volta M., White L., Wind P., Zuber A., 2007. CityDelta: A model intercomparison study to explore the impact of emission reductions in European cities in 2010. *Atmospheric Environment* 41, 189-207.
- Dee D.P., Uppala S.M., Simmons A.J., Berrisford P., Poli P., Kobayashi S., Andrae U., Balmaseda M. A., Balsamo G., Bauer P., Bechtold P., Beljaars A. C. M., van de Berg L., Bidlot J., Bormann N., Delsol C., Dragani R., Fuentes M., Geer A.J., Haimberger L., Healy S. B., Hersbach H., Hólm E.V., Isaksen L., Källberg

P., Köhler M., Matricardi M., McNally A. P., Monge-Sanz B. M., Morcrette J.-J., Park B.-K., Peubey C., de Rosnay P., Tavolato C., Thépaut J.-N., Vitart F., 2011. The ERA-Interim reanalysis: configuration and performance of the data assimilation system, *Q. J. Roy. Meteorol. Soc.*, 137, 553–597, doi:10.1002/qj.828.

Denier van der Gon H.A.C., Visschedijk A., van den Brugh H., Dröge R., 2010. F&E Vorhaben: "Strategien zur Verminderung der Feinstaubbelastung" e PAREST: A high resolution European emission data base for the year 2005. TNO-Report, TNO-034-UT-2010-01895_RPT-ML, Utrecht.

EEA, 2012. Air quality in Europe — 2012 report. European Environmental Agency report No 4/2012, doi:10.2800/55823.

EEA, 2007. Europe's Environment. The Fourth Assessment. EEA, Copenhagen.

EU, 2008: Directive 2008/50/EC of the European Parliament and of the Council on ambient air quality and cleaner air for Europe.

Fink A.H., Brücher T., Krüger A., Leckebusch G.C., Pinto J.G., Ulbrich U., 2004. The 2003 European summer heatwaves and drought e synoptic diagnosis and impacts. Royal Meteorological Society, *Weather* 59, 209-216.

Hendriks C., Kranenburg R., Kuenen J.J.P., van Gijlswijk R.N., Denier van der Gon H.A.C., Schaap M., 2012. Establishing the origin of Particulate Matter concentrations in the Netherlands. TNO-060-UT-2012-00474, TNO report.

Jacob D., Barring L., Christensen O.B., Christensen J.H., de Castro M., Deque M., Giorgi F., Hagemann S., Hirschi M., Jones R., Kjellstrom E., Lenderingk G., Rockel B., Sanchesz E., Schar C., Seneviratne S.I., Somot S., Van ulden A., Van den Hurk B., 2007. An inter-comparison of regional climate models for Europe : model performance in present-day climate. *Climate Change*, 81:31-52.

Jacob D.J. and Winner D.A., 2009. Effect of climate change on air quality. *Atmospheric Environment* 43, 51-63.

John A. and Kuhlbusch T., 2004. Ursachenanalyse von Feinstaub(PM10)-Immissionen in Berlin auf der Basis von Messungen der Staubinhaltsstoffe am Strand, in der Innenstadt und in der Straßenschlucht. IUTA-Bericht Nr. LP 09/2004 – Abschlussbericht.

Jungclaus J.H., Botzet M., Haak H., Keenlyside N., Luo J., Latif M., Marotzke J., Mikolajewicz U., Roeckner E., 2006. Ocean circulation and tropical variability in the AOGCM ECHAM5/MPI-OM, *J. Climate*, 19, 3952–3972.

K-1 Model Developers: K-1 Coupled Model (MIROC) Description, K-1 Technical Report 1, edited by: Hasumi H. and Emori S., Center for Climate System Research, University of Tokyo, Tokyo, Japan, 34 pp., available at: <http://www.ccsr.u-tokyo.ac.jp/kyosei/hasumi/MIROC/tech-repo.pdf>, 2004.

Kjellström E., Boberg F., Castro M., Christensen H.J., Nikulin G., Sánchez E., 2010. Daily and monthly temperature and precipitation statistics as performance indicators for regional climate models. *Clim. Res.* 44, 135-150.

Kuenen J., Denier van der Gon H., Visschedijk A., van der Brugh H., van Gijlswijk R., 2011. MACC European emission inventory for the years 2003-2007. TNO report, TNO-060-UT-2011-00588, Utrecht.

Langner J., Bergström R., Foltescu V., 2005. Impact of climate change on surface ozone and deposition of sulphur and nitrogen in Europe. *Atmospheric Environment* 39, 1129-1141.

Lathière J., Hauglustaine D.A., Friend A.D., De Noblet-Ducoudré N., Viovy N., Folberth G.A., 2006. Impact of climate variability and land use changes on global biogenic volatile organic compound emissions. *Atmospheric Chemistry and Physics* 6, 2129-2146.

Lenderink G., Van den Hurk B., Van Meijgaard E., Van Ulden A. P., Cuijpers J., 2003. Simulation of present-day climate in RACMO2: first results and model developments, KNMI technical report TR 252.

Lenschow P., Abraham H.J., Kutzner K., Lutz M., Prüß J.D., Reichenbächer W., 2001. Some ideas about the sources of PM10. *Atmospheric Environment* 35, Supplement NO.1 S23-S33.

Manders A.M.M., Schaap M., Hoogerbrugge R., 2009. Testing the capability of the chemistry transport model LOTOS-EUROS to forecast PM10 levels in the Netherlands. *Atmospheric Environment* 43, 4050-4059.

Manders A.M.M., van Meijgaard E., Mues A.C., Kranenburg R., van Ulft L.H., Schaap M., 2012. The impact of differences in large-scale circulation output from climate models on the regional modeling of ozone and PM. *Atmospheric Chemistry and Physics Discussion*, 12, 9441-9458.

Meleux F., Solmon F., Giorgi F., 2007. Increase in summer European ozone amounts due to climate change. *Atmospheric Environment* 41, 7577-7587.

Millero F.J., 2004. Physicochemical controls on sea water. In: Holland, H.D., Turkian, K.K. (Eds.), *Treatise on Geochemistry*. Elsevier, Amsterdam (Chapter 6.01).

Moriondo M., Good P., Durão R., Bindi M., Giannakopoulos C., Corte-Real J., 2006. Potential impact of climate change on fire risk in the Mediterranean area, *Clim. Res.*, 31, 85–95, doi:10.3354/cr031085.

Mues A., Manders A., Schaap M., Kerschbaumer A., Stern R., Builtjes P., 2012. Impact of the extreme meteorological conditions during the summer 2003 in Europe on particulate matter concentrations. *Atmospheric Environment* 55, 377-391.

Putaud J.-P. , Raes F., Van Dingenen R., Brüggemann E., Facchini M.-C., Decesari S., Fuzzi S., Gehring R., Hüglin C., Laj P., Lorbeer G., Maenhaut W., Mihalopoulos N., Müller K., Querol X., Rodriguez S., Schneider J., Spindler G., ten Brink H., Tørseth K., Wiedensohler A., 2004. A European aerosol phenomenology - 2:

chemical characteristics of particulate matter at kerbside, urban, rural and background sites in Europe. *Atmospheric Environment* 38, 2579–2595.

Putaud J.-P., Van Dingenen R., Alastuey A., Bauer H., Birmili W., Cyrys J., Flentje H., Fuzzi S., Gehrig R., Hansson H.C., Harrison R.M., Herrmann H., Hitzenberger R., Hüglin C., Jones A.M., Kasper-Giebl A., Kiss G., Kousa A., Kuhlbusch T.A.J., Löschau G., Maenhaut W., Molnar A., Moreno T., Pekkanen J., Perrino C., Pitz M., Puxbaum H., Querol X., Rodriguez S., Salma I., Schwarz J., Smolik J., Schneider J., Spindler G., ten Brink H., Tursic J., Viana M., Wiedensohler A., Raes F., 2010. A European aerosol phenomenology - 3: Physical and chemical characteristics of particulate matter from 60 rural, urban, and kerbside sites across Europe. *Atmospheric Environment* 44, 1308–1320.

Querol X., Alastuey A., Moreno T., Viana M.M., Castillo S., Pey J., Rodríguez S., Artiñano B., Salvador P., Sánchez M., García Dos Santos S., Herce Garraleta M.D., Fernandez-Patier R., Moreno-Grau S., Negral L., Minguillón M.C., Monfort E., Sanz M.J., Palomo-Marín R., Pinilla-Gil E., Cuevas E., de la Rosa J., Sánchez de la Campa A., 2008. Spatial and temporal variations in airborne particulate matter (PM10 and PM2.5) across Spain 1999–2005. *Atmospheric Environment* 42, 3964–3979.

Roeckner E., Bäuml G., Bonaventura L., Brokopf R., Esch M., Giorgetta M., Hagemann S., Kirchner I., Kornblueh L., Manzini E., Rhodin A., Schlese U., Schulzweida U., Tompkins A., 2003. The Atmospheric General Circulation Model ECHAM5, Part I: Model Description, MPI Report 349, Max Planck Institute for Meteorology, Hamburg, Germany, 127 pp..

Sarrat C., Lemonsu A., Masson V., Guedalia D., 2006. Impact of urban heat island on regional atmospheric pollution. *Atmospheric Environment* 40, 1743 – 1758.

Schaap M., Müller K., ten Brink H.M., 2002. Constructing the European aerosol nitrate concentration field from quality analysed data. *Atmospheric Environment* 36, 1323-1335.

Schaap M., Timmermans R.M.A., Sauter F.J., Roemer M., Velders G.J.M., Boersen G.A.C., Beck J.P., Builtjes P.J.H., 2008. The LOTOS-EUROS model: description, validation and latest developments. *International Journal of Environment and Pollution* 32 (2), 270-289.

Schaap M., Manders A.M.M., Hendriks E.C.J., Cnossen J.M., Segers A.J.S., Denier van der Gon H.A.C., Jozwicka M., Sauter F.J., Velders G.J.M., Matthijzen J., Builtjes P.J.H., 2009. Regional modelling of particulate matter for the Netherlands. Technical background report BOP.

Schaap M., Otjes R. P., Weijers E. P., 2011. Illustrating the benefit of using hourly monitoring data on secondary inorganic aerosol and its precursors for model evaluation. *Atmos. Chem. Phys.*, 11, 11041–11053.

Solazzo E., et al., 2012. Model evaluation and ensemble modelling of surface-level ozone in Europe and North America in the context of AQMEII. *Atmospheric Environment* 53, 60-74.

Stern R., Builtjes P.J.H., Schaap M., Timmermans R., Vautard R., Hodzic A., Memmesheimer M., Feldmann H., Renner E., Wolke R., Kerschabumer A., 2008. A model inter-comparison study focusing on episodes with elevated PM10 concentrations. *Atmospheric Environment* 42. 4567-4588.

Stern R., 2010. Anwendung des REM-CALGRID-Modells auf die Ballungsräume Berlin, München und Ruhrgebiet. – PAREST-Project: FKZ 206 43 200/01, Report.

Tagaris E., Manomaiphiboon K., Liao K.-J., Leung L. R., Woo J. H., He S., Amar P., Russell A. G., 2007. The impact of global climate change and emissions on regional ozone and fine particulate matter concentrations over the US, *J. Geophys. Res.-Atmos.*, 112, D14312, doi:10.1029/2006JD008262.

Tai A.P. K., Mickley L.J., Jacob D.J., Leibensperger E.M., Zhang L., Fisher J. A., Pye H.O.T., 2012. Meteorological modes of variability for fine particulate matter (PM2.5) air quality in the United States: implications for PM2.5 sensitivity to climate change. *Atmos. Chem. Phys.*, 12, 3131–3145.

ten Brink H.M., Kruisz C., Kos G.P.A., Berner A., 1997. Composition/size of the light-scattering aerosol in the Netherlands. *Atmospheric Environment*, 31, 23, 3955-3962.

Van Meijgaard E., Van Ulft L.H., Van de Berg W.J., Bosveld F.C., Van den Hurk B.J.J.M., Lendering G., Siebesma A.P., 2008. The KNMI regional atmospheric climate model RACMO version 2.1. KNMI Technical report, TR-302.

Vautard R., Beekman M., Desplat J., Hodzic A., Morel S., 2007a. Air quality in Europe during the summer of 2003 as a prototype of air quality in a warmer climate. *Comptes Rendus Geoscience*, 339, 747-763.

Vercauteren J., Matheeussen C., Wauters E., Roekens E., van Grieken R., Krata A., Makarovska Y., Maenhaut W., Chi X., Geypens B., 2011. Chemkar PM10: An extensive look at the local differences in chemical composition of PM10 in Flanders, Belgium, *Atmospheric Environment*, 45 (1), 108-116.

Weijers E.P., Schaap M., Nguyen L., Matthijsen J., Denier van der Gon H.A.C., ten Brink H.M., Hoogerbrugge R., 2011. Anthropogenic and natural constituents in particulate matter in the Netherlands. *Atmos. Chem. Phys.*, 11, 2281–2294.

Tables

Station code	Station name	Country	Location		Station type of area (all background)	Availability of AirBase data (%)	
			latitude	longitude		2008	2003-2008
Ruhr area							
DENW081	Borken-Gemen	DE	51.86	6.87	rural	92.9	97.1
DEHE046	Bad Arolsen	DE	51.43	8.93	rural	94.0	92.4
DERP016	Westerwald-Herdorf	DE	50.77	7.97	rural	96.5	97.7
DENW022	Gelsenkirchen -Bismarck	DE	51.53	7.10	urban (AirBase: suburban)	98.4	99.1
DENW038	Mülheim-Styrum	DE	51.45	6.87	urban	98.9	99.2
DENW024	Essen-Vogelheim	DE	51.50	6.98	urban	98.1	97.7
DENW008	Dortmund-Eving	DE	51.54	7.46	urban	95.1	98.0
Randstad							
NL00807	Hellendoorn -Luttenbergerweg	NL	52.39	6.40	rural	91.3	69.2
NL00738	Wekerom -Riemterdijk	NL	52.11	5.71	rural	95.4	91.0
NL00131	Vredepeel -Vredeweg	NL	51.54	5.85	rural	95.4	93.8
NL00437	Westmaas -Groeneweg	NL	51.79	4.45	rural	97.5	94.3
NL00444	De Zilk -Vogelaarsdreef	NL	52.30	4.51	rural	95.9	95.9
NL00633	Zegveld -Oude Meije	NL	52.14	4.84	suburban (AirBase: rural)	91.5	86.0
NL00441	Dordrecht -Frisostraat	NL	51.80	4.67	urban	96.5	96.8
NL00446	Den Haag -Bleriotlaan	NL	52.04	4.36	urban (AirBase: suburban)	92.1	47.6
NL00418	Rotterdam -Schiedamsevest	NL	51.92	4.48	urban	97.8	94.5
NL00520	Amsterdam -Florapark	NL	52.39	4.92	urban	13.7	71.3
Berlin							
DEUB030	Neuglobsow	DE	53.14	13.03	rural	100.0	65.2
DEBB053	Hasenholz	DE	52.56	14.02	rural	99.2	33.2
DEBB066	Spreewald	DE	51.90	14.06	rural	99.2	92.8
DEBB065	Lütte (Belzig)	DE	52.19	12.56	rural	98.9	69.4
DEBE056	Friedrichshagen	DE	52.45	13.65	suburban (AirBase: rural)	97.0	91.7
DEBE051	Buch	DE	52.64	13.49	suburban	100.0	93.5
DEBE034	Neukölln -Nansenstraße	DE	52.49	13.43	urban	98.4	96.0
DEBE010	Wedding -Amrumer Str.	DE	52.54	13.35	urban	95.9	94.8

Table 1:

Characteristics of the stations used in this analysis. Station type are given as used in this study, in brackets AirBase characteristic if different than used in the study.

Name	Time period	Grid	Horizontal resolution	Meteorological driver	Emissions	Purpose of run
LE_zoom	2008	1°-14°E 47°-55°N	0.125°x0.0625° regular longitude-latitude grid	12 h forecast data from the operational ECMWF stream with analyses at noon and midnight at a horizontal resolution of about 25x25km	MACC emission database of the year 2005 (Kuenen et al.,2011)	Investigating the impact of the grid resolution on model results.
LE_eu	2003-2008	10°W-40°E 35°-70°N	0.5°x0.25° regular longitude-latitude grid	RACMO2 with ERA-Interim boundaries (RACMO ERA)		Investigating concentration differences between urban and rural regions. A long-term average (6 years) is chosen to avoid inter-annual variability.
RLE_ERA	1989-2009			Output from a SRES-A1B constraint transient run with the GCM ECHAM5r3 have been dynamically downscaled with RACMO2 (RACMO_ECHAM)	2005 MACC emission kept constant in order to concentrate on the effect of changing meteorological conditions	Compared to RLE_ECHAM, RLE_MIROC for the period 1-1-1989 to 31-12-2009 (present-day climate) to identify differences.
RLE_ECHAM	1970-2060	10°W-40°E 35°-70°N	0.5x0.25° regular longitude-latitude grid	Output from a SRES-A1B constraint transient run with the GCM MIROC-hires have been dynamically downscaled with RACMO2 (RACMO_MIROC)		Results of the period 1-1-2041 to 31-12-2060 (future climate) will be compared to the present-day results to study the impact of climate change.
RLE_MIROC						

Table 2:
Characteristics of model simulations.

Ruhr area		Rural stations											
tPM10 ($\mu\text{g}/\text{m}^3$)		Vredepeel (NL00131)			Borken (DENW081)			Bad Arolsen (DEHE046)			Westerwald (DERP016)		
		Obs	LE_zoom	LE_eu	Obs	LE_zoom	LE_eu	Obs	LE_zoom	LE_eu	Obs	LE_zoom	LE_eu
2008 average		23.66	10.08	10.99	22.43	9.79	10.42	16.12	6.42	6.57	11.94	5.20	6.80
2003-2008 ave.		26.75	x	12.52	24.80	x	11.90	17.55	x	7.69	14.83	x	7.90
Standard dev. 2008		13.29	4.72	4.87	10.15	4.44	4.56	7.26	3.66	3.69	8.02	2.93	3.89
Correlation 2008		x	0.67	0.67	x	0.58	0.58	x	0.42	0.42	x	0.34	0.32
Summer ave. 03-08		23.17	x	11.38	21.25	x	10.41	16.00	x	6.07	14.09	x	6.15
Summer ave. 2003		33.61	x	13.72	25.19	x	12.92	20.57	x	6.92	21.99	x	7.58
Climate runs	RLE ERA	RLE ECHAM	RLE MIROC	RLE ERA	RLE ECHAM	RLE MIROC	RLE ERA	RLE ECHAM	RLE MIROC	RLE ERA	RLE ECHAM	RLE MIROC	
Present-day ave.	13.59	12.58	13.83	13.26	12.48	13.45	9.12	8.39	9.01	9.95	9.07	9.87	
Future climate ave.	x	12.64	14.47	x	12.51	14.01	x	8.36	8.99	x	9.03	9.92	
		Urban stations											
		Gelsenkirchen (DENW022)			Mülheim (DENW038)			Essen (DENW024)			Dortmund (DENW008)		
		Obs	LE_zoom	LE_eu	Obs	LE_zoom	LE_eu	Obs	LE_zoom	LE_eu	Obs	LE_zoom	LE_eu
2008 average		27.06	9.78	11.21	25.51	10.52	12.14	27.81	9.25	12.12	26.21	11.88	11.38
2003-2008 average		28.37	x	12.79	27.86	x	13.81	29.45	x	13.82	27.64	x	12.85
Standard dev. 2008		17.95	5.46	5.83	15.90	6.06	7.00	15.40	5.13	6.70	14.10	7.41	5.87
Correlation 2008		x	0.58	0.54	x	0.51	0.55	x	0.53	0.51	x	0.62	0.60
Summer ave. 03-08		24.93	x	11.05	24.34	x	11.92	27.24	x	11.87	25.52	x	11.05
Summer ave. 2003		28.61	x	13.98	31.63	x	15.39	32.42	x	14.82	28.19	x	13.65
Climate runs	RLE ERA	RLE ECHAM	RLE MIROC	RLE ERA	RLE ECHAM	RLE MIROC	RLE ERA	RLE ECHAM	RLE MIROC	RLE ERA	RLE ECHAM	RLE MIROC	
Present-day ave.	14.76	13.57	14.97	16.25	14.79	16.58	16.25	14.79	16.58	14.76	13.57	14.97	
Future climate ave.	x	13.57	15.35	x	14.66	16.88	x	14.66	16.88	x	13.57	15.35	

Table 3a:

Statistics for the rural and urban stations in the Ruhr area

Ruhr area	Rural stations			Urban stations		
tPM10 ($\mu\text{g}/\text{m}^3$)	Obs	LE_zoom	LE_eu	Obs	LE_zoom	LE_eu
2008 average	18.54	7.87	8.70	26.65	10.36	11.71
2003-2008 average	20.98	x	10.00	28.33	x	13.32
Summer ave. 2003-2008	18.63	x	8.50	25.51	x	11.47
Summer ave. 2003	25.34	x	10.29	30.21	x	14.46
Climate runs	RLE ERA	RLE ECHAM	RLE MIROC	RLE ERA	RLE ECHAM	RLE MIROC
Present-day climate average	11.48	10.63	11.54	15.51	14.18	15.78
Future climate average	x	10.64	11.85	x	14.12	16.12
Difference urban - rural stations						
	Obs	LE_zoom	LE_eu			
2008 average	8.11	2.49	3.02			
2008 average rel. difference (%)	43.75	31.57	34.70			
2003-2008 average	7.35	x	3.32			
2003-2008 rel. difference (%)	35.02	x	33.14			
Summer average 2003-2008	6.88	x	2.97			
Summer 2003-2008 rel. difference (%)	36.93	x	34.93			
Summer average 2003	4.87	x	4.18			
Summer 2003 rel. difference (%)	19.23	x	40.59			
Climate runs	RLE ERA	RLE ECHAM	RLE MIROC			
Present-day climate average	4.03	3.55	4.24			
Future climate average	x	3.48	4.27			

Table 3b:**Statistics for stations in the Ruhr area, averaged over stations in the rural, suburban and urban region.**

Randstad	Rural stations			Suburban stations			Urban stations		
tPM10 ($\mu\text{g}/\text{m}^3$)	obs	LE_zoom	LE_eu	obs	LE_zoom	LE_eu	obs	LE_zoom	LE_eu
2008 average	23.92	10.22	11.21	24.75	10.98	12.04	28.64	12.28	13.20
2003-2008 average	26.56	x	12.45	24.98	x	13.25	29.62	x	14.00
Summer average 2003-2008	23.70	x	11.01	22.33	x	11.26	26.93	x	11.67
Summer average 2003	31.20	x	12.66	28.33	x	12.28	29.10	x	12.58
Climate runs	RLE ERA	RLE ECHAM	RLE MIROC	RLE ERA	RLE ECHAM	RLE MIROC	RLE ERA	RLE ECHAM	RLE MIROC
Present-day climate ave.	13.34	12.54	13.49	14.05	13.38	14.14	14.79	14.03	14.85
Future climate average	x	12.55	13.89	x	13.35	14.38	x	14.01	15.16
Differences urban-rural stations									
	Obs	LE_zoom	Le_eu						
2008 average	4.71	2.06	1.99						
2008 ave. rel. difference (%)	19.70	20.12	17.78						
2003-2008 average	3.06	x	1.54						
2003-2008 ave. rel. difference (%)	11.50	x	12.37						
Summer ave. 2003-2008	3.23	x	0.66						
Summer 03-08 rel. difference (%)	13.64	x	6.01						
Summer average 2003	-2.10	x	-0.08						
Summer 2003 rel. difference (%)	-6.74	x	-0.63						
Climate runs	RLE ERA	RLE ECHAM	RLE MIROC						
Present-day climate average	1.45	1.49	1.36						
Future climate average	x	1.46	1.26						

Table 4:**Statistics for stations in the Randstad, averaged over stations in the rural, suburban and urban region.**

Berlin	Rural stations			Suburban stations			Urban stations		
	obs	LE_zoom	LE_eu	obs	LE_zoom	LE_eu	obs	LE_zoom	LE_eu
tPM10 ($\mu\text{g}/\text{m}^3$)									
2008 average	17.04	5.22	5.78	20.14	7.03	6.46	23.93	7.02	7.16
2003-2008 average	18.28	x	6.30	23.29	x	7.35	26.74	x	8.03
Summer average 2003-2008	15.22	x	3.48	18.72	x	4.84	21.55	x	5.46
Summer average 2003	16.34	x	4.13	20.23	x	5.26	23.81	x	5.93
Climate runs	RLE ERA	RLE ECHAM	RLE MIROC	RLE ERA	RLE ECHAM	RLE MIROC	RLE ERA	RLE ECHAM	RLE MIROC
Present-day climate average	7.89	7.68	7.81	8.91	8.61	8.90	9.75	9.40	9.79
Future climate average	x	7.39	7.70	x	8.30	8.77	x	9.08	9.69
Differences urban-rural stations									
	Obs	LE_zoom	Le_eu						
2008 average	6.89	1.80	1.38						
2008 ave. rel. difference (%)	40.45	34.42	23.84						
2003-2008 average	8.46	x	1.73						
2003-2008 ave. rel. difference (%)	46.25	x	27.39						
Summer average 2003-2008	6.33	x	1.48						
Summer 03-08 rel. difference (%)	41.60	x	37.19						
Summer average 2003	7.47	x	1.81						
Summer 2003 rel. difference (%)	45.72	x	43.76						
Climate runs	RLE ERA	RLE ECHAM	RLE MIROC						
Present-day climate average	1.86	1.72	1.98						
Future climate average	x	1.69	1.99						

Table 5:

Statistics for stations in Berlin averaged over stations in the rural, suburban and urban region.

Figures

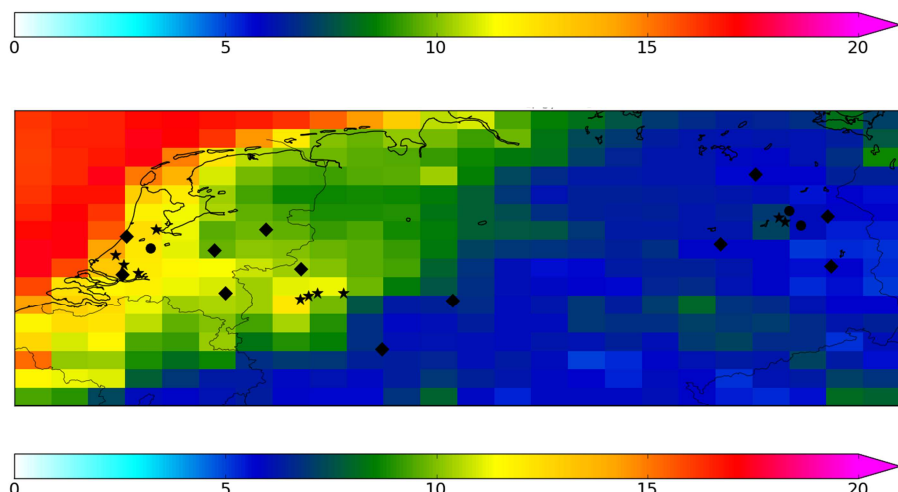
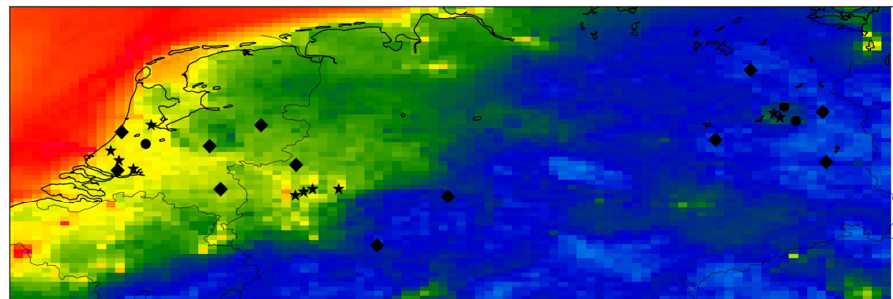
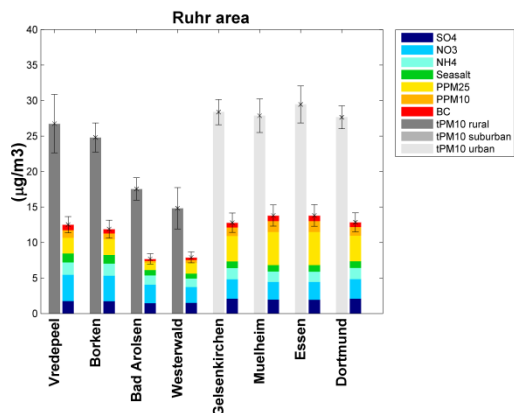


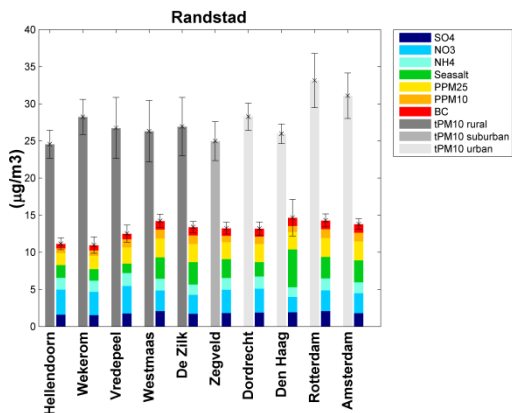
Figure 1.

Distribution of the simulated 2008 average PM10 concentrations ($\mu\text{g}/\text{m}^3$) using a horizontal grid resolution of $7 \times 7 \text{ km}^2$ (LE_zoom) (top) and $25 \times 25 \text{ km}^2$ (LE_eu) (bottom). Included are the location of the stations, Rhomb: rural background stations; Star: urban background stations; Circle: suburban stations.

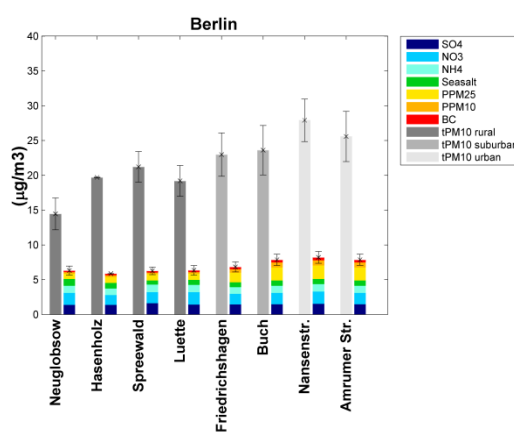
(a)



(b)



(c)

**Figure 2.**

Measured (grey) total PM10 concentrations and simulated (25x25km² resolution run (LE_eu)) (colored) total PM10 concentrations and compositions averaged over the years 2003-2008 for the regions Ruhr area (a), Randstad (b) and Berlin (c). Also shown is the standard deviation of the annual averages of the single years 2003-2008. Note, that the availability of data at the station Hasenholz is only 33%.

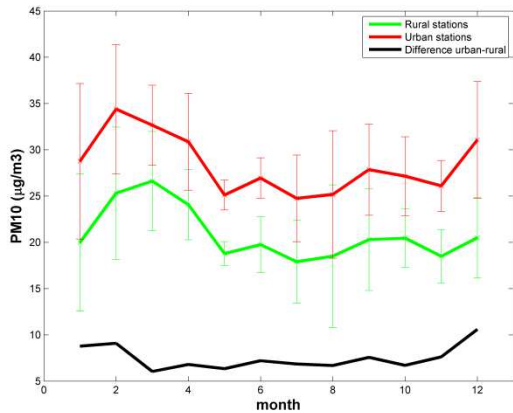


Figure 3.

Averaged annual cycle based on monthly means of the years 2003-2008 of the average of the rural and urban stations in the Ruhr area. Shown is also the standard deviation of the monthly means within the six-year period.

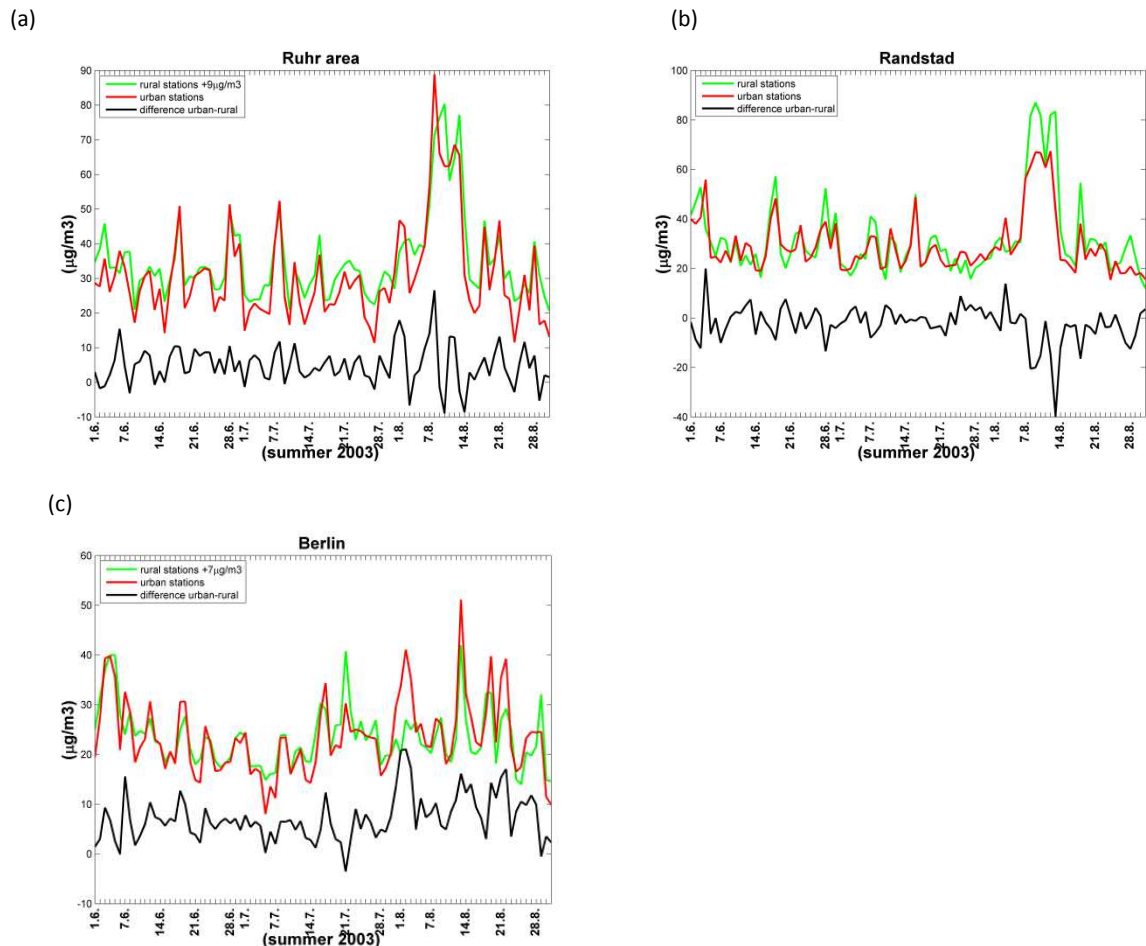


Figure 4.

Time series of measured PM10 concentrations for the summer 2003. For the Ruhr area an offset of $+9\mu\text{g}/\text{m}^3$ is added to the values of the rural stations and for Berlin of $+7\mu\text{g}/\text{m}^3$ in order to be able to better compare the variability of concentrations. For the Randstad no offset is added.

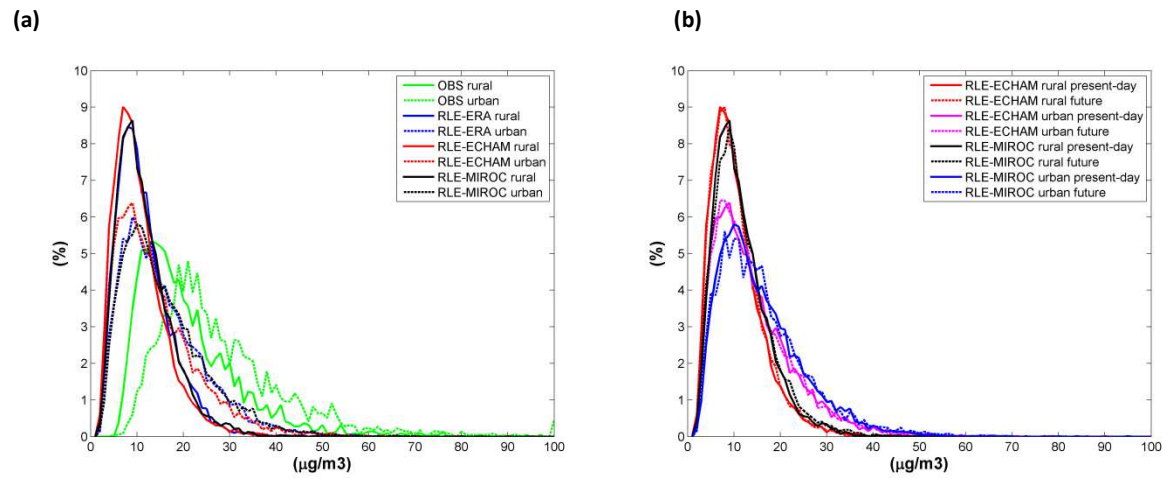


Figure 5.

Frequency distribution (%) of PM10 concentrations ($\mu\text{g}/\text{m}^3$) in the Ruhr area for the present-day period (left) and both the present-day period and the future period (right).

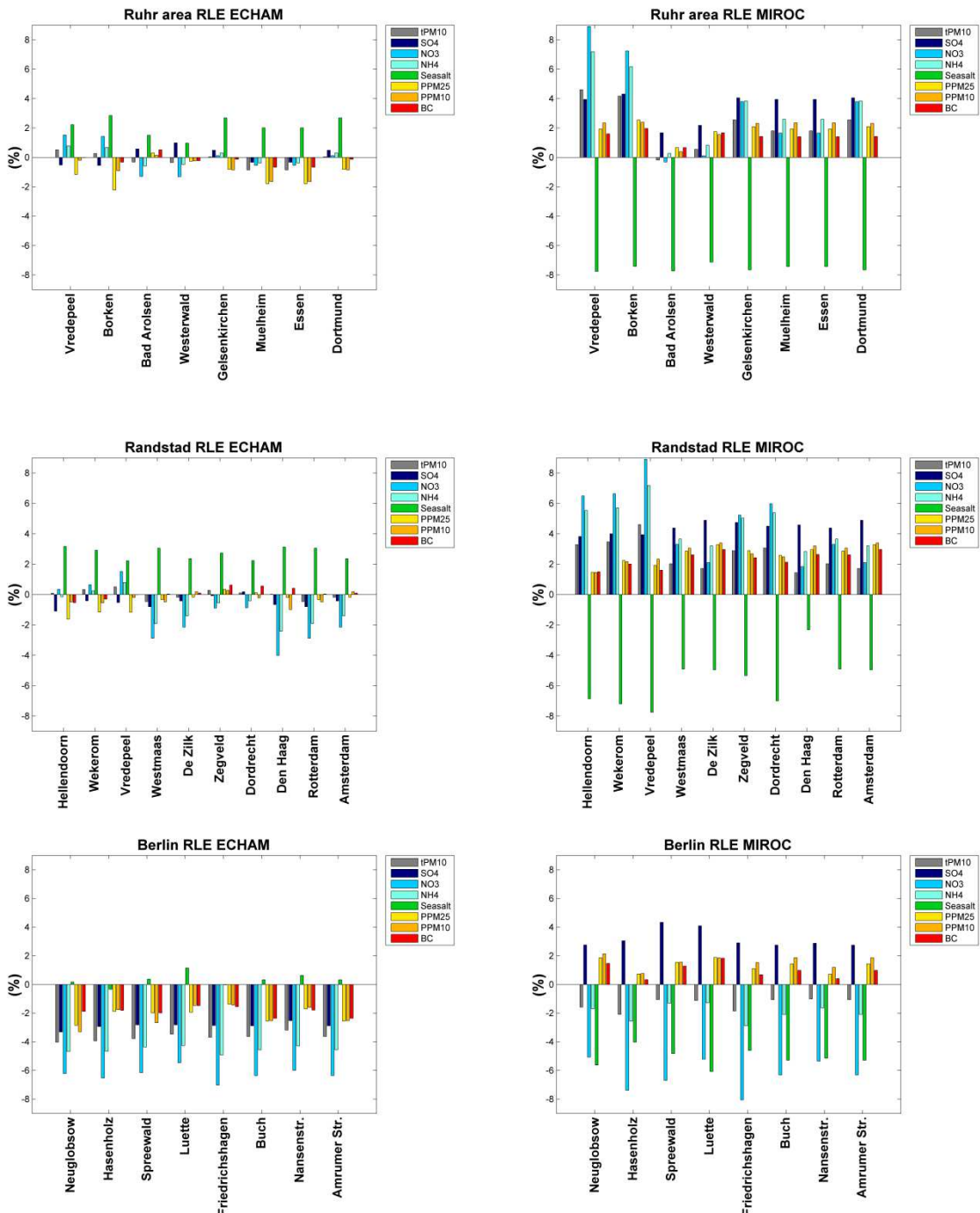


Figure 6.

Relative difference between the future and the present-day period for PM10 and its components for RLE_ECHAM (left) and RLE_MIROC (right).

10 Paper IV: Sensitivity of air pollution simulations with LOTOS-EUROS to temporal distribution of emissions

Sensitivity of air pollution simulations with LOTOS-EUROS to temporal distribution of emissions

A. Mues¹, C. Hendriks², J. Kuenen², A. Manders², A. Segers², Y. Scholz³, C. Hueglin⁴, P. Builjtes^{1,2}, M. Schaap²

1) Freie Universität Berlin, Berlin, Germany, andrea.mues@met.fu-berlin.de

2) TNO, Utrecht, The Netherlands

3) DLR, Stuttgart, Germany

4) EMPA, Dübendorf, Switzerland

To be submitted to Atmospheric Chemistry and Physics

Abstract

In this study the sensitivity of the model performance of the chemistry transport model LOTOS-EUROS to the description of the temporal variability of emissions was investigated. Currently the temporal release of anthropogenic emissions is described by European average diurnal, weekly and seasonal time profiles per sector. These default time profiles largely neglect the variation of emission strength with activity patterns, region, species, emission process and meteorology. The three sources dealt with in this study are combustion in energy and transformation industries (SNAP1), non-industrial combustion (SNAP2) and road transport (SNAP7). First the impact of neglecting the temporal emission profiles for these SNAP categories on simulated concentrations was explored. In a second step, we constructed more detailed emission time profiles for the three categories and quantified their impact on the model performance separately as well as combined. The performance in comparison to observations for Germany was quantified for the pollutants NO₂, SO₂ and PM10 and compared to a simulation using the default LOTOS-EUROS emission time profiles.

In general the largest impact on the model performance was found when neglecting the default time profiles for the three categories. The daily average correlation coefficient for instance decreased by 0.04 (NO₂), 0.11 (SO₂) and 0.01 (PM10) at German urban background stations compared to the default simulation. A systematic increase of the correlation coefficient is found when using the new time profiles. The size of the increase depends on the source category, the component and station. Using national profiles for road transport showed important improvements of the explained variability over the weekdays as well as the diurnal cycle for NO₂. The largest impact of the SNAP1 and 2 profiles were found for SO₂. When using all new time profiles simultaneously in one simulation the daily average correlation coefficient increased by 0.05 (NO₂), 0.07 (SO₂) and 0.03 (PM10) at urban background stations in Germany. This exercise showed that to improve a CTM performance a better representation of the distribution of anthropogenic emission in time by developing a dynamical emission model taking into account regional specific factors and meteorology is recommendable.

1 Introduction

Air pollution levels are controlled by meteorological conditions, atmospheric processing and emission regime. Chemistry transport models (CTM) have been developed to assess the fate of air pollutants. Large efforts have been devoted to improve the process descriptions and meteorological input data. Still, models underestimate the variability of air pollutant levels in general and as function of meteorology compared to observations (Li et al., 2013; Stern et al., 2008). It has been posed by several authors that the emission data used in CTMs are too static (Mues et al., 2012; Menut et al., 2012; Skjøth et al., 2011). Since the early nineties the handling of anthropogenic emissions in CTMs has remained the same. In principle, annual average emission totals are distributed across the domain and combined with average time profiles per sector to arrive at an emission at every point in time. In reality, emission strengths vary with activity patterns, region, species, emission process and meteorology. These variations are currently largely neglected but may be important as atmospheric conditions during release and transport impact the fate of the emitted air pollutants. As an example, accounting for the change in temporal emission characteristics of the energy sector when considering the variability of the contribution of renewable energy with meteorology significantly changes the impact of the power sector in case of energy transition as illustrated by Hendriks et al. (2013). This was explained by the occurrence of the highest emissions from fossil fuel power plants during atmospheric conditions that favor build-up of pollutants (e.g. during night, low wind speeds). Hence, accounting for temporal variability may be important for mitigation strategies as efficiency of measures may be effected. As such, correlations between meteorology and emission strength may impact climate studies for short lived climate forcers. Finally, air quality forecasting (Kukkonen et al., 2012) could be improved with a more detailed description of the temporal distribution of the emission input. Inverse modeling studies are hampered by lack of temporal variation in a-priori emission data (Peylin et al., 2011).

The sensitivity of CTMs to changes in the temporal distribution of emissions is tested in a few studies by comparing simulation results using default time profiles and constant emissions over time. De Meij et al. (2006) found that the daily and weekly temporal distributions of emissions are only important for NO_x, NH₃ and aerosol nitrate, whereas for all aerosol species (SO₄, NH₄, POM, BC) the seasonal temporal variations used in the emission inventory are important. Regional daytime ozone concentrations were found to be not sensitive to changes in the temporal allocation of emissions, while nighttime ozone concentrations are lower under uniform profiles than under time-varying profiles (Tao et al., 2004). Similar results were found when changing the daily cycle of mobile source emission in the CMAQ model which entails substantial changes in simulated ozone concentrations, especially in urban areas at night (Castellanos et al., 2009). Wang et al. (2010) found an increase of correlation when considering different emission factors for the day-of-week and in the diurnal cycle compared to a simulation with constant emissions. However, the impact of neglecting the emission time profiles also depends on the quality of the default time profiles. Observations show that ozone concentrations are higher in the weekend than during weekdays, this signal has been successfully captured by the CMAQ model (Pierce et al., 2010). Pierce et al. (2010) also recommended to improve the estimate of mobile source NO_x emissions and their temporal distributions with special emphasis on diesel cars to better explain observed trends in the extend of the weekend-weekday effect in ozone.

Even less attention has been given in the literature on the development of emission time profiles and their impact on the model performance. Emission time profiles for SNAP2 (non-industrial

combustion) which are based on the actual daily average temperature per grid cell are used in the EMEP (Simpson et al., 2012) and CHIMERE (Bessagnet et al., 2012) model but the impact on the model performance is not documented. Menut et al. (2012) used hourly NO₂ measurements nearby roadside areas as a proxy of road traffic sources to construct new time profiles which were then tested in the CHIMERE model. The most important impact concerns NO₂ concentrations which are by 10-20% higher. The daily ozone peak remains relatively insensitive to this improvement whereas the pollutants concentrations during nighttime are closer to the measurements with the new profiles. The simulation results show very different diurnal variation of emissions from country to country and suggest the use of a new hourly emission factor dataset for various countries. Skjøth et al. (2011) found an improvement in CTM modeling by applying a dynamic ammonium emission model which accounts for local agriculture management and local climate.

In this study we test the sensitivity of the model performance for improved temporal emission information. As such we explore if it is worthwhile to make the effort to improve the emission description to an explicit temporal emission model. The three source categories dealt with in this study are combustion in energy and transformation industries (SNAP1), non-industrial combustion (SNAP2) and road transport (SNAP7). First we explored the impact of neglecting the temporal emission profiles for these SNAP categories on simulated pollutant concentrations with the LOTOS-EUROS chemistry transport model (Schaap et al., 2008). In a second step we constructed more detailed emission time profiles for the three categories and tested them in model simulations using each new profile separately and all three profiles simultaneously in one simulation. We compared the results for the pollutants NO₂, SO₂ and PM₁₀ to measurements and to a model simulation using the default LOTOS-EUROS emission time profiles.

2 Method and data

2.1 The LOTOS-EUROS model

The model employed in this study is the 3D regional chemistry-transport model LOTOS-EUROSv1.8, which is aimed at the simulation of air pollution in the lower troposphere. The model is of intermediate complexity in the sense that the relevant processes are parameterized in such a way that the computational demands are modest enabling hour-by-hour calculations over extended periods of several years within acceptable CPU time. The domain used is bound at 35° and 70° North and 10° West and 40° East. The model projection is normal longitude–latitude and we used the standard grid resolution of 0.50° longitude × 0.25° latitude, approximately 25 × 25 km². In the vertical, the model extends to 3.5 km above sea level and uses the dynamic mixing layer approach to determine the model vertical structure. The meteorological input fields are derived from the ECMWF model. The advection in all directions is handled with a monotonic advection scheme (Walcek et al., 1998). Gas phase chemistry is described using the TNO CBM-IV scheme, which is a condensed version of the original scheme (Whitten et al., 1980). Hydrolysis of N₂O₅ is described explicitly (Schaap et al., 2004a). Cloud chemistry is described following Banzhaf et al. (2012). Aerosol chemistry is represented using ISORROPIA2 (Fountoukis and Nenes, 2007). The dry deposition in LOTOS–EUROS is parameterized following the well-known resistance approach following the EDACS system (Erisman et al., 1994), including a compensation point approach for ammonia (Wichink Kruit et al., 2012). Below cloud scavenging is described using simple scavenging coefficients for gases (Schaap et al., 2004a) and particles (Simpson et al., 2003). Total PM₁₀ in the LOTOS-EUROS model is composed of: Primary chemically unspecified PM in the fine (PPM2.5) and coarse mode (PPMCO), black carbon (BC), dust, ammonium (NH_4^+), sulfate (SO_4^{2-}), nitrate (NO_3^-) and sea salt (Na in the fine and coarse mode). The LOTOS-EUROS model has participated in several international model inter comparison studies addressing ozone (Hass et al., 1997; Van Loon et al., 2007; Solazzo et al., 2012a) and particulate matter (Cuvelier et al., 2007; Hass et al., 2003; Stern et al., 2008; Solazzo et al., 2012b) and shows comparable performance to other European models. For a detailed description of the model v1.8 we refer to Hendriks et al. (2013), Wichink Kruit et al. (2012) and Schaap et al. (2009).

2.2 The emission database

The anthropogenic emissions used in this study are taken from the TNO-MACC emission database for 2005 (Kuenen et al., 2011; Denier van der Gon et al., 2010). This inventory is a European-wide, high-resolution (0.125° × 0.0625° lon-lat) inventory for NO_x, SO₂, NMVOC, CH₄, NH₃, CO, PPM₁₀ and PPM2.5. It is set up using official emissions reported by countries themselves. Emissions have been split in point and area sources and are given in aggregated sources categories (SNAP levels) as a total annual sum. SNAP (Selected Nomenclature for Air Pollutants) level one is the highest aggregation level, distinguishing 10 different source sectors. National emission totals have been disaggregated spatially using actual point source locations and strengths as well as several proxy maps (e.g. population density, traffic intensity) (Kuenen et al., 2011). Elemental carbon emissions are separated from the chemically unspecified primary PM_{2.5} emissions following Schaap et al. (2004b) and primary organic carbon is included as a part of primary PM_{2.5}. Natural emissions are

calculated on-line using the actual meteorological data. The MACC global fire assimilation system (Kaiser et al., 2009) is used on an hourly basis. Biogenic NMVOC and mineral dust emissions are prescribed following Schaap et al. (2009). Sea salt emissions are calculated following Mårtensson et al. (2003) and Monahan et al. (1986) from wind speed at ten meters.

The three source categories dealt with in this study are combustion in energy and transformation industries (SNAP1), non-industrial combustion (SNAP2) and road transport (SNAP7). Non-industrial combustion consists mainly of domestic combustion and is dominated by emissions from heating, though it also includes secondary contributions from processes such as cooking and production of hot water. Road transport within TNO-MACC is subdivided in five categories (road transport exhaust emissions 71: gasoline, 72: diesel, 73: other fuels and non-exhaust emission 74: evaporation of gasoline, 75: road, brake and tyre wear). The three sectors under investigation contribute a significant fraction of the emissions of several pollutants in Europe. As an example, the contribution of the different source sectors to German national emissions totals are given in Table 1. Road transport is the most important source for nitrogen oxides, carbon monoxide and particulate matter with the highest contribution for nitrogen oxide reaching almost half the national total. The power sector is the largest source for sulfur dioxide and contributes significantly to nitrogen oxide emissions. Residential combustion contributes 10-20% to the emissions of a few components. Given the strong seasonal signature, its importance in winter is significantly higher (see below). Combined the three source sectors explain 74, 67, 52 and 35 percent of the national reported emissions of NO_x, SO₂, PM2.5 and PM10 illustrating the potential impact of adaptations to the temporal profiles.

2.3 Model simulations and measurements

To test the sensitivity of the model to the temporal variability of emissions six model simulations were performed. First, a model simulation without emission profiles for SNAP 1, 2 and 7 (LE_const127) and thus using constant emissions for these sectors in time was compared to a base simulation (LE_Default), which uses the default emission time profiles for all SNAP categories. We constructed more detailed emission time profiles for the SNAP1, SNAP2 and SNAP7 categories, which are described in chapter 3. Three simulations were carried out to quantify the impact of each new profile separately (LE_SNAP1, LE_SNAP2, LE_SNAP7), while keeping all other profiles as default. In a last step, all three new time profiles were used simultaneously in one simulation (LE_SNAP127). To include long range transport the runs were performed on the European domain. All model simulations have been performed using emissions for the year 2005 and the meteorology of the year 2006. The model setup, the description and the name of the simulations are summarized in Table 2.

Because the focus of the analyses is on Germany, air pollutant measurements at German stations from the AirBase database (AIRBASE, 2012) were selected and acquired for this study. Due to the horizontal grid resolution of about 25x25km² only rural and urban background stations are used. Only time series with a minimum of 60% data coverage for 2006 for an individual component were chosen for the evaluation. Model data are neglected if no measurements are available on a specific day or hour in the time series.

3 Improved emission time profiles

The default emission time factors currently used in the LOTOS-EUROS model (Buitjes et al., 2003) are given for the hour of the day, the day in the week and the month in the year. The default profiles for SNAP1, SNAP2 and SNAP7 are displayed in Figure 1. Note that a single diurnal profile is applied for all days of the week. These time profiles are applied to every country in the model domain. Except for agriculture, all time profiles were obtained in the early nineties and used ever since. The traffic cycle is based on Dutch urban traffic counts, but the exact origin of the other profiles is not reproducible. Application of these profiles was not limited to LOTOS-EUROS as they have been used within e.g. MACC regional ensemble (Kuenen et al., 2011), AQMEII (Pouliot et al., 2012) and other model exercises (e.g. van Loon et al., 2004). Below, we describe how we replaced the temporal profiles for SNAP1, SNAP2 and SNAP7.

3.1 SNAP7 – Road transport

So far, the default time profiles for road transport do not take into account the temporal release of emissions from road transport based on the driving behavior as a function of location, vehicle type and street type. To study this in more detail we used traffic count data for Light Duty Vehicles (LDV) and Heavy Duty Vehicles (HDV) at twelve highway and six urban street stations (Bundesstraßen) distributed across Germany for the years 2006-2010. First of all, we analyzed these data in view of differences between temporal variation in traffic patterns at highway and urban street locations and differences in the diurnal cycle for each day of the week. We found a considerable difference between the diurnal cycles on weekdays and a weekends, with less pronounced rush our peaks on Saturday and Sunday for both street types. Furthermore, the diurnal profiles for urban streets show much more pronounced morning and afternoon rush-hour peaks than highways. This is explained by the dominance of local commuter traffic at urban roads versus long distance traffic at the highways. Also striking is that on highways, in contrast to urban streets, the total traffic counts are highest on a Friday and do not decrease during the weekend. However, when differentiating between vehicle types HDV traffic counts on highways do significantly decrease in the weekend. In terms of total counts this decrease is compensated by increased LDV traffic on highways.

Although there is a large correspondence between the temporal cycles among highway locations, individual stations show particular features. For instance, at highways near the north coast traffic shows peaks around the weekend (explained by weekend tourism), whereas highway traffic on the highway between Germany and Austria shows a summer maximum in contrast to all other sites due to increased long range traffic during summer holidays. Hence, to be very detailed a traffic model with specific data for all major roads or temporal profiles per road segment should be used. This is far too complicated for our purpose. Therefore, all traffic data were averaged across all urban and highway sites, respectively, to obtain a profile representative for Germany as a whole. In Figure 2 time series of the difference between actual traffic counts and the application of the default and new count time profiles are given for an urban and highway station for the year 2010. The urban and highway profiles based on German traffic counts explain systematically more of the observed traffic counts at all stations than the default profile. As the default cycles are based on urban street traffic counts this is especially striking for the highway stations (Fig.2b). Very high residues occur in March,

May and at the end of December, which is related to holiday impacts (Eastern, Whitsunday, Christmas), which are not explicitly considered in the profiles. Thus, considering the day of the week and the road type helps to improve the description of the temporal driving patterns.

Going one step further, considering the large difference in temporal driving behavior and emissions from HDV and LDV traffic, separate profiles per vehicle type (LDV and HDV) on highways and urban streets were constructed by averaging the traffic count data per vehicle and road type over all five years. Figure 3a shows the diurnal traffic profiles per day of the week and the contribution of each category. Assuming that emissions for all vehicle and street types are the same, the black cycle would represent the total emission time profile. Obviously, traffic emissions are dependent on road (and vehicle) type (through fuel efficiency dependent on speed and driving conditions) (Franco et al., 2013). To account for this feature we used emission split factors that specify the fraction of emission per vehicle and street type in Germany to obtain an emission weighted traffic profile. Note that the emission factors and thereby the importance of each of the four categories differs per pollutant. We chose NOx because traffic has the largest contribution to this component (Tab.2). Figure 3b displays the diurnal traffic profiles per day of the week and the contribution of each category after emission strength weighing. It is clearly shown that the contribution of emissions from the four categories is different, as for example in terms of emissions, the contribution for LDV on highways is much lower than in terms of number (Figure 3a). A comparison between the unweighted, represented by the red line in Figure 3b, and the weighted time cycles illustrates the effect of weighting the emission time profile by the NOx split factor. This effect is especially high on the weekend where the weighted profiles are ~20% lower.

This exercise showed that 1) an update of the time profiles with national data improves the comparison with traffic count data, 2) also within a country traffic regimes shows differences and 3) that the temporal variation for emissions differs from that of traffic counts and should ideally be computed for all species independently.

3.2 SNAP2 – Non-industrial combustion

The default time profile for non-industrial combustion in LOTOS-EUROS reflects a strong (monthly) seasonal variation with a summer minimum. Country specific information is only considered by national emission totals per component but not by the time profiles. Impacts of cold weather spells with increased demand for heating are not accounted for. We applied new emission time profiles for SNAP2, which are based on the method used in the CHIMERE (Bessagnet et al., 2012) and EMEP models (Simpson et al., 2012). This method uses the concept of heating degree days, which is a measure designed to reflect the demand for energy needed to heat a building. The heating degree day factor ($H_{D,C}$) is defined relative to a base temperature (outside temperature) above which a building needs no heating (here: 291.15K) ($H_{D,C} = \max(291.15K - T_{D,C}, 1)$) (1 rather than 0 to avoid numerical problems). This factor increases with increasing difference between the actual 2m daily mean outside temperature $T_{D,C}$ and the base temperature. The heating degree day factors are pre-calculated in the model per day and grid cell. The fraction f of SNAP2 emissions not attributed to heating is a constant, assumed here to be 20% (f=0.2), and is multiplied by the yearly average of the heating degree days per grid cell ($\overline{H_C}$). To come to the SNAP2 emission factor ($F_{D,C}$) the contribution from both terms are added ($D_{D,C} = H_{D,C} + f * \overline{H_C}$) and related to the whole year by calculating an average factor $\overline{D_C}$, ($\overline{D_C} = (1 + f) * \overline{H_C}$). $F_{D,C} = \frac{D_{D,C}}{\overline{D_C}}$ is than the daily SNAP2

emission factor per grid cell. In summertime when the actual temperatures are close to or above the base temperature the emission factor is very small, but in winter the factor is usually significant and can change quite substantially from day to day. To come to the hourly emission factors the default diurnal emission profiles from LOTOS-EUROS (Fig.1a) are used.

The resulting time profiles (Fig.4a) show a stronger temporal variations compared to the default LOTOS-EUROS profiles. Note that the calculations also induce a spatial variability within the country with higher emissions in regions experiencing a colder climate. Especially in the beginning of the year the new emission factors are higher than the default factors. In the summer months both time profiles are very similar to each other because the scaling factor f , used in the new method is close to the default summer emission factor. In the last four months the new time profiles are similar or lower, depending on the location. This described annual cycle of the new emission time profiles corresponds to the yearly cycle of the daily average temperature. In general, the temperature is lower in the first months of a year compared to the ones in the end of the year, which is not taken into account in the default time profiles but which is reflected in the new profiles.

3.3 SNAP1 – Combustion in energy and transformation industries

As for the other sectors the default emission profiles for the power sector (SNAP 1) are assumed to be the same across all countries and invariable with meteorology. This may not be the best representation of reality, since e.g.:

- climate conditions may cause differences in seasonal profiles for countries across Europe;
- variations in electricity consumption (e.g. for heating/cooling) due to changes in meteorology during the year are not represented;
- Variable social habits may induce shifts in diurnal cycles between countries.

Therefore, new time profiles for the power generation sector (SNAP 1) were constructed for 2006 using electricity demand data from each country. In Europe on average, 54% of the electricity is generated using fossil fuels (<http://epp.eurostat.ec.europa.eu>). Nuclear power and hydroelectric power account for 25% and 16% respectively. Intermittent renewable sources only produce a minor part of the total electricity demand (3.7% for wind energy and 0.4% for solar power). Between countries large differences in the electricity mix exist. As only fossil fuels cause emissions during electricity production, the time profiles for SNAP1 are based on the timing of electricity production from fossil fuels. This is calculated for each country by subtracting the power generated from other sources from the hourly electricity demand. For nuclear and hydro power, the production is assumed constant throughout the year. Time profiles for wind and solar power were calculated using the REMix model (Scholz, 2012). REMix is an energy system model that calculates the hourly availability of renewable electricity based on meteorological conditions. The energy system model can also dimension power supply systems with high shares of renewable energy and calculate the least cost operation of the system components, i.e. power generators, power storage and power transmission units. However, international trade and storage of electricity are neglected in this study in order to keep the determination of the time profiles simple

The new seasonal time profiles show a stronger temporal variability between the months and weeks compared to the default LOTOS-EUROS profiles as here illustrated for Germany (Fig.4b). The weekly cycle is more pronounced with a higher amplitude caused by higher emission factors during the week and decreased factors on the weekend. This is especially pronounced in the summer

months where emission at peak production is much higher than in the default profiles. Furthermore, the yearly minimum is shifted to spring and autumn months. Zooming in on a summer week, the daily cycle for the new timing shows peak values in the morning and late afternoon whereas the afternoon peak is not present in the base case (not shown). The daily cycle for the new profiles is especially pronounced in the weekend where the two profiles deviate most from each other.

4 Results

In this chapter the results of the model simulations LE_const127 (4.1.), LE_SNAP7 (4.2.), LE_SNAP2 (4.3.), LE_SNAP1 (4.4.) and the combined run LE_SNAP127 (4.5.) are compared to the LE_Default simulations and to measurements to test the sensitivity of the model to the new constructed time profiles. Table 3 and 4 provides a statistical comparison of all simulations against observations for daily and hourly data, respectively. Figure 5 summarizes the temporal correlation coefficients for selected urban and rural stations, representing different parts of Germany.

4.1 Constant profiles

To demonstrate the impact of the default time profiles for SNAP 1, 2, and 7 on pollution simulations with LOTOS-EUROS the LE_const127 simulation was carried out using constant emissions in time for these three SNAP categories. The largest impact is found for NO₂, which shows an average increase in the correlation coefficient of 0.22 and 0.14 for urban and rural background stations when using the default profiles, respectively (Tab.3). The increase in correlation coefficients on a daily basis is in comparison very modest (Tab.4) showing a strong impact of accounting for the diurnal cycle of NO_x emission from traffic. However, the size of the increase highly depends on the station and varies between -0.01 and 0.17 (Fig.5). Neglecting the emission induced part of the NO₂ temporal variability in the LE_const127 simulations and only considering the part resulting from meteorology and chemistry leads to a diurnal cycle with a concentration maximum during night whereas the LE_Default simulation and the measurements show a night time minimum (not shown). The lower effective dilution leading to the nighttime maximum causes a 10% higher average NO₂ surface concentration in the LE_const127 simulation (Tab.3+4). For SO₂ on an hourly basis an average increase in the correlation coefficient of 0.13 and 0.06 is found for urban and rural background stations, respectively (Tab.3). In contrast to NO₂, a very similar change of correlation was observed for the hourly and the daily time series indicating a more equal relevance of diurnal, weekly and seasonal emission time profiles (Tab.3+4). For SO₂ no systematic impact on the annual mean concentration was shown (Tab.3+4). The smallest impact of the default time profiles are found for PM10, the change of correlation ranges between -0.03 and 0.04 depending on the stations (Fig.5).

The findings in this section illustrate the importance to consider the temporal release of emissions in the model and its impact on the model performance. However, the impact shown here is limited by the quality of the used emission time profiles. Thus below, we assess the impact of using improved time profiles for SNAP 1, 2, and 7 separately.

4.2 SNAP7 – Road transport

On average the impact of using the new SNAP7 time profiles on the NO₂ correlation coefficient is only small (0.01 to 0.04) (Tab.3+4). But the increase in correlation coefficient is found to vary between 0.01 and 0.08 at individual urban and rural background stations (Fig.5). As a result of the higher relevance of NO_x emissions from traffic in urban regions, the increase of correlation is found to be higher at urban (0.04) than at rural (0.01) stations (Tab.3). The model bias for NO₂ is found to decrease only slightly for the LE_SNAP7 simulation (Tab.3+4). In Figure 6 the measured and

simulated (LE_Default and LE_SNAP7) averaged diurnal cycles per day of the week for NO₂ at urban (a) and rural (b) background stations are displayed. Note that the cycles are normalized for a better comparison of the temporal variability. As discussed in chapter 3.1. the strongest changes between the default and the new SNAP7 time profiles appear in the diurnal cycle on the weekend. An improved representation of the NO₂ diurnal cycle on Saturday and Sunday is indeed found for the LE_SNAP7 simulation (Fig.6). This includes a better reproduction of the measured lower concentration maxima in the morning on the weekend compared to weekdays. And also for the maxima in the evening the LE_SNAP7 simulations are closer to the measurements. Overall, the LE_SNAP7 simulation is in better agreement with the lower measured NO₂ concentration level on the weekend. During the week the LE_SNAP7 simulation shows higher concentrations for the minimum during night compared to LE_Default and the measurements. This is due to more emitted mass during night and at early hours in the LE_SNAP7 simulation (see Fig.3b). Furthermore at urban stations the measured maximum in the morning is higher than in the evening, whereas this is the other way around at rural stations. This feature is only captured by the LE_SNAP7 simulation, although differences between urban and rural regions are also in the new SNAP7 profiles not explicitly considered. These findings are verified by a higher correlation coefficient for the average weekly cycle for the LE_SNAP7 (e.g. 0.70 at urban stations) compared to the LE_Default simulation (0.64).

Both model simulations (LE_Default and LE_SNAP7) overestimate the measured NO₂ amplitude in the diurnal cycle (Fig.6), with too high maxima in the morning and evening as well as a too low minimum at noon. The explanation for the different behavior lies in the measurement technique applying molybdenum converters used to monitor NO₂ in Germany (and other networks in Europe). Evaluation of instruments using molybdenum converters against photolytic converters has shown that the molybdenum converters also convert part of the NO_y (Dunlea et al., 2007; Steinbacher et al., 2007). These components maximize during daytime, causing up to a factor 2 difference in measured NO₂ during the afternoon (Villena et al., 2012). To illustrate the impact of the monitoring method we use two three year time series of simultaneous measurements covering 2006-2009 at the site Payerne in Switzerland. A systematic difference in measured NO₂ concentration is indeed found for the two measurement techniques (Fig.7). The normalized weekly cycles for the instruments show a stronger amplitude for the photolytic converter, with both lower minima and higher maxima in the morning. The size of the interference is variable as it depends on the NO_y to NO₂ ratio and therefore on season, pollution regime (NO₂, oxidant levels), air mass age, etc. Thus, the extent of the difference found for the station Payerne cannot be directly translated to the German stations used here. In summary, the monitoring technique explains part of the difference between the measured and simulated NO₂ diurnal cycle. Note that the measurement technique may also partly explain the not captured higher amplitude at urban than at rural stations, as the NO_y to NO₂ ratio is expected to be higher at rural areas than in urban environments.

In short, the new SNAP7 time profiles provide an improvement compared to the default profiles. As expected, the average impact is not as large as in section 4.1, but at some stations the improvement of the NO₂ correlation coefficient is in the same range as found for the LE_Default compared to the LE_const127 simulations. The important improvements of the explained variability over the weekdays as well as the diurnal cycle is observed.

4.3 SNAP2 – non-industrial combustion

An average increase of daily correlation for SO₂ at urban (0.03) and rural (0.05) stations is found for the LE_SNAP2 simulation (Tab.4). The size of the increase depends on the location and shows a positive south-west to north-east gradient across stations in Germany, with a rise of up to 0.08 compared to LE_Default in the east of the domain (Fig.8a). The fact that this is found for urban as well as rural stations hints at a considerable contribution of SNAP2 SO₂ emissions on the total SO₂ concentration from long-range transport processes rather than from the different contribution in rural and urban regions. SO₂ emissions from SNAP2 are considerably higher in regions east of the domain due to heating systems with still a high share of coal and wood use (Kuenen et al., 2011). The use of different fuels (e.g. gas, coal) for heating systems within one country is not accounted for in the spatial distribution of the SNAP2 emissions. In fact, the total amount of emissions is weighted by the population density in a grid cell. Thus the slightly higher impact of the new SNAP2 emission profiles at urban stations (Tab.3+4) suggests a higher contribution of SO₂ emissions from the SNAP2 category in urban than in rural areas. A small increase of correlation and decrease of the model bias is also found for PM10 for the LE_SNAP2 compared to the LE_Default simulation (Fig.5, Tab.3+4). Applying the new approach for SNAP2 in the model results in a systematic increase in the model performance including the consideration of local features.

4.4 SNAP1 – Combustion in energy and transformation industries

The impact of the new SNAP1 profiles on the correlation coefficient for SO₂ is on average only modest with an increase of 0.03 at urban and of 0.01 at rural stations (Tab.3+4) but higher at some individual stations (Fig.8b). The locations of coal-fired power stations in Germany are rather concentrated in the west of the domain. A slightly higher increase of correlation for SO₂ between 0.04 and 0.08 is indeed found in the south-west of the domain, whereas the increase in the east is only modest (0.02), hinting at a local impact of the SNAP1 profiles. The effect of the new time profiles on the SO₂ mean concentration and the model performance for NO₂ and PM10 is only low (Tab.3+4).

4.5 Combined run (LE_SNAP127)

The largest increase of the average correlation coefficient is found if all three new time profiles are used simultaneously in one simulation (LE_SNAP127). The size of the increase depends on the component and is mainly dominated by the most relevant SNAP category for the component. Thus for NO₂ the increase is mainly determined by the SNAP7 profiles and ranges on average from 0.02 to 0.05 (Tab.3+4). For SO₂ on daily basis the correlation coefficient increases with 0.03 and 0.07 at rural and urban stations, respectively (Tab.4). For SO₂ the impact of both the SNAP1 and SNAP2 time profiles is noticeable, but at most stations the correlation coefficient is the same as for the LE_SNAP2 simulation (Fig.5). Compared to every other simulation LE_SNAP127 shows the highest increase of the correlation coefficient for PM10 compared to LE_Default, hinting that profiles from all SNAP categories are relevant for PM10. The increase is 0.03 and 0.02 based on daily and hourly data, respectively (Tab.3+4). Overall the impact on the mean concentrations is only modest for all components.

5 Discussion and Conclusion

In the present study the performance of LOTOS-EUROS was found to be sensitive to the temporal distribution of emissions. This was first indicated by an improvement of the model performance when using the LOTOS-EUROS default time profiles instead of constant emissions for the categories SNAP1, 2 and 7. In a second step new and more detailed emission time profiles for the three emission categories were tested in the model. Separately, each new profile increased the model statistics compared to the default case. The highest increase in model performance was found for the simulation using the three new profiles simultaneously. The improvement was found to be systematic which gives confidence in the robustness of the results.

The correlation coefficient was used as a measure for the presentation of the temporal variability of simulated concentrations in the model. The size of the change of the correlation coefficient between the default and the other simulations depends on the SNAP category, the pollutant, the stations (urban, rural) and the time series (hourly, daily). On average an increase between 0.02 and 0.07 for the combined run (LE_SNAP127) compared to the default run (LE_Default) was found for Germany. To assess whether this impact is significant we compare it to impacts of other model parameters. The impact of improving process descriptions on the correlation coefficient is generally low. For example, using different sea salt emission schemes led to a change of the correlation coefficient in the range of 0.00 to 0.05 at different stations in Europe (Schaap et al., 2009). Also, implementation of a bi-directional surface-atmosphere exchange module for ammonia in the LOTOS-EUROS model did in general not affect the correlation for ammonia (Wichink Kruit et al., 2012). Comparing the performance from LOTOS-EUROS v1.6 to v1.8 (three years of development) shows lower impacts of model development on primary components than shown here, whereas the improvement for PM is larger. Another way to assess the significance of the reported improvement due to the emission temporal profiles is to compare to the spread between model performances of different models. Although the maximum difference between correlation coefficients between individual CTMs is normally larger than the impact of the improved emission profiles, model comparison studies often show several models with very similar correlation coefficients. Stern et al. (2008) computed the correlation coefficients for five different regional CTMs for a winter period in 2003. For SO₂ four models showed correlation coefficients within a range of 0.03. Van Loon et al. (2004) report five out of six models within 0.04, 0.1 and 0.13 for NO₂, SO₂ and PM10, respectively. Van Loon et al. (2007; 2004) compared the model performance for ozone of seven regional CTMs for 2001 and correlation coefficients differed between 0.01 and 0.1 between individual models. In an air quality trend study for Europe by Colette et al. (2011) the performance of six regional and global chemistry transport models were compared. The model performances were tested at suburban stations over 10 years on the daily mean basis. For NO₂ four of the six models showed a correlation coefficient between 0.57 and 0.66, for ozone four models have a correlation between 0.74 to 0.8, and for PM10 three out of four models show a correlation in the range of 0.53-0.57. This comparisons indicate that the improvement using the new emission time profiles in the model is significant compared to the impact of model developments in one model and to the range of model performance between different models.

This sensitivity study also provides information on the importance of the individual emission time profile (diurnal, weekly, seasonal cycle) per SNAP category to the different components. This is for example a strong impact of accounting for the diurnal cycle of NO_x emission from traffic on the NO₂ concentrations as it was also found by de Meij et al. (2006). Replacing the default (Dutch) profiles

with national representative profiles yielded important improvements of the explained variability over the weekdays as well as the diurnal cycle, which was also found by Pierce et al. (2010) and Menut et al. (2012). The largest impact of the SNAP1 and 2 profiles were found for SO₂. The importance of SNAP2 for SO₂ was highlighted as the impact in eastern Germany was high and may deserve more attention. The smallest impact of the temporal profiles was found for PM10 in line with earlier studies (de Meij et al., 2006; Wang et al., 2010). The low impact can be explained by 1) a contribution of only 34.8% of considered SNAP categories to the primary PM10 emissions; 2) a relatively long life time and therefore high background concentration; 3) a large secondary fraction of PM10 increasing the dependence on process descriptions; and 4) a large model underestimation of the total mass due to missing components as secondary organic aerosol. Given the importance of secondary inorganic aerosol accounting for the dependency of emission on agricultural ammonia as a function of location and meteorology following Skjøth et al. (2011) should be investigated in the future.

The findings presented in this explorative study show that a good description of the temporal variability of emissions in chemistry transport models is important and needs further attention. Even though the time profiles presented here for Germany already take into account more detailed information on temporal emission characteristics, a systematic effort is needed to generate time profiles for the different source categories across per European countries. It is important to obtain these profiles at a subsector level, as illustrated for heavy and light duty traffic. Moreover, different emission processes should be differentiated and treated separately such as gasoline evaporation, exhaust emissions and resuspension. For the energy sector the variability of the energy mix in time should be incorporated as coal and gas fired power plants have different use in the energy system and for households cooking and heating should be differentiated. Where possible and relevant, the impact of meteorology should be incorporated. For example, meteorological conditions (rain events; snow) have an effect on observed traffic intensity (Cools et al., 2010). Hence, future emission inventories should contain more detailed information than just SNAP level 1 categories. Moreover, it is anticipated that specific modules should be developed to describe the emission variability per sector. An example is the ammonia emission module accounting for the dependency of agricultural practice as a function of location and meteorology as described by Skjøth et al., (2011). Improved emission modules would provide an improved basis for air quality and climate scenarios, air quality forecasting and emission inversion studies.

In short, to improve a CTM performance in terms of the explained variability of simulated pollutant concentrations a better representation of the distribution of anthropogenic emission in time by developing a dynamical emission model taking into account regional specific factors and meteorology is recommendable.

Acknowledgements

We would like to thank the German Bundesanstalt für Straßenwesen (BASt) for providing the traffic count data. Furthermore, this work was financially supported by TNO and has partly been funded by the FP7 project EnerGEO (see <http://www.energeo-project.eu>).

References

- AIRBASE, 2012. European Topic Centre on Air and Climate Change.
<http://acm.eionet.europa.eu/databases/airbase>.
- Banzhaf S., Schaap M., Kerschbaumer A., Reimer E., Stern R., van der Swaluw E., Builtjes P., 2012. Implementation and evaluation of pH-dependent cloud chemistry and wet deposition in the chemical transport model REM-Calgrid. *Atmospheric Environment* 49, 378-390.
- Bessagnet B., Terrenoire E., Tognrt F., Rouïl L., Colette A., Letinois L., Malherbe L., (Editors), 2012. The CHIMERE Atmospheric Model, EC4MACS Modelling Methodology. Report.
- Builtjes P.J.H., van Loon M., Schaap M., Teeuwisse S., Visschedijk A.J.H., Bloos J.P., 2003. Project on the modelling and verification of ozone reduction strategies: contribution of TNO-MEP. TNO-report, MEP-R2003/166, Apeldoorn, The Netherlands.
- Castellanos P., Stehr J.W., Dickerson R.R., Ehrman S.H., 2009. The sensitivity of modeled ozone to the temporal distribution of point, area, and mobile source emissions in the eastern United States. *Atmospheric Environment* 43, 4603–4611.
- Colette A., Granier C., Hodnebrog Ø., Jakobs H., Maurizi A., Nyiri A., Bessagnet B., D'Angiola A., D'Isidoro M., Gauss M., Meleux F., Memmesheimer M., Mieville A., Rouïl L., Russo F., Solberg S., Stordal F., Tampieri F., 2011. Air quality trends in Europe over the past decade: a first multi-model assessment, *Atmos. Chem. Phys.*, 11, 11657-11678.
- Cools M., Moons E., Wets G., 2010. Assessing the impact of weather on traffic intensity. *Weather, Climate, and Society* 2 ,1, 60-68.
- Cuvelier C., Thunis P., Vautard R., Amann M., Bessagnet B., Bedogni M., Berkowicz R., Brandt J., Brocheton F., Builtjes P., Coppalle A., Denby B., Douros G., Graf A., Hellmuth O., Honoré C., Hodzic A., Jonson J., Kerschbaumer A., de Leeuw F., Minguzzi E., Moussiopoulos N., Pertot C., Pirovano G., Rouil L., Schaap M., Stern R., Tarrason L., Vignati E., Volta M., White L., Wind P., Zuber A., 2007. CityDelta: A model intercomparison study to explore the impact of emission reductions in European cities in 2010, *Atmos. Environ.*, 41, 189–207.
- de Meij A., Krol M., Dentener F., Vignati E., Cuvelier C., Thunis P., 2006. The sensitivity of aerosol in Europe to two different emission inventories and temporal distribution of emissions. *Atmospheric Chemistry and Physics* 6, 4287–4309.

Denier van der Gon H.A.C., Visschedijk A., van den Brugh H., Dröge R., 2010. F&E Vorhaben: "Strategien zur Verminderung der Feinstaubbelastung" e PAREST: A high resolution European emission data base for the year 2005. TNO-Report, TNO-034-UT-2010-01895_RPT-ML, Utrecht.

Dunlea E. J., Herndon S. C., Nelson D. D., Volkamer R. M., San Martini F., Sheehy P. M., Zahniser M. S., Shorter J. H., Wormhoudt J. C., Lamb B. K., Allwine E. J., Gaffney J. S., Marley N. A., Grutter M., Marquez C., Blanco S., Cardenas B., Retama A., Ramos Villegas C. R., Kolb C. E., Molina L. T., Molina M. J., 2007. Evaluation of nitrogen dioxide chemiluminescence monitors in a polluted urban environment. *Atmos. Chem. Phys.*, 7, 2691–2704.

Erisman J.W., van Pul A., Wyers P., 1994. Parametrization of surface-resistance for the quantification of atmospheric deposition of acidifying pollutants and ozone, *Atmos. Environ.*, 28, 2595–2607.

Eurostat website, (<http://epp.eurostat.ec.europa.eu/portal/page/portal/energy/introduction>).

Fountoukis C. and Nenes A., 2007. ISORROPIAII: A computationally efficient thermodynamic equilibrium model for $K^+ + Ca^{2+} + Mg^{2+} + NH_4^+ + Na^+ + SO_4^{2-} - NO_3^- - Cl^- - H_2O$ aerosols. *Atmospheric Chemistry and Physics*, 7 (17), 4639-4659.

Franco V., Kousoulidou M., Muntean M., Ntziachristos L., Hausberger S., Dilara P, 2013. Road vehicle emission factors development: A review. *Atmospheric Environment*, 70, pp. 84-97.

Hass H., van Loon M., Kessler C., Stern R., Matthijzen J., Sauter F., Zlatev Z., Langner J., Foltescu V., Schaap M., 2003. Aerosol Modelling: Results and Intercomparison from 15 European Regional-scale Modelling Systems. *EUROTRAC-2 Special report*. Eurotrac-ISS, Garmisch Partenkirchen, Germany.

Hass H. Builtjes P.J.H, Simpson D., Stern R., 1997. Comparison of model results obtained with several European regional air quality models. *Atmospheric Environment*, 31, 3259–3279.

Hendriks C., Kranenburg R., Kuenen J., van Gijlswijk R., Wichink Kruit R., Segers A., Denier van der Gon H., Schaap M., 2013. The origin of ambient particulate matter concentrations in the Netherlands. *Atmospheric Environment* 69, 289-303.

Kaiser J., Suttie M., Flemming J., Morcrette J.J., Boucher O., Schultz M., 2009. Global real-time fire emission estimates based on space-borne fire radiative power observations. In: AIP Conf. Proc., vol. 1100, pp. 645-648.

Kuenen J., Denier van der Gon H., Visschedijk A., van der Brugh H., van Gijlswijk R., 2011. MACC European emission inventory for the years 2003-2007. TNO report, TNO-060-UT-2011-00588, Utrecht.

Kukkonen J., Olsson T., Schultz D.M., Baklanov A., Klein T., Miranda A.I., Monteiro A., Hirtl M., Tarvainen V., Boy M., Peuch V.-H., Poupkou A., Kioutsoukis I., Finardi S., Sofiev M., Sokhi R., Lehtinen K.E.J., Karatzas K., San José R., Astitha M., Kallos G., Schaap M., Reimer E., Jakobs H., Eben K., 2012. A review of operational, regional-scale, chemical weather forecasting models in Europe. *Atmospheric Chemistry and Physics*, 12 (1), pp. 1-87.

Li R., Wiedinmyer C., Baker K.R., Hannigan M.P., 2013. Characterization of coarse particulate matter in the western United States: a comparison between observation and modeling. *Atmos. Chem. Phys.*, 13, 1311–1327.

Mårtensson E.M., Nilsson E.D., de Leeuw G., Cohen L.H., Hansson H.-C., 2003. Laboratory simulations and parameterization of the primary marine aerosol production. *J. Geophys. Res.* 108.

Menut L., Goussebaile A., Bessagnet B., Khvorostyanov D., Ung A., 2012. Impact of realistic hourly emissions profiles on air pollutants concentrations modelled with CHIMERE. *Atmospheric Environment* 49, 233-244.

Monahan E.C., Spiel D.E., Davidson K.L., 1986. A model of marine aerosol generation via whitecaps and wave disruption. In *Oceanic Whitecaps and their role in air/sea exchange*, edited by Monahan, E.C., and Mac Niocaill, G., pp. 167-174, D. Reidel, Norwell, Mass., USA.

Mues A., Manders A., Schaap M., Kerschbaumer A., Stern R., Builtjes P., 2012. Impact of the extreme meteorological conditions during the summer 2003 in Europe on particulate matter concentrations. *Atmospheric Environment* 55, 377-391.

Peylin P., Houweling S., Krol M.C., Karstens U., Rödenbeck C., Geels C., Vermeulen A., Badawy B., Aulagnier C., Pregger, T., Delage, F., Pieterse, G., Ciais, P., Heimann, M., 2011. Importance of fossil fuel emission uncertainties over Europe for CO₂ modeling: Model intercomparison. *Atmospheric Chemistry and Physics*, 11 (13), pp. 6607-6622.

Pierce T., Hogrefe C., Rao T.S., Porter P.S., Ku J.Y., 2010. Dynamic evaluation of a regional air quality model: Assessing the emissions-induced weekly ozone cycle. *Atmospheric Environment* 44, 3583-3596.

Pouliot G., Pierce T., Denier van der Gon H., Schaap M., Moran M., Nopmongcol U., 2012. Comparing emission inventories and model-ready emission datasets between Europe and North America for the AQMEII project. *Atmospheric Environment* 53, 4-14.

Schaap M., Manders A., Hendriks E.C.J., Cnossen J.M., Segers A.J., Denier van der Gon H.A.C., Jozwicka M., Sauter F.J., Velders G.J.M., Matthijzen J., Builtjes P.J.H., 2009. Regional modeling of particulate matter for the Netherlands. BOP report (Nr. 500099008).

Schaap M., Timmermans R.M.A., Sauter F.J., Roemer M., Velders G.J.M., Boersen G.A.C., Beck J.P., Builtes P.J.H., 2008. The LOTOS-EUROS model: description, validation and latest developments. *International Journal of Environment and Pollution* 32 (2), 270-289.

Schaap M., van Loon M., ten Brink H. M., Dentener F. J., Builtjes P. J. H., 2004a. Secondary inorganic aerosol simulations for Europe with special attention to nitrate, *Atmos. Chem. Phys.*, 4, 857–874, doi:10.5194/acp-4-857-2004.

Schaap, M., Denier Van Der Gon, H.A.C., Dentener, F.J., Visschedijk, A.J.H., van Loon, M., ten Brink, H.M., Putaud, J.-P., Guillaume, B., Lioussse, C., Builtjes, P.J.H., 2004b. Anthropogenic black carbon and fine aerosol distribution over Europe. *Journal of Geophysical Research* 109, D18201.

Scholz Y., 2012. Renewable energy based electricity supply at low costs - development of the REMix model and application for Europe. Dissertation; University of Stuttgart, Stuttgart 2012.

Simpson D., Benedictow A., Berge H., Bergström R., Emberson L. D., Fagerli H., Flechard C. R., Hayman G. D., Gauss M., Jonson J. E., Jenkin M. E., Nyíri A., Richter C., Semeena V. S., Tsyro S., Tuovinen J.-P., Valdebenito Á., Wind P., 2012. The EMEP MSC-W chemical transport model – technical description. *Atmospheric Chemistry and Physics* 12, 7825–7865.

Simpson D., Fagerli H., Jonson J. E., Tsyro S., Wind P., Tuovinen J.-P., 2003. Transboundary 20 Acidification, Eutrophication and Ground Level Ozone in Europe, Part 1: Unified EMEP Model Description, EMEP Report 1/2003, Norwegian Meteorological Institute, Oslo, Norway.

Skjøth C.A., Geels C., Berge H., Gyldenkærne S., Fagerli H., Ellermann T., Frohn L.M., Christense, J., Hansen K.M., Hansen K., Hertel O., 2011. Spatial and temporal variations in ammonia emissions – a freely accessible model code for Europe. *Atmospheric Chemistry and Physics*, 11, 5221-5236.

Solazzo E., Bianconi R., Vautard R., Wyat Appel K., Moran M. D., Hogrefe C., Bessagnet B., Brandt J., Christensen J. H., Chemel C., Coll I., Denier van der Gon H. A. C., Ferreira J., Forkel R., Francis X. V., Grell G., Grossi P., Hansen A. B., Jericevic A., Kraljevic L., Miranda A. I., Nopmongcol U., Pirovano G., Prank M., Riccio A., Sartelet K. N., Schaap M., Silver J. D., Sokhi R. S., Vira J., Werhahn J., Wolke R., Yarwood G., Zhang J., Rao S. T., Galmarini S., 2012a Model evalution and ensemble modelling of surface-level ozone in Europe and North America in the context of AQMEII, *Atmos. Environ.*, 53, 60–74.

Solazzo E., Bianconi, Pirovano G., Matthias V., Vautard R., Moran M. D., Wyat Appel K., Bessagnet B., Brandt J., Christensen J. H., Chemel C., Coll I., Ferreira J., Forkel R., Francis X. V., Grell G., Grossi P., Hansen A. B., Miranda A. I., Nopmongcol U., Prank M., Sartelet K. N., Schaap M., Silver J. D., Sokhi R. S., Vira J., Werhahn J., Wolke R., Yarwood G., Zhang J., Rao S. T., Galmarini S., 2012b. Operation model evaluation for particulate matter in Europe and North America in the context of AQMEII. *Atmos. Environ.*, 53, 75–92.

Steinbacher M., Zellweger C., Schwarzenbach B., Bugmann S., Buchmann B., Ordóñez C., Prévot A. S. H., Hueglin C., 2007. Nitrogen oxide measurements at rural sites in Switzerland: Bias of conventional measurement techniques, *J. Geophys. Res.*, 112, D11307, doi:10.1029/2006JD007971.

Stern R., Builtjes P.J.H., Schaap M., Timmermans R., Vautard R., Hodzic A., Memmesheimer M., Feldmann H., Renner E., Wolke R., Kerschabumer A., 2008. A model inter-comparison study focusing on episodes with elevated PM10 concentrations. *Atmospheric Environment* 42. 4567-4588.

Tao Z., Larson S.M., Williams A., Caughey M., Wuebbles D.J., 2004. Sensitivity of regional ozone concentrations to temporal distribution of emissions. *Atmospheric Environment* 38, 6279–6285.

Van Loon M., Vautard R., Schaap M., Bergström R., Bessagnet B., Brandt J., Builtjes P. J. H., Christensen J. H., Cuvelier K., Graf A., Jonson J. E., Krol M., Langner J., Roberts P., Rouil L., Stern R., Tarrasón L., Thunis P., Vignati E., White L., Wind P., 2007. Evaluation of long-term ozone simulations from seven regional air quality models and their ensemble average, *Atmospheric Environment* 41, 2083–2097.

Van Loon M., Roemer M.G.M., Builtjes P.J.H., 2004. Model inter-comparison in the framework of the review of the unified EMEP model. TNO-Report R2004/282, Apeldoorn, The Netherlands.

Villena G., Bejan I., Kurtenbach R., Wiesen P., Kleffmann J., 2012. Interferences of commercial NO₂ instruments in the urban atmosphere and in a smog chamber. Atmospheric Measurement Techniques, 5, 149-159.

Walcek C.J. and Aleksic N.M., 1998. A simple but accurate mass conservative peak-preserving, Mixing ratio bounded advection algorithm with fortran code, Atmospheric Environment, 32, 3863–3880.

Wang X., Liang X.-Z., Jiang W., Tao Z., Wang J.X.L., Liu H., Han Z., Liu S., Zhang Y., Grell G.A., Peckham S.E., 2010. WRF-Chem simulation of East Asian air quality: Sensitivity to temporal and vertical emissions distributions. Atmospheric Environment 44, 660-669.

Whitten G., Hogo H., Killus J., 1980. The Carbon Bond Mechanism for photochemical smog. Env. Sci. Techn. 14, 14690-700.

Wichink Kruit R.J., Schaap M., Sauter F. J., van Zanten M. C., van Pul W. A. J., 2012. Modeling the distribution of ammonia across Europe including bi-directional surface-atmosphere exchange. Biogeosciences 9, 5261–5277.

Tables:

SNAP	NOx	SO2	NH3	NMVOC	CO	PM10	PM2.5
1	19,3	53,7	0,5	6,4	3,6	5,2	8,2
2	6,4	12,9	0,5	3,3	20,5	11,1	18,6
3+4	14,4	28,9	2,2	4,0	30,1	37,8	24,4
5	0,7	3,8	0,0	6,8	0,1	0,0	0,0
6	0,0	0,0	0,3	63,8	0,0	4,8	8,5
7	48,5	0,1	1,7	13,3	41,5	18,4	25,5
8	10,7	0,6	0,1	2,3	4,2	5,7	10,0
9	0,0	0,0	0,0	0,0	0,0	0,0	0,0
10	0,1	0,0	94,7	0,0	0,0	17,0	4,8
1 + 2 + 7	74,1	66,7	2,7	23,0	65,6	34,8	52,3
All (kTon)	1457	540	578	1163	3731	218	123

Table 1.

Contribution of the different source sectors to German national emissions (%). Besides single sectors also the relative contribution for the three sectors studied here are given. Finally, the last row provide the national emission total for all species (KTon).

Name	Time period	Grid & Horizontal resolution	Meteorological input	Description of run
LE_Default	Emission: 2005 Meteorology: 2006	10°W-40°E 35°-70°N; 0.5°x0.25° regular lon-lat grid	12 h forecast data from the operational ECMWF stream with analyses at noon and midnight at a horizontal resolution of about 25x25km	Default emission time profiles (see Fig.1) for all SNAP categories
LE_const127				Default emission time profiles for all SNAP categories but constant profiles for SNAP1, SNAP2 and SNAP7.
LE_SNAP7				Default emission time profiles for all SNAP categories beside for SNAP7. For SNAP7 the new profiles were used for Germany and the Netherlands (see Fig.3) .
LE_SNAP2				Default emission time profiles for all SNAP categories beside for SNAP2. For SNAP2 the new profiles were used for Europe (see Fig.4a) .
LE_SNAP1				Default emission time profiles for all SNAP beside for SNAP1. For SNAP1 the new profiles were used for Europe (see Fig.4b) .
LE_SNAP127				Default emission time profiles for all SNAP categories beside for SNAP1, SNAP2 and SNAP7. For the SNAP 1 and SNAP 2 categories the new profiles for Europe and for SNAP7 the new profiles for Germany and the Netherlands were used.

Table 2.

Description of the model simulations.

Rural background stations									
Simulation name	NO2			SO2			PM10		
	Correlation	Mean year	Bias	Correlation	Mean year	Bias	Correlation	Mean year	Bias
LE_Default	0.71	9.88	1.80	0.70	2.05	0.78	0.46	11.22	7.60
LE_const127	0.57	11.17	0.51	0.64	2.01	0.82	0.46	11.22	7.60
LE_SNAP1	0.72	9.89	1.79	0.71	2.04	0.79	0.47	11.20	7.62
LE_SNAP2	0.71	9.91	1.77	0.74	2.08	0.75	0.47	11.25	7.58
LE_SNAP7	0.72	9.98	1.70	0.70	2.05	0.78	0.46	11.20	7.62
LE_SNAP127	0.73	10.02	1.66	0.74	2.07	0.76	0.48	11.20	7.62
Urban background stations									
Simulation name	NO2			SO2			PM10		
	Correlation	Mean year	Bias	Correlation	Mean year	Bias	Correlation	Mean year	Bias
LE_Default	0.70	13.33	13.42	0.62	2.80	2.08	0.51	12.70	12.36
LE_const127	0.48	15.15	11.60	0.49	2.76	2.12	0.49	12.75	12.31
LE_SNAP1	0.71	13.33	13.43	0.65	2.79	2.09	0.52	12.68	12.38
LE_SNAP2	0.70	13.35	13.41	0.67	2.83	2.05	0.52	12.73	12.33
LE_SNAP7	0.72	13.49	13.26	0.62	2.80	2.08	0.51	12.69	12.38
LE_SNAP127	0.72	13.51	13.25	0.69	2.83	2.06	0.53	12.69	12.37

Table 3.

Statistical overview of model performance averaged over all available stations based on hourly data.

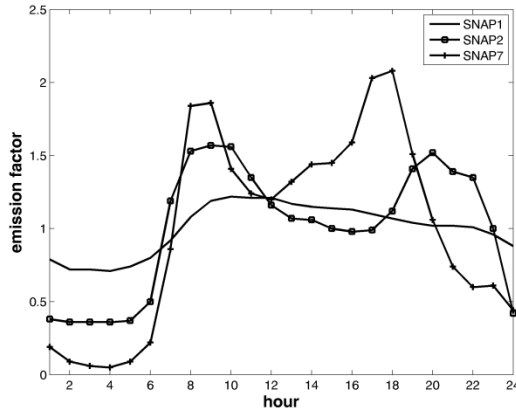
Rural background stations									
Simulation name	NO2			SO2			PM10		
	Correlation	Mean year	Bias	Correlation	Mean year	Bias	Correlation	Mean year	Bias
LE_Default	0.78	10.14	1.57	0.73	2.09	0.82	0.46	11.15	7.06
LE_const127	0.76	11.55	0.15	0.67	2.06	0.86	0.47	11.16	7.06
LE_SNAP1	0.79	10.14	1.56	0.74	2.08	0.83	0.47	11.13	7.08
LE_SNAP2	0.78	10.17	1.54	0.76	2.12	0.79	0.48	11.18	7.04
LE_SNAP7	0.79	10.24	1.46	0.73	2.09	0.82	0.47	11.13	7.09
LE_SNAP127	0.80	10.28	1.42	0.76	2.12	0.80	0.49	11.13	7.08
Urban background stations									
Simulation name	NO2			SO2			PM10		
	Correlation	Mean year	Bias	Correlation	Mean year	Bias	Correlation	Mean year	Bias
LE_Default	0.77	13.03	13.69	0.71	2.64	2.18	0.54	12.55	12.38
LE_const127	0.73	14.84	11.88	0.60	2.60	2.22	0.53	12.59	12.34
LE_SNAP1	0.78	13.03	13.69	0.74	2.63	2.19	0.55	12.53	12.40
LE_SNAP2	0.77	13.05	13.67	0.76	2.67	2.14	0.56	12.58	12.35
LE_SNAP7	0.81	13.19	13.53	0.71	2.64	2.18	0.54	12.53	12.40
LE_SNAP127	0.82	13.20	13.52	0.78	2.66	2.15	0.57	12.54	12.39

Table 4.

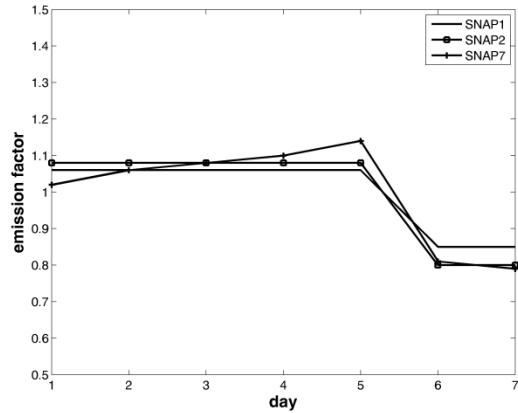
Statistical overview of model performance averaged over all available stations based on daily data.

Figures:

(a)



(b)



(c)

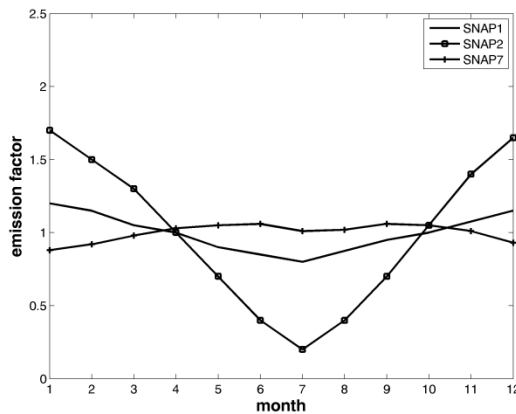
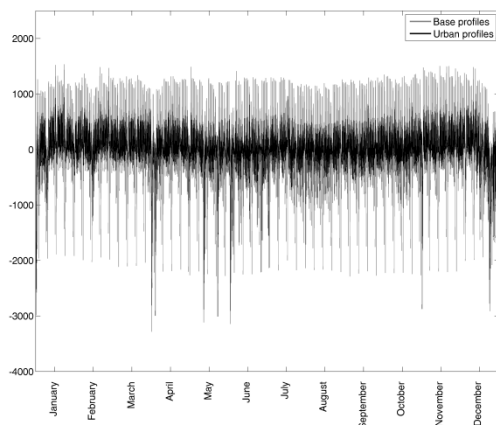


Figure 1.

Overview of the LOTOS-EUROS default diurnal cycle (a), weekly cycle (b) and seasonal cycle (c) of emission factors for the SNAP1, SNAP2 and SNAP7 categories.

(a)



(b)

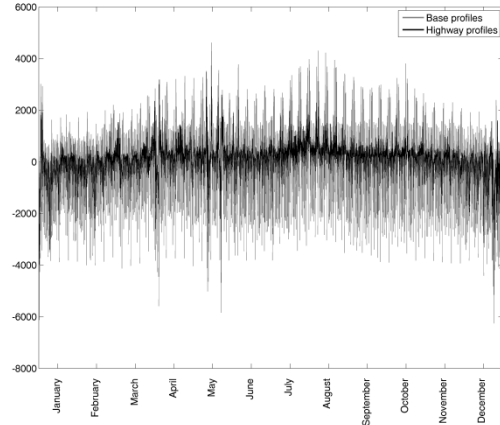
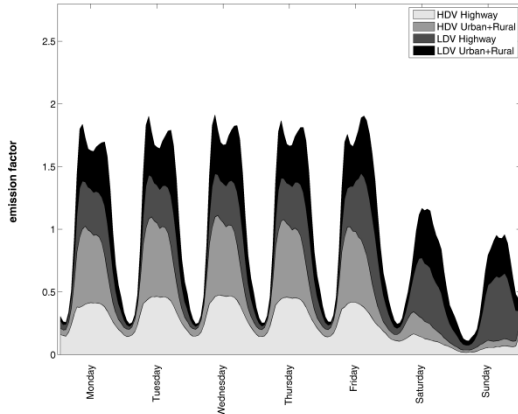


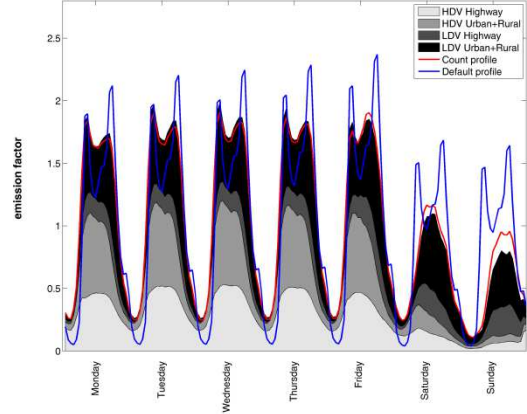
Figure 2.

Comparison of the traffic hourly count residues for the default, urban and highway time profiles at an urban street station (a) and a highway station (b) in Germany for the year 2010.

(a)

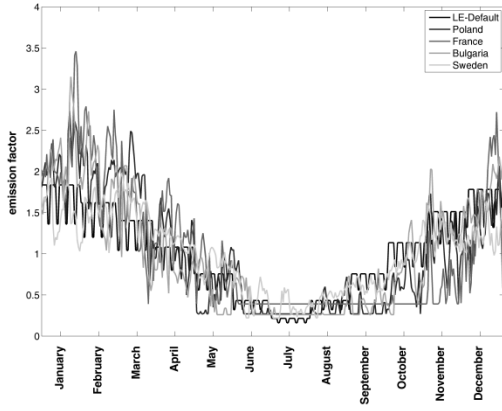


(b)

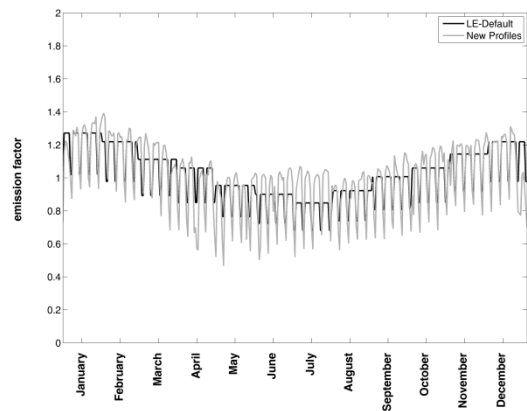
**Figure 3.**

Summation of diurnal cycles per day of the week for LDV and HDV on urban streets and highways equally weighted (a) and weighted with the NOx split factors (b). The red line in Figure (b) is the same as the black line in Figure (a), the blue line represents the default time profiles.

(a)



(b)

**Figure 4.**

Comparison between the new and the default seasonal (daily) emission factors at five locations for SNAP 2 (a) and for Germany for SNAP1 (b).

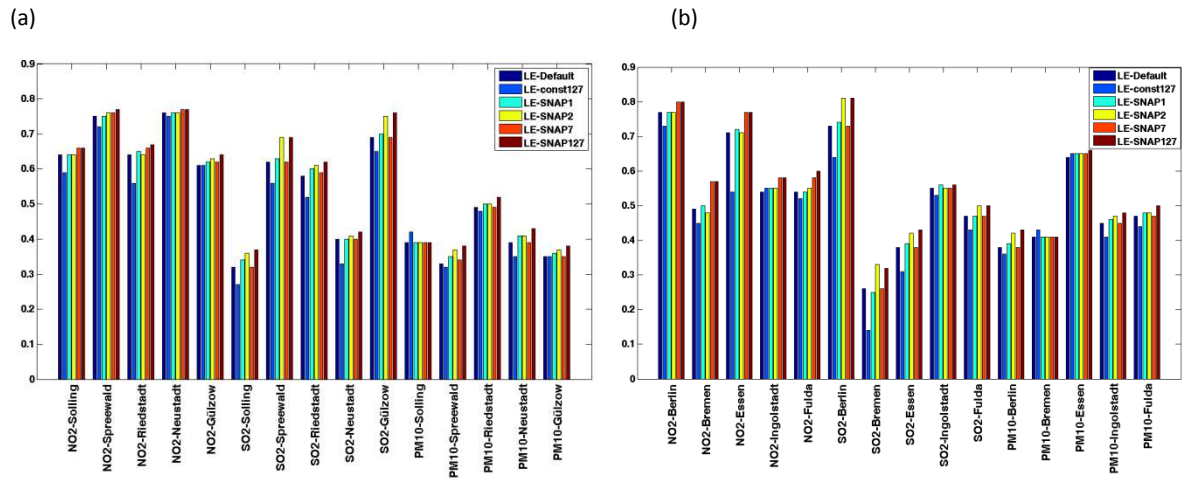


Figure 5.

Bar charts of the daily correlation coefficients for all simulations at selected urban (a) and rural (b) background stations across Germany.

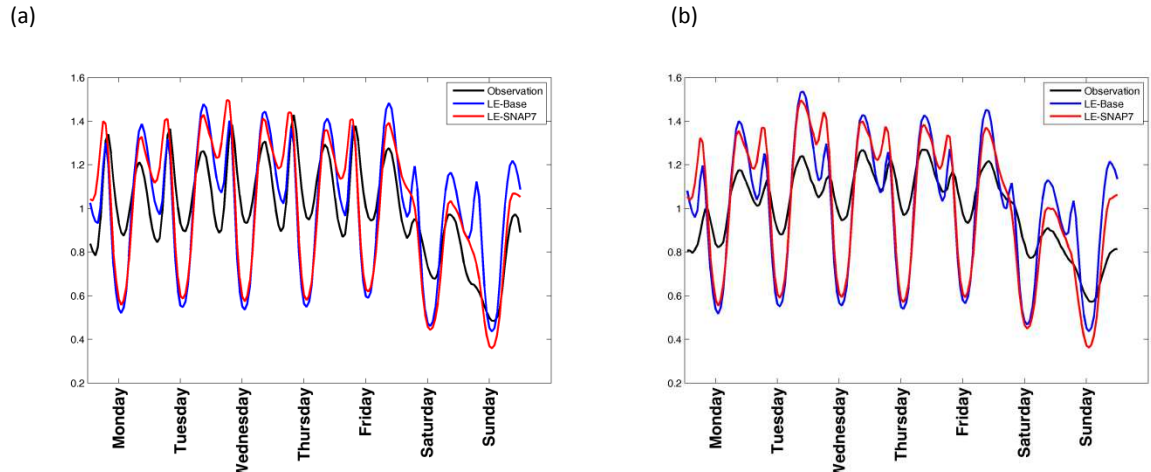


Figure 6.

Simulated and measured normalized weekly cycle of NO2 at all available urban (a) and rural (b) stations.

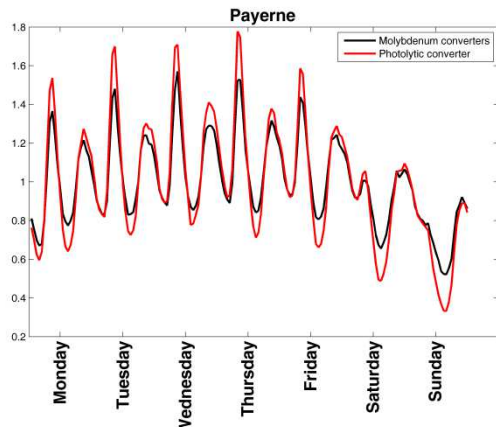


Figure 7.

Normalized weekly cycle of NO₂ of simultaneous measurements using a molybdenum converter and a photolytic converter averaged over a three year time series (2006-2009) at the site Payerne in Switzerland.

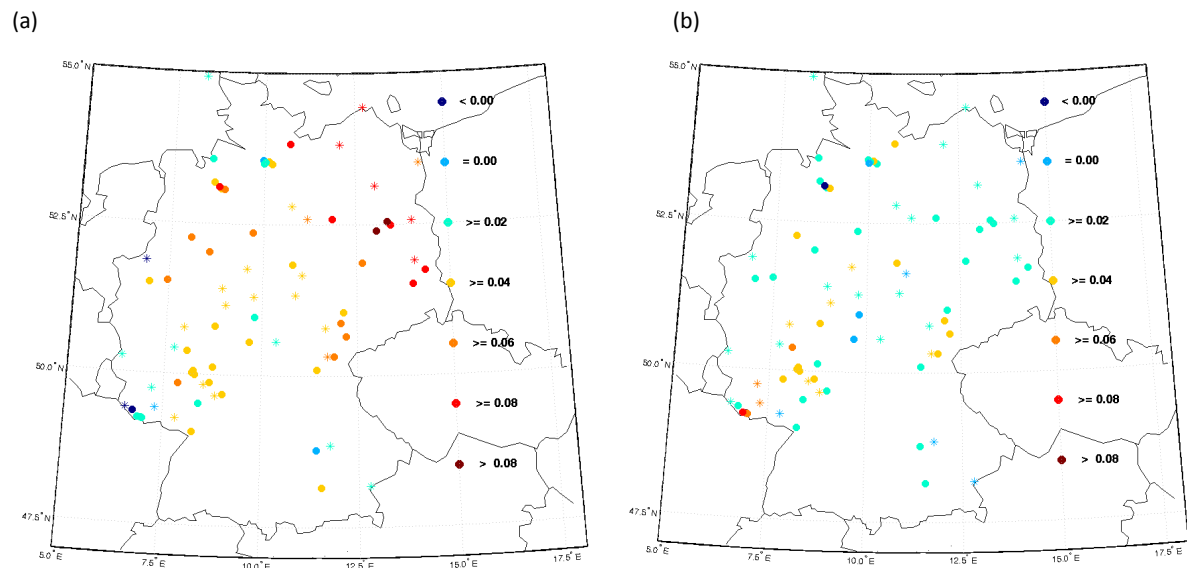


Figure 8.

Difference of daily correlation coefficient for SO₂ between the model simulations using the new (LE_SNAP2, LE_SNAP1) and the default (LE_Default) emission time profiles for SNAP2 (a) and SNAP1 (b) across German urban (circle) and rural (stars) stations.

11 Publication list

11.1 Scientific articles

A. Mues, A. Manders, M. Schaap, A. Kerschbaumer, R. Stern, P. Builtjes, 2012. Impact of the extreme meteorological conditions during the summer 2003 in Europe on particulate matter concentrations. *Atmospheric Environment*, 55 (2012), 377-391.

A. Manders, E. van Meijgaard, A. Mues, R. Kranenburg, L.H.van Ulft, M.Schaap, 2012. The impact of differences in large-scale circulation output from climate models on the regional modeling of ozone and PM. *Atmospheric Chemistry and Physics*, 12, 9441-9458.

A. Mues, A. Manders, B. van Ulft, E. van Meijgaard, M. Schaap, P. Builtjes, 2012. Investigating differences in air quality between urban and rural regions under current and future climate conditions. Extended abstract to be published in the book of the ITM 2012, 32st NATO/SPS International Technical Meeting on Air Pollution Modeling and its Application 7-11 May 2012, Utrecht, The Netherlands.

A. Mues, A. Manders, M. Schaap, L.H. van Ulft, E. van Meijgaard, P. Builtjes, 2012. Differences in particulate matter concentrations between urban and rural regions under current and changing climate conditions. Submitted to *Atmospheric Environment*, November 2012.

A. Mues, C. Hendriks, J. Kuenen, A. Manders, A. Segers, Y. Scholz, C. Hueglin, P. Builtjes, M. Schaap. Sensitivity of air pollution simulations with LOTOS-EUROS to temporal distribution of emissions. To be submitted to *Atmospheric Chemistry and Physics*.

11.2 Presentations

A. Mues, A. Manders, M. Schaap, R. Stern, A. Kerschbaumer, P. Builtjes, 2012. Modeling the impact of meteorology on particulate matter, implications for emissions. 24th GLOREAM/ACCENT workshop on tropospheric chemical transport modeling, 17-19 October 2012, Barcelona, Spain.

A. Mues, A. Manders, B. van Ulft, E. van Meijgaard, M. Schaap, P. Builtjes, 2012. Investigating differences in air quality between urban and rural regions under current and future climate conditions. ITM 2012, 32st NATO/SPS International Technical Meeting on Air Pollution Modeling and its Application, 7-11 May 2012, Utrecht, the Netherlands.

A. Mues, A. Manders, B. van Ulft, E. van Meijgaard, M. Schaap, P. Builtjes, 2011. Evaluation of a coupled climate – air quality model system. 11th EMS Annual Meeting, 10th European Conference on Applications of Meteorology, 12-16 September 2011, Berlin, Germany.

A. Mues, A. Manders, B. van Ulft, E. van Meijgaard, M. Schaap, P. Builtjes, 2011. Modeling air quality in a changing climate using LOTOS-EUROS. UAQCC – Urban Air Quality and Climate Change – Joint Workshop of WMO and KlimaCampus, University of Hamburg, 16-18 August 2011, Hamburg, Germany.

11.3 Posters

A. Mues, A. Manders, M. Schaap, P. Builtes, R. Stern, 2011. Impact of the extreme meteorological conditions during the summer 2003 in Europe on air quality – an observation and model study. EGU 2011, European Geosciences Union General Assembly 2011, 3-8 April 2011, Vienna, Austria.

A. Mues, A. Manders, M. Schaap, P. Builtes, R. Stern, 2010. Air quality in cities – aerosol-modelling in relation to climate. 1st – 3rd CLM-Community Assembly 2010, 1-3 September 2010, Berlin, Germany.

Appendix

Contribution to the paper I, III, IV:

The main topic of the study was formulated for the FU Berlin Milieu-Project (<http://www.milieu.fu-berlin.de/>). The set-up of the study was developed by myself in discussions with colleagues at TNO. The chemistry transport models LOTOS-EUROS and REM/Calgrid used to address the scientific questions were used in the default set-up and the simulations for paper I, III and IV were performed by myself and in cooperation with TNO. The RACMO2 – LOTOS-EUROS simulation used in paper III was performed at KNMI (Dutch Weather Service). The literature studies, post-processing of model and measurement data including plotting of figures and the analyses of results were mainly conducted by myself. In paper III the new time profiles for SNAP7 were constructed by myself, I constructed the SNAP2 profiles based on concepts described in literature and the SNAP1 profiles were developed by colleagues at TNO. Discussion and interpretation of the results were done in cooperation with the colleagues at TNO. The papers were written by myself aided by the co-authors.

Contribution to the paper II:

The main work on this study has been done at TNO and KNMI (Dutch Weather Service) in framework of the Dutch Knowledge for Climate Program. As a result of the close cooperation between the institute of Meteorology of the FU Berlin and TNO Utrecht, it was possible to join the work and use the model data. I contributed to interpretation and discussion of the simulation results. The paper was mainly written by A. Manders.

Danksagung

Nun ist es an der Zeit mich bei all denjenigen zu bedanken, die mich bei der Erstellung dieser Arbeit unterstützt haben. Ich habe viel von den unterschiedlichsten Personen gelernt und viel fachliche und moralische Unterstützung erfahren. Vielen Dank!

Mein besonderer Dank gilt:

Den (ehemaligen) Mitarbeitern der Trumf-Gruppe am Institut für Meteorologie, insbesondere Dr. Rainer Stern und Dr. Andreas Kerschbaumer, die mir auch schon während meiner Diplomarbeit immer mit Rat und Tat zur Seite standen. Ich habe viel von euch gelernt und danke euch für die Zusammenarbeit in den letzten Jahren. Ich freu mich euch auch in Zukunft bei unseren Stammtischen zu sehen.

A big ‚Dank jullie wel‘ to the air quality modeling group at TNO! I enjoyed my time in Utrecht and I always felt welcome. Thank you very much for your support and the help, especially from the LOTOS-EUROS helpdesk!

Des Weiteren bedanke ich mich bei den Initiatoren des Milieu-Projektes an der FU Berlin, insbesondere bei Herrn Prof. Ulrich Cubasch, und bei TNO für die Finanzierung meiner Stelle. Insbesondere durch das Milieu-Projekt hatte ich die Möglichkeit in völlig andere Fachgebiete einen Einblick zu erhalten.

Ich möchte mich herzliche bei Prof. Peter Builtjes bedanken, der mir die Stelle im Milieu-Projekt geben hat und damit auch die Möglichkeit diese Arbeit zu schreiben. Ich danke dir auch für deine Vorlesung ‚Luftchemie‘, durch die ich für dieses Fachgebiet begeistert wurde. Die Zusammenarbeit mit TNO war besonders wichtig für mich. Danke, dass du meine Aufenthalte dort ermöglicht und organisiert hast. Ich danke dir auch vielmals für die vielen Gespräche über meine Arbeit in den letzten Jahren.

Ein ganz besonderer Dank gilt auch Dr. Astrid Manders und Dr. Martijn Schaap bei TNO, die mich während der gesamten Zeit unterstützt haben. Ich danke dir Astrid, für die vielen fachlichen Diskussionen ob bei TNO oder am Telefon und vor allem auch für dein unermüdliches Korrekturlesen und die technische Hilfe! I would like to thank you Martijn for all your help and that you always arranged time to discuss my work! I always enjoyed working with both of you and I learnt a lot from you especially about writing papers!

Mein Dank gilt auch Sabine Banzhaf für die vielen (un)erheblichen Überminuten, die wir zusammen im Büro gearbeitet haben und für dein stets offenes Ohr! Du bist einfach ein Trum(p)f!

Thomas Bergmann, der einfach viel besser ist als der Helpdesk bei TNO.

Ute Zahn, vielen Dank für deinen Sachverstand im Bereich der englischen Sprache!

Carsten Nierlein, ich danke für deine ‚Word‘-Hilfe.

Meinen Eltern und Geschwistern, die immer an mich geglaubt haben und mich immer unterstützt haben! Das hat mir sehr geholfen, ich danke euch dafür! Bei meinen Eltern möchte ich mich insbesondere auch für die kulinarische Verpflegung während der besonders arbeitsintensiven Phase bedanken.